DOCTOR OF PHILOSOPHY

A basic region in the Elp1 subunit of the budding yeast Elongator complex is essential for wobble uridine tRNA modification

Di Santo, Rachael Teresa Ann

Award date:
2013

DOCTOR OF PHILOSOPHY

A basic region in the Elp1 subunit of the budding yeast Elongator complex is essential for wobble uridine tRNA modification

Rachael Teresa Ann Di Santo

2013

University of Dundee

A basic region in the Elp1 subunit of the budding yeast Elongator complex is essential for wobble uridine tRNA modification

Rachael Teresa Ann Di Santo

A thesis submitted for the degree Doctor of Philosophy

University of Dundee

4th September 2013

Contents

List of Figures

List of Tables

Abbreviations

ADH1	Alcohol dehydrogenase 1
AEBSF	4-(2-Aminoethyl) benzenesulfonyl fluoride hydrochloride
AID	Auxin inducible degron
AMP	Ampicillin
Arg4	Argininosuccinate lyase
ATM	Ataxia-telangiectasia mutated
BSA	Bovine serum albumin
Cbp80	Cap binding protein 80
Cex1	Cytoplasmic export protein 1
Crm1	Chromosome region maintenance 1
CTD	C-terminal domain
DHU LOOP	Dihydrouridine loop
Dph	Dipthamide biosynthesis protein
DTT	Dithiothreitol
ECL	Enhanced chemiluminescence
EDTA	Ethylenediaminetetraacetic acid
eEF1	Eukaryotic elongation factor 1
eEF2	Eukaryotic elongation factor 2

Elp	Elongator protein
EMSA	Electrophoretic mobility shift assay
EV	Empty vector
FD	Familial Dysautonomia
G418	Geneticin
GAL	Galactose
Gcn4	General Control nonderepressible 4
Gcn5	General Control nonderepressible 5
GEF	Guanine nucleotide exchange factor
GFP	Green fluorescence protein
Gln4	Glutamine metabolism 4
GST	Glutathione S-transferase
GuSCN	Guanidine isothiocyanate
HA	Human influenza hemagglutinin
HAT	Histone acetyl transferase
HEPES	2-[4-(2-hydroxyethyl)piperazin-1-yl]ethanesulfonic acid
Hrr25	HO and radiation repair 25
IKAP	IKK complex-associated protein
IKBKAP	Inhibitor of kappa light polypeptide gene enhancer in B-cells, kinase complex-associated protein
KTI	Killer toxin insensitive
MEC-17	Mechanosensory abnormality protein 17
MMS	Methyl methanesulfonate
MOPS	3-(N-morpholino)propanesulfonic acid
mQH_20	Mill-Q filtered water
mTOR	Mammalian target of rapamycin
Ncs2	Needs Cla4 to Survive 2
NES	Nuclear export sequence
NLS	Nuclear import sequence

NTPase	Nucleotide triphosphatase
OD_{600}	Optical density at 600 nm
PCNA	Proliferating cell nuclear antigen
PEG	Polyethylene glycol
PTSK	*O*-phosphoseryl-$tRNA^{Sec}$ kinase
SAM	S-Adenosylmethionine
Sap	Sit4 associated protein
SCF	Skp, Cullin, F-box containing complex
SDS-PAGE	Sodium dodecyl sulphate polyacrylamide gel electrophoresis
Sec2	Secretory protein 2
Sit4	Suppressor of initiation of transcription 4
ssDNA	Single stranded DNA
TBS	Tris buffered saline
TEV	Tobacco etch virus
TIR1	Transport inhibitor response 1
Trm112	tRNA Methyltransferase 112
Trm9	tRNA Methyltransferase 9
tRNA	Transfer RNA
Tuc1	tRNA 2-thiolation protein 1
Tum1	Thiouridine Modification 1
Uba4	Ubiquitin-like protein activating 4
Urm1	Ubiquitin related modifier 1

All culture media abbreviations are given in the Appendix

Acknowledgements

I would first of all like to say a huge thank you to my supervisor Professor Mike Stark for all his guidance throughout this work and for making my time in the lab so valuable and enjoyable. I would also like to say a special thank you to Dr Ashwin Bhat, Mr Stephen Corbishley (Corbo) and Dr Vasso Makrantoni for patiently teaching me the basics of yeast during my rotation project and for helpful discussions. Other past lab members have also been brilliant for discussions about Elongator and have made significant contributions to this work; Dr Wael Abdel-Fattah (who did phosphopeptide mapping of Elp1), Miss Susie Bandau (who made the *SUP4 ochre* suppressor system or 'Susies system' as I like to call it), Miss Kasia Kozyrska (an honours student who worked on the 'other half' of Elp1), Miss Charlotte Lloyd (the first honours student under my wing who made the pGAL-TEV strains used in this study). I would also like to thank all the members of the Schaffrath Lab with whom we collaborate with on many aspects of Elongator; especially Professor Raffael Schaffrath and Mr Daniel Jablownowski for all the helpful meetings and advice given throughout this work. A big thank you to Dr Subbu Sundaramoorthy for lots of recombinant protein advice as well the rest of the TOH lab who are great neighbours. Other thanks go out to; Dr Etsushi Kitamura, Dr Mark Larance and Mr Michael Porter (for reagents and advice); Dr Sam Swift and Dr Alan Prescott (for extensive help with microscopy); Miss Kelly Hodge, Dr Sara ten Have and the proteomics facility (for carrying out mass spectrometry sample prep and runs); The media kitchen, wash-up and stores (for keeping everything ticking over). Finally thanks to all my family and friends who stood by me during the stressful times- you probably deserve medals but you just get this little mention instead I'm afraid.

Declaration

I hereby declare that this thesis is based on my own work and is of my own composition. Work that is not my own is clearly indicated by references to the appropriate researchers and/or their publications. The work described here has to my knowledge never been presented for a higher degree or publication excluding where work is clearly referenced.

Rachael Teresa Ann Di Santo

I certify that Rachael Di Santo has spent at least nine terms in research in the Wellcome Trust Centre for Gene Regulation and Expression, University of Dundee, has fulfilled the conditions of Ordinance General No. 39 of the University of Dundee and is qualified to submit this thesis for the degree of Doctor of Philosophy.

Professor Michael. J. R Stark

Professor of Yeast Molecular Biology

University of Dundee

Abstract

Elongator is a conserved, multi-subunit protein complex (Elp1-6) that was first discovered in *Saccharomyces cerevisiae* (Budding yeast). The complex is nonessential in yeast but loss of function leads to pleiotropic phenotypes such as temperature sensitivity and slow growth adaptations. In higher eukaryotes Elongator is required for normal growth and development and in humans, a mutation in the largest subunit (Elp1) causes Familial Dysautonomia, a severe autosomal recessive neuropathy.

It has now been shown that the main role of yeast Elongator is to promote mcm^5 and ncm^5 tRNA wobble uridine modifications that are required for these tRNAs to function efficiently in protein translation. This function is conserved in higher eukaryotes, including mammals, and it is now thought that a common translation defect may underlie the pleiotropic phenotypes associated with Elongator dysfunction.

The Elp1 subunit has a C-terminal domain that is predicted to be mainly alpha-helical in structure and contains a highly conserved arginine/lysine rich region that was previously annotated as a putative nuclear localisation sequence (NLS). Since tRNA modifications are thought to occur in the cytoplasm, which is where Elongator is mainly localised, it was not immediately clear why an NLS would be required.

In order to define the function of this basic region, an *elp1-KR9A* mutant was created with nine alanine substitutions throughout its sequence. The Elp1 basic region was found to be essential for the tRNA wobble uridine modification function of Elongator. However, the distribution of Elp1 between the cytoplasm and nucleus was unaffected by the *elp1-KR9A* mutation and therefore it is unlikely to function as a nuclear localisation sequence. Since the Elp1 basic region is of functional importance we

hypothesised that it could be involved in binding tRNA to the Elongator complex. This was tested by examining the binding of tRNA to recombinant Elp1 and Elp1-KR9A C-terminal domains. The wild-type Elp1 C-terminal domain formed a complex with tRNA that was abolished by mutations in the basic region, indicating that the conserved basic region in Elp1 is essential for tRNA wobble uridine modification most likely through its role as a tRNA binding motif.

Chapter 1: Introduction

1.1 Overview of the budding yeast Elongator complex

The complexity of higher eukaryotes, particularly mammalian cells, can make the study of basic cellular functions difficult. *Saccharomyces cerevisiae* (budding yeast) is a unicellular eukaryote that is well established as a model organism. In contrast to higher eukaryotes, yeast are simpler and more amenable to genetic manipulations that are invaluable for the analysis of proteins function. Although higher eukaryotes have larger genomes and therefore correspondingly larger proteomes, many proteins are highly conserved across eukaryotes. In studies of basic cellular functions such as the cell cycle, gene transcription and protein translation, research in yeast as a eukaryotic model have provided valuable contributions to the understanding of these processes. Proteins that are conserved from yeast to man can therefore be studied in yeast to provide meaningful insight into the function of their human counterparts.

Elongator is a six subunit protein complex, which is present in all eukaryotes. It was first discovered in budding yeast associated with chromatin bound RNA polymerase II (Otero et al., 1999). Due to this association and the finding that one of the subunits (Elp3) contained a histone acetyl transferase (HAT) domain (Wittschieben et al., 1999), the principle function of the complex was proposed to be as a histone acetyltransferase, acting on nucleosomes during transcript elongation(Otero et al., 1999, Wittschieben et al., 1999). However, this role of Elongator is now disputed due to various other data that have emerged from work in yeast and other organisms, including the finding that most of the cellular pool of Elongator is present in the cytoplasm rather than the nucleus (Pokholok et al., 2002). Subsequently, a number of other functions have been proposed for the complex and it was suggested that

Elongator could have distinct functions in both the nucleus and the cytoplasm (Svejstrup, 2007).

The Elongator complex was first described as a heterotrimer made up of subunits Elp1-Elp3 (Otero et al., 1999) .A smaller, more salt labile subcomplex was later discovered consisting of Elp4-Elp6 (Krogan and Greenblatt, 2001, Winkler et al., 2001), which together with the Elp1-3 heterotrimer was proposed to form a hexameric holocomplex (Figure 1.1).

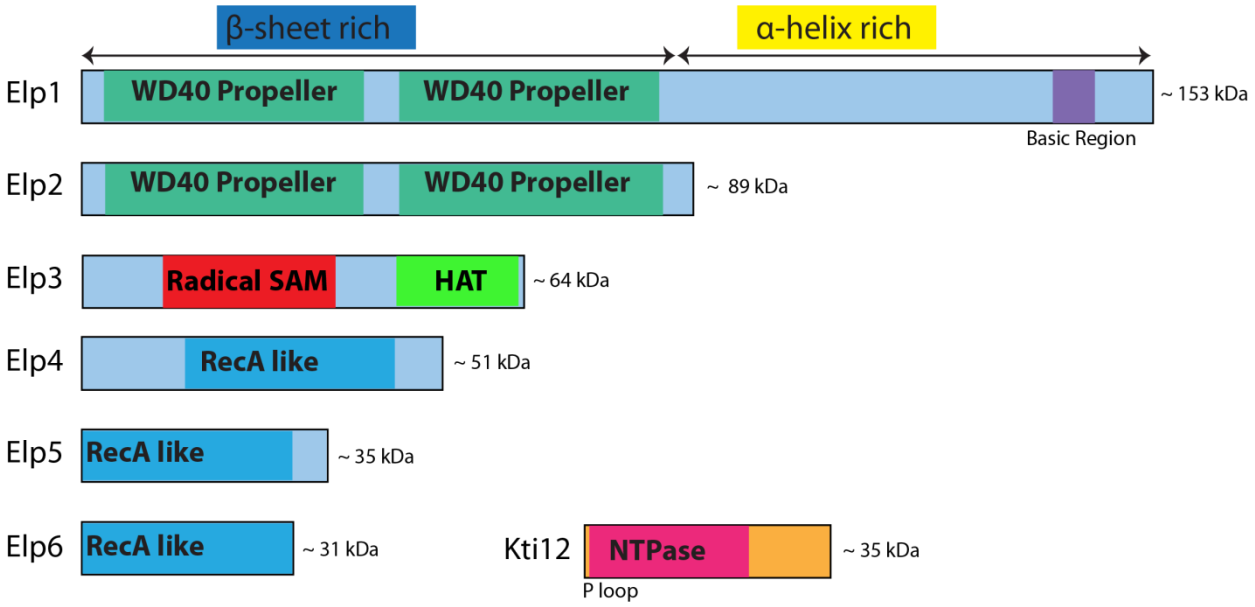

Figure 1.1: Schematic of the Elongator subunits. The Elp1-6 subunits and accessory protein Kti12 are displayed showing known structural and functional domains, features and molecular weights.

i) Elp1

Elp1 is the largest Elongator subunit and is thought to act as a core scaffold, since it is essential for assembly of the complex. Interactions between Elp2, Elp3 and across the two subcomplexes are lost when Elp1 is deleted (Frohloff et al., 2003, Fichtner et al., 2002b). Elp1 has an interesting proposed secondary structure, the N-terminal portion is predicted to be mainly beta-sheet and the C-terminal portion largely alpha-helix (Figure 1.2). The N-terminus contains WD40 repeat domains, which are predicted to form beta propellers connected to a more flexible C-terminus. The Elp1 C-terminus also has a basic region, annotated as a putative Nuclear localisation sequence (Fichtner et al., 2003), which is highly conserved across eukaryotes.

ii) Elp2

The Elp2 subunit has multiple WD40 repeats that are predicted to form two seven-bladed beta propeller domains (Glatt and Muller, 2013). Unlike the other subunits of Elongator, although Elp2 is required for function, it is not essential for Elongator complex assembly as its deletion does not disrupt subunit contacts between Elp1, Elp3 or the Elp4-6 subcomplex (Frohloff et al., 2003, Petrakis et al., 2004). Since Elp2 is made up of WD40 repeats, which are reported to mediate protein-protein interactions (Fellows et al., 2000), it has been suggested that Elp2 may mediate the binding of other factors. In support of this the Elp2 C-terminus is required for binding of the accessory factor Kti12 (see below) to the assembled complex (Frohloff et al., 2003, Fichtner et al., 2002b).

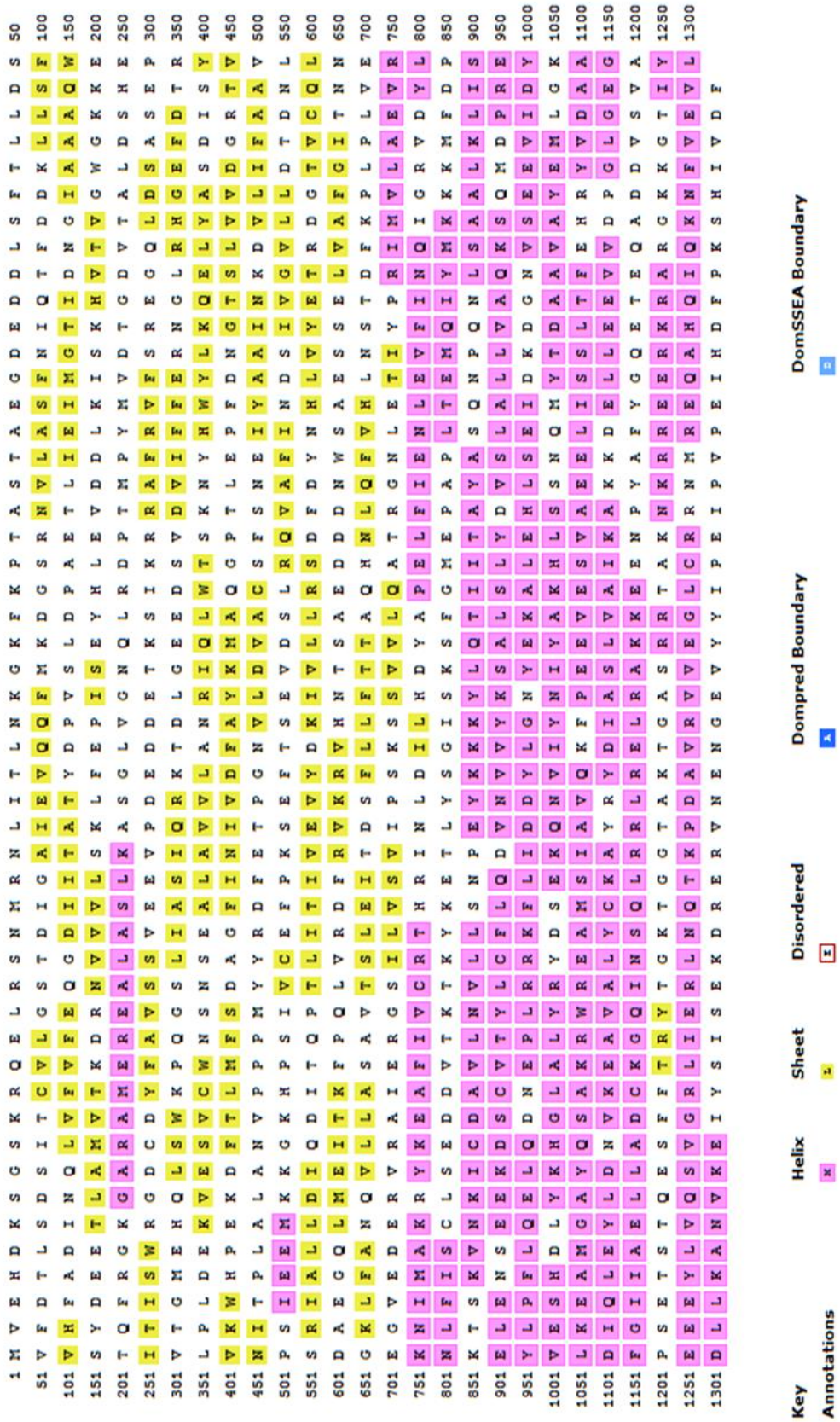

Figure 1.2: The predicted secondary structure of the yeast Elp1 subunit. The N-terminal half of Elp1 is mainly beta sheet while the C-terminal half is predicted to consist of alpha helix. Generated by the server PSIPred (McGuffin et al., 2000) using NCBI sequence accession NP_013488.3.

iii) Elp3

The Elp3 subunit is presumed to be the catalytic core of Elongator since it contains two functionally important enzymatic domains (Figure 1.1). Elp3 has an N-terminal Radical S-Adenosylmethionine (SAM) like domain (Chinenov, 2002) and a C-terminal GNAT-type histone acetyltransferase (HAT) like domain (Wittschieben et al., 1999).

Radical SAM domains use a bound iron-sulphur cluster as an electron donor for cleavage of their SAM substrate into methionine and a 5'-deoxyadenosyl radical. The generated radical is then able to remove protons from other substrate molecules in order to carry out a number of functions, such as the transfer of methyl groups (Frey et al., 2008). Members of the GNAT-type HAT family share common core A, B and D sequence motifs that mediate the binding of Acetyl CoA and transfer of Acetyl groups onto the N-terminal Lysine residues of Histone tails (Marmorstein, 2001).

In Elp3, these domains are highly conserved and essential to Elongator function. Point mutations of cysteines predicted to co-ordinate the iron-sulphur cluster in the Radical SAM domain (Paraskevopoulou et al., 2006, Greenwood et al., 2009) and in the B motif of the HAT domain (Wittschieben et al., 2000) result in dysfunctional Elongator phenotypes (Section 1.2). Both of these domains also appear to be enzymatically active, since Elongator can acetylate Histone H3 and H4 *in vitro* and Elp3 has been shown to co-ordinate an iron-sulphur cluster, which can bind and may cleave SAM (Paraskevopoulou et al., 2006, Greenwood et al., 2009). Although the HAT-like domain of Elp3 has activity towards Histones, it does not appear to be coupled to a chromatin binding domain, unlike other HATs of this family (Marmorstein, 2001). It seems likely that this domain works in conjunction with the Radical SAM domain for its unknown *in*

vivo enzymatic role. Unlike other Elongator subunits, Elp3 is also conserved in Archaea, which illustrates the importance of this coupled enzymatic function (Chinenov, 2002).

Elp1 is required for Elp3 stability (Petrakis et al., 2004) and these subunits directly interact (Fichtner et al., 2002b, Frohloff et al., 2003). The Elp3 subunit also mediates the Elp2-Elp1 interaction (Fichtner et al., 2002b, Petrakis et al., 2004) and the iron-sulphur cluster of the Elp3 Radical SAM domain is integral to the overall assembly of Elongator (Greenwood et al., 2009).

iv) Elp 4,5,6

Very little was previously known about the Elp4-6 subcomplex of Elongator but all of its subunits have homologues in humans and it was suggested that this complex binds across interfaces created by assembled Elp1-3 (Hawkes et al., 2002, Close et al., 2012b, Petrakis et al., 2004). Recently the crystal structure of this subcomplex was solved. The Elp4-6 subunits all contain a common RecA-like fold, made up of a nine-stranded parallel beta sheet between alpha helices. Further to this, the subcomplex was assembled as a heterohexameric ring complex made up of two copies of each subunit (Glatt et al., 2012).

This architecture is related to the RecA-like NTPase superfamily, which hydrolyse nucleoside triphosphates and couple this to movements along substrates. Each subunit of a RecA-like NTPase hexamer donates residues to the NTPase active site of the adjacent subunit allowing for coordinated hydrolysis. This is coupled to conformational changes that allow translocation of a substrate molecule, such as DNA or RNA into the central cavity of the hexamer (Lyubimov et al., 2011). The bacterial Rho factor is

classic example of this superfamily and functions as a transcription terminator. Rho uses the energy from ATP hydrolysis to power the translocation of RNA transcripts through its central pore using transient associations with the protruding helices that line this pore. The dynamic movement of RNA through this cavity has the effect of pulling the mRNA away from the RNA polymerase II complex and the template gene (Kaplan and O'Donnell, 2003).

Like RecA-like NTPase family counterparts, the Elp4-6 hexamer has a basal ATPase activity, which is comparable in levels to other members of the family. This was unexpected since key signature residues of a P-loop motif, required for nucleotide binding (Ponting, 2002, Glatt et al., 2012, Lyubimov et al., 2011) are not present in these subunits. Mutations in other potential catalytic residues of Elp5 and Elp6 led to reduced ATPase activity and these mutant proteins can only a partially rescue the equivalent gene deletions (Glatt et al., 2012). Therefore the Elongator subcomplex hexamer has a functionally important basal ATPase activity.

The work by Muller and colleagues has also changed our view of the overall architecture of the complex. It was shown that, as in the Elp4-6 subcomplex, each Elp1-3 subunit can associate with itself, suggesting at least two copies are present in the holocomplex. Further to this the Elongator complex purified by gel filtration was estimated to be ~850 kDa. Elongator is therefore likely to be made up of two copies of each of its six subunits, forming a dodecamer. It is now proposed that two Elp1-3 heterotrimers are bridged by the Elp4-6 hexameric ring (Figure 1.3, Glatt et al., 2012, Glatt and Muller, 2013).

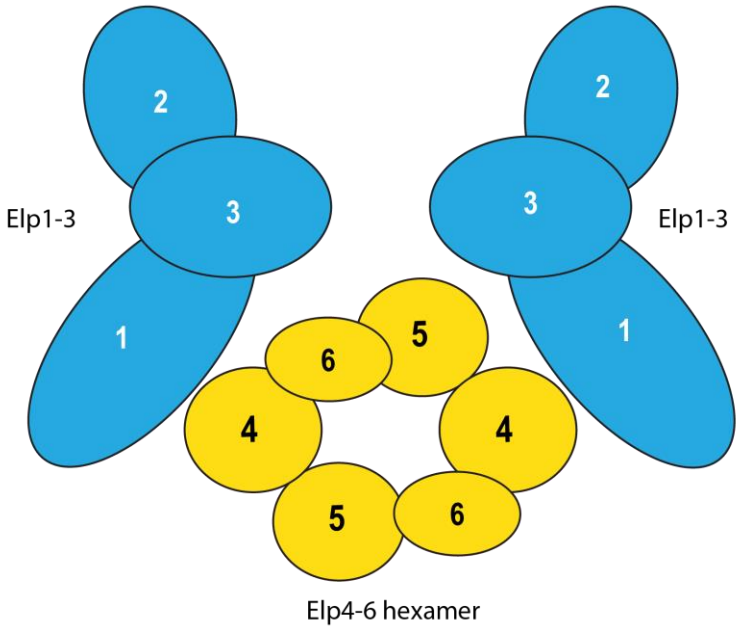

Figure 1.3: Proposed dodecamer assembly of the Elongator complex. In this model, proposed by Glatt et al (2012), Elongator is made up of two copies of each of its six subunits. The Elp4-6 hexamer bridges two Elp1-3 complexes. The schematic shown here is not representative of the exact contacts between all subunits.

v) Kti12

Kti12 is an accessory factor that binds to the preassembled Elongator complex, since the interaction is lost when complex assembly is disrupted (Fichtner et al., 2002a). Therefore it is likely that Kti12 binds across interfaces created by assembled subunits and the C-terminus of Elp2 is required for this (Fichtner et al., 2002b).

The role of Kti12 is unknown but like the Elongator subunits, Kti12 has homologues in other eukaryotes, including humans (Fichtner et al., 2002a). It has a highly conserved P-loop containing NTPase domain (Figure 1.1, Fichtner et al., 2002a, Petrakis et al., 2005) and is closely related to *O*-phosphoseryl-tRNA^{Sec} kinase (PSTK), an enzyme involved in selenocysteine-tRNA biosynthesis (Sherrer et al., 2008, Araiso et al., 2009). Deletion or multicopy expression of *KTI12* phenocopies loss of Elongator function, suggesting that the correct balance of Kti12 is essential in this regard (Butler et al., 1994). The P-loop motif is also functionally important, since truncation of this region

alone causes these dysfunctional phenotypes (Fichtner et al., 2002a). It is likely that Kti12 regulates Elongator complex function or participates directly in its poorly understood enzymatic mechanism.

1.2 Phenotypes associated with Elongator dysfunction

A mutation in the human homologue of the *ELP1* gene, IKBKAP, causes Familial Dysautonomia, a severe recessive neurodevelopmental disease (Anderson et al., 2001, Slaugenhaupt et al., 2001). Familial Dysautonomia is characterised by autonomic and sensory nervous system defects caused by the improper development and progressive loss of neurons. The symptoms of the disorder include dysphagia, gastric dysmotility, postural hypotension, loss of overflow tears as well as reduced sensitivity to pain and temperature. The disorder is fatal in adulthood due to the progressive loss of autonomic nervous system functions (Gold-von Simson and Axelrod, 2006).

Familial Dysautonomia (FD) has a high carrier frequency in the Ashkenazi Jewish population and within this faction the disease occurs every 1 in 3,600 births (Slaugenhaupt et al., 2001). The most common causative IKBKAP mutation is a single (T to C) base change in intron 20 of the gene. This causes a splicing defect that results in exon 20 skipping in the RNA transcript and production of a truncated protein (Anderson et al., 2001, Slaugenhaupt et al., 2001). This splicing defect is tissue specific as both the wild-type and mutant transcripts can be detected in patients at varying ratios in different cell types. The mutant transcript is most prominent in brain tissues where IKBKAP is normally highly expressed and loss of the wild-type protein causes the severe neurological defects of the disease (Slaugenhaupt et al., 2001).

The human homologues of *ELP3* and *ELP4* genes have also been linked to the neurological disorders Amyotrophic Lateral Sclerosis and Rolandic Epliepsy, respectively (Simpson et al., 2009, Strug et al., 2009). In human derived cell lines, Elongator dysfunction results in cell migration defects that may contribute to defects in neurodevelopment (Close et al., 2006, Johansen et al., 2008, Lee et al., 2009, Close et al., 2012b). Taken together there is a clear requirement for functional Elongator in the proper development and function of human neurons.

In mice deletion of *ELP1* is embryonic lethal, suggesting that Elongator function is also required during embryogenesis. The defects resulting in lethality are rescued by expression of the human IKBKAP transgene, which demonstrates the functional conservation of the Elongator complex (Chen et al., 2009b). Elongator is also required for meiotic progression and fertility in mice (Lin et al., 2013) and therefore plays a fundamental role in mammalian development. There are no human mutations yet identified corresponding to complete deletion of any Elongator subunits, this is in agreement with evidence that the complex plays an essential role during development.

In other higher eukaryotes, loss of Elongator function is also associated with a range of developmental and growth defects. Deletion of the *ELP3* homolog in *Drosophilia* leads to larval lethality (Walker et al., 2011) and targeted depletion of Elp3 results in neurological defects, such as a hyperactive phenotype and sleep loss (Singh et al., 2010). The *Drosophilia ELP3* gene was also identified in a screen for genes required for neuronal communication and survival (Simpson et al., 2009). In *C. elegans* mutations in either *ELP1* or *ELP3* homologs causes salt avoidance learning defects, slow growth and reduced fertility (Chen et al., 2009a). Mutation of Elongator subunits in *Arabadopsis* is associated with defective leaf and root growth and development as well

as altered responses to environmental stresses (Nelissen et al., 2005, DeFraia and Mou, 2011). The Elongator complex is therefore essential for normal development and growth in a range of higher eukaryotes.

In yeast, Elongator subunits are non-essential but deletion of any of the Elongator genes results in common pleiotropic phenotypes. Combined subunit gene deletions do not alter these phenotypes illustrating that each subunit is required independently for formation of a fully functional complex (Fellows et al., 2000). Deletion of Elongator genes causes slow growth adaptations, temperature sensitivity and sensitivity to various chemicals such as hydroxyurea, caffiene and rapamycin (Otero et al., 1999, Li et al., 2009, Frohloff et al., 2001, Schaffrath., personal communication). Mutations in Elongator subunits also result in resistance to the *Kluyveromyces lactis (K. lactis)* derived toxin, Zymocin (Frohloff et al., 2001, see section 1.5). Interestingly, complementation studies have demonstrated that expression of human Elp3 can partially rescue the equivalent yeast deletion phenotypes (Li et al., 2005), suggesting that the structure and function of Elongator is highly conserved across all eukaryotes.

1.3 The many proposed functions of the Elongator complex

A role in gene transcription was originally proposed for the Elongator complex, since it was first purified from yeast chromatin, associated with the elongating form of RNA polymerase II. Since the Elp3 subunit contained a conserved HAT domain, it was suggested that the complex facilitated transcription by the acetylation of histones ahead of the elongating RNA polymerase (Otero et al., 1999, Wittschieben et al., 1999). This was supported by the observed "slow start" phenotypes in Elongator mutants, which were characterised by delayed induction of genes required for new growth conditions. For example, deletion of *ELP1* caused a slow growth phenotype upon switching cells from glucose to galactose and this was shown to be due to a delayed accumulation of galactose induced transcripts (Otero et al., 1999). In fact subsets of mRNAs were differentially expressed in Elongator mutants when analysed by microarray (Krogan and Greenblatt, 2001).

Deletions of Elongator subunits displayed synthetic growth defects with a number of RNA polymerase II regulatory subunit gene deletions as well as Gcn5, a HAT involved in transcriptional co-activation as part of the SAGA complex (Jona et al., 2001, Van Mullem et al., 2002, Kong et al., 2005, Wittschieben et al., 2000). Deletion of histone tails or point mutations in histone acetylation sites were also synthetically lethal with Elongator gene deletions, suggesting these could be a substrate for the complex (Wittschieben et al., 2000). Further to this, the complex was able to acetylate histones *in vitro* and in Elongator mutants levels of *in vivo* acetylated histone H3 were reduced (Winkler et al., 2002).

A role for Elongator in transcription was also proposed in higher eukaryotes. *Arabidopsis,* mice and human cells lacking Elongator function have lower levels of

acetylated histone H3 and display differential gene expression (Nishimura et al., 2009, Close et al., 2006, Chen et al., 2009b). The patterns of gene expression were argued to correlate with phenotypes. In *Arabadopsis,* genes involved in auxin dependent responses were misregulated; this is an essential signalling pathway during growth and development (Nelissen et al., 2010). Several genes required for cell migration in FD patient fibroblasts (Close et al., 2006) and for embryo development in mice (Chen et al., 2009b) were also shown to be down-regulated. In *Drosophila,* deletion of *ELP3* is also associated with differential gene expression and the phenotypes and transcription profile were suggested to be similar to deletion of *Domino*, a SWI/SNF like chromatin remodelling enzyme (Walker et al., 2011).

A direct role in transcription was argued since depletion of Elongator from human cell extracts resulted in an Acetyl-CoA dependent reduction in RNA polymerase II transcription *in vitro,* which was rescued by addition of purified Elongator (Kim et al., 2002). Elongator was also shown to be associated with chromatin in higher eukaryotes, suggesting that it directly affects gene expression (Metivier et al., 2003, Close et al., 2006, Nelissen et al., 2010).

Taken together, it was therefore initially proposed that the pleiotropic phenotypes caused by Elongator dysfunction resulted from misregulation of transcription and that the complex was directly involved in this process. However, the function of Elongator in transcription has been questioned for a number of reasons. A global role for the complex in transcript elongation is not in line with the finding that only certain genes were affected in Elongator mutants (Krogan and Greenblatt, 2001). Elongator subunits also could not be detected associated with Chromatin or any RNA polymerase II elongation factors in yeast (Pokholok et al., 2002, Close et al., 2012a). Further, deletion

of the *ELP2* subunit still supported the assembly and *in vitro* HAT activity of the complex but displayed identical phenotypes *in vivo* to other subunit deletions (Petrakis et al., 2004). Although in higher eukaryotes Elongator was shown to interact with chromatin, association was at both target and non-target genes (Kouskouti and Talianidis, 2005, Close et al., 2006) and Elongator's HAT activity was also found to be less efficient against nucleosomes compared with purified histones (Winkler et al., 2002, Kim et al., 2002). Purified yeast and human Elongator also failed to stimulate RNA pol II transcription *in vitro*, unlike other known elongation factors (Kim et al., 2002, Krogan et al., 2002). Therefore despite a large amount of data implicating Elongator in transcription, it remained difficult to pinpoint the exact role of the complex in this process.

An alternative hypothesis for Elongator function was in the regulation of histone coupled chromatin assembly. This was initially suggested since yeast Elongator deletion strains show genetic interactions with several histone chaperone gene deletions, display telomeric silencing defects and are sensitive to DNA damaging agents (Li et al., 2009). An interaction between Elongator and the DNA clamp protein PCNA was also demonstrated in yeast and plants (Li et al., 2009, Xu et al., 2012). Based on these data it was proposed that Elongator may function to acetylate histones to aid assembly into chromatin during DNA replication and DNA damage.

Surprisingly, despite these proposed roles, Elongator was found to be mainly localised to the cytoplasm of cells (Pokholok et al., 2002), which does not support a central role in transcription or other nuclear processes. Given the cytoplasmic localisation of Elongator a number of other functions were proposed for the complex.

The Elongator complex was implicated in the regulation of exocytosis. Deletion of yeast *ELP1* supresses the defect caused by a mutation in the *SEC2* gene (*sec2-59*), encoding a guanine nucleotide exchange factor involved in the regulation of vesicle docking and secretion. Exocytosis is blocked in *sec2-59* mutants, which have a premature stop codon in the coding region of the gene, resulting in truncation and mislocalisation of Sec2. Deletion of *ELP1* rescued the secretion defect of *sec2-59* strains and Elp1 could also be crosslinked to wild-type Sec2 in cell extracts. It was therefore argued that the major role of Elongator was to negatively regulate Sec2 dependent exocytosis (Rahl et al., 2005).

There has also been some evidence that Elongator may be directly involved in cytoplasmic protein acetylation. In *C. elegans* and mice, mutation of *ELP1* and *ELP3* subunits was reported to decrease endogenous α-tubulin acetylation and these subunits could be co-purified from microtubules (Solinger et al., 2010, Creppe et al., 2009). Elongator gene deletions displayed genetic interactions with gene deletions of various α-tubulin regulators and Elp3 could also acetylate α-tubulin *in vitro* (Gardiner et al., 2007, Creppe et al., 2009). However, the levels of acetylated α-tubulin in *C. elegans* and various other organisms, including FD patient fibroblasts, have since been reported to be normal when Elongator is deleted and this brings these data in question (Chen et al., 2009a, Simpson et al., 2009, Cheishvili et al., 2011, Miskiewicz et al., 2011). A major α-tubulin acetylase, MEC-17, has also since been described and is present across multiple organisms (Akella et al., 2010). In *Drosophila,* Elp3 was also implicated in the acetylation of Bruchpilot, a protein involved in synaptic morphology and function. The levels of acetylated Bruchpilot were also reduced in Elongator mutants and a weak acetylation of the protein by Elp3 was shown *in vitro* (Miskiewicz et al., 2011). It should be noted that acetylation of α-tubulin and Bruchpilot by Elp3

was demonstrated *in vitro* alongside Histone H3, which appeared to be acetylated more efficiently in both cases. This makes it difficult to argue whether either of these substrates is physiologically relevant.

The substrate specificity and function of the Elongator complex has historically been controversial and this has shaped the idea that Elongator may have multiple roles in the cell (Versees et al., 2010). However, a convincing alternative to the functions of Elongator proposed above is a central role in the modification of wobble uridine containing transfer RNAs (tRNAs) that has emerged as a conserved function of Elongator. This role may underlie all of the seemingly unrelated functions of Elongator and will be discussed in the following sections.

1.4 Transfer RNA function and modification

The amino acid sequence of a protein is coded within its corresponding gene by a universal genetic code consisting of 61 triplet nucleotide codons that are transcribed into messenger RNA (mRNA). Codons are interpreted during the process of translation in cytoplasmic ribosomes such that the corresponding amino acids are incorporated into a growing polypeptide chain. This is how the transcribed genes act as a blueprint for the synthesis of functional proteins and the process must be both rapid and accurate to meet the cell's demands (Alberts, 2008, Berg et al., 2007).

Transfer RNAs (tRNAs) act as adaptor molecules in the process of translation, since they read the genetic code and couple this to the incorporation of an amino acid at the ribosome. These small molecules are made up of ~73-93 RNA bases and all share a similar 'cloverleaf' secondary structure made up of base paired stem regions and

loops. Further structure is governed by hydrogen bonding between these various structural regions to form an upside down 'L shape' made up of several helices and loops (Figure 1.4). The 3' end of each tRNA protrudes out of this structure and contains a single stranded three nucleotide CCA sequence with a free 3'-hydroxyl group for the attachment of a particular amino acid. The attachment of amino acids to tRNA is carried out by aminoacyl-tRNA synthetases, which bind substrate tRNAs and amino acids and catalyse the formation of an aminoacyl-tRNA, or a 'charged' tRNA. Another important functional feature of tRNA is a loop that resides at the bottom of the structure, termed the anticodon loop. This contains a three nucleotide sequence, bases 34-36 in the universal structure, which 'decodes' or complements a particular codon of the genetic code (Figure 1.4A). The accurate charging of tRNAs with amino acids and codon recognition by tRNAs at the ribosome are both essential for maintenance of the universal genetic code (Berg et al., 2007).

Eukaryotic ribosomes are made up of a small (40S) and large (60S) subunits consisting of proteins and ribosomal RNAs (rRNAs) that associate to form the active translation machinery (80S). The 40S subunit contains an 18S rRNA and is the site at which decoding occurs, it binds the mRNA molecule and interacts with the anticodon loop portion of the tRNA. The 60S subunit contains 28S, 5.8S and 5S rRNAs and interacts with the amino acid charged portion of tRNA. This subunit contains the catalytic centre for peptide bond formation between a growing polypeptide and a bound aminoacyl-tRNA (Berg et al., 2007, Alberts, 2008).

The process of mRNA translation proceeds by formation of an initiation complex, assembly of the 80S ribosome, elongation of the growing polypeptide chain and finally

termination and release of the synthesised protein. A brief overview of Elongation will be described, for review of general translation please refer to Steitz (2008).

The assembled ribosome contains three sites for the binding of tRNA molecules, the Aminoacyl site (A-site), the Peptidyl site (P-site) and the Exit site (E-site). The A-site positions the mRNA codon for recognition and accepts tRNA as an active ternary complex associated with GTP-bound Elongator factor 1 (EF1). The correct anticodon-codon contacts form a small mini-helix, which is proofread by hydrogen bonding with the 18S rRNA in the 40S subunit. This converts the small subunit to a closed conformation causing GTP hydrolysis and release of EF1 and places the aminoacyl region of the tRNA into the catalytic centre of the ribosome. Peptide bond formation is catalysed by the 28S rRNA (a ribozyme) and the growing polypeptide chain is transferred to the A site bound tRNA. Binding of GTP-bound Elongator factor 2 (EF2) to the ribosome and coupled GTP hydrolysis causes movement of the A-site bound tRNA into the P-site, moving the mRNA along with it. This displaces the previous P-site tRNA into the E-site for exit from the ribosome and positions the next codon in the mRNA at the empty A-site (Figure 1.5). These cycles are repeated until termination is signalled by a stop codon in the mRNA, which rather than specifying a tRNA leads instead to the binding of release factors that free the completed polypeptide and break apart the assembled ribosome (Berg et al., 2007, Alberts, 2008, Steitz, 2008). The process of polypeptide elongation at the ribosome proceeds rapidly and with high fidelity (Cochella et al., 2007).

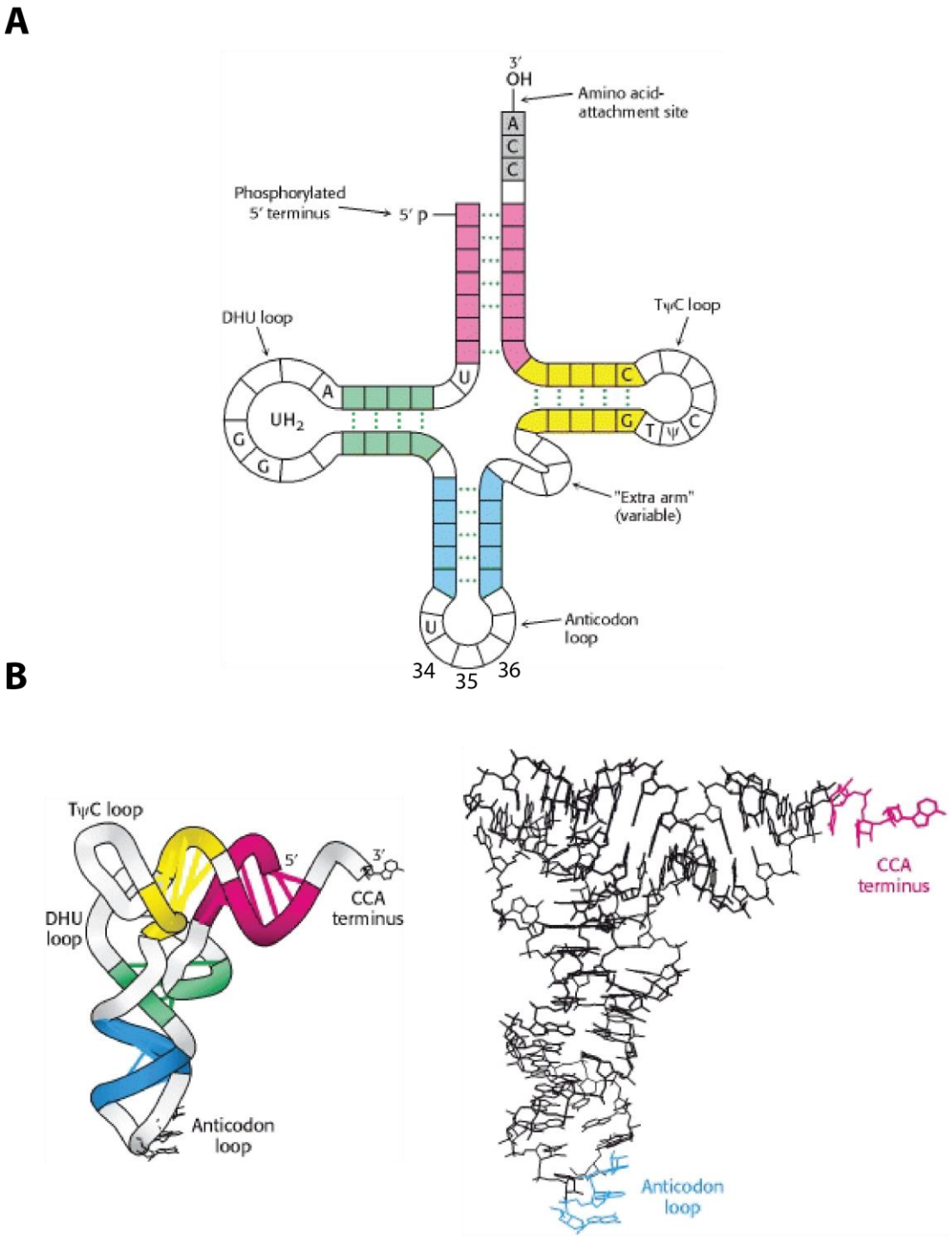

Figure 1.4: Universal structural features of tRNA molecules. A) Schematic of general tRNA secondary structure illustrating conserved features, stems and loops. B) Views of higher order tRNA structure. Schematic of L shaped folded tRNA with stacked helices and loop regions (left) and skeletal model showing bases in yeast $tRNA^{Phe}$ (right). Images are adapted from Berg et al (2007).

A

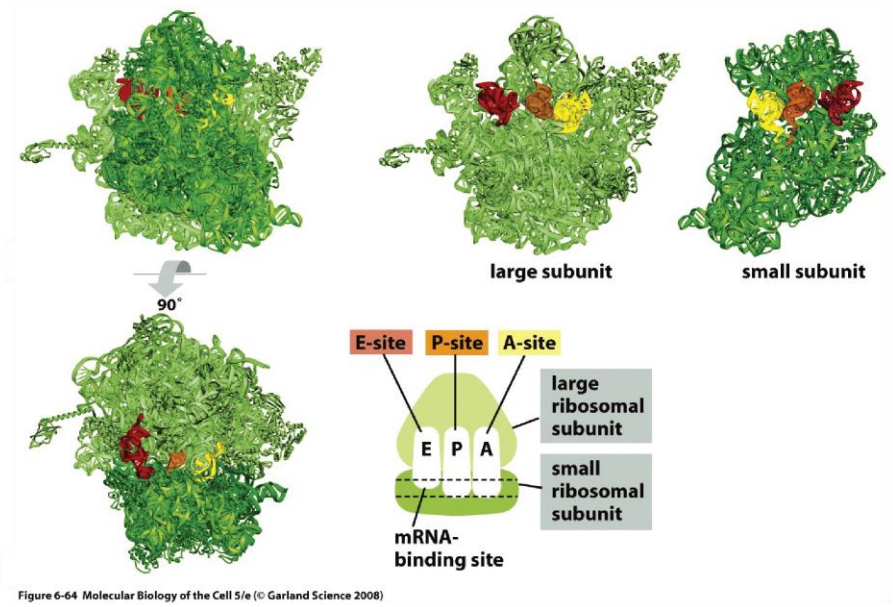

B

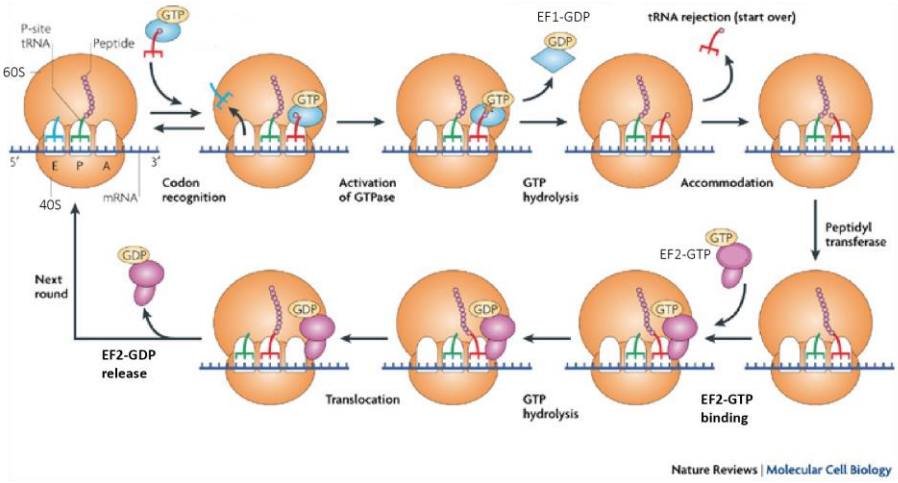

Figure 1.5: Translation elongation at the ribosome. A) Structure of the bacterial ribosome with bound tRNAs to illustrate conserved overall architecture and schematic of tRNA binding sites, A-site, P-site and E-site. Image taken from Alberts (2008). B) Schematic overview of the Elongation steps of translation at the eukaryotic ribosome adapted from Steitz (2008).

In all organisms the genetic code is degenerate such that most amino acids can be specified by more than one codon during translation. In fact of the 20 amino acids only methionine and tryptophan are specified by a single triplet codon. However, not all of the 61 codons have an exact match to the anticodon of the tRNA molecule that decodes them and cells have a lot less than 61 specific tRNA species. This means that many tRNAs recognise more than one codon and this is due to 'wobble' at the first base of the anticodon (third base in the codon) that allows relaxation of the usual rules of base pairing (Crick, 1966). Interactions between the first and second bases of a codon have to be strictly complemented by Watson-Crick base pairing with the tRNA anticodon, this is monitored by the conserved hydrogen bonding contacts with the 18S rRNA in the A-site of Ribosome, mentioned above. The third base of a codon is less restrictive so that non-cognate base pairing can occur with the first base of the anticodon (Ogle et al., 2001, Selmer et al., 2006). This nucleotide (position 34 in the universal structure) is therefore termed the 'wobble' position. An overview of the decoding capacity of tRNAs across the genetic code in yeast is summarised in Figure 1.6.

codon	anticodon	amino acid	codon	anticodon	amino acid	codon	anticodon	amino acid	codon	anticodon	amino acid
UUU	-	Phe	UCU	IGA	Ser	UAU	-	Tyr	UGU	-	Cys
UUC	GmAA		UCC	-		UAC	GΨA		UGC	GCA	
UUA	**ncm^{5}UmAA**	Leu	UCA	**ncm^{5}UGA**		UAA	-	n.a.	UGA	-	n.a.
UUG	m^{5}CAA		UCG	CGA		UAG	-		UGG	CmCA	Trp
CUU	-	Leu	CCU	AGG	Pro	CAU	-	His	CGU	ICG	Arg
CUC	GAG		CCC	-		CAC	GUG		CGC	-	
CUA	UAG		CCA	**ncm^{5}UGG**		CAA	**mcm^{5}s^{2}UUG**	Gln	CGA	-	
CUG	-		CCG	-		CAG	CUG		CGG	CCG	
AUU	IAU	Ile	ACU	IGU	Thr	AAU	-	Asn	AGU		Ser
AUC	-		ACC	-		AAC	GUU		AGC	GCU	
AUA	ΨAΨ		ACA	**ncm^{5}UGU**		AAA	**mcm^{5}s^{2}UUU**	Lys	AGA	**mcm^{5}UCU**	Arg
AUG	CAU	Met	ACG	CGU		AAG	CUU		AGG	CCU	
GUU	IAC	Val	GCU	IGC	Ala	GAU	-	Asp	GGU	-	Gly
GUC	-		GCC	-		GAC	GUC		GGC	GCC	
GUA	**ncm^{5}UAC**		GCA	**ncm^{5}UGC**		GAA	**mcm^{5}s^{2}UUC**	Glu	GGA	**mcm^{5}UCC**	
GUG	CAC		GCG	-		GAG	CUC		GGG	CCC	

Figure 1.6: The genetic code and distribution of tRNA molecules in yeast. Modifications on particular tRNA species are also shown. A= Adenosine, U= Uridine, G= Guanosine, C= Cytosine, I= Inosine, Gm= 2'-O-methylguanosine, ncm^{5}U= 5-carbamoylmethyluridine, mcm^{5}U= 5-methoxycarbonylmethyl, mcm^{5}s^{2}U= 5-methoxycarbonylmethyl-2-thio-uridine, Ψ= Pseudouridine. Taken from Johansson et al (2008)

Although tRNA molecules must conform to a rigid global structure in order to bind efficiently to the A-site of the ribosome they each have particular identities. These are imparted not only by their nucleotide sequences but also by extensive nucleoside modifications that occur in both the loop and stem regions of the tRNA (Figure 1.7). These modifications can affect the folding, stability, charging and decoding properties of a tRNA species and are conserved in all kingdoms of life (Björk, 1995).

Modifications in the anticodon loop affect the translational properties of a given tRNA species, contribute to reading frame maintenance, efficient codon recognition at the A-site and restrict misreading (Agris et al., 2007, Agris, 2008). The wobble position 34 and position 37 of the tRNA anticodon loop are the most commonly and extensively modified bases. These modifications appear to be especially important in structuring anticodon loops that are enriched in pyrimidines (U and C) and the wobble uridine in eukaryotic tRNA is almost never unmodified. Modification of wobble uridine imparts extra stability and improves base stacking contacts, while modification of the conserved purine 37 position is important for maintaining the width of the loop (Agris, 2008, Agris et al., 2007). Modifications play a key role in the function of tRNAs and so are essential to the accurate and efficient translation of the genetic code.

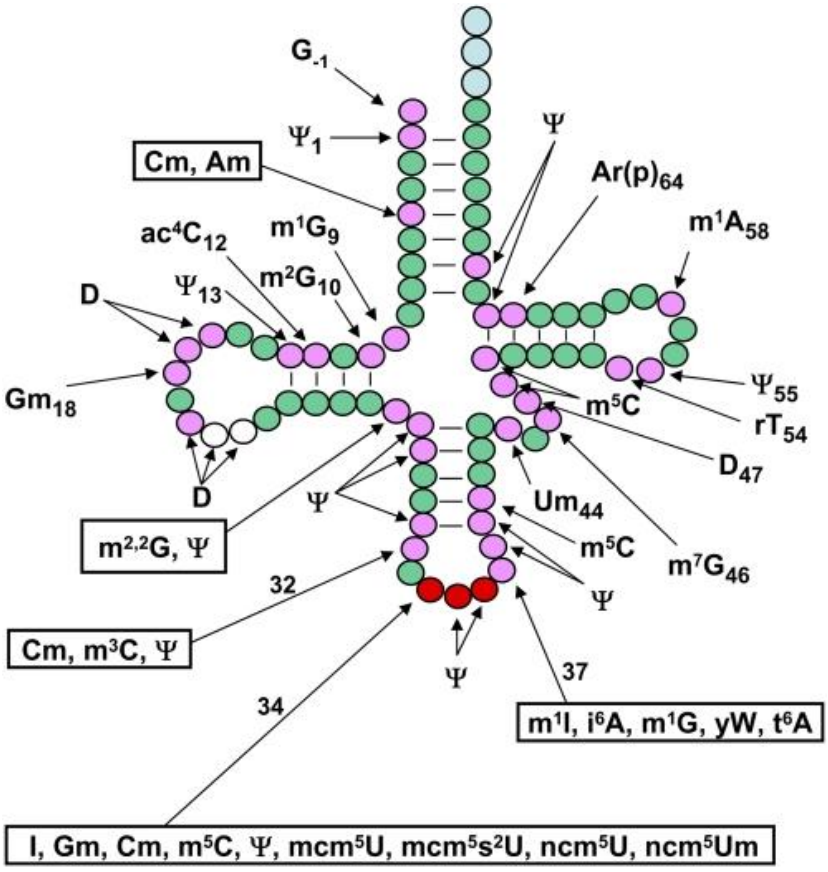

Figure 1.7: Schematic overview of tRNA modifications in yeast. Green circle=Unmodified base, Pink circle=Modified base in some or all tRNAs, Red circle=Anticodon base, Blue circle=Amino acid acceptor stem base. Modifications are as follows; Ψ=Pseudouridine, m^1G= 1-methylguanosine, m^2G= 2-methylguanosine, ac^4C= 4acetylcytidine, D= dihydrouridine, Gm= 2'-O-methylguanosine, $m^{2,2}G$= N2,N2-dimethylguanosine, m^3C= 3-methylcytidine, I= Inosine, m^5C= 5-methylcytidine, mcm^5U= 5-methoxycarbonylmethyl, mcm^5s^2U= 5-methoxycarbonylmethyl-2-thiouridine, ncm^5U= 5-carbamoylmethyluridine, ncm^5Um= 5-carbamoylmethyl-2'-O-methyuridine, m^1I= 1-methylinosine, i^6A= N6-isopentenyladenosine, yW= wybutosine, t^6A= N6-threonylcarbamoyladenosine, Um= 2'-O-methyluridine, m^7G= 7-methylguanosine, rT= Ribothymidine, Ar(p)= 2'-O-ribosyladenosine(phosphate). Taken from Phizicky and Hopper (2010a)

1.5 Elongator's role in Zymocin resistance and tRNA wobble uridine modification

In order to gain a growth advantage the dairy yeast *Kluyveromyces lactis* has gained 'Killer' capabilities that allow it to inhibit the growth of other yeasts. This is mediated by secretion of a toxin, Zymocin, which is taken up by budding yeast and consequently induces a G1 cell cycle arrest (Butler et al., 1991c). Zymocin is a trimeric toxin, made up of α, β and γ subunits that are encoded by a linear plasmid system. Zymocin's killer activity resides in the γ subunit whereas the α and β subunits mediate entry into the cell (Tokunaga et al., 1989, Butler et al., 1991b). Zymocin likely docks onto cell wall chitin using the α subunit, which has exochitinase activity, and the hydrophobic β subunit may then mediate interactions with the exposed membrane for insertion of the γ subunit (Butler et al., 1991a, Jablonowski et al., 2001b, Zink et al., 2005).

A number of mutations in budding yeast have been identified that confer resistance to Zymocin and these can be separated into two classes (Table 1.1, Butler et al., 1991b). Mutants that are defective in proteins involved in binding and uptake of Zymocin are resistant to extracellular Zymocin but sensitive to expression of the intracellular expression of the γ subunit. These 'Class I' mutants include strains with mutations in genes of the chitin synthesis pathway, such as chitin synthase. The 'Class II' mutants are resistant to both extracellular Zymocin and intracellular γ subunit expression and encode proteins involved in regulating the intracellular target of the toxin. Among the Class II mutants were deletions of genes encoding the Elongator complex, which implicated the complex in the cellular response to the toxin (Frohloff et al., 2001).

Gene	Protein Description	Role in Zymocin Toxicity
	Class I	
CHS3	Chitin synthase III	Docking
CHS4	Activator of Chitin Synthase III	Docking
CHS5	Chitin targetting protein	Docking
CHS6	Regulation of Chitin synthesis	Docking
CHS7	Regulation of Chitin synthesis	Docking
*ISR1**	Putative Kinase	Docking
*UGP1**	UDP-glucose pyrophosphorylase	Docking
*GRX3**	Glutaredoxin	Not known, activation?
IPT1	Inositolphosphotransferase	Import
PMA1	H^+-ATPase	Not known, activation?
PTK2	Activator of Pma1	Not known, activation?
	Class II	
ELP1	Elongator subunit	Target tRNA modification
ELP2	Elongator subunit	Target tRNA modification
ELP3	Elongator subunit	Target tRNA modification
ELP4	Elongator subunit	Target tRNA modification
ELP5	Elongator subunit	Target tRNA modification
ELP6	Elongator subunit	Target tRNA modification
KTI11	Elongator accessory factor	Target tRNA modification
KTI12	Elongator accessory factor	Target tRNA modification
KTI13	Elongator accessory factor	Target tRNA modification
HRR25	Caesin Kinase 1	Target tRNA modification
SIT4	Sit4 phosphatase	Target tRNA modification
SAP185/SAP190	Sit4 binding partners	Target tRNA modification
TRM9	tRNA methyltransferase	Target tRNA modification
TRM112	Trm9 accessory factor	Target tRNA modification
NCS2	Sulphur relay factor	Target tRNA modification
TUC1	Sulphur relay factor	Target tRNA modification
URM1	Sulphur carrier	Target tRNA modification
UBA4	Urm1 activator	Target tRNA modification
TUM1	Sulphur transferase	Target tRNA modification
	Class II Multicopy suppressors	
$tRNA^{Glu}_{(UUC)}$	-	Toxin target
$tRNA^{Lys}_{(UUU)}/tRNA^{Gln}_{(UUG)}$	-	Toxin target
KTI12	Elongator accessory factor	Target tRNA modification

Table 1.1. Summary of Zymocin resistant mutants in yeast. Class I genes when deleted confer resistance to the extracellular Zymocin. Class II genes when deleted confer resistance to both extracellular and intracellular toxin. Multicopy suppressors cause Zymocin resistance when expressed in multicopy. Genes separated with ' /' denote that only the double mutant causes Zymocin resistance. The '*' denotes multicopy Class I suppressors. This table summaries data from Butler et al.,(1994) Huang et al., (2008) Jablonowski et al., (2001a, 2001b, 2006), Dephoure et al., (2005), Mehlgarten et al., (2007), Zink et al., (2005), Mehlgarten and Schaffrath, (2003, 2004), Frohloff et al.,(2001) Fichtner and Schaffrath (2002), Fichtner et al., (2003).

Interestingly, it was also shown that the tRNA gene encoding $tRNA^{Glu}_{UUC}$ is a multicopy suppressor of Zymocin action and this led on to the discovery that transfer RNAs are the intracellular target of the toxin (Butler et al., 1994, Lu et al., 2005). The γ subunit of Zymocin is a tRNA anticodon nuclease that cleaves $tRNA^{Glu}_{UUC}$ (and to a lesser extent $tRNA^{Lys}_{UUU}$ and $tRNA^{Gln}_{UUG}$) containing a 5-methoxycarbonymethyl-2-thio-uridine (mcm^5s^2U) at the anticodon wobble position (Lu et al., 2005). The mcm^5s^2U modification is essential for substrate recognition, targetting $tRNA^{Glu}_{UUC}$ for cleavage at the 3' side of the wobble position (Figure 1.8). Depletion of substrate tRNA by Zymocin is thought to cause defects in translation resulting in G1 cell cycle arrest of sensitive yeasts (Figure 1.8, Lu et al., 2005).

The resistance of Elongator mutants to Zymocin was shown to be due to lack of the mcm^5 moiety at the wobble uridine position in substrate tRNA, which protects them from recognition and cleavage by the toxin. This uncovered a novel function of the complex: Elongator is required for an early step in synthesis of 5-methyoxycarbonylmethyl (mcm^5) and 5-carbamoylmethyl (ncm^5) modifications on wobble uridine containing tRNAs (Huang et al., 2005). In yeast, out of a total of 42 tRNAs, 11 require Elongator dependent modifications (Figure 1.9A) and these are required for efficient decoding at the wobble position during translation (Percudani et al., 1997, Huang et al., 2005, Lim, 1994).

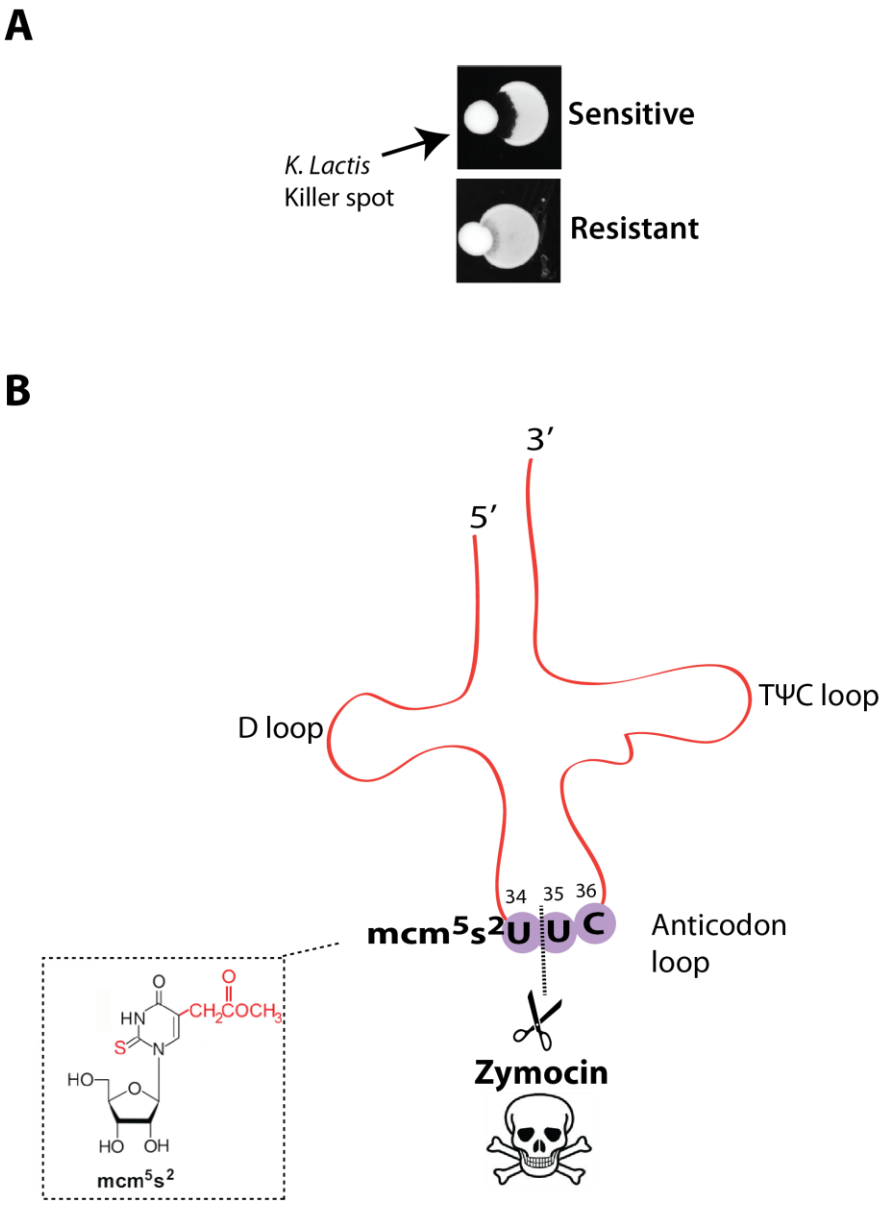

Figure 1.8: Zymocin mechanism of action. A) Zymocin inhibits the growth of sensitive yeast strains. Sensitivity is assayed by innoculating the edge of the strain of interest with *K. lactis*. This is called an 'Eclipse' assay as Zymocin sensitive yeast show a halo of growth inhibition around the *K. lactis* colony. B) Zymocin is a tRNA anticodon nuclease that cleaves at the 3' side of a mcm^5s^2U at the wobble position. To illustrate the Zymocin mechanism of action $tRNA^{Glu}(mcm^5s^2UUC)$ is shown.

It is not yet known if Elongator acts directly in the catalysis of the cm^5 step of these tRNA modifications but the Radical SAM and HAT domains of Elp3 are essential to this function (Huang et al., 2005, Chen et al., 2011b). The combination of these two functional domains in Elp3 is highly conserved and Radical SAM domain containing enzymes have already been implicated in a number of RNA modification reactions (Agarwalla et al., 2002, Pierrel et al., 2004, Anton et al., 2008, Yan et al., 2010, Grove et al., 2011). Labelling experiments have shown that carbon atoms from acetyl-CoA are not immediate donors for synthesis of the mcm^5 and ncm^5 modifications and the actual donor remains unknown (Tumaitis and Lane, 1970). It is tempting to speculate that the HAT and Radical SAM domains may work cooperatively for synthesis of precursors and attachment of these tRNA modifications. In line with this, immunoprecipitated Elp1 and Elp3 subunits could be specifically crosslinked to exogenous substrate tRNAs and the Elp4-6 subcomplex has been shown to bind tRNAs *in vitro* (Huang et al., 2005, Glatt et al., 2012).

Other class II Zymocin resistant genes have also been shown to be required for target tRNA modifications; these include proteins involved in the thiolation and final methylation steps of the mcm^5s^2U modification and putative Elongator accessory factors (Table 1.1 and Figure 1.9B).

In a screen for Zymocin resistant mutants, a number of factors were discovered whose substrate tRNAs were subsequently shown to lack their 2-thio moiety, which is also required for toxin recognition (Huang et al., 2008, Fichtner et al., 2003). The Ubiquitin like modifier Urm1 and its activating enzyme Uba4, are required for 2-thio incorporation along with Tuc1, Ncs2 and Tum1. The pathway for this modification proceeds by a sulphur relay system (Noma et al., 2009, Leidel et al., 2009).

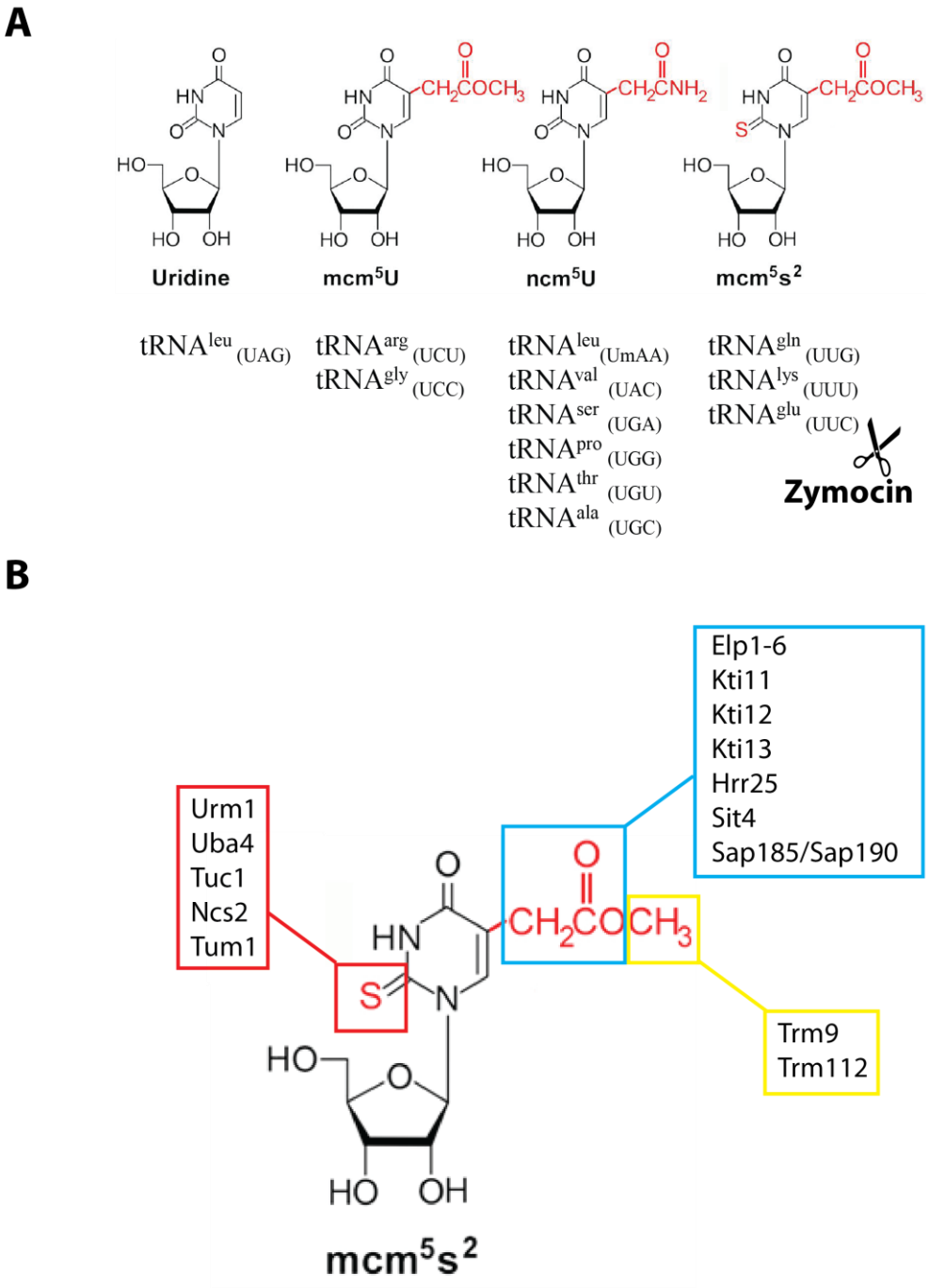

Figure 1.9: Elongator is required for tRNA wobble uridine modifications. A) Summary of yeast tRNAs with a modified uridine at the wobble position of the anticodon. ncm^5U= 5-carbamoylmethyluridine, mcm^5U= 5-methoxycarbonylmethyl, mcm^5s^2U= 5-methoxycarbonylmethyl-2-thio-uridine. B) Proteins required for the synthesis of the different moieties (boxed) of mcm^5s^2U. Elongator is thought to be required for cm^5 incorporation.

Urm1 has been implicated in the urmylation of proteins but is also related to bacterial sulphur carriers (Goehring et al., 2003, Zhang et al., 2009). It acts as a sulphur carrier in the modification of tRNA alongside its binding partner, Uba4. A model has been proposed whereby thiolated Tum1 donates the sulphur moiety to Uba4, which adenylates and then thiolates Urm1 using two different functional domains. This thiocarboxylated group in Urm1 acts as a donor for the tRNA modification and sulphur is transferred onto uridine by an unknown mechanism that may involve Tuc1 and Ncs2 (Noma et al., 2009, Leidel et al., 2009). In yeast this thiolation pathway occurs independently of Elongator, since the normally undetectable intermediate s^2U modification is detected in Elongator deletion strains (Huang et al., 2005).

The final methylation step in the synthesis of mcm^5 modifications is catalysed by a SAM dependent tRNA methyltransferase, Trm9 alongside its accessory partner Trm112 (Kalhor and Clarke, 2003, Jablonowski et al., 2006, Studte et al., 2008). Apart from Zymocin resistance, deletion of *TRM9* does not result in other *elp* like phenotypes and so it acts downstream of the Elongator dependent step (Jablonowski et al., 2006). This also suggests that loss of the methyl group of mcm^5 may not have a particularly severe effect on tRNA function, though such effects have been suggested to become more severe under stress conditions (Kalhor and Clarke, 2003).

Mutations in the Killer insensitive genes *KTI11-KTI13* result in loss of mcm^5U and ncm^5U modification, suggesting that these act in the same pathway as the Elongator complex (Huang et al., 2008). Deletion of these genes also results in typical *elp* phenotypes and homologues of these factors are also found from yeast to man (Frohloff et al., 2001, Fichtner and Schaffrath, 2002).

KTI12 causes Zymocin resistance when deleted or expressed in multicopy and this suggests that wild-type levels are essential for Elongator dependent tRNA modification (Butler et al., 1994, Section 1.1 for Kti12 details). Deletion of *KTI12* completely abolishes Elongator dependent tRNA modification (Huang et al., 2008).

Kti11 is a small, highly acidic protein containing a zinc ribbon motif that is required for Elongator dependent tRNA modifications (Sun et al., 2005, Huang et al., 2008). Kti11 has also been identified as Dph3, a factor involved in the synthesis of the Diphthamide (2-[3-carboxyamido-3-(trimethylamino)-propyl]-histidine), a unique modification that occurs on Translation Elongation Factor 2 (eEF2) and is the target of Diphtheria toxin (Liu et al., 2004). The function of this modification is unknown but it may be required for the fidelity of translation and is conserved from yeast to man (Liu et al., 2012, Collier, 2001). Kti11 forms a trimeric complex with Dph1 and Dph2, other factors in the Diphthamide synthesis pathway, and is thought to be involved in an early step of synthesis (Liu et al., 2004). Consequently, deletion of *KTI11* causes concurrent Zymocin and Diphtheria toxin resistance due to lack of mcm^5U and Diphthamide modifications respectively (Fichtner and Schaffrath, 2002, Liu et al., 2006). It has been proposed that Kti11 is involved in multiple processes, since it interacts independently with the Elongator complex, the accessory factor Kti13, eEF2 and ribosomal proteins (Fichtner and Schaffrath, 2002, Liu et al., 2004). Truncation of the Kti11 C-terminus results in resistance to Zymocin but not Diphtheria toxin, demonstrating that its cellular roles can be uncoupled (Bar et al., 2008). Deletion of *KTI11* also causes an increase in the level of an N-terminally truncated form of Elp1 that may reflect a role for Kti11 in stability of this subunit (Fichtner et al., 2003).

Kti13 does not appear to interact with the Elongator complex directly but rather is associated through its tight interaction with Kti11 (Fichtner and Schaffrath, 2002). Unlike *KTI11* and *KTI12*, deletion of *KTI13* does not completely abolish Elongator dependent tRNA modifications but these are significantly reduced (Huang et al., 2008). This suggests that Kti13 may play a regulatory role in Elongator function; this is supported by the fact that it contains a guanine nucleotide exchange factor (GEF) like domain at its N-terminus. Like its binding partner Kti11, Kti13 may also play roles in other complexes. It was originally identified in a screen for suppressors of α-tubulin mutants and interacts with Nap1, a protein involved in microtubule dynamics (Kirkpatrick and Solomon, 1994, Kellogg and Murray, 1995).

Deletions of *KTI11* and *KTI13* display genetic interactions with Elongator gene deletions, suggesting they are not part of the same complex but rather are acting as regulatory factors that may have other independent functions. When *kti13* and *elp3* deletions are combined there is a more severe growth defect than either alone. Deletion of *KTI11* alone confers a severe growth defect that can be partially rescued by deletion of *ELP3* (Fichtner and Schaffrath, 2002). Combined deletion of both *KTI11* and *KTI13* is lethal and each single deletion can be partially rescued by overexpression of *KTI12*, suggesting functional interplay between these factors (Zabel et al., 2008, Butler et al., 1991b).

Interestingly, the casein kinase Hrr25 and Sit4 protein phosphatase are also class II mutants and are required for the Elongator dependent tRNA modifications (Mehlgarten and Schaffrath, 2003, Jablonowski et al., 2001a, Huang et al., 2008), this will be discussed in Section 1.8. Although not yet well understood there appear to be a number of factors that impinge on Elongator's role in tRNA wobble uridine

modification. The fact that so many genes have been shown to be required for these modifications demonstrates their likely functional importance.

1.6 The central function of the Elongator complex is in tRNA wobble uridine modification

It is now thought that the major role of the Elongator complex in yeast is to promote mcm^5 and ncm^5 tRNA wobble uridine modifications. This is because multicopy expression of two hypomodified tRNAs in yeast, which normally receive the mcm^5s^2 modification, is sufficient to rescue nearly all *elp* mutant phenotypes tested so far (Esberg et al., 2006, Chen et al., 2011b). This suppression is presumed to be due to elevated levels of the encoded tRNAs, which are increased two-fold, compensating for their reduced function due to lack of wobble uridine modification (Bjork et al., 2007). This is strong evidence that these mutant phenotypes could all be caused by a common translational defect.

Increased levels of both $tRNA^{Lys}_{UUU}$ and $tRNA^{Gln}_{UUG}$ suppresses the slow start phenotypes of *elp* mutants, including the underlying delay in gene activation and histone H3 hypoacetylation. Elevated levels of these tRNAs also reverses the synthetic defects associated with combining an *ELP3* deletion with deletions of *GCN5* or genes encoding other histone chaperones, as well as suppressing sensitivity to caffiene, hydroxyurea and high temperature. Overexpression of $tRNA^{Lys}_{UUU}$ and $tRNA^{Gln}_{UUG}$ also mimics the presence of functional Elongator in the *elp1Δ sec2-59* double mutant (Esberg et al., 2006). This argues against a direct role of Elongator in transcription,

chromatin assembly and exocytosis and suggests that these phenotypes occur due to a defect in the translation of proteins involved in these processes.

To further corroborate this, deletion of genes involved in the thiolation step of tRNA wobble uridine modifications were shown to confer identical phenotypes to Elongator deletions strains that were also rescued by overexpression of these specific tRNAs (Esberg et al., 2006, Chen et al., 2011b). Taken together, this illustrates that these pleiotropic phenotypes are likely to arise from the reduced function of these tRNAs. The fact that only these particular hypomodified tRNAs can rescue the defects suggests that the mcm^5s^2 modification must have the most important consequences for tRNA function.

The requirement of Elongator for tRNA wobble uridine modification is conserved in higher eukaryotes since it has been demonstrated in plants, worms and mice (Chen et al., 2009a, Mehlgarten et al., 2010, Lin et al., 2013). The accessory factors Kti11-13 also have homologs in higher eukaryotes including humans, suggesting a common mode of regulation. The phenotypes associated with Elongator dysfunction in these organisms have also been proposed to be caused by a translational defect. This has important implications for Familial Dysautonomia, as defects in translation may be central to the pathogenesis of the disease. A central role for Elongator in tRNA wobble uridine modification is also in agreement with the reported localisation of the complex, as these tRNA modifications normally occur in the cytoplasm (Hopper and Phizicky, 2003). In this work, any further references to Elongator function will therefore relate to its role in tRNA wobble uridine modification.

1.7 Elongator and translational defects

Modifications on the anticodon loop of tRNA frequently occur at the wobble position and are thought to structure the anticodon for efficient decoding at the ribosome (Agris et al., 2007, Agris, 2008). In eukaryotes tRNA wobble uridine can be modified to ncm^5U, mcm^5U and mcm^5s^2U and the Elongator complex is essential for an early step in the synthesis of these groups (Figure 1.9, Huang et al., 2005). These modifications are generally involved in the recognition of A ending codons and mcm^5U and ncm^5U may also be important in 'wobbling' to allow recognition of G ending codons (Johansson et al., 2008).

The $mcm^5s^2U_{34}$ modification is found on tRNA species that decode –AA ending codons ($tRNA^{Lys}_{UUU}$, $tRNA^{Gln}_{UUG}$, $tRNA^{Glu}_{UUC}$) and both the mcm^5 and s^2 groups work cooperatively to increase the efficiency of cognate codon binding (Johansson et al., 2008, Yarian et al., 2000, Murphy et al., 2004, Bjork et al., 2007). This is important because the stability of the pyrimidine-rich UUN anticodon loops is very poor and it has been reported that affinity of the hypomodified tRNAs for the ribosome A-site is reduced two-fold (Agris, 2008, Yarian et al., 2000). It should be noted that the hypomodified tRNAs isolated from Elongator mutants show no steady state defects in stability or charging with amino acid (Johansson et al., 2008, Bjork et al., 2007). These tRNAs decode in 'split' codon boxes where the U/C ending codons specify a different amino acid than A/G ending codons and where the G ending codons are read by a synonymous cognate tRNA (Figure 1.6).

In yeast, phenotypes associated with Elongator dysfunction are nearly all rescued by multicopy expression of hypomodified $tRNA^{Lys}_{UUU}$ and $tRNA^{Gln}_{UUG}$ but no other Elongator dependent tRNAs, which suggests these are the most compromised in terms

of function (Esberg et al., 2006). This also suggests that loss of Elongator-dependent modifications results in less efficient codon recognition at the A-site, rather than misreading errors, since it would be expected that the latter would be exacerbated by overexpression of the hypomodified tRNAs. The importance of the $mcm^5s^2U_{34}$ modification for tRNA function is further illustrated by the fact that deletion of *ELP* genes alongside *TUC1*, which abolishes both mcm^5 and s^2 modifications, is lethal in budding yeast. Amazingly, this lethality can be rescued by overexpression of the pyrimidine rich hypomodified $tRNA^{Lys}_{UUU}$, suggesting this tRNA is the most reliant on modification for function (Bjork et al., 2007).

The phenotypes associated with Elongator dysfunction are hypothesised to be caused by inefficient translation of particular mRNAs that require decoding by Elongator dependent tRNAs. Overexpression of these tRNAs likely increases the formation of A-site binding ternary complexes, which may compensate for reduced efficiency of translation in susceptible mRNA transcripts and thus reverse phenotypes. Recent work has begun to address these translational defects in Elongator mutants.

In *Schizosaccharomyces pombe* deletion of *ELP3* is non-lethal even though it results in loss of both mcm^5 and s^2 modifications, suggesting that the thiolation occurs downstream in this organism. These *elp3* knockouts have defects in mitosis and cytokinesis and have negative genetic interactions with several mitosis inducing genes. To assess translation defects in *S. pombe elp3Δ* strains, the relative expression levels of all proteins was determined and compared to wild-type: 494 proteins were down-regulated but the overall changes were two-fold or less. This constituted only a moderate defect in overall translation with approximately 87% of the proteome unaffected. The down-regulated proteins could all be categorised into four functional

groups in which the AAA lysine codon was over-represented. The levels of mRNAs in these functional groups were largely unaffected but they were highly dependent on Elongator for their efficient translation. This was exemplified by a candidate kinase, Cdr2, which is involved in cell cycle control in fission yeast. Cdr2 was strongly down-regulated in *elp3Δ* cells but overexpression of hypomodified $tRNA^{Lys}_{UUU}$ restored its protein levels. Codon re-engineering of *CDR2* to replace all AAA codons with the synonymous AAG lysine codon uncoupled its expression from dependence on Elongator function. Since deletion of *ELP3* causes similar cell cycle defects to deletions of *CDR2* the dependence of Cdr2 translation on Elongator function was suggested to be at least partially responsible for this phenotype in *elp3Δ* cells (Bauer et al., 2012). Another study in *S. pombe* highlighted a connection between Elongator and the expression of certain stress response genes that could also similarly be uncoupled from Elongator dependency by altering their codon usage (Fernandez-Vazquez et al., 2013). Therefore in *S. pombe*, certain mRNAs involved in cell cycle control and stress responses require Elongator dependent tRNA modifications for efficient translation.

In budding yeast the translation defects associated with loss of Elongator or Urm1 function have also been investigated. Similar to the findings in fission yeast, deletion of *ELP3* had little effect on the overall translation of the proteome and only a small subset of proteins appeared to be affected. The down-regulated proteins were enriched in AAA, CAA and GAA codons, which suggests that these mRNAs were particularly dependent on Elongator function for expression. Deletion of *URM1* conferred an almost identical pattern of altered protein expression and the levels of altered proteins were almost all rescued by multicopy expression of $tRNA^{Lys}_{UUU,}$ $tRNA^{Gln}_{UUG}$ and $tRNA^{Glu}_{UUC}$. *In vitro* ribosome binding assays using an mRNA construct with the AAA codon and $tRNA^{Lys}_{UUU}$ isolated from wild type, *urm1Δ* and *elp3Δ* strains

showed a 60% reduction in A-site binding and a five-fold reduced rate of dipeptide bond formation with the hypomodied $tRNA^{Lys}_{UUU}$ compared to wild-type (Rezgui et al., 2013).

Recently it was also shown by ribosome profiling in yeast that AAA, CAA and GAA codon occupancy by the ribosome is generally increased in *elp3Δ* and *urm1Δ* cells. This directly demonstrates that hypomodified $tRNA^{Lys}_{UUU}$, $tRNA^{Gln}_{UUG}$ and $tRNA^{Glu}_{UUC}$, function less efficiently in translation under normal growth conditions (Zinshteyn and Gilbert, 2013). The authors suggest that the slowing of Elongation due to lack of wobble uridine modification is insufficient to affect global protein levels and no ribosome queuing was detected in codons surrounding mcm^5s^2 dependent codons. Targets have been identified in *S. pombe* that can be uncoupled from Elongator function by altering codon usage, suggesting that certain proteins are nonetheless affected in expression due to bias codon usage (Bauer et al., 2012, Fernandez-Vazquez et al., 2013).

Taken together, this suggests that loss of Elongator does not globally disrupt translation and that the majority of proteins are still translated normally. Rather, certain mRNAs are susceptible, due to a skewed Elongator dependent codon content, to reduced efficiency of translation at the ribosome. It is possible that under different growth or stress conditions that elongation defects may become more pronounced and this has not been investigated. Other defects arising from lack of tRNA modifications may also play a significant role in phenotypes associated with Elongator mutants, but how these could be mediated is not understood (Zinshteyn and Gilbert, 2013).

Deletion of *TRM9*, encoding the tRNA methyltransferase responsible for methylation of the mcm^{5}U moiety, has also been linked to codon dependent regulation of translation (Begley et al., 2007, Chen et al., 2011a). Interestingly, the translation defect in *trm9* knockouts may be distinct from that seen in Elongator and *urm1* knockouts. It has been shown that in *trm9Δ* strains ncm^{5}U accumulates in tRNA$^{Arg}_{UCU}$ and tRNA$^{Glu}_{UUC}$ and the loss of the methyl group has been suggested to increase misreading of U/C ending codons (Chen et al., 2011a, Johansson et al., 2008). This is in agreement with the fact that *trm9Δ* cells show increased frameshifting and missense errors and are associated with activation of heat shock and unfolded protein responses (Patil et al., 2012).

The modification of tRNA by Elongator appears to be a basic function that should be required in all cells for the proper translation of mRNAs. However, analyses so far have reported that certain functional groups of proteins are particularly over-represented in modification dependent codons (Bauer et al., 2012, Rezgui et al., 2013, Begley et al., 2007, Bauer and Hermand, 2012). For example, yeast proteins down-regulated in *elp3Δ* cells were reported to be generally associated with anabolic functions whereas up-regulated proteins were associated with catabolic functions (Rezgui et al., 2013). This has led to the suggestion that tRNA modifications could be modulated in order to rapidly down-regulate the expression of a subset of mRNAs based on the reduced decoding efficiency of the tRNAs that read them. This would result in preferential down-regulation of mRNAs that require these Elongator-dependent tRNAs for efficient translation. Under the influence of external stimuli or developmental cues, reduced tRNA modification would allow rapid mRNA expression control at the post-transcriptional level.

There are a few lines of evidence that support this hypothesis. In yeast, the levels of several tRNA modifications have been shown to change in response to certain stresses. However, this does not take into account tRNA turnover and the changes do not always reflect phenotypes associated with loss of the corresponding modification. For example, Elongator mutant strains are sensitive to hydrogen peroxide but mcm^5s^2 levels are not altered upon hydrogen peroxide treatment and so it remains to be seen if these modifications could be dynamically regulated (Chan et al., 2010). The levels of thiolation in mcm^5s^2 containing tRNAs are also dependent on the availability of cysteine and methionine amino acids, which links tRNA modification and translational efficiency to nutrient status. It appears that s^2U_{34} is a gauge for the sulphur status of the cell and reduced levels of this modification results in general down-regulation of translation and carbohydrate metabolism and up-regulation of cysteine, methionine and lysine biosynthesis and sulphur salvage pathways (Laxman et al., 2013). It has also been suggested that mcm^5s^2U modifications could be regulated by mTOR signalling, since Uba4 reportedly interacts with TORC1 and *elp* and *urm1* mutants are hypersensitive to rapamycin, although no such crosstalk has been identified for the Elongator pathway (Laxman and Tu, 2011, Schaffrath., Personal Communication , Leidel et al., 2009, Jablonowski et al., 2009). The expression of the human homologue of *TRM9* (ABH8) has been shown to be induced by the ATM DNA damage response kinase, which implies that higher eukaryotes may regulate these tRNA modifications in response to stress (Fu et al., 2010). The distribution of Elongator subunits in some higher eukaryotes is tissue specific and this may underlie a modulation of translation in certain tissues and developmental stages (Chen et al., 2009a, Nelissen et al., 2010, Lin et al., 2013, Cuajungco et al., 2003).

The possible regulation of tRNA modification provides an exciting new level of gene expression control but this requires further investigation. Since the tRNA modification function of Elongator relies on the function of Hrr25 (a casein kinase) and Sit4 (a protein phosphatase), such regulation could potentially be mediated through reversible phosphorylation of Elongator subunits.

1.8 The regulation of Elongator by phosphorylation

Mutations that disrupt the kinase activity of Hrr25 or deletion of the protein phosphatase Sit4 cause Class II Zymocin resistance (Table 1.1), which suggested a role for reversible protein phosphorylation in Elongator-dependent tRNA modification (Mehlgarten and Schaffrath, 2003, Jablonowski et al., 2001a, Butler et al., 1991b). In fact the Elp1 subunit is subject to phosphorylation, since it is recognised by generic anti-phospho-serine and anti-phospho-threonine antibodies. In wild-type strains, Elp1 can be separated into distinct 'phospho' and 'non-phospho' forms based on loss of the slower migrating form upon phosphatase treatment and immunoreactivity with phosphospecific antibodies (Jablonowski et al., 2004, Mehlgarten et al., 2009). This indicates that under normal conditions Elp1 is balanced between 'hyper' and 'hypo' phosphorylated forms. Hrr25 kinase dead mutants alter this balance and only the 'hypo' phosphorylated Elp1 can be detected (Mehlgarten et al., 2009). In contrast, deletion of *SIT4* causes accumulation of the 'hyper' phosphorylated form (Mehlgarten et al., 2009, Jablonowski et al., 2004). These proteins therefore appear to have opposing roles in regulating the phosphorylation state of the Elp1 subunit. Since both *HRR25* and *SIT4* mutations cause Zymocin resistance then a balance between these phospho-forms must be essential for Elongator function.

Hrr25 is a member of the Caesin Kinase I (CKI) family, of which there are four members in yeast. It contains an N-terminal serine/threonine kinase domain, a P/Q rich C-terminus and has homologues in higher eukaryotes, including humans (Hoekstra et al., 1994). The kinase is involved in multiple cellular processes, including DNA damage responses, meiosis and Ca^{2+}/Calmodulin signalling (Ho et al., 1997, Kafadar et al., 2003, Petronczki et al., 2006). Interestingly, Hrr25 is also implicated in ribosome biogenesis (Schafer et al., 2006, Ray et al., 2008). Zymocin resistant mutants of *HRR25* were isolated initially with a point mutation in a conserved residue (E52D) that rendered the kinase inactive. The levels of Elongator subunit mRNAs are not altered in this mutant and deletion of downstream targets and inactivation of other CKI family members do not cause Zymocin resistance (Mehlgarten and Schaffrath, 2003). However, the mcm^5 and ncm^5 modifications were absent in the *hrr25* mutant (Huang et al., 2008) and therefore the kinase activity of Hrr25 is essential to Elongator tRNA modification. Consistent with a role in DNA damage repair, *hrr25* mutant strains are sensitive to methyl methanesulfonate (MMS). Truncation of the Hrr25 P/Q rich domain rescues this phenotype but this mutant is still Zymocin resistant, demonstrating that the cellular functions of the kinase can be uncoupled (Mehlgarten and Schaffrath, 2003).

Sit4 is a PP2A-like serine/threonine protein phosphatase that is implicated in a large number of processes including Protein Kinase C and mTOR signalling (Arndt et al., 1989, Angeles de la Torre-Ruiz et al., 2002, Di Como and Arndt, 1996). It is required for normal cell cycle progression and stress responses (Sutton et al., 1991, Lopez-Mirabal et al., 2008, Douville et al., 2004). The different functions of Sit4 are mediated by its interaction with Sit4 associated proteins, or Saps, that direct its activity towards different substrates. There are four Sap proteins in yeast Sap4, Sap155, Sap185 and Sap190. The Sap4/Sap155 and Sap190/185 proteins are functionally distinct and likely

direct Sit4 towards different groups of substrates (Luke et al., 1996). Deletion of both *SAP190* and *SAP185* results in Zymocin sensitivity so these direct its activity towards the Elongator complex (Jablonowski et al., 2009). Like Hrr25 mutants, there were no changes in the mRNA or protein levels of Elongator subunits in Sit4 deletion strains, which suggested post-translational regulation of the complex (Jablonowski et al., 2001a). Both Sit4 and Hrr25 have been demonstrated to interact, which is consistent with a combined regulatory role (Jablonowski et al., 2004, Ho et al., 2002).

The Hrr25 kinase interacts with the assembled Elongator complex but this interaction is dependent on the accessory factor Kti12. Deletion of *KTI12* abolishes this interaction and mutations in *hrr25* also cause increased association of Kti12 with Elongator (Mehlgarten et al., 2009). Further to this, Kti12 also appears to regulate Elongator phosphorylation, deletion or multicopy expression of *KTI12* causes Elp1 'hypo' or 'hyper' phosphorylation, respectively (Jablonowski et al., 2004).

It has been proposed that Hrr25 is bridged to Elongator by its interaction with Kti12 and that both factors may regulate Sit4 activity towards Elp1. Such a role as a regulator of Sit4 is supported by the fact that 'kinase-dead' *hrr25* in combination with a *SIT4* deletion results in a wild-type balance of Elp1 phospho-forms, as described above, suggesting that Hrr25 cannot be the only Elp1 kinase and that both these proteins have functional interplay (Mehlgarten et al., 2009). Multicopy *KTI12* in combination with multicopy *SIT4* also results in a wild-type balance of phosphorylated Elp1, suggesting that Kti12 antagonises Sit4 phosphatase activity (Jablonowski et al., 2004). Therefore the balance of phosphorylated Elp1 is dependent on the interplay between Hrr25, Sit4 and Kti12, but this is not yet well understood (Figure 1.10).

In order to understand better the regulation of Elp1 by phosphorylation, our lab carried out phosphopeptide mapping combined with alanine substitutions in putative phosphorylation sites (Abdel-Fattah and Stark unpublished). Several putative phosphorylation sites at the C-terminus of Elp1 were found to be functionally essential and are currently under investigation (Figure 1.11). Of significance to this work, serine 1209 was found to be functionally essential since mutation to alanine caused Elongator dysfunction, as did the combined mutation of serines 1198 and 1202 to alanine.

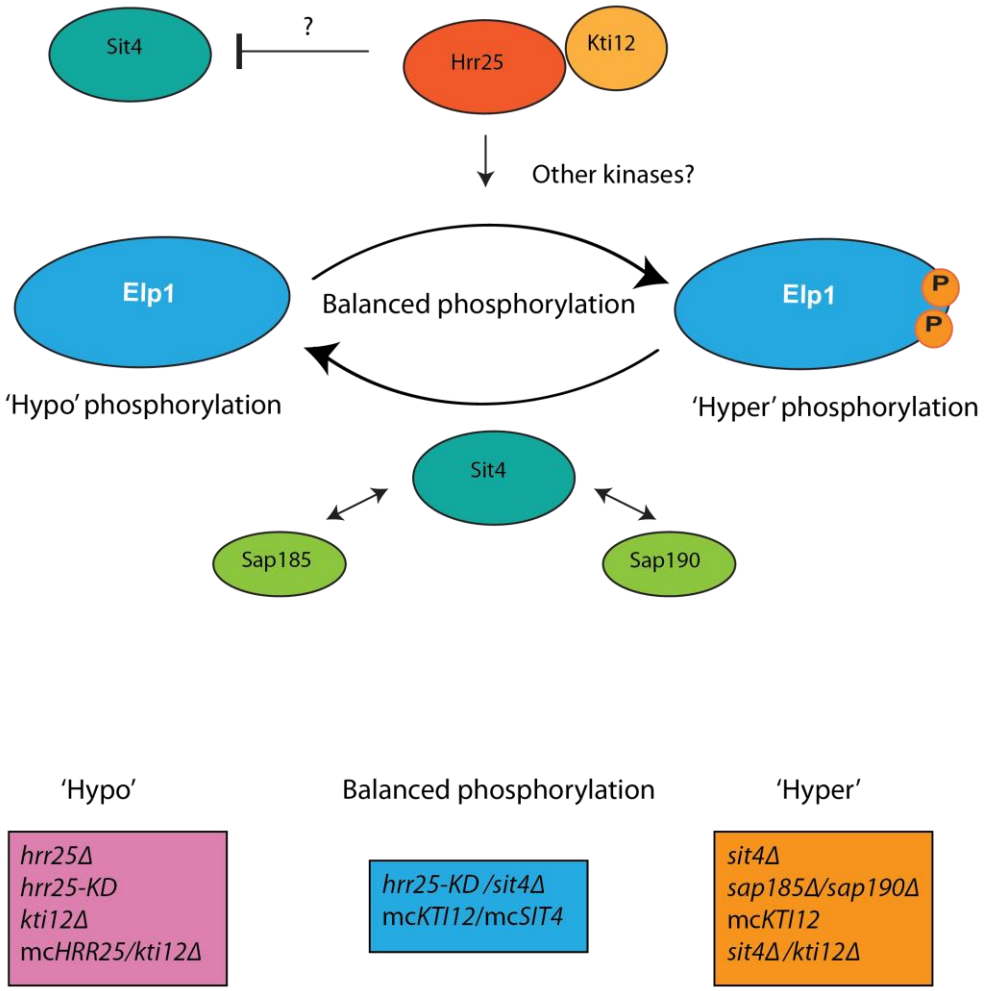

Figure 1.10: Balanced Elp1 phosphorylation depends on the interplay between Hrr25, Sit4 and Kti12. Kti12 and Hrr25 promote phosphorylation that is opposed by Sit4 dephosphorylation. Hrr25 may work alongside Kti12 to inhibit Sit4 dephosphorylation of Elp1. Boxes denote the various gene deletions and multicopy expressions that correspond to each Elp1 phosphorylation state. This schematic summaries data from Mehlgarten and Schaffrath (2003), Mehlgarten et al (2009), Jablonowski et al (2001a, 2004, 2009)

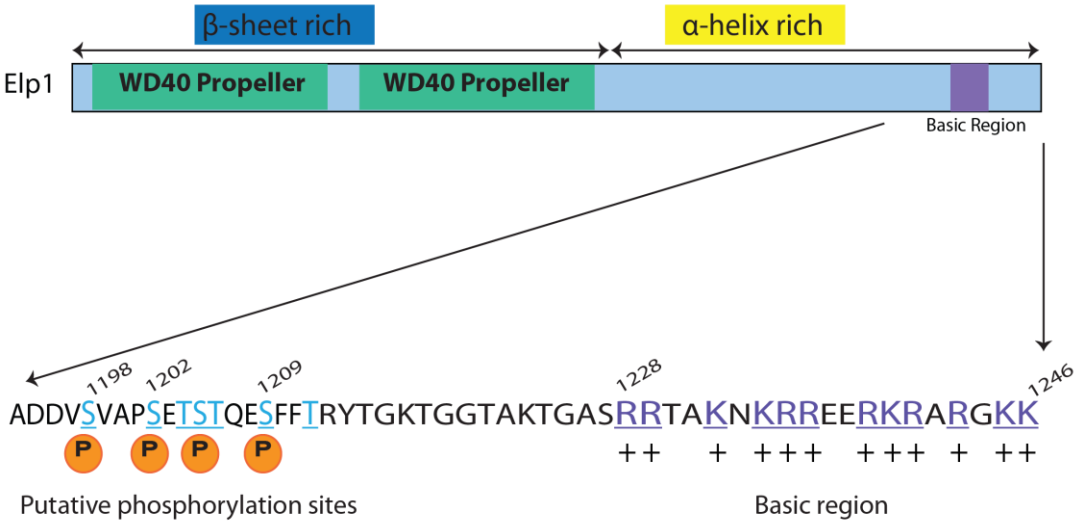

Figure 1.11: Putative phosphorylation sites and basic region in the Elp1 subunit.
Phosphopeptide mapping has revealed putative phosphorylation sites that lie near a basic region in the Elp1 C-terminus. Orange balls indicate phosphorylation and the residue number is shown where the exact site has been mapped. Blue residues indicate putative phosphorylation sites and purple residues indicate the basic region.

1.9 A basic region in the Elp1 C-terminal domain

The Elp1 C-terminal domain contains a lysine/arginine rich basic region (Figure 1.11) that is highly conserved across eukaryotes, including humans. This region has been annotated as a putative bipartite nuclear localisation sequence (NLS) but this potential function has not yet been fully investigated. In yeast, truncation of the Elp1 C-terminus, including this basic region, results in loss of Elongator function and it was shown that when fused to GFP, the Elp1 C-terminal domain (CTD) can direct import of the fusion protein into the nucleus (Fichtner et al., 2003). It was suggested by the authors that Elp1 may require import into the nucleus for a role in transcription. However, Elp1 has been reported to be mainly cytoplasmic in both yeast and human cells (Pokholok et al., 2002, Kim et al., 2002).

A cytoplasmic localisation is consistent with a role in anticodon tRNA modification so it was unclear why Elp1 would require nuclear import (Hopper and Phizicky, 2003). Other work has also shown that addition of a *bona fide* NLS (from Cap binding protein 80, Cbp80) onto the Elp1 C-terminus traps the subunit in the nucleus but causes loss of Elongator function, consistent with a cytoplasmic role (Rahl et al., 2005). The C-terminus of Elp1 is predicted to be mainly α-helical indicating that it may be quite flexible (Figure 1.2). Furthermore, the functionally important phosphorylation sites discussed above also lie just upstream of this basic region (Figure 1.11) raising the possibility that there could be some interplay between these regions. The importance and function of the Elp1 basic region has not yet been extensively studied.

1.10 Aims of this work

The key aim of this thesis is to investigate the role of the highly conserved basic region in the Elp1 subunit of Elongator using budding yeast as a eukaryotic model organism. Budding yeast is an excellent tool for basic research and to date a significant amount of work on the Elongator complex has been carried out using this organism as a model.

The Elp1 basic region resides in the C-terminal domain and although annotated as a putative NLS this function has not been extensively studied. The work presented in this thesis addresses several aspects of how this basic region in Elp1 impinges on Elongator function. It is hoped that the conclusions of this thesis will provide valuable information on the function of the Elp1 basic region from yeast to man.

i) **The functional significance of the Elp1 basic region**

In order to study the function of the Elp1 basic region alanine substitutions were created throughout its sequence. Various functional assays were used to determine the effect of these mutations on Elongator tRNA wobble uridine modification. To assay the effects of these mutations on the distribution of Elp1 between the nucleus and cytoplasm of cells microscopy of GFP tagged Elp1 and Elp1 mutant proteins was used.

ii) **What effects do mutations in the Elp1 basic region have on Elongator complex assembly and phosphorylation?**

To determine whether the basic region in Elp1 is important for the assembly of the Elongator complex the association of tagged subunits in the context of wild-type and mutant Elp1 were analysed by pulldowns and

western blotting. Phosphorylation could also be altered in Elp1 basic region mutants if certain sites regulated the recognition or function of this region. To investigate the possible relationship between the Elp1 basic region and functionally important phosphorylation, wild-type and mutant Elp1 proteins were analysed by western blotting using an Elp1 phospho-specific antibody against the functionally important serine 1209 site.

iii) If the Elp1 basic region is not required for nuclear import then is it required for interaction with tRNA?

We hypothesised that the basic region may be required for tRNA binding to Elongator. This alternative function was addressed using recombinant Elp1 fusion proteins and electromobility shift assays with yeast tRNA.

Chapter 2: Materials and Methods

2.1 Yeast Cell Culture and Strain Construction

Standard *Saccharomyces cerevisiae* (yeast) culture and molecular biology techniques were used, unless otherwise stated (Sherman, 2002, Stansfield, 2006, Amberg et al., 2005, Sambrook and Russell, 2001). All culture media used in this study were provided by Media Services, University of Dundee and media recipes along with working drug concentrations are described in the Appendix. Unless otherwise stated ultrapure water was purified by a 0.22 µm milli-Q filter (denoted mQH_20 throughout) and sterilised by autoclaving.

2.1.1 Yeast Cell Culture

Haploid budding yeast strains were cultured in rich Yeast-Peptone-Adenine-Dextrose (YPAD) medium or the appropriate selective dropout media (DOA) at 26°C or 30°C unless otherwise stated. Strains were stored long term at -80°C as glycerol stocks, made by growing strains from single colonies on agar media and then scraping into 20% (v/v) Glycerol. To recover strain from these stocks, a small amount of cells were plated from glycerol stocks on the appropriate agar medium and grown overnight. Overnight cultures were made by inoculating ~5 ml of medium with yeast from an agar plate and incubated with shaking. The concentration of cells in liquid culture was determined using optical density at 600 nm (OD_{600}). For log phase cultures, overnights were diluted to the appropriate OD_{600} (~ 0.1) in fresh medium and grown for at least 2 doublings (usually around 6-8 hours) to reach log phase (OD_{600} of ~1). Unless stated otherwise all strains were derived from BY4741 (*MAT***a** *his3Δ1 leu2Δ0 met15Δ0 ura3Δ0*). A list of strains used and/or generated in this study is shown (Table 2.1).

Table 2.1: List of strains used and/or generated in this study.

Strain	Genotype	Source
	K. lactis	
IFO1267	*MAT***a** prototroph [pGLK2^{+} pGLK1^{+}]	Lab Stock
	S. cerevisiae	
BY4741	*MAT***a** *his3Δ1 ura3Δ0 leu2Δ0 met15Δ0*	Lab Stock
BY4742	*MAT*α *his3Δ1 ura3Δ0 leu2Δ0 lys2Δ0*	Lab Stock
WAY034	BY4741 *elp1Δ::KanMX4*	Euroscarf
YRDS250	BY4741 *elp1Δ::*HIS3MX	This Study
YRDS225	BY4742 *elp1Δ::*hph	This Study
SBY128	BY4741 *his3Δ1*::URA3-SUP4-NatRMX	S. Bandau
SBY132	BY4741 *his3Δ1::ura3^{oc22}*-SUP4-NatRMX	S. Bandau
SBY134	WAY034 *his3Δ1*::*URA3*-SUP4-NatRMX	S. Bandau
SBY138	WAY034 *his3Δ1:: ura3^{oc22}*-SUP4-NatRMX	S. Bandau
YRDS1	BY4741 NIC96-4mcherry-NatRMX	This Study
YRDS59	YRDS1 *ELP1*-L-GFP-HIS3MX [1]	This Study
YRDS84	*MAT***a** NIC96-4mcherry-NatRMX6 *lys2Δ*	This Study
YRDS228	BY4741 *elp1::*CORE	This Study
YRDS229	YRDS59 *elp1::*CORE-L-GFP-HIS3MX	This Study
YRDS256	YRDS228 *ELP1* (*delitto perfetto*)[2]	This Study
YRDS258	YRDS228 *elp1-KR9A* (*delitto perfetto*)	This Study
YRDS253	YRDS229 *ELP1*-L-GFP-HIS3MX (*delitto perfetto*)	This Study
YRDS255	YRDS229 *elp1-KR9A*-L-GFP-HIS3MX (*delitto perfetto*)	This Study
YRDS317	YRDS229 *elp1-KR5A*-L-GFP-HIS3MX (*delitto perfetto*)	This Study
YRDS319	YRDS229 *elp1-KR4A*-L-GFP-HIS3MX (*delitto perfetto*)	This Study
YRDS321	YRDS229 *elp1-1209A*-L-GFP-HIS3MX (*delitto perfetto*)	This Study
YRDS323	YRDS229 *elp1-1198A-1202A*-L-GFP-HIS3MX (*delitto perfetto*)	This Study
YRDS270	YRDS228 *ELP1* (*delitto perfetto*) *his3Δ1*::*URA3*-SUP4-NatRMX	This Study
YRDS272	YRDS228 *ELP1* (*delitto perfetto*) *his3Δ1*:: *ura3^{oc22}*-SUP4-NatRMX	This Study
YRDS278	YRDS228 *elp1-KR9A* (*delitto perfetto*) *his3Δ1*::*URA3*-SUP4-NatRMX	This Study
YRDS280	YRDS228 *elp1-KR9A* (*delitto perfetto*) *his3Δ1*:: *ura3^{oc22}*-SUP4-NatRMX	This Study
YRDS153	YRDS1 *ELP1*-L-NES(Rev)-GFP-HIS3MX	This Study
YRDS545	YRDS1 *ELP1*-L-NLS(Cbp80)-L-GFP-HIS3MX	This Study
YRDS539	YRDS1 *ELP1*-L-*NLS4A*(Cbp80)-L-GFP-HIS3MX	This Study
YRDS269	BY4741 *ELP1*-L-3HA-HIS3MX	This Study

CLY6	WAY034 *TRP1::*(p*GAL*-TEV-myc$_3$-*HIS3::TRP1*)$_n$ [3]	C. Lloyd
YRDS331	*MAT*α *Δelp1::*hph *TRP1::*(p*GAL*-TEV-3myc-*HIS3::TRP1*)$_n$	This Study
YRDS370	YRDS269 *elp1::*CORE-L-3HA-HIS3MX	This Study
YRDS450	*MAT***a** *elp1::*CORE-L-3HA-HIS3MX *TRP1::*(p*GAL*-TEV-3myc-*HIS3::TRP1*)$_n$ *met15Δ0*	This Study
YRDS494	YRDS450 *ELP1*-TEV-L-3HA-HIS3MX (*delitto perfetto*)	This Study
YRDS338	YRDS269 *ADH1*::TIR1-9myc-*URA3*	This Study
YRDS393	YRDS338 *ADH1*::TIR1-9myc-*URA3* *ELP1*-L-3HA-AID-NatRMX	This Study
YRDS439	YRDS1 *ARG4*-L-GFP-HIS3MX	This Study
YRDS437	YRDS1 *KTI12*-L-GFP-HIS3MX	This Study
YRDS447	YRDS1 *ELP3*-L-GFP-HIS3MX	This Study
YRDS443	YRDS1 *ELP5*-L-GFP-HIS3MX	This Study
YRDS526	YRDS439 *KTI12*-L-3HA-KanMX	This Study
YRDS461	YRDS253 *KTI12*-L-3HA-KanMX	This Study
YRDS467	YRDS255 *KTI12*-L-3HA-KanMX	This Study
YRDS529	YRDS321 *KTI12*-L-3HA-KanMX	This Study
YRDS537	YRDS439 *ELP3*-L-3HA-KanMX	This Study
YRDS463	YRDS253 *ELP3*-L-3HA-KanMX	This Study
YRDS482	YRDS255 *ELP3*-L-3HA-KanMX	This Study
YRDS528	YRDS439 *ELP5*-L-3HA-KanMX	This Study
YRDS474	YRDS253 *ELP5*-L-3HA-KanMX	This Study
YRDS487	YRDS255 *ELP5*-L-3HA-KanMX	This Study
YRDS492	BY4741 *GLN4*-GFP-HIS3MX	Invitrogen
YRDS493	BY4741 *CEX1*-GFP-HIS3MX	Invitrogen
YRDS531	YRDS253 *kti12Δ*::KanMX	This Study
YRDS533	YRDS255 *kti12Δ*::KanMX	This Study
YRDS535	YRDS321 *kti12Δ*::KanMX	This Study

[1] "L" indicates the linker region discussed in Section 2.1.5. [2] Integration by 'delitto perfetto' method discussion in Section 2.1.12. [3] Integration of >1 copy pCAL7(copy number not determined).

2.1.2 Eclipse Assays and Growth Tests

For Eclipse assays, cells from overnight cultures were suspended in sterile mQH_20 at an OD_{600}=1.0 and 5 µl was spotted onto YPAD (made with Roth agar). Once dry, the edge of each spot was inoculated with *Kluyveromyces lactis* (IFO1267) and assays were incubated at 30°C for 1-2 days. Strains with functional Elongator are sensitive to the Zymocin toxin secreted by *K. lactis* resulting in a halo of growth inhibition.

For Growth tests, cells from overnight cultures were resuspended in sterile mQH_20 at an OD_{600}=1.0. Four or five ten-fold serial dilutions were made and 5 µl of each dilution was spotted on the appropriate media. These were incubated at the appropriate temperature, usually 30°C for 2-3 days.

2.1.3 Crossing and tetrad dissection

Strains were crossed and sporulated by standard methods (Stansfield, 2006, Amberg et al., 2005). Briefly, haploid strains of *MAT**a*** and *MATα* mating types were mixed together in a small volume of sterile mQH_20 and spread in a small patch on YPAD agar. This was incubated overnight at 30°C and diploids were selected on the appropriate medium (commonly DOA -Met -Lys for crosses involving BY4741/BY4742 derivatives). For sporulation, diploids were grown on GNA medium overnight and then thickly patched onto VB Sporulation media and incubated at 26°C for 5-10 days. Sporulation of diploids occurs in response to nitrogen starvation and was confirmed by visualisation of meiotic tetrad spores under the microscope. Tetrads consist of four haploid spores within an ascus (protective sac) and have a distinctive cruciform appearance. Cells were suspended in sterile mQH_20 and the asci digested with Zymolyase (0.5 mg/ml) for ~10 mins so that tetrad spores could be separated on a YPAD agar plate using a tetrad dissection microscope (Sporeplay, Singer instruments).

Dissected spores were allowed to grow for 2-3 days at 30°C, patched onto YPAD and then screened for the appropriate marker to obtain haploids of the desired genotypes. If required, these were confirmed by colony PCR and fluorescent microscopy (Sections 2.1.8 and 2.3.1).

2.1.4 Yeast Transformation

Yeast transformations were carried out using the Lithium acetate/PEG method (Gietz and Woods, 2002). Overnight cultures were diluted into fresh media at an OD_{600} of ~0.25 and grown for 6 hours to allow at least two doublings. Cells were then harvested by centrifugation at 3000 rpm for 2 min, washed once in sterile mQH_20 and resuspended in $1/50^{th}$ the culture volume of sterile mQH_20 (i.e. 0.5 ml for 25 ml culture). In general $1/5^{th}$ of this was used per transformation reaction and cells were aliquoted and harvested as before. Cell pellets were resuspended in 360 µl of T-Mix (33% (w/v) PEG, 0.3 mg/ml boiled single stranded Herring sperm DNA, 0.1 M lithium acetate and 34 µl of transforming DNA). For plasmid transformations a maximum of 50 ng of DNA was used whereas for PCR generated cassettes the full allowed volume (34 µl) was used without dilution to allow an excess for the less efficient process of homologous recombination. Transformation reactions were heat shocked at 42°C for 40 min and then cells were harvested. Transformed cell pellets were resuspended in sterile mQH_20, plated on the appropriate selective medium and grown at 30°C for 2-3 days. For drug selection transformed cell pellets were first resuspended in YPAD medium and incubated at 26°C with shaking for 3-4 hours before plating out as above. Positive transformants were streaked out on selective agar to single colonies and then checked by colony PCR (Section 2.1.8). Usually at least 2 verified clones from each transformation were saved as glycerol stocks.

2.1.5 Yeast Gene Manipulation

Knockout and tagging cassettes for transformation were generated using Longtine vectors (Longtine et al., 1998) with the appropriate gene-specific primers unless otherwise indicated. Gene specific knockout cassettes were amplified by polymerase chain reaction (Section 2.1.7) for transformation into the appropriate yeast strain. This method deletes the open reading frame of the gene and replaces it with a marker gene. Each set of knockout primers was designed with a gene specific sequence of around 50-55 base pairs upstream (forward primer) and downstream (reverse primer) of the open reading frame. A forward F1 primer sequence (CGGATCCCCGGGTTAATTAA) and a reverse R1 primer sequence (GAATTCGAGCTCGTTTAAAC), which are used as generic sequences for amplification of the marker gene from a Longtine plasmid template, were added onto the 3' end of these gene specific sequences. Gene specific primers for amplification were therefore generically designed as; Forward 5'-Gene specific sequence-F1-3' and Reverse 5'-Gene specific sequence-R1-3'.

C-terminal tagging of genes was carried out similarly, except the gene specific forward primer was designed just upstream of the stop codon of the gene. A forward F2 primer sequence (CGGATCCCCGGGTTAATTAA) and the R1 reverse sequence (GAATTCGAGCTCGTTTAAAC) bind within the appropriate Longtine tagging plasmid template to amplify the Tag sequence and a marker gene. This generates a cassette that excludes the stop codon of the gene and inserts a C-terminal tag followed by the *ADH1* transcription terminator and a selectable marker gene when transformed into the appropriate strain. When necessary to preserve full functionality, the forward primer for C-terminal tagging also contained a linker sequence (encoding the amino acid sequence GSAGSAAGSG) between the end of the gene specific sequence and the

tag. To visualise the nuclear periphery of yeast strains, the nuclear pore complex component Nic96 was tagged with 4mCherry as outlined above, using pT909 as the template (gift from Tomo Tanaka). Correct integration of gene knockout or C-terminal tagging cassettes were confirmed by colony PCR and if appropriate by fluorescence microscopy (Sections 2.1.8 and 2.3.1).

2.1.6 Integration of *SUP4 ochre* suppressor system

Plasmids containing the *SUP4 ochre* suppressor system (Susanne Bandau, unpublished; see Appendix) were linearised by restriction digest using *Msc*I and transformed into appropriate strains for integration at the *his3Δ1* locus. The system cassettes contain either the wild-type *URA3* gene (pSB1) or *ura3*^{o22} with a premature stop codon (pSB3) as well as the *SUP4* suppressor tRNA gene and the NatRMX marker for selection. Positive integrants were selected for by growth on YPAD + ClonNAT and verified by colony PCRs (Section 2.1.8).

2.1.7 Polymerase chain reactions for amplification of DNA

For the amplification of certain cassettes and for colony PCR *Taq* DNA polymerase (prepared as described in Pluthero, (1993)) was used, under the following standard reaction conditions: Reactions contained 1× *Taq* DNA polymerase buffer (10 mM Tris-HCl pH 8.8, 1.5 mM $MgCl_2$, 50 mM KCl and 0.08% (v/v) NP40), 0.2 mM of each dNTP, 0.2 µM of each primer, template DNA and *Taq* DNA polymerase enzyme (typically 1/10 the final reaction volume). Cycling conditions were 95°C for 1 min then 30-35 cycles of denaturation at 95°C for 30 s, annealing at 55°C for 30 s and extension at 72°C for 1 min/kb product. A final extension step at 72°C for 10 min was always used and the annealing temperature was sometimes adjusted based on the melting temperature of the primer pair.

For the amplification of cassettes where product fidelity was especially important we used Phusion DNA polymerase (Finnzymes) under the following standard conditions: Reactions contained 1× Phusion High fidelity polymerase buffer (proprietary), 0.2 mM of each dNTP, 0.5 µM of each primer, template DNA and 0.02 U/µl of Phusion DNA Polymerase. Cycling conditions were 98°C for 30 s then 25-30 cycles of denaturation at 98°C for 30 s, annealing at 55°C for 30 s and extension at 72°C for 30 s/kb product. A final extension step at 72°C for 10 min was always used and the annealing temperature was sometimes adjusted based on the melting temperature of the primer pair.

Template DNA was either plasmid DNA, generally used at no more than 1 ng/µl, or a standard yeast genomic DNA prep used at $1/10^{th}$ the final reaction volume (Section 2.1.8). A list of primers used in this study are provided in the Appendix.

2.1.8 Colony PCRs

For yeast colony PCRs, genomic DNA was prepared by digestion of the yeast cell wall by Zymolyase. A small amount of cells were resuspended in SPZ buffer (1.2 M Sorbitol, 81 mM Na_2HPO_4, 19 mM NaH_2PO_4, 2.5 mg/ml Zymolyase) and incubated at 37°C for 30 min, then 95°C for 5 min. The reactions were then diluted 10 fold and used as a template for colony PCR at $1/10^{th}$ of the final reaction volume. Amplification is carried out using *Taq* DNA polymerase as described (Section 2.1.7).

To check for correct integration of cassettes at the target gene locus, primers that bind upstream or downstream of the integration were used in combination with primers that bind within the integration cassette. Only positive integrants at that locus will give a PCR product. Often a PCR reaction diagnostic for negative integration was also assayed using primers that amplify a product from within the replaced region.

For bacterial colony PCRs, a small amount of cells were resuspended directly in the *Taq* polymerase reaction mix and this was boiled at 95°C for 5 min before PCR amplification with appropriate primers.

2.1.9 DNA sequencing

DNA sequencing was carried out by the DNA Sequencing Service, University of Dundee (http://www.dnaseq.co.uk/). Between 500-600 ng of plasmid DNA was typically sent for sequencing along with the appropriate primer at a stock concentration of 3.2 µM. For PCR products, typically a 1 in 10 dilution of the final reaction in mQH_20 was sent directly. Problematic PCR products were treated with Antarctic phosphatase (Section 2.2) to dephosphorylate residual dNTPs and primers, which would otherwise interfere with the sequencing reaction.

2.1.10 Agarose Gel Electrophoresis

All PCR and restriction digest reactions were analysed by Agarose gel electrophoresis. Gels were made by dissolving 1% (w/v) ultrapure agarose in 1× TAE (40 mM Tris, 0.1% Acetic acid, 1 mM EDTA) buffer by boiling. This mixture was cooled before adding 5 µl/100 ml of SYBR Safe gel stain, to allow visualisation of DNA bands by UV exposure. The gel was poured and allowed to set. DNA samples were mixed with 6x DNA loading dye (10 mM Tris-HCl pH 7.6, 0.15% (w/v) orange G, 0.03% (w/v) xylene cyanol FF, 60% (v/v) Glycerol, 60 mM EDTA) before loading. Gels were run at 120 V for 30-45 min in 1× TAE running buffer and DNA Hyperladder I (Bioline) was used as size markers.

2.1.11 Mutant *elp1* Plasmids

All *elp1* mutant plasmids used in this study were synthesised by DNA2.0 (https://www.dna20.com/) and the mutations made are listed elsewhere (Figure 3.1).

These were generated from YCplac111-*ELP1*-6HA by replacing the relevant part of the gene with a synthesized *elp1* mutant sequence. The original YCplac111 vector was used as an empty vector control (Gietz and Akio, 1988).

2.1.12 Site Directed Mutagenesis by '*delitto perfetto*'

The '*delitto perfetto*' method allows for 'clean' integrations as site directed mutations are introduced into a gene of interest without the need for marker selection (Storici and Resnick, 2006). A region within the gene of interest is first replaced with a marker cassette, which in turn is replaced by a mutant sequence. This second event is identified by counterselection for the marker.

A CORE knockout cassette containing the *KlURA3* and KanMX6 markers was amplified using *Taq* DNA polymerase and pCORE (Storici and Resnick, 2006) as a template. The primers appended forward P1 (GAGCTCGTTTTCGACACTGG) and reverse P2 (TCCTTACCATTAAGTTGATC) plasmid specific sequences onto ~50 bps *ELP1* specific sequence. The cassette was transformed into appropriate stains to replace the region of *ELP1* encoding amino acids 1164-1277. Positive *elp1::CORE* transformants were selected by growth on DOA -Ura and confirmed by growth on YPAD + G418 and colony PCR.

Primers flanking the deleted region of *ELP1* were used to amplify a replacement sequence from YCp-*ELP1*-6HA or the equivalent mutant vector using Phusion DNA polymerase. These were transformed into *elp1::CORE* strains to reconstitute the deleted region with the wild type or mutant *ELP1* sequence. Transformants were grown on YPAD at 30°C overnight and then replica plated twice over 2 days on 5-FOA medium to select for loss of the *KlURA3* marker. Positive transformants were further

confirmed by lack of growth on YPAD + G418, colony PCR and sequencing across the replaced region.

2.1.13 Elongator "switch off" strain construction and analysis

To generate strains in which Elp1 levels were controlled through fusion to an Auxin inducible degron (Nishimura et al., 2009) , a strain that expressed TIR1-9myc under the control of the ADH1 promoter was made. The pNHK53 plasmid (kind gift from Tomo Tanaka) containing the *Os*TIR1-9myc gene under control of the *ADH1* promoter was linearised by restriction digest using *Sph*I. This unique restriction site is within the *ADH1* promoter sequence and generates a cassette that can be integrated at the endogenous *ADH1* promoter. This cassette was transformed into a strain expressing C-terminal 3HA tagged Elp1 and selected for by growth on DOA -Ura. Colony PCR was used to distinguish single and multiple integration at the *ADH1* locus. Primers were then designed for C-terminal tagging of Elp1-3HA with an auxin inducible degron sequence (AIDD17) using pT1450 as a template (kind gift from Tomo Tanaka). The tagging cassette was transformed into a single integrant TIR1-9myc strain to replace *ELP1*-3HA-HIS3MX with *ELP1*-3HA-AID-NatRMX. Transformants were selected for by growth on YPAD+ ClonNAT, checked for lack of growth on DOA-His and verified by colony PCR.

For inducible inactivation of Elongator through *in vivo* C-terminal truncation of Elp1, a previously made strain containing a pGAL-TEV-3myc-HIS3MX cassette integrated in multicopy at the *TRP1* locus (Charlotte Lloyd, unpublished) was used. This was crossed with a *MAT*α strain to generate pGAL-TEV-3myc-HIS3MX containing haploids of the opposite mating type. These were crossed with a strain containing *ELP1*-3HA disrupted with a pCORE cassette (*elp1::CORE*-3HA). Haploids containing both the pGAL-TEV-

3myc-HIS3MX and *elp1::CORE*-3HA loci in the *MAT***a** mating type were selected for and verified by colony PCR. The CORE cassette in these strains was reconstituted by *'delitto perfetto'* using a version of *ELP1* encoding a TEV protease cleavage site (ENLYFQGDDV) immediately before Ser-1202 in Elp1 using the YCp-Elp1::TEV-6HA plasmid as template. Thus induction of TEV protease expression by growth on galactose results in cleavage of the last 147 amino acids of Elp1. Strains were verified using colony PCR and sequencing across the replaced region of Elp1.

Cleavage/degradation of Elp1 in our strains was analysed by time course experiments. TEV cleavage strains were grown overnight in YPAR (2% raffinose), inoculated into fresh YPAR medium at an OD_{600}= 0.2 and grown at 30°C for two doublings. A sample of cells equivalent to 10 OD_{600} units was harvested, washed with 1x Phosphate buffered saline (PBS) and the pellets snap frozen in liquid nitrogen and stored at -80°C ('Pre' sample). Cultures were harvested at 3000 rpm for 1 min and resuspended at OD_{600}= 0.5 in YPARG (2% raffinose, 2% galactose). Additional 10 OD_{600} samples were taken at 0, 30, 60, 90, 120, 150, 180, 210 min after switching to YPARG medium. As a control a small scale glucose switch culture was also grown and samples were taken 0 and 210 min after inoculating into YPAD (2% glucose).

Auxin inducible degron strains were inoculated from overnight cultures into fresh YPAD (2% glucose) media at an OD_{600}= 0.1 and grown at 30°C for around two doublings. A 10 OD_{600} unit sample was processed as above ('Pre' sample) and then 0.5 mM of 1-naphthalene acetic acid (NAA), an auxin related compound, was added to cultures. Additional 10 OD_{600} unit samples were taken at 0, 15, 30, 60, 90, 120, 150, 180, 360 min after NAA addition to the medium.

The pelleted samples from each experiment were all processed in parallel by the NaOH/TCA protein extraction method and analysed by western blotting (Sections 2.4.1 and 2.4.7).

2.2 Molecular Cloning

Cloning was carried out using standard methods (Sambrook and Russell, 2001) and all kits and reagents were used according to manufacturer's instructions unless otherwise stated. Restriction enzymes were supplied by New England Biolabs (NEB) or Fermentas.

For restriction digests, typically up to 0.5-1 µg of plasmid DNA or insert was digested in a final reaction volume of 25 µl, containing 1× reaction buffer and 10 units of each restriction enzyme. Reactions were incubated at the appropriate temperature for 1-1.5 hours and either heat inactivated or immediately separated by agarose gel electrophoresis. For fast digest enzymes (Fermentas), reactions were incubated for 20 min only.

Plasmid vectors and inserts digested with the appropriate restriction enzymes and purified using a Gel extraction kit (QIAGEN) after separation by agarose gel electrophoresis. Briefly, bands were visualised and cut from the gel. The appropriate volume of QG buffer (20 mM Tris HCl pH 6.6, 5.5 M GuSCN) was added to the gel piece and this was incubated at 50°C until the agarose dissolved. DNA was bound to a silica column by spinning at 10,000 × g for 1 min and then washed with QG buffer and PE buffer (10 mM Tris-HCl pH 7.5, 80% ethanol). The DNA was eluted in 10 mM Tris-HCl pH 8.5 or mQH_20.

To reduce background from self-ligation of single cut vectors, plasmid digests were treated with 5 Units of Antarctic phosphatase (NEB) in 1× Antarctic phosphatase buffer (5 mM Bis-Tris-Propane-HCl , 0.1 mM $MgCl_2$, 10 µM $ZnCl_2$ pH 6.0) for 30 min-1 hour at 37°C and then reactions were heat inactivated at 75°C.

Ligations were carried out using the Rapid DNA ligation kit (Roche) in general using 1:3 or 1:5 molar ratio of vector to insert. The insert and vector were mixed and added to an equal volume of 2× T4 DNA ligase buffer (usually to a final volume of 20 µl) and 5 U of T4 DNA ligase. Reactions were left at room temperature for 30 min - 2 hours and transformed directly into competent DH5 alpha *E. coli* (Section 2.2.5). Usually no more than $1/20^{th}$ of the ligation reaction was used for bacterial transformation and reactions omitting DNA ligase were used as negative controls.

Plasmids were purified from *E. coli* with a Plasmid miniprep kit (Bioline) using 5 ml or 10 ml overnight cultures for high copy and low copy plasmids respectively, with appropriate selection. In brief, cultures pellets were lysed in alkaline NaOH/SDS buffer for no more than 5 min. Lysates were then neutralised in a high salt buffer and precleared by centrifugation at 20,000 × g for 10 mins. Lysates were passed through a silica column by spinning at 10,000 × g for 1 min and then DNA bound to the column was washed with an acidic/salt buffer and then an ethanol based buffer. Plasmid DNA was eluted from the column using 10 mM Tris-HCl pH 8.5 or mQH_20.

Details of plasmids used and/or generated in this study are provided in the Appendix.

2.2.1 Cloning part of the Elp1 C-terminal domain into the GFP tagging vector pUG34

Sequences encoding part of the Elp1 C-terminal domain (amino acids 1181-1349) were amplified using Phusion DNA polymerase with primers containing built in *Spe*I (Forward primer) and *Xho*I (Reverse primer) restriction sites. The plasmid YCp-*ELP1*-6HA (or the equivalent plasmid carrying mutations in the basic region) were used as templates. The amplified Elp1 C-terminal sequences were subcloned using blunt end ligation into the pJET1.2 vector (Thermo scientific) and verified by diagnostic restriction digests and sequencing across the insert. The C-terminal fragments were then digested out from pJET1.2 using *Spe*I and *Xho*I enzymes and cloned into complementary sites in the pUG34 N-terminal green fluorescence protein (GFP) tagging vector. Diagnostic restriction digests were used to verify integration of the C terminal fragments.

2.2.2 Cloning the NES from HIV Rev into pFa6a-GFP(S65T)-HIS3MX6

Complementary primers encoding nuclear export sequence (NES) from HIV Rev were designed containing *Bam*HI (forward) and *Pac*I (reverse) overhangs. These primers were mixed in a 1:1 molar ratio (0.1 µM each), placed in boiling water and then allowed to cool slowly to room temperature for annealing to form a double stranded NES insert sequence. The annealed template was cloned between *Bam*HI and *Pac*I sites in frame with the GFP coding sequence in the Longtine pFa6a-GFP(S65T)-HIS3MX6 plasmid to make pFa6a-NES-GFP(S65T)-HIS3MX6. Positive clones were verified by bacterial colony PCR and sequencing across the cloned sequence. The final cloned plasmid was used as a template for C-terminal tagging of *ELP1* with an NES sequence.

2.2.3 Cloning the NLS from Cbp80 into pFa6a-GFP(S65T)-HIS3MX6

A 462 bp dsDNA sequence ('gBlock'; Integrated DNA technologies) was synthesised and used to replace the plasmid sequence between endogenous *Pac*I and *BsrG*I sites in pFa6a-GFP(S65T)-HIS3MX6. The *Pac*I and *Bsr*GI restriction sites lie upstream and within the GFP gene respectively. The gBlock was designed to reinstate the plasmid sequence, but with the inclusion upstream of the GFP gene of a sequence encoding the first 30 amino acids of the Cap binding protein 80 (Cbp80). This sequence contains a strong nuclear localisation sequence (NLS, Rahl et al., 2005). A mutant NLS version of this construct containing four alanine substitution mutations was also similarly generated. The 'gBlocks' (100 ng) were digested with *Pac*I and *Bsr*GI and cloned between the equivalent sites in pFa6a-GFP(S65T)-HIS3MX6, creating a plasmid with the Cbp80 NLS or mutant NLS encoded upstream of the GFP gene. Positive clones were verified by diagnostic restriction digests and sequencing across the cloned sequence. The final cloned plasmids pFa6a-NLS(Cbp80)-GFP(S65T)-HIS3MX6 and pFa6a-*NLS4A*(Cbp80)-GFP(S65T)-HIS3MX6 plasmids were used as templates for C-terminal tagging of *ELP1*.

2.2.4 Cloning the C-terminal domain of Elp1 into pGEX4T-1

For recombinant expression of Elp1, primers were designed to amplify the region encoding the C-terminal half (amino acids 730-1349) with built in *Eco*RI (forward primer) and *Xho*I (reverse primer) restrictions sites. The reverse primer also included a His_6 tag. This region of Elp1 is predicted to be mainly alpha helical. The C-terminus was amplified using Phusion DNA polymerase and genomic DNA preps from *ELP1*-GFP and *elp1-KR9A*-GFP strains as template. The amplified C-terminal sequence was cloned between *Eco*RI and *Xho*I sites in the Glutathione-S-transferase (GST) fusion expression vector pGEX4T-1 (kind gift from Angus Lamond). Positive clones were verified by

diagnostic restriction digests and DNA sequencing across the cloned insert in both directions to ensure there were no PCR based mutations.

2.2.5 Bacterial plasmid transformations

Bacterial transformations were carried out in chemically competent DH5 alpha *E. coli* (F^- *Φ80lacZΔM15 Δ(lacZYA-argF)U169 recA1 endA1 hsdR17* (r_K^-, m_K^+) *phoA supE44 λ– thi-1 gyrA96 relA1*) as previously described (Sambrook and Russell, 2006). Briefly, around 50-100 ng of plasmid DNA was added to competent *E. coli* cells and incubated for 30 min on ice with intermittent gentle swirling to mix. The cells were heat shocked for 90 sec at 42°C and immediately replaced on ice to recover for 2 min. Cells were allowed to recover in Super optimal broth (SOC) medium at 37°C with shaking for 45 min before being plated on Luria broth (LB) agar with plasmid selection (normally Ampicillin, abbreviated Amp). Transformation plates were grown overnight at 37°C and single colonies were inoculated into liquid LB with selection. These were cultured at 37°C overnight with shaking and plasmids isolated (Section 2.2).

For transformation of expression plasmids into chemically competent BL21 (DE3) *E. coli* (Stratagene: *F^- ompT gal dcm lon hsdSB*(r_B^- m_B^-) *λDE3* [*lacI lacUV5-T7 gene 1 ind1* s^{am}*7 nin5*]). The manufacturer's protocols were followed but differ from the above only in the time of heat shock at 42°C, which is reduced to 20 s. For long term storage of plasmid containing strains liquid overnights from single colonies were stored at -80°C in 20% (v/v) glycerol.

2.3 Fluorescence Microscopy

2.3.1 Checking yeast strains for fluorescent protein-tagged fusions

To check strains for expression of fluorescent protein-tagged fusions, cells from overnight cultures were harvested by centrifugation at 3000 rpm for 2 min and washed once with sterile mQH_20. Cell pellets were resuspended in low fluorescence synthetic complete (SC) medium or the appropriate selective medium and a small volume was inoculated onto a microscope slide and compressed with a coverslip. Cells were visualised with a Delta Vision RT microscope (Applied Precision) connected to a CCD camera (CoolsnapHQ / ICX285) using the appropriate channel setting to assay for a particular fluorescent tag.

2.3.2 Preparing fixed log phase yeast cells for fluorescence imaging

For fixed cell imaging, strains from overnight cultures were subcultured to log-phase (OD_{600}~ 1) at 30°C in the appropriate medium, allowing at least 2 doublings. Strains containing pUG34-*ELP1*-CTD plasmids were cultured in DOA -His -Met media to select for the plasmid and to induce the GFP tagged C-terminus. Strains containing genomic GFP tagged fusions were grown without selection in YPAD. The equivalent of 4.5 OD_{600} units (4.5 ml culture at OD_{600}=1) of each strain was fixed by adding formaldehyde at 3.7% (v/v) for 30 min with gentle agitation. Cells were harvested at 3000 rpm for 2 min, washed three times with 1× PBS and pipetted onto 0.2% (w/v) Concanavalin A (Sigma) treated coverslips. After immobilising for ~3-5 min, coverslips were placed on microscope slides onto which a small spot of antifade solution (0.5% (w/v) p-phenylenediamine, 20 mM Tris pH 8.8, 90% (v/v) glycerol) had been placed and then

sealed with nail varnish. Slides were allowed to dry for at least 2 hours, stored in the dark and imaged within 4 days.

2.3.3 Acquisition of 2D fluorescent images

Cells were visualised with a Delta Vision RT microscope (Applied Precision) connected to a CCD camera (CoolsnapHQ / ICX285) using an 100x lens (Olympus 1X-71) and 1.514 immersion oil. 2D images (512 x 512) were captured with Bin 2 x 2 mode (0.132 µm pixel size) under the following standard conditions;

Excitation/Emission Channel: mCherry, Exposure: 0.5 sec, ND filter: 100%

Excitation/Emission Channel: YFP-ET, Exposure: 1 sec, ND filter 100%

Excitation/Emission Channel: OPEN, Exposure: 0.05 sec, ND filter 10%

Flat field calibration was carried out before imaging for the YFP-ET channel using a fluorescent calibration slide (488-519 nm, Applied Precision) and applied during image acquisition. The mCherry exposure was sometimes altered within the range 0.35- 1 sec across experiments depending on factors such as bulb strength and age of slide. In any given experiment all settings were constant across samples and each field of view focused so the majority of cells were imaged through the middle of the cell. For quantification experiments at least 5-10 different fields of view were captured for each sample. Images were initially visualised using SoftWoRx (Applied Precision).

2.3.4 Quantification of 2D fluorescent images

Raw images were visualised and processed for figures using OMERO insight v4.4.0 (Allan et al., 2012). Quantification of raw images was performed using Volocity 6.0 (Perkin Elmer) and data processed with Microsoft Excel (Office 2010). Briefly, quantification protocols identified whole cell objects using YFP-ET channel and nuclear objects using the mCherry channel. The intensity values were calculated for each compartment and the GFP signal within the nucleus intersected with the whole cell object. Thresholds for identification of whole cell objects were applied using strains without a GFP tag as a guide to identify intensities generated by autofluoresence. The intensity information for each object was exported to Microsoft Excel and averages were calculated for each set of images.

2.4 Protein Biochemistry

2.4.1 Protein extraction using NaOH/TCA method

Strains were grown to log phase (OD_{600}~ 1) and typically 5-10 OD_{600} units were harvested by centrifugation at 3000 rpm, 2 min. Yeast protein extracts were prepared using the NaOH-TCA method (Horvath and Riezman, 1994) as follows. Cell pellets were resuspended in 200 µl of NaOH buffer (1.85 mM NaOH, 7.4% (v/v) β-mercaptoethanol) by vortexing and incubated on ice for 10 min. An equal volume of 20% (v/v) TCA was added, mixed by inverting and incubated on ice for a further 10 min. Protein pellets were harvested at 14,000 rpm for 2 min, washed with acetone and allowed to air dry briefly. Pellets were incubated with 200 µl of 2× Laemmli buffer (125 mM Tris-HCl pH 6.8, 4% (w/v) SDS, 20% (v/v) glycerol, 0.01% (w/v) Bromophenol Blue, 5% (v/v) β-

mercaptoethanol) for 10 min at room temperature then resuspended by disrupting the pellet with a pipette tip. Samples were incubated at 75 °C for 15 min and centrifuged at 14,000 rpm for 30 sec. The supernatant containing dissolved proteins was removed into a fresh tube and 5-10 µl used for SDS-PAGE analysis (Section 2.4.5).

2.4.2 Yeast protein extraction by bead beating lysis

Strains were grown to log phase (OD_{600}~ 1) and typically 50-100 OD_{600} units (50-100 ml at an OD_{600}=1) were harvested by centrifugation at 3000 rpm, 2 min. Cell pellets were snap frozen and stored at -80°C until use. Lysis by bead beating was used to prepare yeast protein extracts as described below. To minimise protein degradation all further steps are carried out at 4°C.

Pellets were defrosted slowly on ice and resuspended in cold Lysis Buffer (50 mM HEPES pH 7.5, 2 mM $MgCl_2$, 150 mM NaCl, 0.1% (v/v) Triton X-100, 50 mM NaF, 50 mM Na-β-glycerophosphate) supplemented with Complete EDTA free Protease inhibitor (Roche), PhosSTOP (Roche), 1 mM AEBSF and 2 mM Na_3VO_4 . Typically 10 µl /OD_{600} was added to pellet (i.e. 0.5 ml to 50 OD_{600} unit pellet). The resuspended cell pellets were added to 1.5 ml screw cap tubes filled two thirds full with cold 0.5 mm glass beads (BioSpec products) so that liquid and beads completely filled the tube. If necessary multiple tubes were set up to accommodate each resuspended pellet and these were mixed well by vortexing. Cells were lysed using a bead beater (BioSpec products) at intervals of 4 × 30 sec with 1 min hold and then 2 × 1 min with 2 min hold. Cell suspensions were checked using a bright field microscope (Zeiss) and typically around 70-90% cell lysis was achieved. Lysates were separated from the glass beads by pricking the bottom of the screw cap tubes with a microlance syringe needle and quickly placing into 1.5 ml microfuge tubes on ice, followed by centrifugation at 3000

rpm for 30 sec. Lysates were then cleared by centrifugation at 14,000 rpm for 10 min and the supernatant removed into a fresh tube. For larger cultures, above 100 $OD_{600,}$ resuspended cell pellets were added to 7 ml specimen tubes filled two thirds full with cold 0.5 mm glass beads. Cell lysis by bead beating was as described above but using the larger sized tube holder for the bead beater.

Protein extracts were normalised using Bradford Coomassie reagent (Pierce) by standard methods. Briefly, a dilution of protein extract (typically 1 in 10) was added to Bradford reagent and then OD_{595} values were measured. Protein concentrations were estimated using the relationship Absorbance OD_{595} /(mg/ml) = 0.05.

2.4.3 Expression, purification and coupling of GFP-Trap to Sepharose

GFP-Trap is a single heavy chain antibody derived from Llama which recognises GFP (Rothbauer et al., 2008). GFP-Trap was expressed from a pGEX4T-1 plasmid in BL21 (DE3) *E. coli* (kind gift from Angus Lamond), purified using standard GST affinity purification techniques (GE Healthcare, 2012) and coupled to cyanogen bromide (CNBr) activated Sepharose.

For expression of GFP-Trap, starter cultures in LB-Amp were grown at 37°C with shaking for 8-12 hours and then inoculated 1 in 100 into Autoinduction medium containing Amp (i.e. 5 ml starter in 500 ml). Expression cultures were grown at 25°C with shaking for 72 hours and induction of GST tagged GFP-Trap occurred upon saturation of the culture. Cultures were harvested by centrifugation at 5250 × g, 4°C with slow deceleration and pellets were resuspended (25 ml/500 ml culture) in cold 1× PBS with Complete EDTA Protease inhibitors (Roche). The resuspended pellets were snap frozen and stored at -80°C. Unless stated otherwise all further steps were carried out at 4°C to minimise protein degradation.

For lysis, resuspended pellets were defrosted slowly and then treated with Lysozyme (1 mg/ml, Sigma) for 30 min with rotation. The lysates were supplemented with $MgCl_2$ to 10 mM and treated with DNase I (~4 µg/ml, Sigma) for a further 30 min. Finally, Triton X-100 at 1% (v/v) was added and lysates were sonicated on ice with 10 sec bursts at 60% power until no longer cloudy (typically 40 sec total). Sonicated lysates were cleared by centrifugation at 20,000 × g for 30 min and the supernatant retained for affinity purification using the GST tag.

Lysates were added to Glutathione-Sepharose Fast flow 4 resin (GE Healthcare) prewashed with 1× PBS (2 ml bead resin/ 500 ml culture) and incubated overnight with end-over rotation. The resin was harvested at 1000 rpm and washed twice with 1 x PBS before being added to a purification column (Pierce). The resin was further washed by gravity flow with 30 ml 1× PBS, 20 ml 1× Tris buffered Saline (TBS) and then 20 ml 1× Thrombin cleavage buffer (50 mM Tris HCl pH 8, 10 mM $CaCl_2$). The resin was incubated with 10 U of Thrombin in 1× Thrombin cleavage buffer at room temperature overnight for cleavage of the GST tag. The GFP-Trap protein was eluted from the column at room temperature using 10 ml 1× Thrombin cleavage buffer and fractions were collected and analysed by SDS-PAGE (Section 2.4.5). The concentration of GFP-Trap was determined by absorbance at 280 nM using the calculated extinction coefficient.

Fractions containing GFP-Trap were pooled and coupled to CNBr Sepharose (GE Healthcare) at a concentration of 5-10 mg/ml protein per ml of Sepharose, as follows. GFP-Trap was dialysed overnight using 6-8 kDa cut off dialysis tubing (SpectroPor) into CNBr Sepharose coupling buffer (0.1 M Na_2CO_3, 0.5 M NaCl pH 8.3) and concentrated using a 10 kDa cut off column (Amicon), if required. CNBr Sepharose was rehydrated in

10 mM HCl for 30 min at room temperature, pelleted by centrifugation at 1000 rpm and then washed three times with 10 mM HCl. Working quickly, the beads were washed in CNBr coupling buffer and then completely drained. Purified GFP-Trap was added to the beads to make a 50% slurry and then left to couple for 2-8 hours at room temperature with gentle rotation. The beads were pelleted and then blocked with 10 bead volumes of 100 mM Tris-HCl pH 7.4 for 8 hours at room temperature with gentle rotation. The GFP-Trap Sepharose was stored at 4°C as 50% slurry in TBS with 0.02% (v/v) sodium azide.

2.4.4 GFP tagged protein pulldowns using GFP-Trap Sepharose

Protein extracts from GFP tagged strains, made by bead beating lysis, were normalised typically to ~8 mg/ml in cold Lysis Buffer (50 mM HEPES pH 7.5, 2 mM $MgCl_2$, 150 mM NaCl, 0.1% (v/v) Triton X-100, 50 mM NaF, 50 mM Na-β-glycerophosphate) supplemented with Complete Protease Inhibitors (Roche), PhosSTOP (Roche), 1 mM AEBSF and 2mM Na_3VO_4. To minimise protein degradation extracts were kept on ice or at 4°C throughout. A small sample ($1/10^{th}$ volume) of each normalised extract was added to an equal volume of 2× Laemmli buffer and incubated at 75°C for 15 min; this served as the input sample.

Protein extracts were precleared with Sepharose-4B beads (Sigma) for 30 min with end-over rotation. In general 0.5 µl of bead slurry was used per 1 OD_{600} unit of extract (i.e. 25 µl was used for 50 OD_{600} units of cells). Precleared extracts were harvested by centrifugation at 1000 rpm for 1 min and added to GFP-Trap slurry for 2 hours with end-over rotation. In general 1 µl of GFP-Trap slurry was used per 1 OD_{600} unit of extract (i.e. 50 µl was used for 50 OD_{600} units of cells). GFP-Trap pulldowns were harvested by centrifugation at 1000 rpm for 1 min. A small sample ($1/10^{th}$ volume) of

the supernatant was added to an equal volume of 2× Laemmli buffer and incubated at 75°C for 15 min, this served as the flow through sample. GFP-Trap pulldown beads were washed three times with Lysis buffer and proteins were eluted from the beads by adding 50 µl 2× Laemmli buffer and incubating at 75°C for 15 min. This elution step was repeated twice and the two sequential eluates were pooled.

In general, for GFP pulldowns to assay complex assembly the equivalent of 50 OD_{600} units of cells were used and for pulldowns coupled to mass spectrometry 250 OD_{600} units were used.

2.4.5 Separation of proteins by SDS-PAGE

Precast 4-12% NuPage Bis-Tris Gels were used to separate protein samples in 1× MOPS SDS running buffer (50 mM MOPS, 50 mM Tris Base, 0.1% SDS, 1 mM EDTA, pH 7.7, LifeTech) supplemented with NuPage Antioxidant (Proprietary). Gels were run in an XCell Surelock electrophoresis tank at 200V for 60-80 min and then either stained or used for western blotting. All equipment and reagents were supplied by Novex.

2.4.6 Protein Gel staining

Gels were added to Instant Blue stain (Expedeon) in petri dishes with gentle agitation for 1 hour-overnight and protein bands visualised with a light box. For SYPRO Ruby staining (Molecular probes) gels were first fixed with 50% methanol, 7% acetic acid for 60 min and then stained overnight with SYPRO Ruby in foil wrapped petri dishes with gentle agitation. Gels were then washed once with 10% methanol, 7% acetic acid for 30 min , rinsed with mQH_20 and then scanned using a fluorescent image analyser (FLA-5100 Fujifilm) using the LPB setting (473 nm).

2.4.7 Western Blotting

Protein samples separated by SDS-PAGE were electrotransferred to a PVDF membrane (Immobilon) in 1× Towbin buffer (25 mM Tris, 192 mM glycine, 10% methanol). Briefly, the membrane was activated using Methanol before being placed over the SDS-PAGE gel and sandwiched between two filter papers and two foam sponges, rolling out all air bubbles between layers. This was sealed inside a transfer cassette and placed into a Mini Trans Blot tank (Bio-Rad) with the gel side nearest the cathode. Transfer was carried out at 100 V for 60-80 min with an ice pack for cooling. Membranes were then blocked with gentle agitation for 1 hour in TBS-T (Tris buffered saline, 0.02% (v/v) Tween) with 5% (w/v) dried non-fat milk. When using phosphospecific antibodies milk was substituted with 4% (w/v) Bovine serum albumin (BSA). Primary antibodies were diluted in the equivalent blocking solution and added to membranes overnight at 4°C with rotation. After incubation with primary antibody membranes were washed three times for 10 min with TBS-T before being incubated with the appropriate secondary antibody conjugated to horse radish peroxidase (HRP). All secondary antibodies were diluted 1 in 10,000 in 5% (w/v) dried non-fat milk TBS-T and incubated with blots for 1 hour with rotation. The blots were washed three times for 10 min with TBS-T before being developed using Enhanced Chemiluminescent HRP Substrate (Immobilon) and visualised using the LAS-4000 chemiluminescence imager (Fujifilm). Details of all antibodies used in this study are shown in Table 2.2. Analysis by densitometry of bands was carried out using Aida Image Analyzer v.3.27 and values exported to Microsoft Excel (Office 2010). Statistical analyses were carried out using SigmaPlot 12.0 (Systat Software, Inc).

Table 2.2. Antibodies used in this study

Antibody	Dilution	Host	Source	Code
Anti-GFP	1 in 1000	Mouse	Roche	11814460001
Anti-HA	1 in 3000	Mouse	Santa Cruz	sc-7392
Anti-Cdc28	1 in 10,000	Goat	Santa Cruz	sc-6709
Anti-Myc	1 in 10,000	Rabbit	Santa Cruz	sc-789
Anti-His	1 in 5000	Rabbit	Santa Cruz	sc-803
Anti-GST	1 in 5000	Mouse	Sigma	G1160
Anti-pSer	1 in 1000	Rabbit	ImmunoK	220-15-1PSER
Anti-1209p-Elp1	1 in 3000	Rabbit	This Study	-
Anti-Non phospho-Elp1	1 in 3000	Rabbit	This Study	-
Anti-Mouse IgG	1 in 10,000	Donkey	GE Healthcare	NA931V
Anti-Rabbit IgG	1 in 10,000	Donkey	Santa Cruz	sc-2004
Anti-Goat IgG	1 in 10,000	Donkey	Santa Cruz	sc-2020

2.4.8 Antibody Production

An anti-phospho-1209S Elp1 antibody was generated for use in this study using a peptide antigen and Rabbit hosts. The peptide sequence used for immunisation was H_2N-CTSTQE-pS-FFTRY-$CONH_2$ where pS indicates phosphoserine. The antipeptide antibody was produced and purified by Biogenes using standard procedures as indicated on their website (http://www.biogenes-antibodies.com). Briefly, the phosphospecific fraction of the final bleed was purified by serum depletion using immobilised non-phosphorylated peptide (H_2N-CTSTQESFFTRY-$CONH_2$). The phosphospecific antibodies were then isolated from the depleted serum using the immobilised phosphopeptide. This procedure also generated a non-phosphospecific fraction from the first step. The purified antibody was tested for phosphospecificity by loss of signal against protein extracts prepared from an *elp1-1209A* mutant and by competition with the phosphopeptide. The antibody was stored at -20°C in 50% (v/v) glycerol and the conditions for use are described (Table 2.2). A small excess of the non-

phosphorylated peptide was normally added to the primary dilution before use to prevent any cross-reaction with the non-phosphorylated epitope.

2.4.9 Expression and purification of the Elp1 C-terminal domain

The C-terminal domains of Elp1 and Elp1-KR9A were expressed from a pGEX4T-1 plasmid transformed into BL21 (DE3) *E. coli* (Stratagene). The constructs express these proteins with an N-terminal GST tag and C-terminal His_6 tag for dual affinity purification. A GST-His_6 plasmid was expressed and purified alongside these as a control (kind gift from Tom Owen Hughes).

For expression of the Elp1 and Elp1-KR9A fusion proteins, starter cultures in LB-Amp were grown at 37°C with shaking for 8-12 hours and then inoculated 1 in 50 into Autoinduction medium with Amp (i.e. 10 ml starter into 500 ml). Expression cultures were grown at 30°C with shaking for 4-5 hours and then the temperature was reduced to 25°C overnight. Expression was induced upon saturation of cultures and was tested by taking a small sample of culture and boiling in an equal volume of 2× Laemmli buffer for western blotting against affinity tags.

Cultures were harvested by centrifugation at 5250 × g, 4 °C with slow deceleration and pellets were resuspended (25 ml/500 ml culture) in cold Lysis buffer (20 mM Tris HCl pH 7.5, 300 mM NaCl) supplemented with Complete EDTA free Protease inhibitors (Roche). The resuspended pellets were snap frozen and stored at -80°C. All further steps are carried out at 4°C to prevent protein degradation.

For lysis, resuspended pellets were defrosted slowly and then treated with Lysozyme (1 mg/ml, Sigma) for 30 min with rotation. The lysates were supplemented with $MgCl_2$ to 10 mM and treated with DNAse I (~4 µg/ml, Sigma) for a further 30 min. Lysates

were sonicated on ice with 10 sec bursts at 60% power until no longer cloudy (typically 40 sec total) and lysis was checked by bright field microscopy. Sonicated lysates were cleared by centrifugation at 20,000 × g for 30 min and the supernatant used for affinity purification.

Lysates were added to HisPur Cobalt resin (Thermo scientific) prewashed with Lysis Buffer (1 ml bead resin/500 ml culture) and incubated for 2 hours at 4°C with rotation. The resin was harvested at 1000 rpm and added to a purification column (Pierce). The resin was further washed by gravity flow with 20 ml of Lysis Buffer and then His_6 tagged proteins were eluted using 1 ml, 2 ml and 3 ml of HisPur Elution Buffer (20 mM Tris HCl pH 7.5, 300 mM NaCl, 300 mM Imidazole). For each elution step the resin was incubated in HisPur Elution Buffer for 10 min with rotation before the eluate was collected by gravity flow.

Eluates from the HisPur resin were pooled and Dithiothreitol (DTT) to 10 mM was added. The HisPur eluate was added to Glutathione-Sepharose Fast Flow 4 resin (GE Healthcare), prewashed with HisPur Elution buffer (2 ml bead resin/500 ml culture) and incubated for 3 hours with rotation. The resin was harvested at 1000 rpm and washed with 10 ml HisPur elution buffer before being added to a purification column (Pierce). The resin was further washed by gravity flow with 20 ml Lysis Buffer and then GST tagged proteins eluted with 2 ml then twice with 3 ml of GST elution buffer (50 mM Tris HCL pH 8, 50 mM reduced Glutathione). For each elution step the resin was incubated in GST elution buffer for 10 min at 4°C with rotation before the eluate was collected by gravity flow.

Eluates from the Glutathione resin were pooled and diafiltered into Protein Binding Buffer (20 mM Tris HCl pH 7.5, 150 mM NaCl, 2 mM $MgCl_2$) using a 10 kDa cut off

column (Amicon) according to manufacturer's instructions. Briefly, the pooled eluates were added to the column, made up to 10 ml with Protein binding buffer and concentrated 10-20 fold by centrifugation at 14,000 rpm for 10-15 min. This step was repeated twice and then the concentrated eluate was collected.

The recombinant protein preps were stored at -20°C in 50% glycerol until use when they were diafiltered back into Protein Binding Buffer as above. Recombinant proteins were normalised by absorbance at 280 nM using the extinction coefficient of the full length tagged proteins. Throughout the purification, samples of inputs, bound, flowthroughs, eluates and post elution bound were boiled in 2× Laemmli buffer for SDS-PAGE analysis. Recombinant protein preps were checked by western blotting for affinity tags and by peptide mass fingerprinting.

2.4.10 Mass spectrometry analysis of protein samples

Preparation of samples by in-gel trypsin digest was carried out by Kelly Hodge and processed by the University of Dundee Mass spectrometry facility (http://proteomics.lifesci.dundee.ac.uk/). Briefly, each band was incubated in 100 mM NH_4HCO_3 ,100% (v/v) acetonitrile (ACN) and incubated at room temperature for 10 min with shaking. This step was repeated and liquid removed before sequential addition of 100% (v/v) ACN then 100 mM NH_4HCO_3 and incubation for 30 min at 37°C with shaking. Gel pieces were dried and then incubated in 10 mM DTT for 45 min at 55°C. Liquid was again removed and gel pieces incubated in 55 mM iodoacetamide for 30 min in the dark. Gel pieces were washed twice, as above, with 100 mM NH_4HCO_3 , 100% (v/v) ACN and then dried. For digestion, 20 ng/µl of trypsin was added in 50 mM NH_4HCO_3 and left overnight at 37°C. To the digests a roughly equivalent volume of 0.1% (v/v) trifluoroacetic acid (TFA) followed by 100% (v/v) ACN was added and the gel

pieces were sonicated on ice for 15 min. The supernatant containing tryptic peptides was removed into a new tube and sonication of the gel pieces was repeated with 0.1% (v/v) TFA, 30% (v/v) ACN and then 0.1% (v/v) TFA, 50% (v/v) ACN. The supernatants from all sonication steps were pooled, concentrated in a vacuum centrifuge at 60°C and then cleaned on a C18 column.

For pulldown experiments, samples were analysed on a Velos Pro (Thermo Scientific Fisher, Boston) Orbitrap mass spectrometer coupled to an Ultimate 3000 RSLC nanoflow HPLC system (Dionex, Sunnyvale California). Sample volumes of 5 µl were eluted over a 100 min run on a 50 cm C18 column (75 µm × 50 cm nanoviper column, Thermo Scientific Boston). Samples were injected using the EasySpray source and run gradient was a 2–40% linear gradient of solvent A (0.1% formic acid): solvent B (80% ACN with 0.8% formic acid) at a flow rate of 0.3 µl/min. For recombinant protein fingerprinting samples were run on the XL Orbitrap mass spectrometer coupled to the HPLC system described above. The run gradient was as described above except that samples were eluted over a 40 min run on a 15 cm C18 column (15cm × 75µm pepmap column, Thermo Scientific Boston). Raw data was analysed using Maxquant version 1.3.0.5 run against the appropriate protein databases. Microsoft Excel (Office 2010) was used for further analysis. For pulldown experiments, the intensity values of proteins detected in the pulldowns was normalised by the total intensity value (intensity in sample plus intensity in bead control) of the corresponding protein to give an enrichment value. Population statistics were used to check the distribution of the data. In general, a ratio lower than 0.75-0.8 was classed as non-significant enrichment. A ratio of 1 for a protein indicates that there was no protein detected in the bead control sample. Posterior error probability (PEP) values act as a p value for probability of correct protein identification.

2.5 RNA Analysis and binding

2.5.1 GFP tagged protein pulldowns for analysis for associated RNAs

Typically around 100 OD_{600} units of cells were used for each GFP-Trap pulldown. These were carried out essentially as described previously (Sections 2.4.2 and 2.4.4), up to the point of elution from the GFP-Trap beads, with minor changes as follows. Separate RNase free reagents, tubes and pipettors were used throughout and gloves were changed frequently. Lysis buffer was also supplemented with 100 U/ml of Ribolock RNase inhibitor (Fermentas) and the concentration of normalised protein extract was higher, typically around 10-12 mg/ml. As the RNA input sample $1/10^{th}$ the volume of normalised extract was added to 300 µl Tripure Reagent (Roche), snap frozen and stored at -80°C.

After the final wash step, elution was carried out by adding to the beads 100 µl of TE buffer (10 mM Tris-Cl, pH 7.5. 1 mM EDTA, Ambion) supplemented with 1% (v/v) SDS and 2.5% (v/v) β-Mercaptoethanol. These were incubated at 75°C for 15 min and the supernatant removed to a new RNase free tube. This elution step was repeated and the supernatants pooled. To check GFP pulldown efficiency, 50 µl of eluate was added to an equal volume of 2× Laemmli buffer for western blot analysis. The remaining 150 µl of eluate was added to 300 µl Tripure Reagent (Roche), snap frozen and stored at -80°C. RNA extractions were carried out as described in Section 2.5.2.

2.5.2 RNA Extraction

RNA was extracted from samples in Tripure reagent (a mixture of phenol and guanidine thiocyanate, pH 4, Roche) following the manufacturer's protocols. Briefly, chloroform was added to the samples (0.3 ml/ml of Tripure) and shaken for 15 sec.

Once mixed these were left at room temperature for 15 min to allow phases to separate. Samples were centrifuged at 12,000 × g, 4°C for 15 min and the aqueous phase containing RNA was carefully removed into a new tube. RNA was precipitated at -20°C using 2.5 volumes of 100% ethanol, 0.3 M sodium acetate pH 5.5, 10 mM $MgCl_2$ and 20 µg of glycogen. The RNA pellet was harvested by centrifugation at 20,000 × g, 4°C for 30 min and then washed once using 75% cold ethanol. The pellet was air dried and resuspended in an appropriate volume of RNase free water (10-100 µl). To remove any small contamination with genomic DNA, the resuspended RNA was treated with RNase free DNase I (Fermentas). RNA was mixed with 1 × DNase I buffer (10 mM Tris-HCl pH 7.6, 2.5 mM $MgCl_2$, 0.5 mM $CaCl_2$) and 2 Units of DNase I and incubated at 37°C for 15 min. The enzyme was inactivated by the addition of EDTA to 5 mM and heating to 75°C. The yield of RNA was calculated by absorbance at 260 nm and samples were snap frozen and stored at -80 °C. Small RNA extractions were carried out as described above except after obtaining the aqueous phase a subtractive precipitation using ~2.5 M LiCl was carried out at -20 °C for 3 hours to remove RNAs larger than ~200 bp. The supernatant was then precipitated and processed as above.

2.5.3 Radiolabelling of DNA oligonucleotide probes

Radiolabelling of oligonucelotide (oligo) DNA probes for northern blot analysis was carried out using T4 polynucleotide kinase (Fermentas) and [γ-^{32}P]ATP (Perkin Elmer), under the following conditions. For each labelling reaction 10 pmol of oligo was heated at 95°C for 30 sec and then immediately placed on ice. The oligo was added to 1× Forward buffer A (50 mM Tris-HCl pH7.6, 10 mM $MgCl_2$, 5 mM DTT, 0.1 mM spermidine), 10 units of T4 polynucleotide kinase and ~1 µM of [γ-^{32}P]ATP (specific activity 6000 Ci/mmol). Reactions were incubated at 37°C for 1-2 hours and then

unincorporated nucleotides were removed using a G-25 microspin column (GE healthcare). For each northern blot, 10 pmol of 5' end labelled oligo was used as a probe. The sequences of oligo probes used in this study are shown in the Appendix.

2.5.4 Radiolabelling yeast tRNA

Yeast tRNA (R9001, Sigma) was resuspended in RNase free water and the concentration determined using absorbance at 260 nm. The quality of tRNA was also checked by small RNA gel electrophoresis (Section 2.5.5). Yeast tRNA was treated with Fast alkaline phosphatase (Fermentas) to remove the endogenous 5' phosphate before radiolabelling. For each reaction 4 pmol of yeast tRNA was mixed with 1× FAP buffer (10 mM Tris-HCl pH 8.0, 5 mM $MgCl_2$, 0.1 M KCl, 0.02% (v/v) Triton X-100, and 0.1 mg/ml BSA), 10 U of Ribolock RNase inhibitor and 2 U of Fast alkaline phosphatase. Reactions were incubated at 37°C for 1 hour and then heat inactivated. Radiolabelling was carried out using T4 polynucleotide kinase (Fermentas) and [γ-^{32}P]ATP (Perkin Elmer), under the following conditions. The inactivated phosphatase reactions were made up with 1× Exchange buffer B (50 mM imidazole-HCl pH 6.4 , 18 mM $MgCl_2$, 5 mM DTT, 0.1 mM spermidine and 0.1 mM ADP), 8 units of Ribolock RNase inhibitor, 10 U of T4 polynucleotide kinase and ~1 µM of [γ-^{32}P]ATP (specific activity 6000 Ci/mmol). Reactions were incubated at 37°C for 2 hours and then the kinase was inactivated by addition of EDTA at 8 mM and heating. Unincorporated nucleotides were removed using a G-25 microspin column (GE healthcare) and radiolabelled tRNA was snap frozen and stored at -20°C.

2.5.5 Small RNA gel electrophoresis

Precast 10% TBE-Urea Gels were used to separate RNA samples in ultrapure 1× TBE running buffer (100 mM Tris-base pH 8.4, 90 mM boric acid, and 1 mM EDTA, LifeTech)

made up in twice autoclaved mQH_20. RNA samples were added to 2× TBE-Urea loading dye, incubated at 75°C for 5-10 min then immediately placed on ice, to denature secondary structure. Typically around 100-300 ng of RNA was loaded per lane. Gels were run in an XCell Surelock electrophoresis tank at 180 V, 4°C for 60-80 mins, until the Bromophenol Blue dye front was near the bottom of the gel. All equipment and reagents were supplied by Novex (LifeTech).

2.5.6 SYBR Gold nucleic acid staining

RNA gels were added to SYBR Gold stain (Molecular probes), diluted 1 in 10,000 in 1× TBE. Staining was carried out in sterile petri dishes, covered in foil, with gentle agitation for 30 min then rinsed briefly with sterile mQH_20. To visualise bands, gels were scanned using a fluorescent image analyser (FLA-5100 Fujifilm) on the LPB setting (473 nm).

2.5.7 Northern Blotting

RNA samples were separated by RNA gel electrophoresis (Section 2.5.5) and then electrotransferred to a Hybond XL membrane in ultrapure 0.5× TBE (50 mM Tris, 45 mM boric acid, and 0.5 mM EDTA, LifeTech). Briefly, the membrane was soaked in transfer buffer before being placed over the RNA gel and sandwiched between four filter papers and foam sponges, rolling out all air bubbles between layers. This was sealed inside the transfer module and placed into an X Cell Blotting tank (Novex) with the gel side nearest the cathode. Transfer was carried out at 30 V for 1-2 hours at 4°C. Membranes were auto crosslinked on both sides using a UV Stratalinker (254 nm) and blocked with Perfecthyb Plus hybridisation buffer (Sigma) for 2-3 hours at 42°C with rotation. For each blot 10 pmol radiolabelled oligo probe was added to the hybridisation buffer and allowed to bind at 42°C overnight with rotation. Membranes

were typically washed twice for 10 min at 42°C with 4× SSC (750 mM NaCl and 75 mM sodium citrate pH 7.0) and then 2× SCC (375 mM NaCl and 37.5 mM sodium citrate pH 7.0). Between washes the counts on the membrane were monitored with a Geiger counter to determine when enough background radioactivity had been removed. Autoradiography was carried out by exposures to Phosphoimager film and bands visualised by scanning using the fluorescent image analyser (FLA-5100 Fujifilm) on the IP-S setting. Analysis by densitometry of bands was carried out using Aida Image Analyzer v.3.27 and values exported to Microsoft Excel (Office 2010).

2.5.8 Electrophoretic Mobility Shift Assays

For Electrophoretic mobility shift assays (EMSAs), recombinant protein was mixed with tRNA in binding buffer (20 mM Tris HCl pH 7.5, 150 mM NaCl and 2 mM $MgCl_2$) and allowed to equilibrate for 45 min at room temperature.

For EMSAs with excess tRNA, each binding reaction consisted of 0.4 mM (~200 ng) of tRNA, 5% (v/v) glycerol and 20 U Ribolock RNase inhibitor mixed with the appropriate concentration of protein in a final volume of 20 µl. Binding reactions were separated on 6% polyacrylamide gels in ultrapure 0.5× TBE running buffer at 100 V for 1 hour. A small amount of 6× Gel Pilot loading dye (Qiagen) was run alongside reactions to monitor separation and gels were pre run for 15-30 min. Gels were stained with SYBR gold (Section 2.5.6) and scanned using a fluorescent image analyser (FLA-5100 Fujifilm) on the LPB filter (473 nm). Immunoblot EMSAs were carried out the same way, except part of the gel was treated with 0.5% (v/v) SDS for 15 min before being transferred to PVDF membrane, as described (Section 2.4.7), using 1× Towbin buffer without methanol. The blots were then soaked in 10% acetic acid and air dried before western blotting to detect GST and His_6 tags.

For EMSAs with radiolabelled tRNA, each binding reaction consisted of 1 nM ^{32}P-tRNA, 8% (v/v) glycerol and 10 U Ribolock RNase inhibitor mixed with the appropriate concentration of protein in a final volume of 12 µl. Binding reactions were typically separated on 4-20% polyacrylamide gels in ultrapure 0.25× TBE running buffer (25 mM Tris, 22.5 mM boric acid, 0.25 mM EDTA, LifeTech) at 100 V in an ice bucket. Reactions were run into the gel at 300 V for 10-15 min and then the voltage was reduced to 150 V-180 V (to give a current of ~7 mA) for a total time of 90 min. For 5% polyacrylamide gels the running time was 45 min. A small amount of 6× Gel pilot loading dye (Qiagen) was run alongside reactions to monitor separation and gels were pre run for 45 min. Gels were dried at 80°C for 90 min on a vacuum gel drier (Bio-Rad) before autoradiography was carried out by exposures to Phosphoimager film. Bands were visualised by scanning using the fluorescent image analyser (FLA-5100 Fujifilm) on the IP-S setting. Analysis by densitometry of bands was carried out using Aida Image Analyzer v.3.27and values exported to Microsoft Cxcel (Office 2010). For estimation of dissociation constant EMSA experiments the conditions were as described above except that 0.1 nM ^{32}P-tRNA was used per binding reaction. Competitor EMSA experiments were as described above, except binding reactions were allowed to proceed without competitor for 25 min and then the complexes were challenged by the addition of competitor for a further 25 min. Competitor binding reactions were also made up for a final volume of 15 µl.

For EMSA separation on agarose gels, binding reactions were as described above except that these were separated on a 1.5% agarose gel in ultrapure 0.5× TBE running buffer at 120 V in an ice bucket. Reactions were run at 120 V for a total time of ~70 min. A small amount of 6× Gel pilot loading dye (Qiagen) was run alongside reactions to monitor separation and gels were pre run for 30 min. Gels were fixed for 5 min in

10% methanol, 10% acetic acid and dried at room temperature for 3 hours on a vacuum gel drier (Bio-Rad) before autoradiography as described above.

Chapter 3: A basic region in the Elp1 subunit of Elongator is essential for tRNA modification but does not affect localisation of the complex

3.1 Introduction

A putative nuclear localisation sequence (NLS) was previously annotated in the C-terminal domain of the Elp1 subunit of Elongator (Fichtner et al., 2002b). Truncation of the C-terminus, including this lysine/arginine rich basic region results in resistance to Zymocin indicating that it may be essential to Elongator function (Fichtner et al., 2003). A high level of sequence conservation from yeast to humans also highlights its likely importance (Figure 3.1A). The consensus sequence for a classical bipartite NLS is $(K/R)(K/R)X_{10\text{-}12}(K/R)_{3/5}$ (i.e. two basic residues followed by a spacer of 10 amino acids then 3/5 basic residues) and this would be expected to bind importin-α (Lange et al., 2007, Kosugi et al., 2009a). The putative Elp1 NLS resembles this bipartite type NLS and is compared with a "classical" NLS sequence from *X. laevis* Nucleoplasmin in Figure 3.1B. The Elp1 putative NLS is not highlighted by the NLS prediction programme cNLS Mapper (Kosugi et al., 2009b) as a bipartite nuclear localisation sequence even at the lowest cut-off, but is identified using NLSstradumus (Nguyen Ba et al., 2009). The programs use different methods of prediction; cNLS Mapper marks each amino acid to give an NLS score based on known NLS sequences to predict nuclear import activity, whereas NLSstradumus relies on the frequency of lysine and arginine within a region. It should be noted that although the putative NLS of Elp1 does resemble the classical bipartite NLS, many annotated NLS sequences are non-functional in the context of the full protein. This is exemplified by the fact that the number of predicted NLS sequences in the yeast genome exceeds the number of nuclear localised proteins (Kosugi et al., 2009a). Basic regions in proteins may therefore be required for other interactions and never see the cell's nuclear import machinery. It is also worth noting that in the

alignments (Figure 3.1A) the general basicity of the region in Elp1 is conserved but the exact consensus of the putative bipartite NLS is not.

A

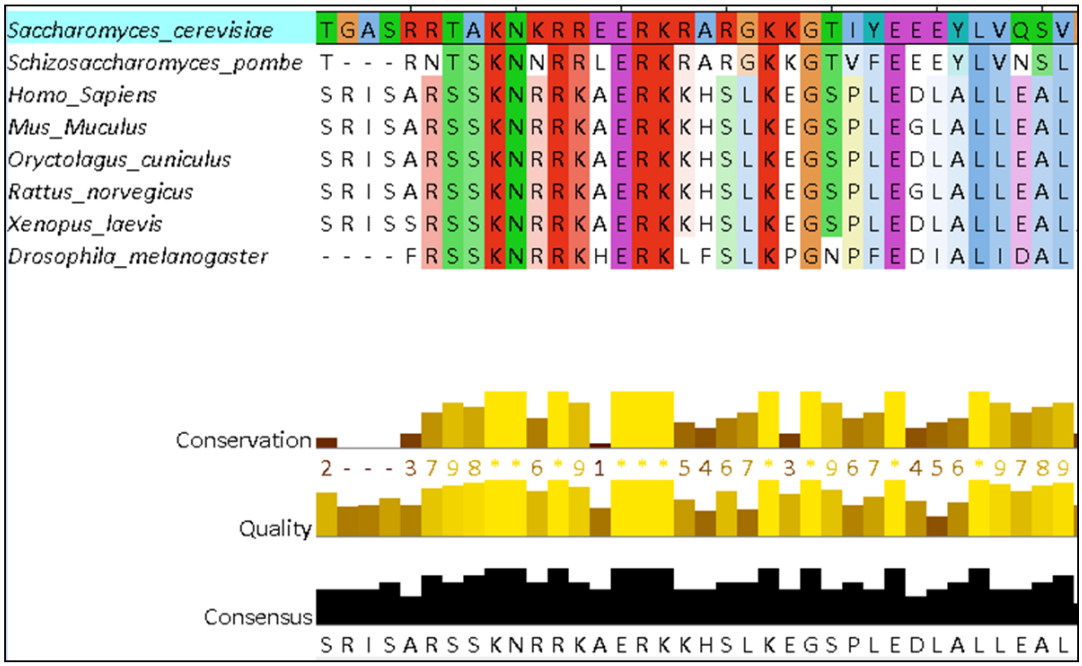

B

(K/R)(K/R)X$_{10\text{-}12}$(K/R)$_{3/5}$	Bipartite NLS consensus
RRTAKNKRREERKRARGKK	Elp1 putative NLS
KRPAATKKAGQAKKKK	Nucleoplasmin NLS

Figure 3.1: A basic region in Elp1 is highly conserved and annotated as a putative NLS.
A) Multiple sequence alignment of the Elp1 subunit of Elongator from various eukaryotic organisms. The basic region is displayed to highlight conservation, indicated by matching colours and the conservation bars. Alignment was carried out using Clustal Omega (http://www.ebi.ac.uk/Tools/msa/clustalo/) and Jalview v2.8 (Waterhouse et al., 2009) for display. B) For comparison the bipartite NLS consensus sequence, the *S. cerevisiae* Elp1 putative NLS and the *X. laevis* Nucleoplasmin NLS are shown. Basic residues are highlighted in purple.

Since tRNA anticodon modifications are thought to occur in the cytoplasm of cells (Hopper and Phizicky, 2003) and it is known that Elp1 is mainly cytoplasmic (Pokholok et al., 2002, Huh et al., 2003), it is interesting to hypothesise why the Elongator complex may require a nuclear import sequence. It is possible that Elongator may have an evolutionary conserved NLS in order to undergo import and re-export alongside tRNAs, which have been shown to shuttle constitutively between the nucleus and cytoplasm in yeast (Takano et al., 2005). Certain nuclear factors may be required for the tRNA modification function of Elongator or nuclear-cytoplasmic shuttling may regulate the modification of tRNA. It is also possible that nuclear localised Elongator participates in other distinct functions such as transcription, though such functions are now disputed (Esberg et al., 2006). A further possibility is that the basic region in Elp1 may never normally interact with the cell's import machinery and could have a distinct function in the context of the Elongator complex.

3.2 Results (Part 1)

3.2.1 Characterising the effects of mutations in the Elp1 basic region on Elongator function.

In order to more extensively study the function of this conserved basic region in Elp1 a series of mutations were designed throughout its sequence (Figure 3.2). A mutant allele, *elp1-KR9A*, with nine alanine substitutions in basic residues hypothesised to be important for nuclear import was created (Figure 3.2). To dissect this sequence more closely 'proximal' (first half) and 'distal' (second half) alanine substitutions in this sequence were also made creating *elp1-KR5A* and *elp1-KR4A* respectively (Figure 3.2).

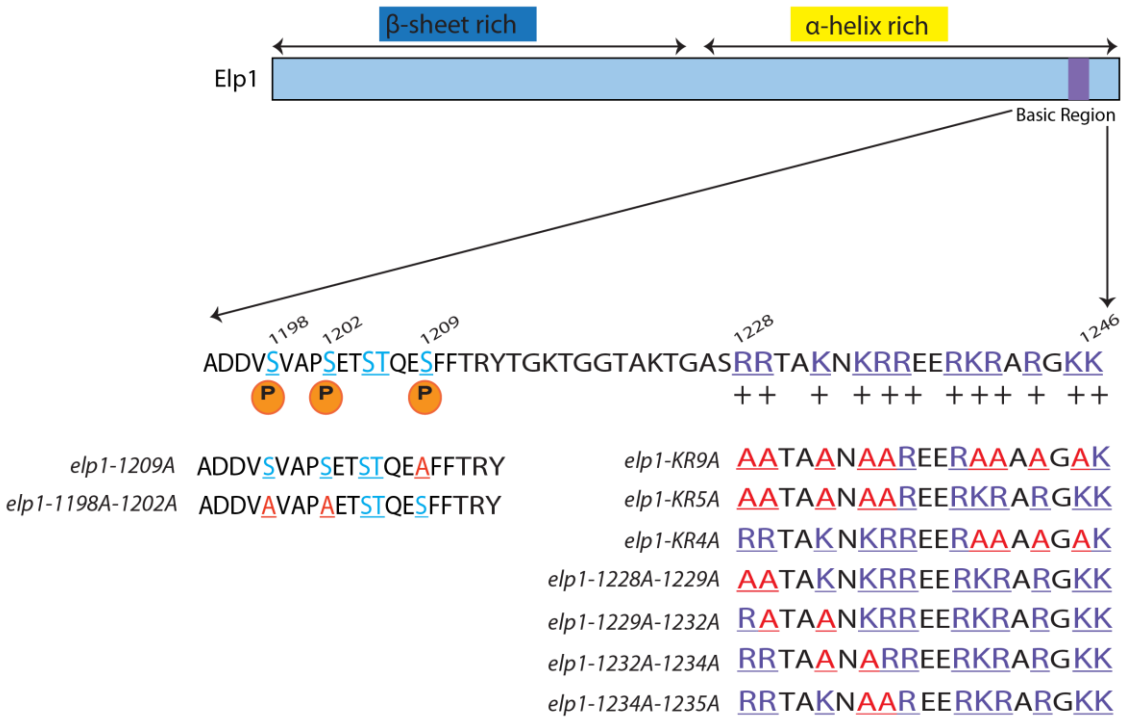

Figure 3.2: Summary of alanine substitutions created in the C-terminal domain of Elp1. Schematic of the Elp1 subunit of Elongator, including secondary structure predictions. A part of the C-terminal domain is highlighted, indicating functionally important phosphorylation sites in blue and basic residues within the conserved basic region in purple. Alanine substitutions in each mutant are highlighted in red.

Alanine substitution mutants were introduced into YCp-*ELP1*-6HA, a plasmid construct containing 6HA tagged Elp1 under the control of its endogenous promoter, which was then transformed into an *elp1Δ* strain. Sensitivity to Zymocin is a convenient method of assessing Elongator function as loss of Elongator dependent tRNA modification results in resistance to this toxin. The ability of each of these mutant versions of Elp1 to rescue the Zymocin resistance of *elp1Δ* was assayed by Eclipse assay (Figure 3.3).

Wild-type *ELP1* rescued the resistance of *elp1Δ* whereas *elp1-KR9A* did not indicating that the Elp1-KR9A protein does not support Elongator function. The *elp1-KR5A* mutant was resistant whereas the *elp1-KR4A* mutant was sensitive and so based on this assay it seemed that mutation of the distal region alone had a minimal effect on Elongator function compared with mutating the proximal region. To further dissect the region required for Elongator function, additional mutants that contained progressive Alanine substitutions within the proximal NLS region were made, *elp1-1228A-1229A, elp1-1229A-1232A*, *elp1-1232A-1234A* and *elp1-1234A-1235A* (Figure 3.2). These mutants all appeared Zymocin-sensitive by Eclipse assay (Figure 3.3), therefore based on these assays it appears that substituting just two basic residues within the proximal region does not lead to significant loss of function.

To study the effects of these mutants on Elongator function more quantitatively a plasmid (pAE1) expressing the toxic gamma subunit of Zymocin under control of a galactose inducible promoter was used (Butler et al., 1994). The intracellular expression of the gamma subunit is induced by growth on galactose containing media allowing sensitivity or resistance to the toxin to be assayed by growth test.

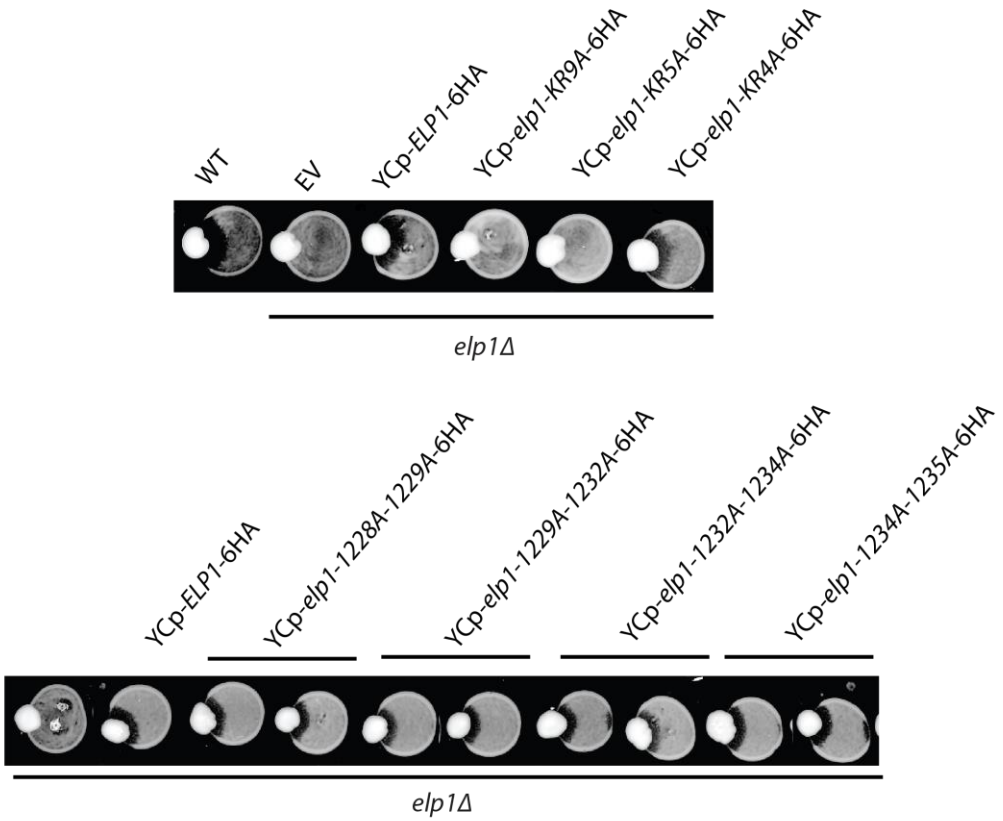

Figure 3.3: Mutations in the Elp1 basic region disrupt Elongator function. Eclipse assay of *elp1Δ* (WAY034) strains containing plasmids carrying wild-type and mutant versions of *ELP1* (YCplac111-*ELP1*-6HA and derivatives; see Figure 3.2). Wild-type (WT, BY4741) and *elp1Δ* (WAY034) with empty vector (EV) served as controls for Zymocin sensitivity and resistance respectively.

elp1Δ strains containing Elp1 mutant plasmids together with pAE1 were assayed for Zymocin resistance on galactose containing medium (Figure 3.4). The *elp1-KR9A* mutant was fully resistant compared with the empty vector control. The proximal *elp1-KR5A* mutant was resistant but slightly less so than *elp1-KR9A*. The distal *elp1-KR4A* mutant appeared sensitive by eclipse assay, but in this more quantitative assay of Zymocin sensitivity some level of resistance was seen, though less than that conferred by *elp1-KR9A* and *elp1-KR5A.*

In summary the proximal and distal mutants all displayed some level of Elongator dysfunction in this assay. Comparing the level of defect shown by these mutant alleles it appears that the *elp1-KR5A* and *elp1-KR4A* mutations are additive in the context of the *elp1-KR9A* allele. This suggests that both proximal and distal mutations contribute to the phenotype but with a greater contribution made by the proximal *elp1-KR5A* mutant. Since the *elp1-KR9A* is the most severe then the entire basic region is influencing Elongator function.

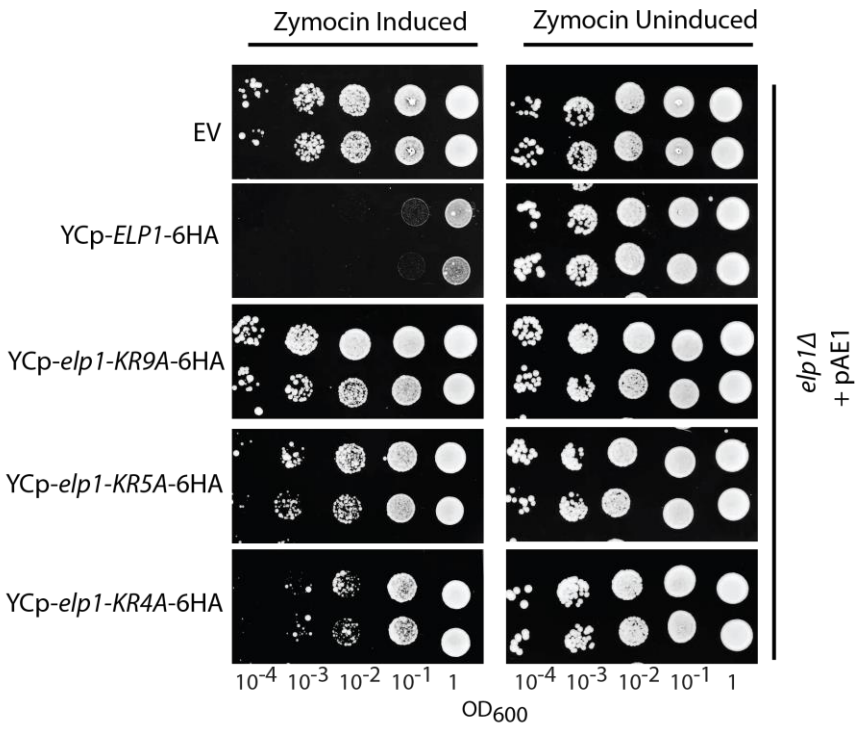

Figure 3.4: The *elp1-KR9A* mutations result in a loss of Elongator function that is comparable to *elp1Δ*. Growth test of *elp1Δ* (WAY034) strains containing plasmids carrying wild-type and mutant versions of *ELP1* (YCplac111-ELP1-6HA and derivatives; see Figure 3.2) together with pAE1. pAE1 contains the gamma toxin subunit of Zymocin under control of a galactose inducible promoter. Zymocin expression is induced by growth on galactose and repressed on glucose. *elp1Δ* (WAY034) containing empty vector (EV) and YCp-*ELP1*-6HA plasmids served as controls for Zymocin resistance and sensitivity respectively.

Our lab has created a *SUP4 ochre* suppressor system (Bandau and Stark, unpublished) that allows assay of Elongator dependent tRNA modification and its effect on translational efficiency. This *SUP4* suppressor system monitors the efficiency of *ochre* stop codon suppression by the *SUP4* tRNA that requires Elongator-dependent wobble uridine modification for activity. These *SUP4* system strains carry a ura^{oc22} marker, containing a premature *ochre* stop codon within the coding region of the gene, as well as a *SUP4 ochre* suppressor tRNA gene (Figure 3.5A). The *SUP4* gene encodes $tRNA^{Tyr}_{U\Psi A}$ that can read through the *ochre* mutation in $ura3^{oc22}$, supressing its stop codon function and allowing full translation of the marker protein. However, the *SUP4* $tRNA^{Tyr}_{U\Psi A}$ requires an Elongator dependent wobble mcm^5U modification for efficient *ochre* suppression (Huang et al., 2005). Consequently only strains with functional Elongator can read-through $ura3^{oc22}$ and grow on medium lacking uracil (Figure 3.5B). Strains that have compromised Elongator function show defective growth on media lacking uracil (DOA-Ura).

elp1Δ SUP4 system strains containing *ELP1* or *elp1* mutant plasmids were assayed for Elongator dependent *SUP4 ochre* suppression by growth on DOA -Ura (Figure 3.6). Wild-type *ELP1* $ura3^{oc22}$ strains containing empty vector and *elp1Δ* $ura3^{oc22}$ strains complemented by wild-type *ELP1* on a plasmid each showed slightly defective growth on DOA-Ura compared with control strains that lacked the *ochre* mutation in *URA3* (note smaller colonies on the two highest dilutions). This is most likely due to the fact that the read through is probably not completely efficient even in the presence of the mcm^5U modification. The difference in growth between *elp1Δ SUP4* system strains with empty vector or complemented with a wild-type *ELP1* plasmid indicate the extremes of phenotype against which the various mutant *elp1* alleles can be compared (* in Figure 3.6).

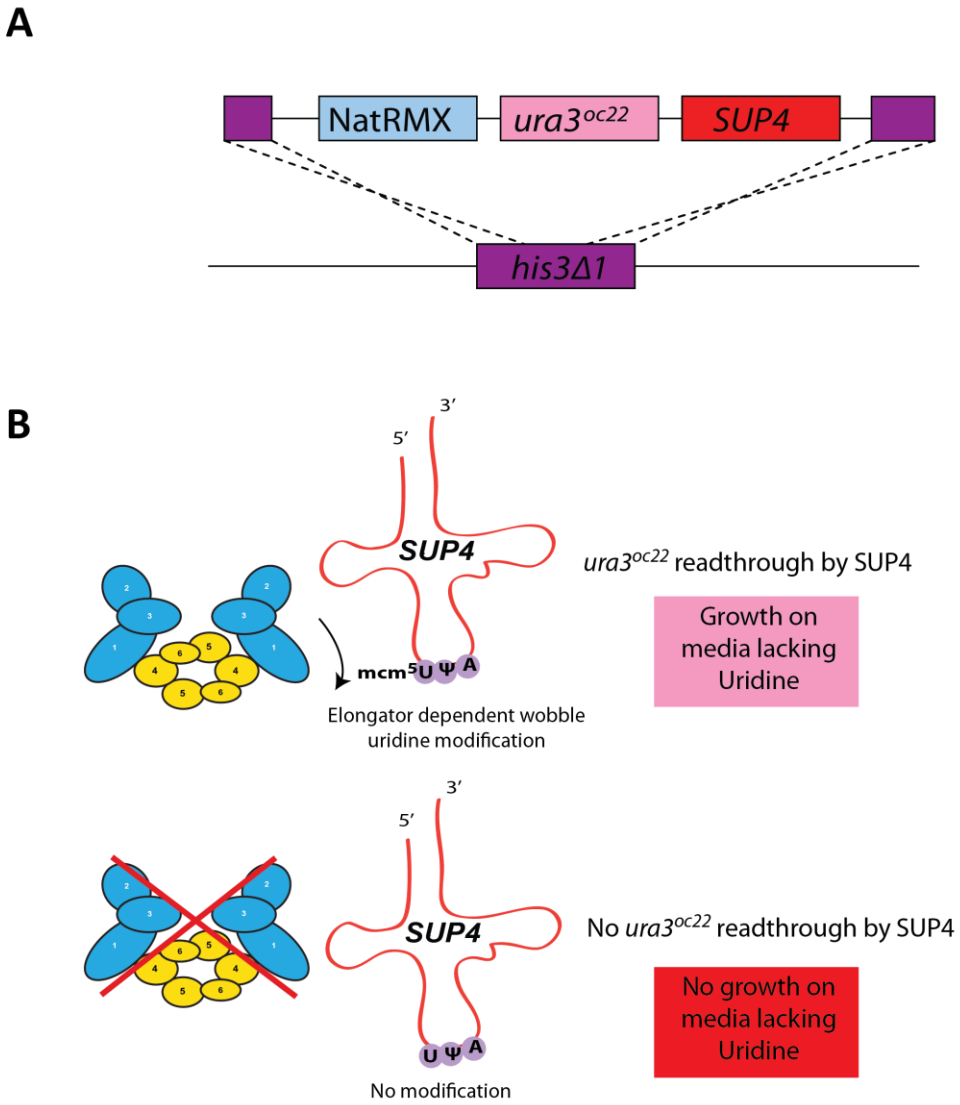

Figure 3.5: A *SUP4 ochre* suppressor system to assay the levels of Elongator dependent tRNA modification. A) Schematic of the cassette system integrated at the *his3Δ1* locus. The *ura3*^{oc22} gene has a premature stop codon that disrupts expression of the marker gene. *SUP4* encodes tRNA$^{Tyr}_{UΨA}$ and NatRMX is a marker gene for integration. B) Schematic of the Elongator dependent *SUP4 ochre* suppression system. The *SUP4* encoded tRNA can read through the premature stop codon in *ura3*^{oc22} to allow expression of the marker. However, this tRNA requires mcm^5 modification at the wobble uridine position for its suppressor function. Strains that lack Elongator function do not express the *ura3*^{oc22} marker and cannot grow on media lacking uridine.

The *elp1-KR9A* mutant showed a considerable growth defect on DOA-Ura that was comparable to that shown by the *elp1Δ* empty vector control. The *elp1-KR5A* proximal mutant and *elp1-KR4A* distal mutants both looked similar to *elp1Δ* complemented with wild-type *ELP1* in terms of growth (i.e. wild-type *ELP1* from now on). The proximal mutant may show a very minor defect in comparison, having slightly smaller colonies in the last two dilutions. However, this suggests that there is some level of Elongator dependent tRNA modification in both the proximal and distal mutants that allows *SUP4 ochre* suppression levels comparable to wild-type *ELP1*. The *elp1-KR9A* mutant is more severe in terms of defective *SUP4 ochre* suppression, suggesting there is little to no Elongator dependent tRNA modification in this strain.

The proximal basic region mutants *elp1-1228A-1229A, elp1-1229A-1232A*, *elp1-1232A-1234A* and *elp1-1234A-1235A* were also tested using the system but showed wild-type levels of *SUP4 ochre* suppression and this is in agreement with Eclipse assays (Figure 3.7 and Figure 3.4).

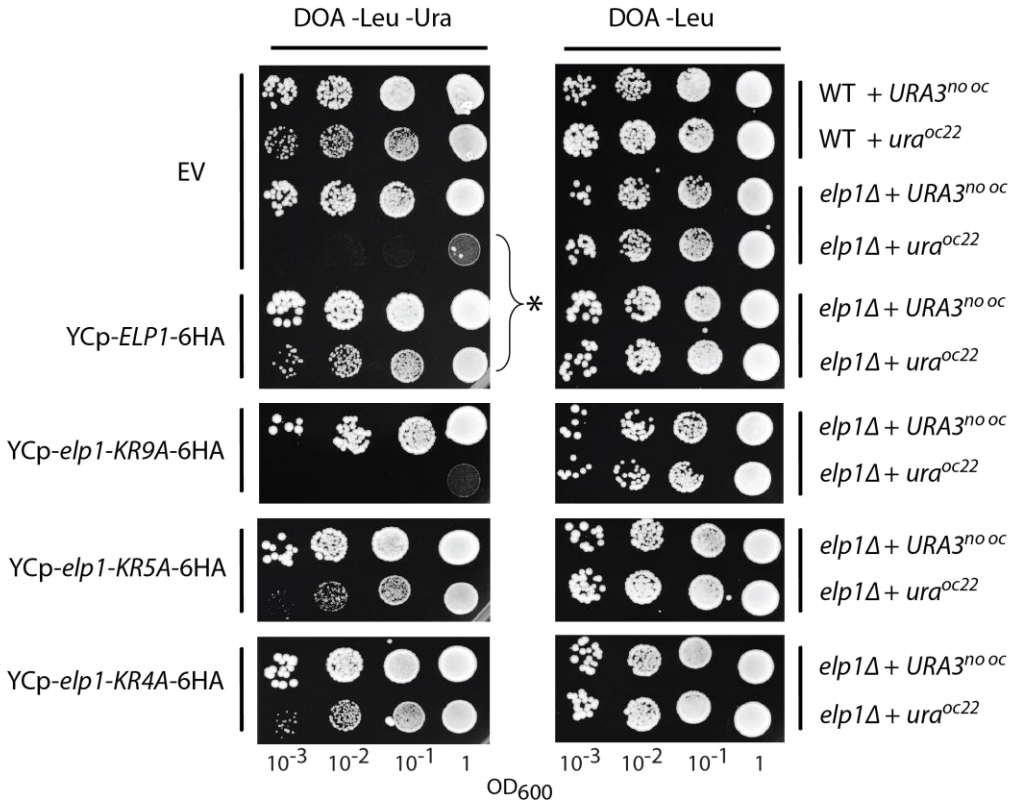

Figure 3.6: The *elp1-KR9A* mutant is defective in Elongator dependent *SUP4 ochre* suppression. Growth test of *SUP4* system integrated strains (SBY128, 132, 134, 138) containing plasmids carrying wild-type and mutant versions of *ELP1* (YCplac111-ELP1-6HA and derivatives; see Figure 3.2). Strains were assayed on DOA -Leu -Ura for *SUP4 ochre* suppression and subsequent expression of the *ura3* marker. The * indicates the effect of loss of Elongator function on *SUP4 ochre* suppression in *ura3*^{oc22} strains.

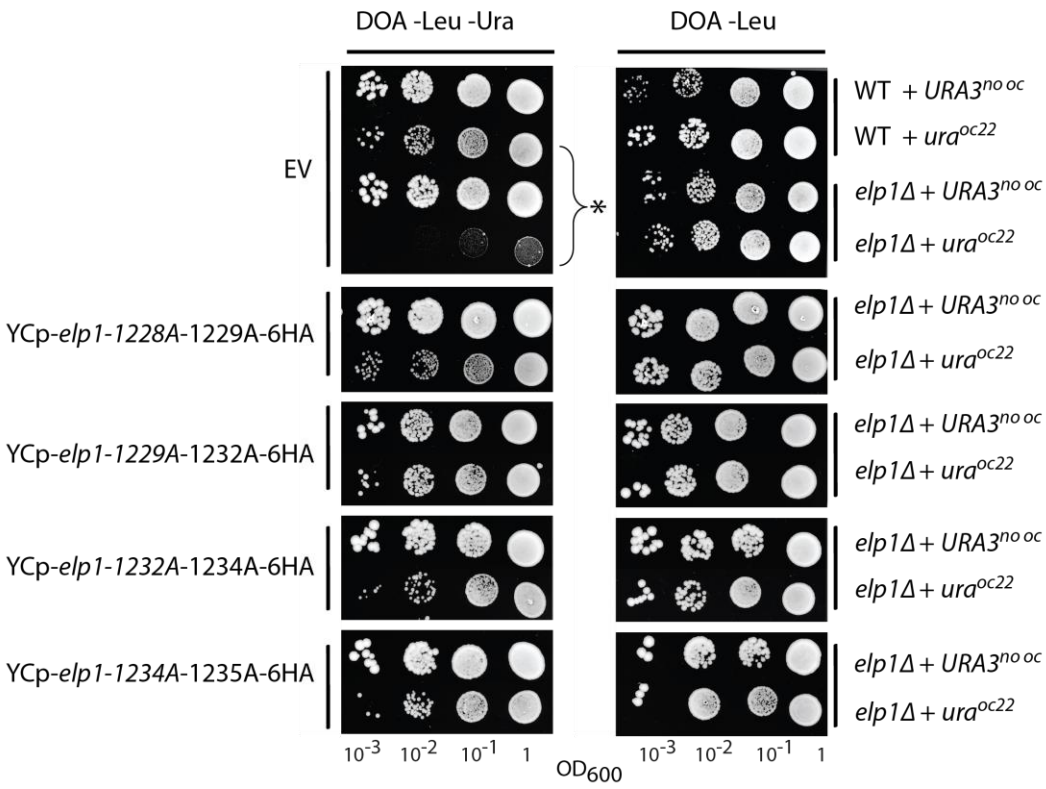

Figure 3.7: 'Alanine scanning' substitutions across the proximal part of the Elp1 basic region do not disrupt Elongator dependent *SUP4 ochre* suppression. Growth test of *SUP4* system integrated strains (SBY128, 132, 134, 138) containing plasmids carrying wild-type and mutant versions of *ELP1* (YCplac111-ELP1-6HA and derivatives; see Figure 3.2). Strains were assayed on DOA -Leu -Ura for *SUP4 ochre* suppression and subsequent expression of the *ura3* marker. The * indicates the effect of loss of Elongator function on *SUP4 ochre* suppression in *ura3*^{oc22} strains.

3.2.2 Genomic integration of *elp1* mutants by '*delitto perfetto*'

In order to characterise the phenotypes of the basic region mutants further without plasmid selection these mutants were integrated into the yeast genome using a '*delitto perfetto'* approach (Figure 3.8A). This makes use of a counter selectable CORE cassette to allow for a small region of the endogenous copy of *ELP1* to be replaced by the corresponding region containing specific mutations. This method has the advantage of giving a clean integration, since the mutants replace a region of the wild-type gene locus without leaving a selectable marker integrated as well. This was carried out in the background of GFP tagged Elp1 to generate strains in which the endogenous *ELP1* allele was replaced with *elp1-KR9A*, *elp1-KR5A*, *elp1-KR4A* and functionally important serine phosphorylation site mutants *elp1-1209A* and *elp1-1198-1202A*. Expression of the GFP tagged integrants was checked by western blot and was equivalent to that of wild-type *ELP1*-GFP before integration, as shown for '*delitto perfetto'* integrated wild-type *ELP1* and *elp1-KR9A* (Figure 3.8B and C).

Integrated GFP tagged versions of *ELP1* were tested for Elongator function using Eclipse assays (Figure 3.9). The CORE cassette deletes part of the Elp1 C-terminal domain (amino acids 1164-1277) and as expected this resulted in non-functional Elongator as this strain was resistant to Zymocin. The *elp-KR9A* and *elp1-KR5A* mutants were resistant and the *elp1-KR4A* mutant was sensitive, in agreement with the Eclipse assays performed on strains expressing these *elp1* alleles from a plasmid (Figure 3.3). The phosphorylation site mutants *elp1-1209A* and *elp1-1198A-1202A* were resistant, consistent with the previous finding that these alleles block Elongator activity (Abdel-Fattah and Stark, unpublished). The *'delitto perfetto'* integrated wild-type *ELP1* is

sensitive to Zymocin as expected and is shown alongside wild-type and *elp1Δ* controls to validate the integration method.

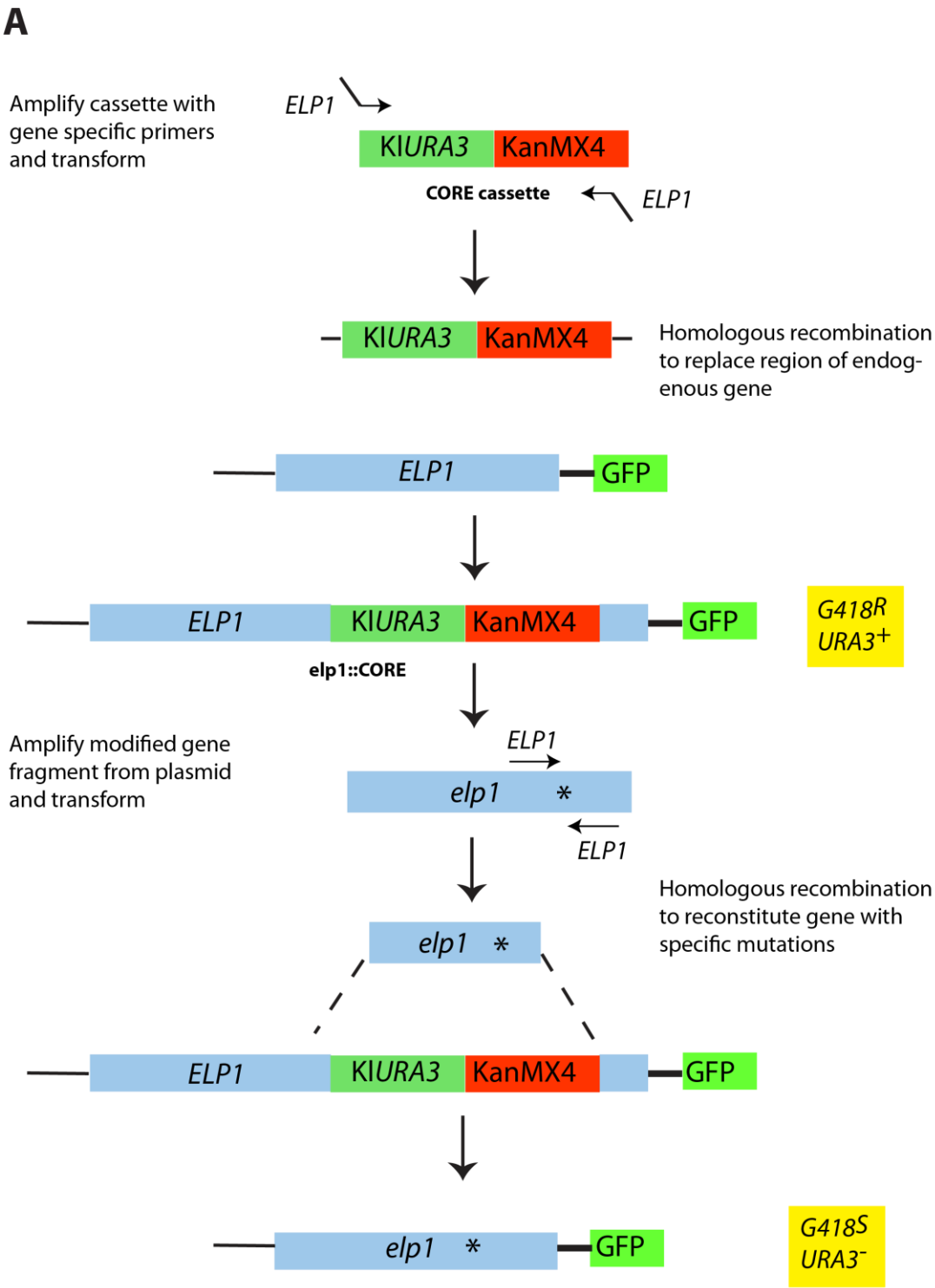

Figure 3.8: Precise replacement of the wild-type *ELP1* locus with mutant alleles by *'delitto perfetto'*; See next page for figure legend.

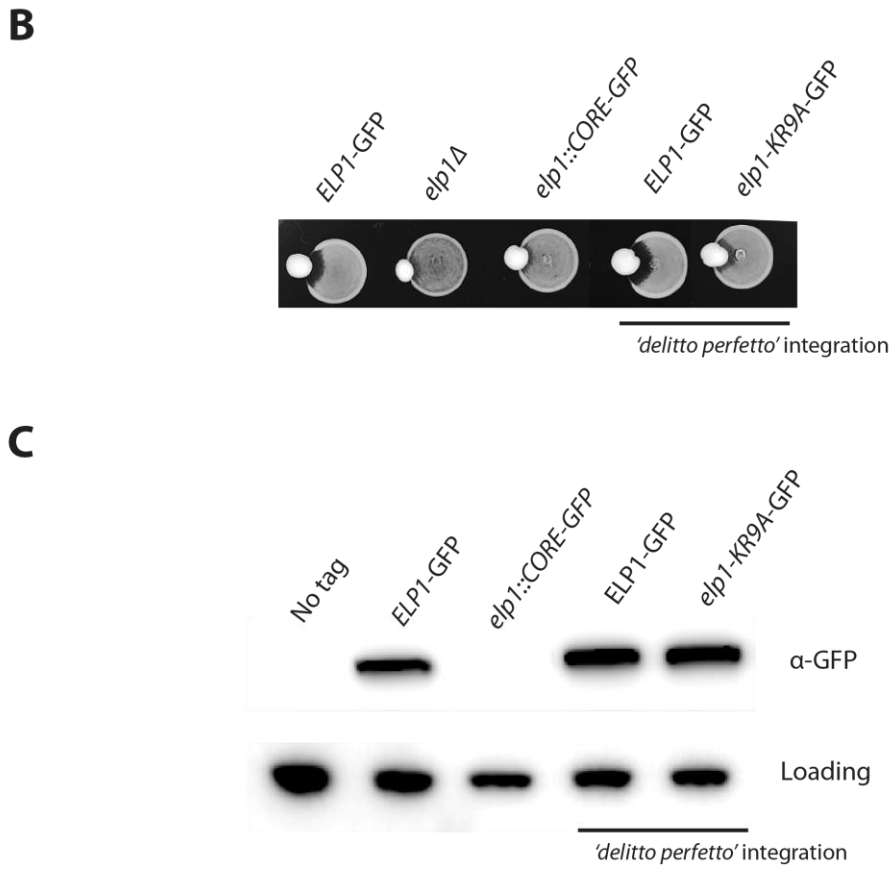

Figure 3.8: Precise replacement of the wild-type *ELP1* locus with mutant alleles by *'delitto perfetto'*. A) Schematic outlining the '*delitto perfetto'* method of integration (Storici and Resnick, 2006). This allows for reconstitution of the wild-type *ELP1* gene with mutant versions by counterselection. B) Eclipse assay of '*delitto perfetto'* strains. *ELP1*-GFP (starting strain, YRDS59) and *elp1Δ* (YRDS250) served as controls for Zymocin sensitivity and resistance respectively. C) Protein extracts from '*delitto perfetto'* strains were analysed by western blotting with anti-GFP. The untagged (YRDS1) and *ELP1*-GFP (starting strain, YRDS59) samples served as controls. As a loading control blots were also analysed with anti-Cdc28.

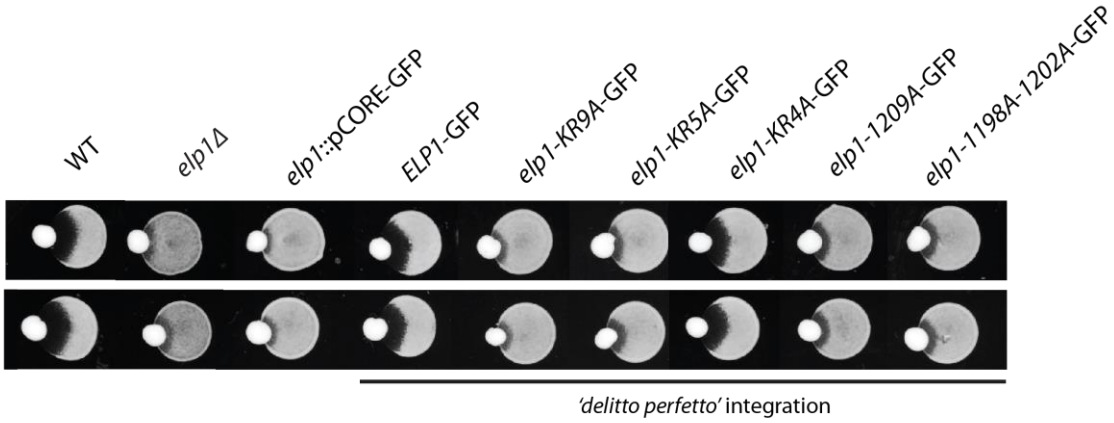

Figure 3.9: The integrated *elp-KR9A* mutant disrupts Elongator function. Eclipse assay of strains containing chromosomal copies of *ELP1* and *elp1* mutants. Wild-type (WT, BY4741) and *elp1Δ* (YRDS250) served as controls for Zymocin sensitivity and resistance respectively.

Mutant *elp1* alleles were also assayed for Elongator function using the pAE1 Zymocin plasmid (Figure 3.10). The *elp1-KR9A* mutant was resistant to galactose-induced intracellular Zymocin expression and this was comparable to *elp1Δ,* as in the plasmid based assays (Figure 3.4). The proximal *elp1-KR5A* mutant was resistant but less so than *elp1-KR9A,* while the distal mutant *elp1-KR4A* appeared sensitive. The result with *elp1-KR4A* may indicate that the 6HA tag used in plasmid based assays could adversely affect Elongator function to a small degree when compared with the integrated GFP tagged versions, since *elp1-KR4A* showed more Zymocin resistance in the plasmid based assay (compare Figures 3.4 and 3.10). The levels of Zymocin resistance shown by *elp1-KR4A*, *elp1-KR5A* and *elp1-KR9*A is progressively increased respectively, with *elp1-KR9A* having the most severe phenotype (Figure 3.10). Phosphorylation site mutants *elp1-1209A* and *elp1-1198A-1202A* also showed resistance comparable to that of the *elp1Δ* control.

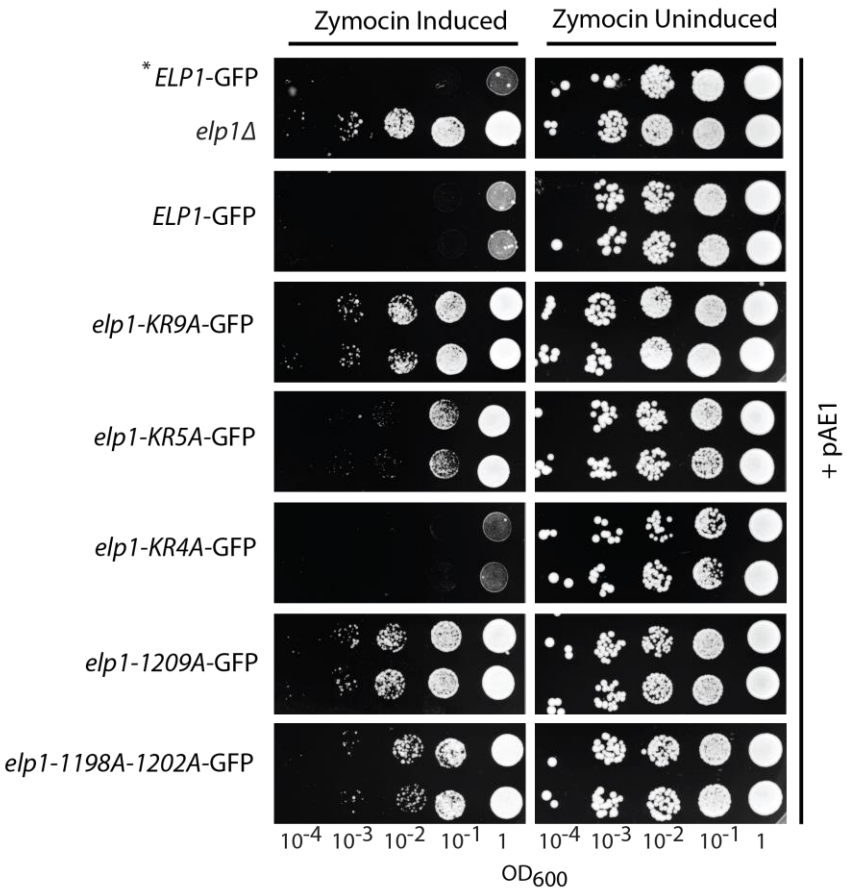

Figure 3.10: The integrated *elp1-KR9A* mutant results in a loss of Elongator function that is comparable to *elp1Δ*. Growth test of strains containing chromosomal copies of *ELP1* and *elp1* mutants. pAE1 contains the gamma toxin subunit of Zymocin under control of a galactose inducible promoter. Zymocin expression is induced by growth on galactose and repressed on glucose. * indicates the *ELP1*-GFP starting strain for *'delitto perfetto'* integrations. **ELP1*-GFP (YRDS59) and *elp1Δ* (YRDS250) served as controls for Zymocin sensitivity and resistance respectively.

Since *elp1-KR9A* showed a severe phenotype in the *SUP4 ochre* suppressor assay (Figure 3.6), this phenotype was retested with integrated wild-type *ELP1* and *elp1-KR9A* mutant in the *SUP4* system strains (Figure 3.11). As in the plasmid-based assays, the *elp1-KR9A* mutant showed defective growth on DOA-Ura, comparable to that of the *elp1Δ* control. Note that the first spot (OD_{600}=1) for this mutant shows slightly better growth than *elp1Δ* in this case, whereas on the plasmid the *elp1-KR9A* mutant was just as compromised as the knockout. This is probably to do with the effects of the 6HA tag as suggested above for *elp1-KR4A*. Nevertheless the *elp1-KR9A* mutant has a severe defect in Elongator dependent *SUP4 ochre* suppression, suggesting little to no Elongator dependent tRNA modification in this mutant. The integrated wild-type *ELP1* (denoted *ELP1*) showed equivalent growth on DOA-Ura as non-integrated wild-type ELP1 (denoted WT), which validates integration method.

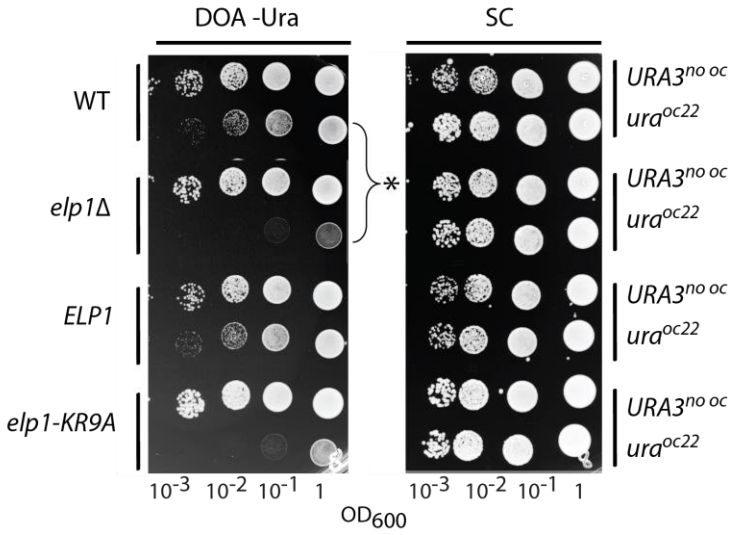

Figure 3.11: The integrated *elp1-KR9A* mutant is defective in Elongator dependent *SUP4 ochre* suppression. Growth test of *SUP4* system strains containing chromosomal copies of *ELP1* and *elp1-KR9A*. Wild-type (WT) denotes starting strains (SBY128, 132) and *ELP1* denotes integrated wild-type *ELP1*. The lack of difference between these strains validates the *'delitto perfetto'* method. Strains were assayed on DOA-Ura for *SUP4 ochre* suppression and subsequent expression of the *ura3* marker. The * indicates the effect of loss of Elongator function on *SUP4 ochre* suppression in *ura3*^{oc22} strains.

In summary, the *elp1-KR9A* mutant was comparable to an *elp1* knockout strain in terms of resistance to Zymocin and Elongator dependent *SUP4 ochre* suppressor function and was the most severe of all basic region mutants tested using each of the assays. The proximal mutant (*elp1-KR5A*) is also resistant to Zymocin but less so than *elp1-KR9A* and shows only a minor defect in Elongator dependent *ochre* suppression. The distal mutant (*elp1-KR4A*) showed some level of resistance to Zymocin in plasmid based assays, though marginally less than *elp1-KR9A* and *elp1-KR5A*, but was wild-type in terms of Elongator dependent *SUP4 ochre* suppression. Since *elp1-KR9A* is more severe than either *elp1-KR5A* or *elp-KR4A* alone then the entire basic region must contribute to the tRNA modification function of the complex. Taken together, these results show that the Elp1 basic region is essential for the tRNA modification function of Elongator.

Strain	Zymocin resistance	*SUP4 ochre* suppressor defects	Elongator function
Wild-type	**-**	**-**	**Functional**
elp1-1228A-1229A	-	-	Functional
elp1-1229A-1232A	-	-	Functional
elp1-1232A-1234A	-	-	Functional
elp1-1234A-1235A	-	-	Functional
elp1-KR4A	+/-	-	Functional
elp1-KR5A	++	+/-	Partial
elp1-KR9A	+++	+++	Non Functional
elp1Δ	**+++**	**+++**	**Non Functional**

Table 3.1: Summary of the effects of Elp1 basic region mutations on Elongator function. The effects of the various Elp1 basic region mutations on Elongator function, as assayed by Zymocin resistance and *SUP4 ochre* suppression are summarised. The extremes of phenotype are denoted by '+++' as shown by *elp1Δ* strains and '-' as shown by wild-type strains. The relative severity across mutants can be compared by the number of '+'s in comparison to these strains. A partial or minor phenotype in either assay is denoted by '+/-'.

3.2.3 Testing *elp1* basic region mutants for other phenotypes associated with non-functional Elongator

Deletion of Elongator subunits in yeast leads to pleiotropic phenotypes, including rapamycin hypersensitivity and temperature sensitivity (Frohloff et al., 2001, Schaffrath., personal communication, Otero et al., 1999). The temperature sensitivity of *elp1* basic region and phosphorylation site mutants was assayed (Figure 3.12 and 3.13). Apart from *elp1Δ* there was no obvious growth defect associated with any of these mutants when grown at high temperature (38°C). The rapamycin sensitivity of the *elp1-KR9A* mutant was also tested and it was found to be was rapamycin hypersensitive, although slightly less so than an *elp1Δ* (Figure 3.13).

The differences in severity of these phenotypes compared with *elp1Δ* suggests that there is a greater defect associated with having no Elp1 (as in *elp1Δ)* than having a mutant version of Elp1. Although *elp1-KR9A* is equivalent to *elp1Δ* in terms of Zymocin sensitivity, this assays for the mcm^5s^2 modification on $tRNA^{Glu}_{UUC}$ and perhaps to a lesser extent $tRNA^{Lys}_{UUU}$ and $tRNA^{Gln}_{UUC}$ (Lu et al., 2005). The other phenotypes associated with Elongator dysfunction are likely to arise from secondary defects associated with accumulation of defective translation, occurring due to loss of modifications on multiple tRNAs. Any small level of tRNA modification may allow these secondary phenotypes to become less pronounced and the threshold of tRNA modifications that allow these to be assayed is likely to be different. This is exemplified by differences in the phenotypes for *elp1-KR5A*. In the *SUP4 ochre* suppression system some level of modification may support read through of the $ura3^{oc22}$ gene to allow growth on DOA-Ura that is comparable to wild-type *ELP1* despite this mutant showing considerable resistance to Zymocin (Figure 3.7 and Figure 3.3).

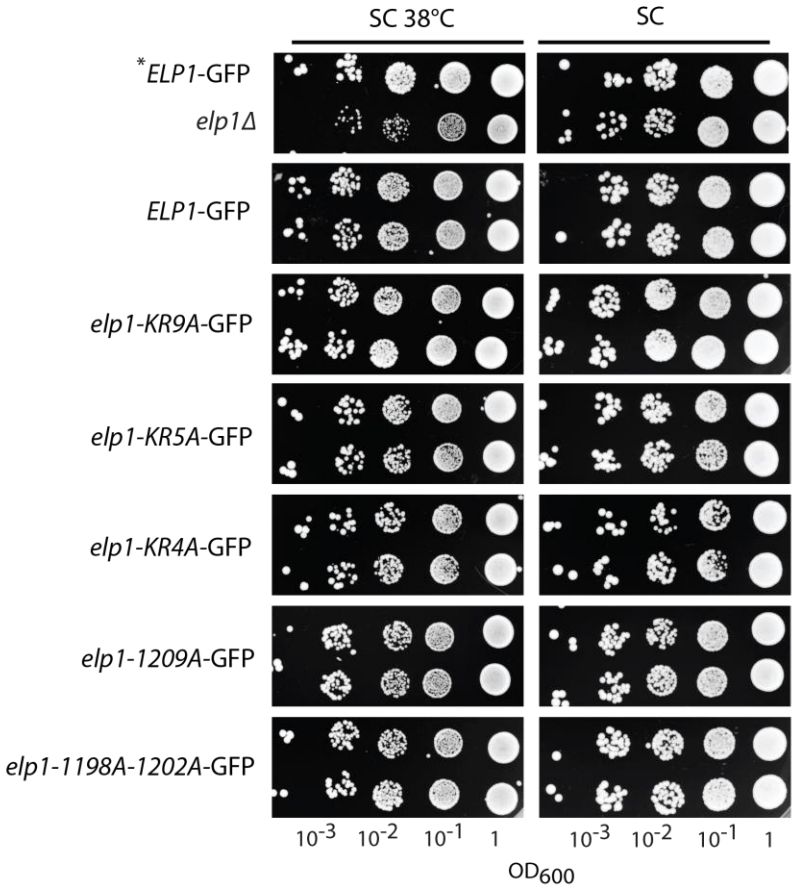

Figure 3.12: Mutations in the Elp1 basic region do not display a temperature sensitive phenotype. Growth test of strains containing chromosomal copies of *ELP1* and *elp1* mutants at 30°C and 38°C. Two clones of each strain were assayed. * *ELP1*-GFP indicates the starting strain for *'delitto perfetto'* integrations. **ELP1*-GFP (YRDS59) and *elp1Δ* (YRDS250) served as controls for extremes of phenotype.

It can be argued that many of the described phenotypes associated with Elongator dysfunction may result from other functions of the complex. However, it has been demonstrated that most of these phenotypes are rescued by multicopy expression of hypomodified $tRNA^{Gln}_{UUG}$ and $tRNA^{Lys}_{UUU}$, which normally receive mcm^5s^2 wobble uridine modifications (Esberg et al., 2006). This suggests that these all arise from a common translational defect that is countered by the approximately two-fold excess in the pool of these tRNAs when expressed from a high copy plasmid (Bjork et al., 2007).

Since a temperature sensitive phenotype in *elp1-KR9A* was not detected a test of tRNA rescue in this strain could not be attempted. However, the expression of these tRNAs from a high copy plasmid rescued the temperature sensitivity of *elp1Δ* (Figure 3.14A), which confirms previous work (Esberg et al., 2006). The rapamycin hypersensitivity phenotype of *elp1Δ* was not rescued in our hands by tRNA overexpression (Figure 3.14B). More extensive work would be required to test whether other tRNAs may rescue this phenotype. It is possible that this phenotype may arise due the combination of lack of tRNA modifications and the more general decrease in translation initiation caused by inactivation of the mTOR pathway that may worsen existing defects.

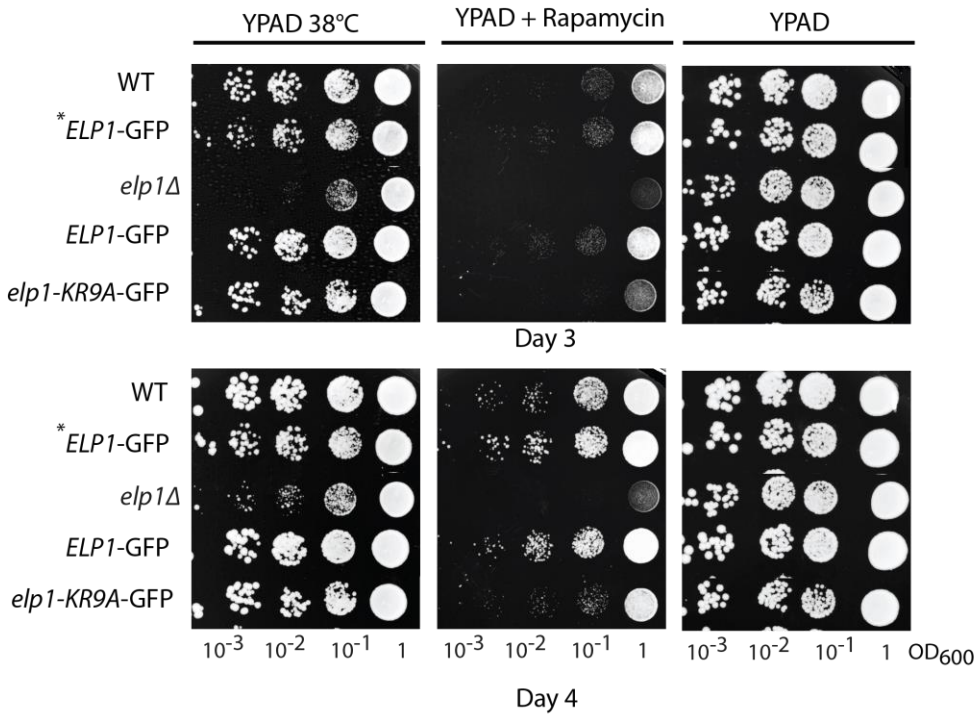

Figure 3.13: The *elp1-KR9A* mutant is rapamycin hypersensitive. Growth test of strains containing chromosomal copies of *ELP1* and *elp1* mutants at 30°C, 38°C and at 30°C on medium containing 1 µg/µl of Rapamycin. **ELP1*-GFP indicates the starting strain for *'delitto perfetto'* integration. Wild-type (WT, BY4741),*ELP1-GFP (YRDS59) and *elp1Δ* (YRDS250) served as controls for extremes of phenotype.

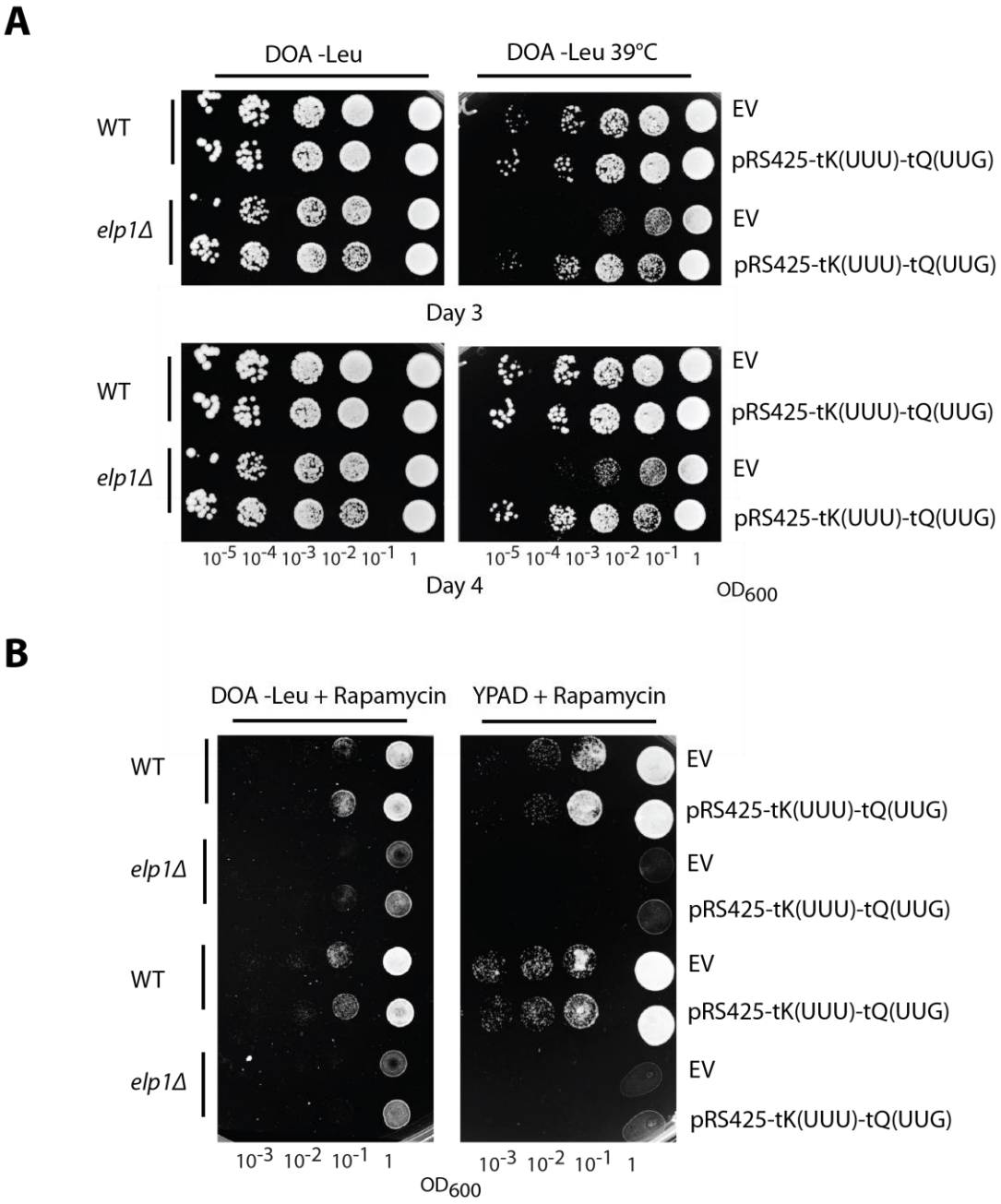

Figure 3.14: Multicopy expression of $tRNA^{Gln}_{UUG}$ and $tRNA^{Lys}_{UUU}$ rescues the temperature sensitivity of *elp1Δ* but not rapamycin hypersensitivity. Growth tests of wild-type (WT, BY4741) and *elp1*Δ (YRDS250) strains containing empty vector (EV) or a multicopy tRNA vector (pRS425-tK(UUU)-tQ(UUG)). Two clones of each strain were tested A) at 30°C and 38°C and B) on medium containing 1 µg/µl of Rapamycin.

3.3 Results (Part 2)

3.3.1 The Elp1 C-terminal domain can drive nuclear import

The basic region in the Elp1 subunit is essential for tRNA wobble uridine modification and this was previously annotated as a putative NLS. Since most of the Elp1 pool is cytoplasmic rather than nuclear (Pokholok et al., 2002, Rahl et al., 2005) it was unclear why the complex would require a nuclear import sequence for this function.

To investigate whether the Elp1 putative NLS was capable of driving nuclear import and whether this was affected by basic region mutations, the region of *ELP1* encoding part of the Elp1 C-terminus (amino acids 1181-1349) was cloned from plasmids carrying wild-type *ELP1*, *elp1-KR9A*, *elp1-KR5A* and *elp1-KR4A* into an N-terminal GFP tagging vector (pUG34) to enable expression of the corresponding GFP-Elp1 fusions. These constructs are regulated by a *MET25* promoter that allows conditional expression of the fusion proteins in DOA-Met media. The effect of the Elp1 C-terminus on the distribution of GFP between the nucleus and cytoplasm can be assayed using a strain where the nuclear boundary is defined by fusion of a 4mCherry tag to Nic96, a nuclear pore complex protein.

The localisation of GFP tagged constructs was visualised in unsynchronised fixed cells grown to log phase in DOA-Met-His medium (Figure 3.15). The GFP tagged wild-type Elp1 C-terminus was concentrated in the nucleus of the cell and this is in agreement with previous work (Fichtner et al., 2003). In contrast, all of the *elp1-KR* mutants had a diffuse localisation comparable to the empty vector control, suggesting that the C-terminus can no longer influence GFP localisation. The presence of GFP in both the nucleus and cytoplasm in the empty vector and *elp1-KR* mutant strains is most likely a

result of diffusion throughout the compartments. In general globular proteins of up to 50-60 kDa can enter the nucleus by diffusion (Macara, 2001, Dingwall and Laskey, 1986) and our GFP-Elp1 fusions have a molecular weight of ~47 kDa. However, based on these experiments we cannot rule out that *elp1-KR9A, elp1-KR5A* or *elp1-KR4A* may retain some level of nuclear import function. The C-terminus of Elp1 in isolation can therefore function to drive nuclear import and mutation of basic residues in this region disrupts this property.

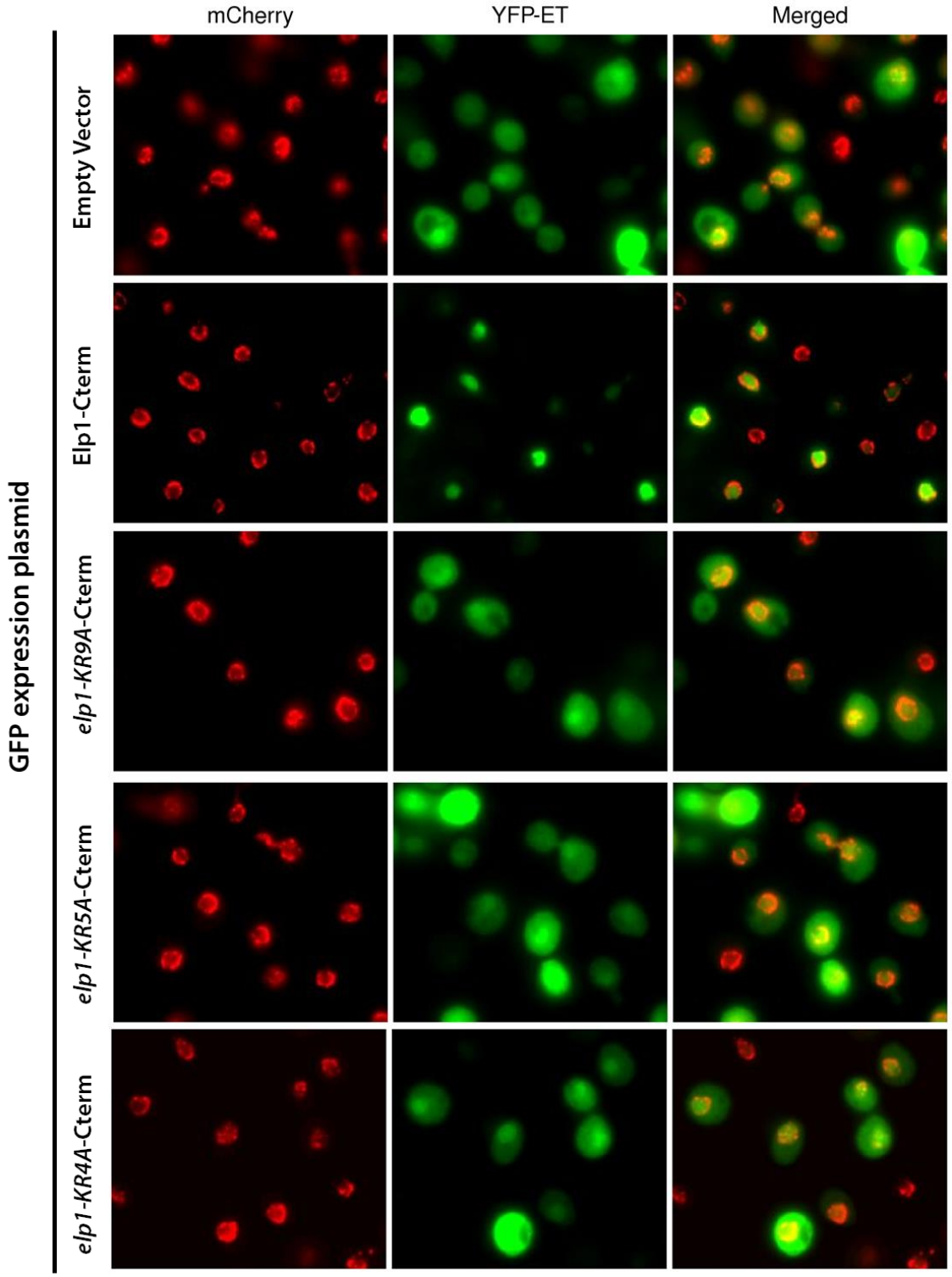

Figure 3.15: The Elp1 C-terminal domain can drive nuclear import of GFP and this is disrupted by basic region mutations. Representative images of Nic96-4mCherry nuclear boundary tagged strains containing pUG34 plasmids expressing N-terminal GFP tagged wild-type and mutant Elp1 sequences (C-terminal residues 1181-1349). The pUG34 empty vector served as a GFP only control. The nuclear boundary (red) and GFP signals (green) were visualised by mCherry and YFP-ET channels respectively.

3.3.2 Basic region mutations do not disrupt the localisation of Elp1

Although it is known that Elongator is mainly cytoplasmic rather than nuclear (Pokholok et al., 2002), the relative levels of Elp1 present in these compartments has not yet been quantified. We wanted to determine the relative pools of Elp1 in these compartments and examine how mutations in the Elp1 basic region might affect this. The localisation of Elp1-1209A, in which a serine to alanine substitution at an *in vivo* phosphorylation site leads to loss of Elongator function, was also assayed to see whether phosphorylation might regulate the distribution of Elp1.

A strain was constructed in which Elp1 was C-terminally tagged with GFP and which had the nuclear boundary labelled by Nic96-4mCherry. This allowed the distribution of Elp1 between the nucleus and cytoplasm to be visualised and quantified. As described above (Figure 3.9), we introduced the required *elp1* mutations into the wild-type *ELP1*-GFP construct in this strain using *'delitto perfetto'*. The localisation of Elp1-GFP in unsynchronised fixed log phase cells was analysed by taking 2D images of multiple fields of view. An untagged strain was used as a control to remove intensities caused by autofluorescence.

The wild-type Elp1-GFP was mainly cytoplasmic (Figure 3.16A) with this compartment having a bright and granular distribution of GFP. This is in agreement with other reports, including that of the Yeast GFP collection (Huh et al., 2003, Tkach et al., 2012, Pokholok et al., 2002). The nucleus appeared darker compared with the cytoplasm indicating little to no nuclear localisation. None of the *elp1-KR* mutants showed any obvious defects in the distribution of Elp1, it is again mainly cytoplasmic in each case and any small nuclear pool of Elp1 appeared unchanged. It would be expected that if Elp1 was no longer being imported into the nucleus that a more obvious change

compared to wild-type Elp1 would be visible under steady state conditions. The *elp1-1209A* mutant also showed no observable defect in its nucleo-cytoplasmic distribution, suggesting that phosphorylation at this functionally important site does not regulate Elongator localisation.

The relative nuclear and cytoplasmic pools of Elp1-GFP were quantified in order to assay any more subtle changes that may not be visualised (Figure 3.16B). The GFP tagged wild-type or mutant Elp1 proteins were all mainly cytoplasmic as calculated from summed GFP intensities for each strain. A small nuclear pool could be quantified, but notably there were no major changes in this despite mutation of the basic region. The averages measured vary slightly but the standard deviations overlap. These small differences in the average could be due to small differences in the maximum intensities measured in each set of images or minor sampling differences. It is also possible that the basic residues affect the uptake of low levels of unassembled or unfolded Elp1 into the nucleus and this results in the small differences in the average pools (i.e. ~3% increase in cytoplasmic pool) when mutated. Since there are no clear differences in Elp1 distribution, any substantial role of the basic region as a determinant of the nucleo-cytoplasmic localisation of Elp1 is very unlikely. The effects of basic region mutations on Elongator function cannot be attributed to mutation of a functionally important nuclear localisation sequence.

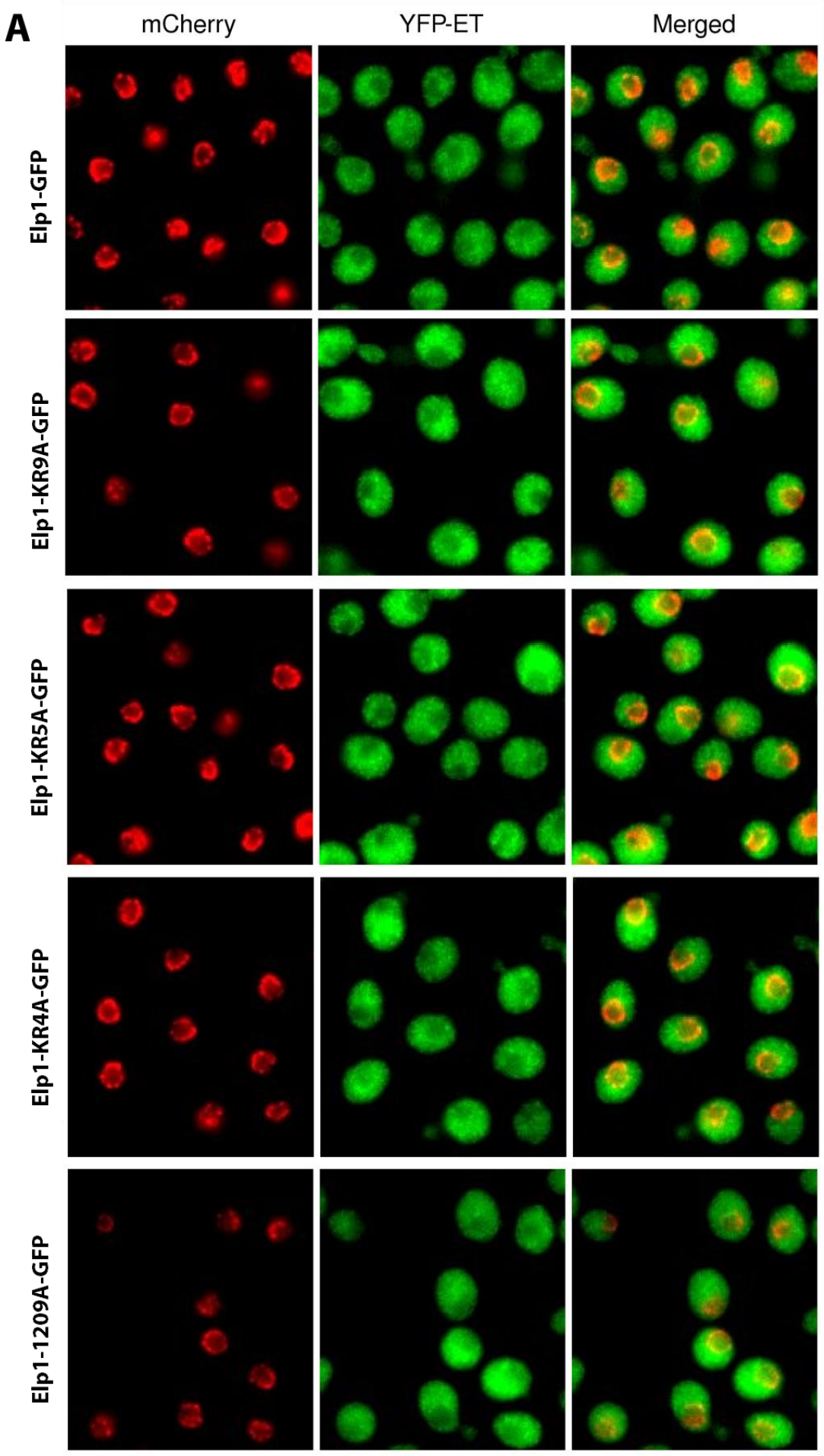

Figure 3.16: Elp1 has a cytoplasmic localisation that is not disrupted by mutations in the basic region; See next page for figure legend

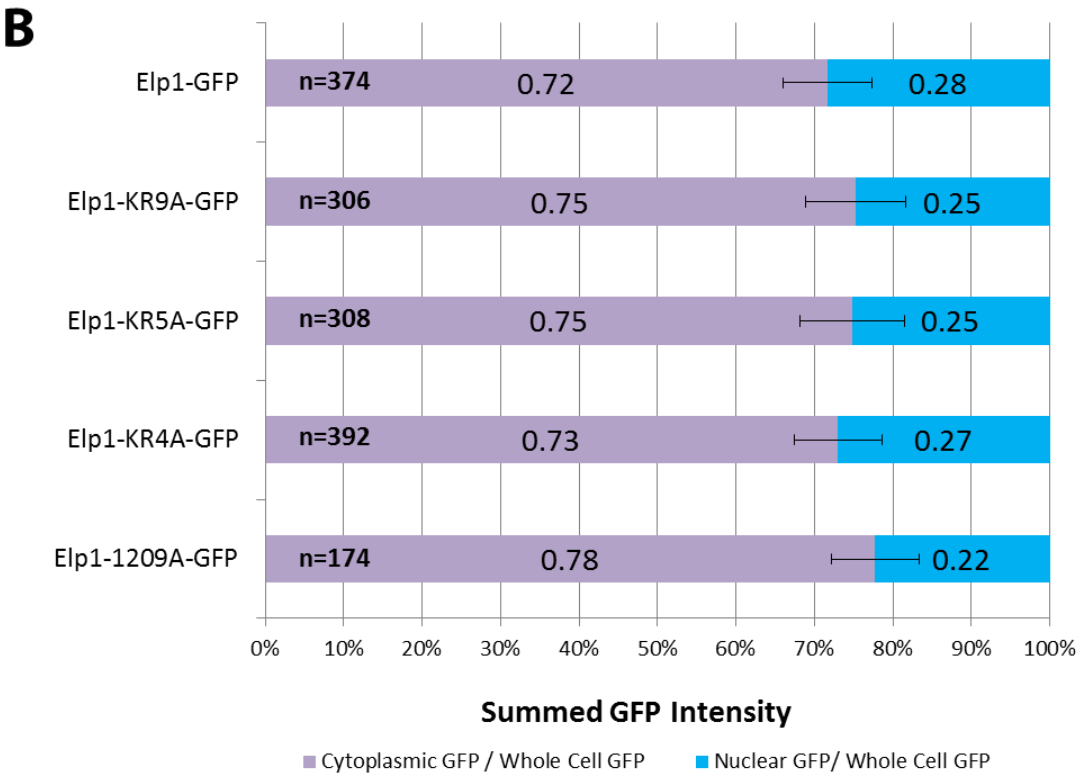

Figure 3.16: Elp1 has a cytoplasmic localisation that is not disrupted by mutations in the basic region. A) Representative images of strains expressing GFP tagged wild-type and mutant Elp1 with a Nic96-4mCherry nuclear boundary tag. The nuclear boundary (red) and GFP signals (green) were visualised by mCherry and YFP-ET channels respectively. B) Quantification of the average % nuclear and cytoplasmic pools of wild-type and mutant Elp1. Percentages were calculated using the summed intensity of GFP and the number of cells (n) analysed for each strain is shown. The error bars represent the standard deviation of the averages.

A small nuclear localisation of Elp1 has been reported in the literature (Collum et al., 2000, Fichtner et al., 2003, Kim et al., 2002, Rahl et al., 2005) and the results presented here agree that there support the presence of a nuclear pool, apparent upon quantification of images. The functional significance of any Elp1 nuclear pool is not immediately clear since tRNA modifications at the anticodon loop generally occur in the cytoplasm (Hopper and Phizicky, 2003). It is possible that the intensities present in the nucleus could represent some form of unaccounted for background or a degraded version of Elp1-GFP, small enough to enter the nucleus, although the latter is not obvious from western blotting (data not shown). It should be noted that use of 2D images will overestimate the pool of GFP in the nucleus, since the smaller volume of this compartment cannot be taken into account in a single image section. Unfortunately, quantification of images in 3D cannot be carried out due to technical issues to do with photobleaching. It appears that a small nuclear pool of Elp1 is present but whether this could represent some form of background is impossible to rule out based on these data alone, but could be further addressed in the future by fractionation of the cells and analysis of Elp1 distribution by western blotting.

Importantly, it is clear that the wild-type distribution of Elp1 is not disrupted by any of the mutations so far assayed under our conditions. Although the basic region of Elp1 can drive nuclear import in isolation, in the context of the whole polypeptide this property does not appear to be functionally relevant. Mutation of the basic region does not alter the steady state distribution of Elp1 between the nucleus and cytoplasm. Under our conditions this basic region is not required for nuclear import of Elp1, although it is important for Elongator function.

Like Elp1, the other subunits of Elongator, Elp2-6 have been reported to be mainly cytoplasmic and this is in agreement with their assembly into a multiprotein complex (Tkach et al., 2012, Huh et al., 2003, Kim et al., 2002, Breker et al., 2013). The localisation of the accessory protein Kti12 has not been extensively investigated, and though reported cytoplasmic it does not appear to be excluded from the nucleus (Huh et al., 2003). Kti12 is a binding partner of Elp1 but has also been shown to interact with Chromatin independently of Elongator, which may suggest that it has other functions (Fichtner et al., 2002b, Petrakis et al., 2005).

In order to assay its distribution throughout the nucleus and the cytoplasm Kti12 was GFP tagged at its C-terminus and the GFP tag was shown by eclipse assay not to disrupt Kti12 function (data not shown). Kti12-GFP had lower overall GFP intensities compared with Elp1-GFP but a higher relative nuclear pool (Figure 3.17). The Kti12-GFP fusion protein is ~67kDa so this construct should be too large to freely diffuse across compartments, suggesting another means of nuclear import. It should be noted that no obvious nuclear import or export sequences in the Kti12 protein sequence can be identified. It is not yet known whether Kti12 may play a role in other distinct functions in either the nucleus or the cytoplasm, but other work indicates that not all of it is associated with Elongator (Fichtner et al., 2002a). Since deletion of *KTI12* results in loss of Elongator function it was possible that it might influence the distribution of the Elp1 subunit. To test this, *KTI12* was knocked out in strains containing *ELP1*-GFP or *elp1-KR9A*-GFP and the localisation of Elp1 assayed. The distribution of Elp1 was largely unchanged when compared with wild-type *KTI12* strains and so Kti12 does not appear to influence the distribution of Elp1 (Figure 3.18).

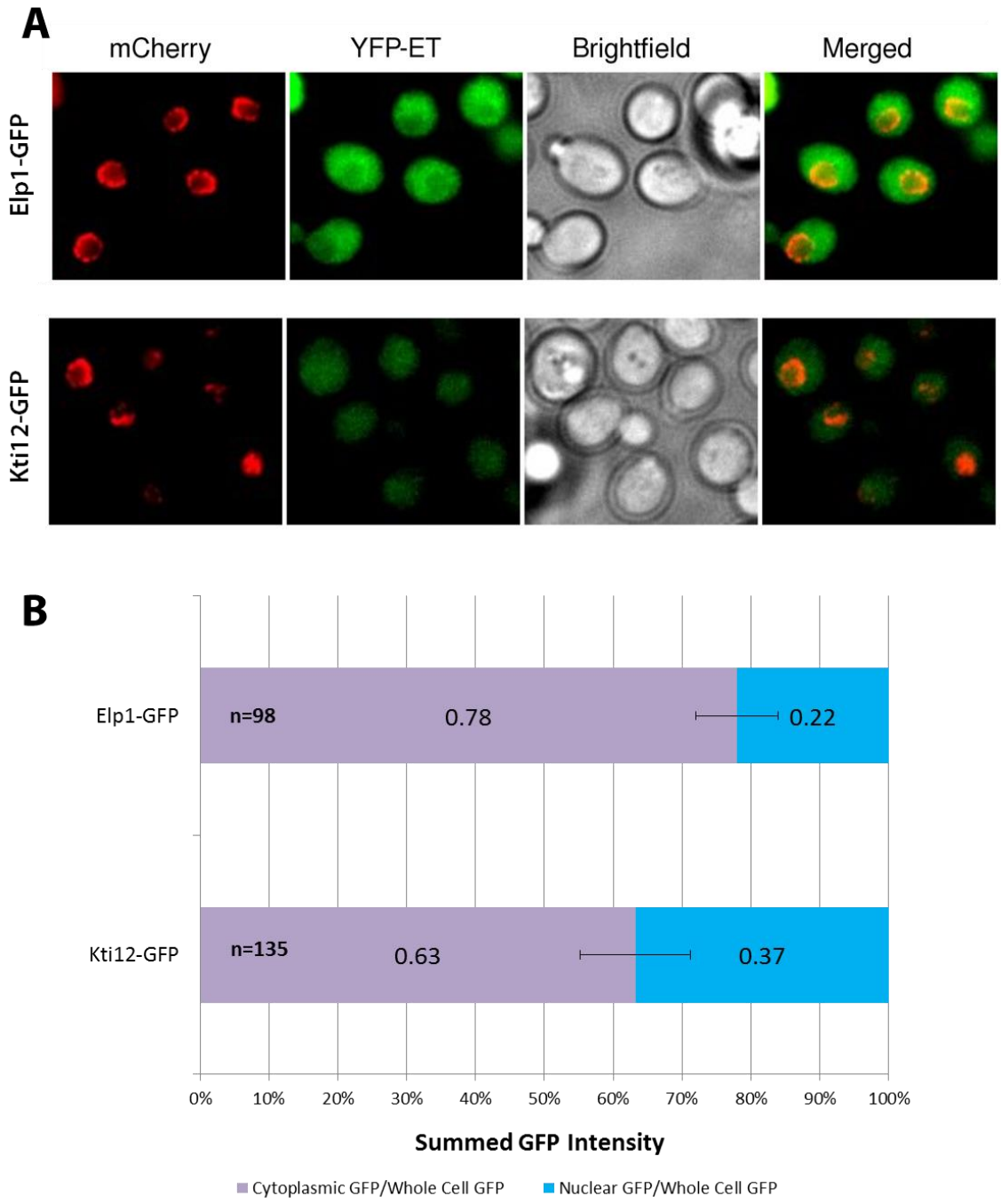

Figure 3.17: Kti12 has a different nucleo-cytoplasmic distribution than Elp1. A) Representative images of strains expressing GFP tagged Elp1 and Kti12 with a Nic96-4mCherry nuclear boundary tag. The nuclear boundary (red) and GFP signals (green) were visualised by mCherry and YFP-ET channels respectively. B) Quantification of the average % nuclear and cytoplasmic pools of Elp1 and Kti12. Percentages were calculated using the summed intensity of GFP and the number (n) of cells analysed for each strain is shown. The error bars represent the standard deviation of the average.

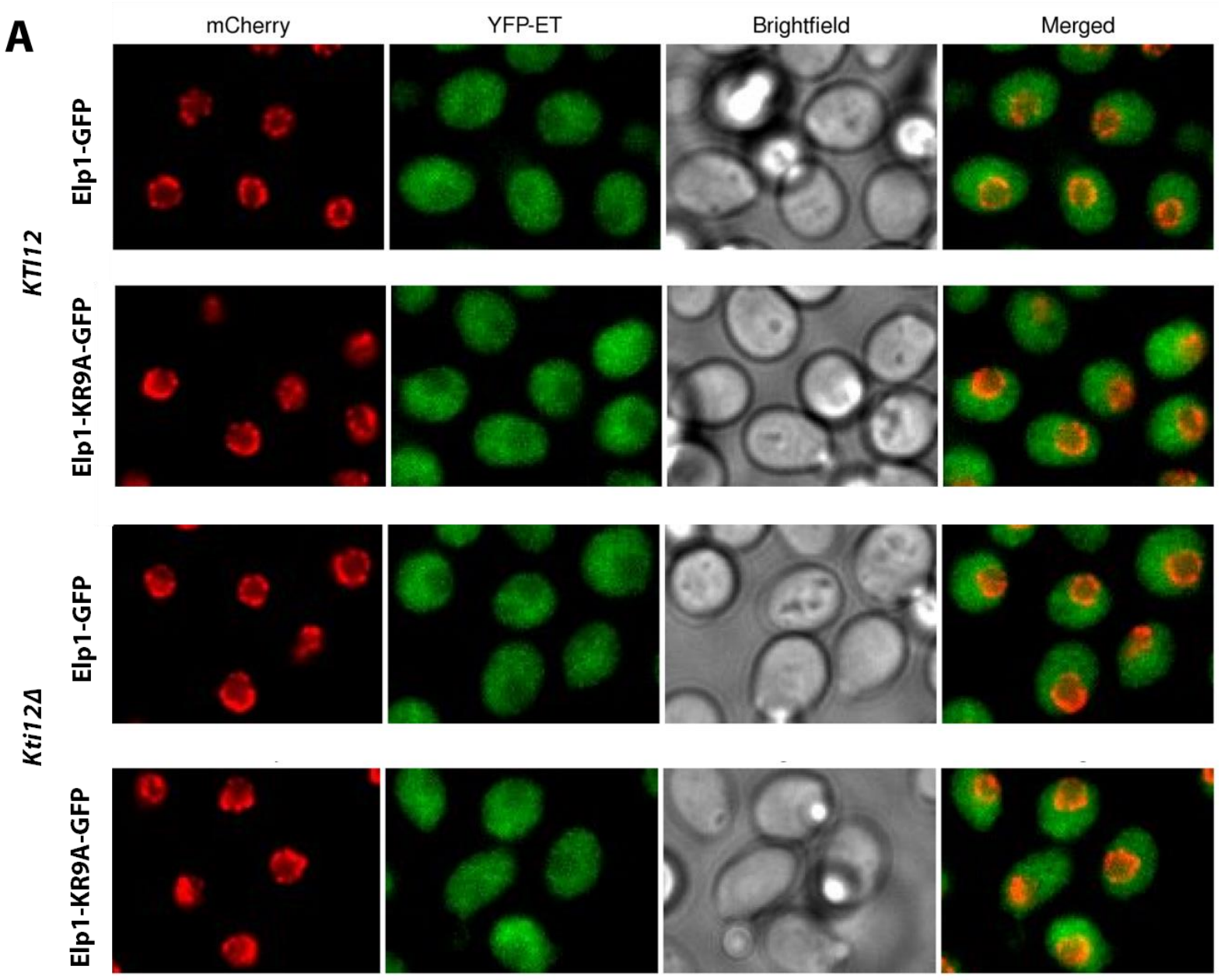

Figure 3.18: Kti12 does not influence the localisation of Elp1; See next page for figure legend.

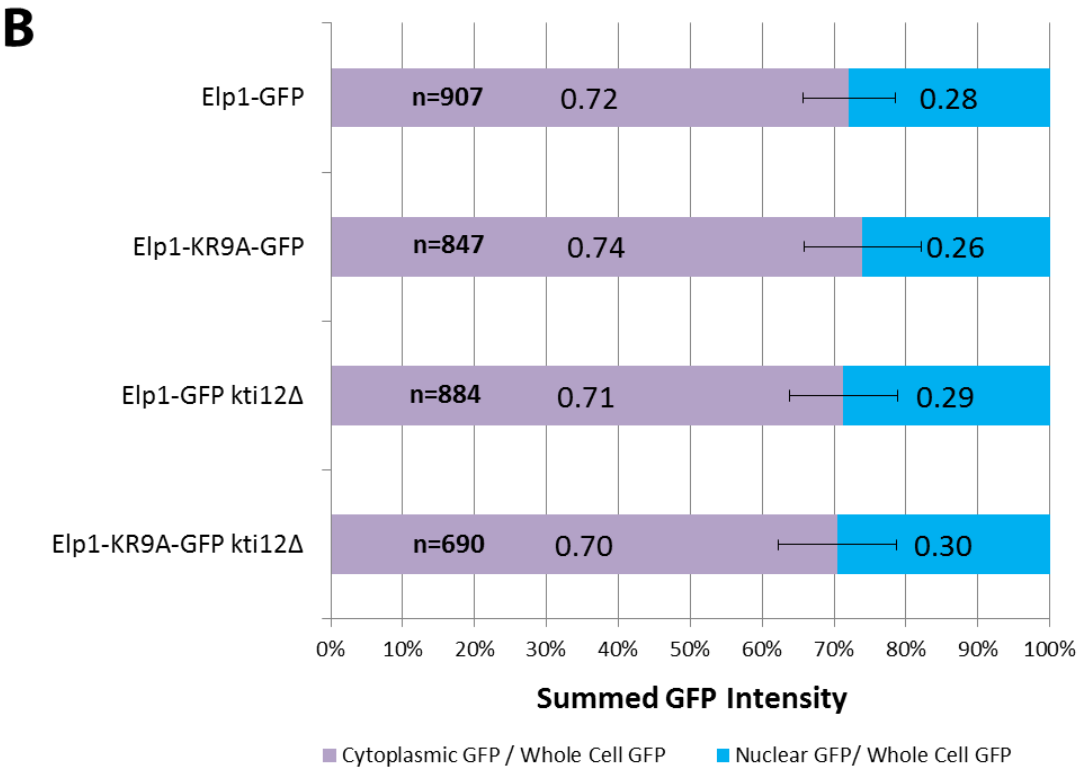

Figure 3.18: Kti12 does not influence the localisation of Elp1. A) Representative images of strains expressing GFP tagged Elp1 and *elp1* mutants with a Nic96-4mCherry nuclear boundary tag. These are in the context of either wild-type *KTI12* or *kti12Δ*. The nuclear boundary (Red) and GFP signals (Green) were visualised by mCherry and YFP-ET channels respectively. B) Quantification of the average % nuclear and cytoplasmic pools of Elp1 and *elp1-KR9A* mutants. Percentages were calculated using the summed intensity of GFP and the number (n) of cells analysed for each strain is shown. The error bars represent the standard deviation of the average.

3.3.3 Fusing a nuclear export sequence onto Elp1 does not affect Elongator function

It was clear from our data that the putative NLS of Elp1 was not driving nuclear import under steady state conditions. However, since a small nuclear pool of Elongator was quantified in the above work it was tested whether this nuclear pool of Elp1 could be important for tRNA modification. To this end the classical nuclear export sequence (NES) of the HIV Rev protein (Fischer et al., 1995, Pollard and Malim, 1998) was cloned downstream of the Elp1 C-terminus (Figure 3.19). This is a well-annotated Leucine Rich type 2-2-1 export sequence that is transported out of the nucleus by Crm1 (Fornerod et al., 1997). The HIV Rev NES has been shown to function when fused to yeast proteins and should deplete any nuclear localised Elp1 to create a strain in which Elp1 is completely cytoplasmic (Ohira and Suzuki, 2011, Fritz and Green, 1996).

The localisation of Elp1-NES(Rev)-GFP was assayed and strikingly it showed that there were no visible or major quantifiable difference in the distribution of Elp1 (Figure 3.20). Like wild-type Elp1, the nucleus of the cell appeared darkened with a mainly cytoplasmic distribution of GFP. This lack of clear difference in the nuclear pool of Elp1 with or without the NES may suggest that there is very little Elp1 in the nucleus and so a strong export sequence cannot drastically affect its distribution. However, it is also possible that in context of Elp1 this export sequence might be masked from the export machinery.

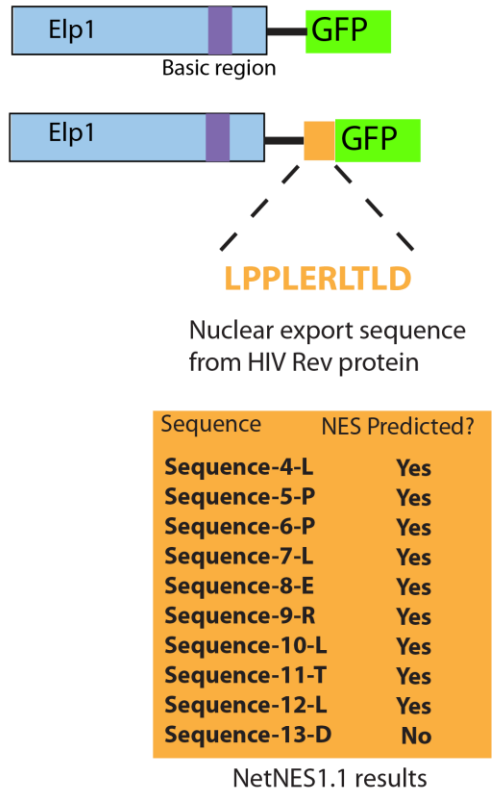

Figure 3.19: A nuclear export sequence from HIV Rev built into Elp1-GFP. Schematic showing the nuclear export sequence (NES) of HIV Rev fused downstream of the Elp1 C-terminus. The NES predictor programme NetNES1.1 annotation of this sequence is also shown (http://www.cbs.dtu.dk/services/NetNES-1.1/). The 'Yes' annotation denotes that the programme has predicted a score for the amino acid that suggests it is part of a putative NES.

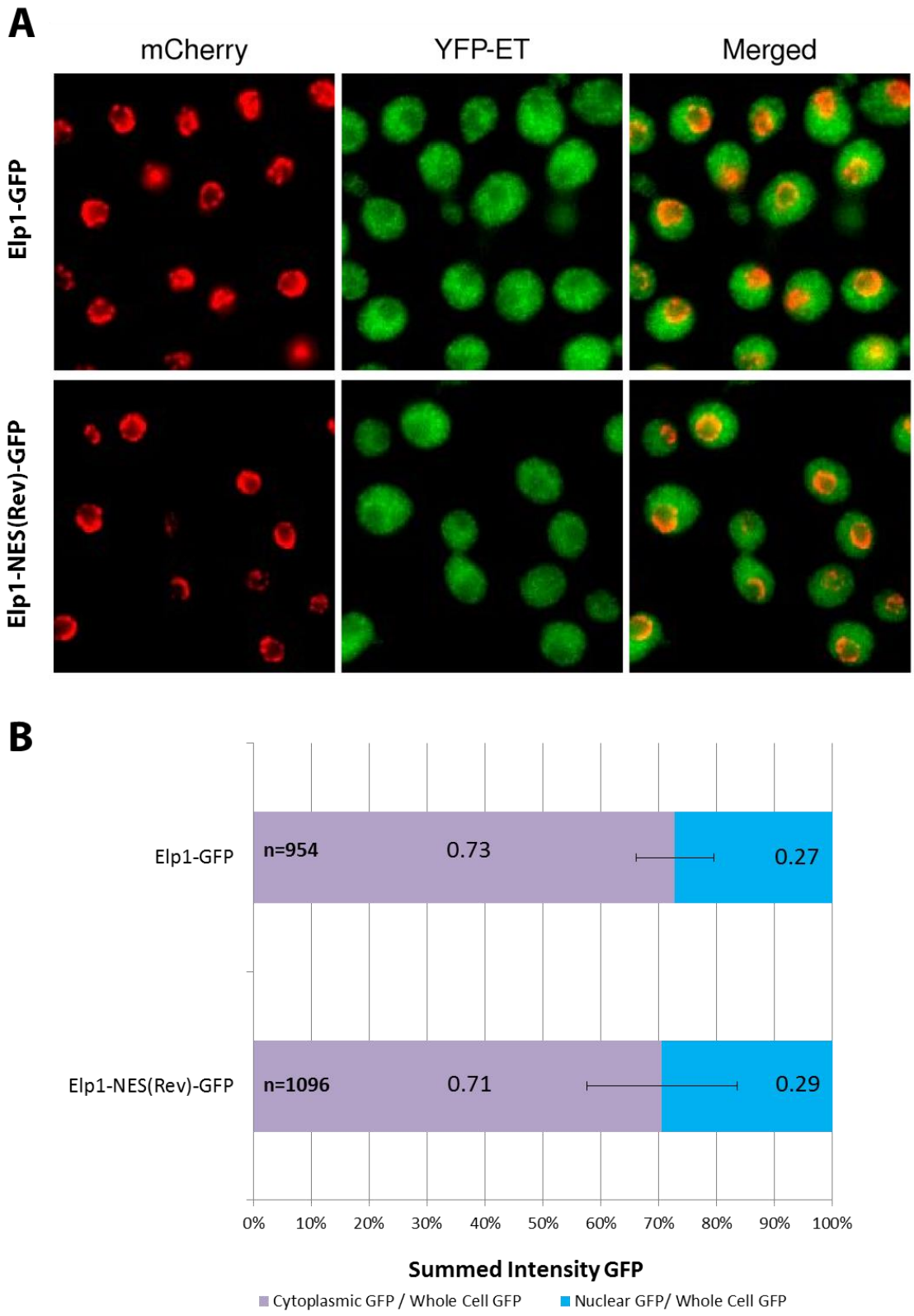

Figure 3.20: The distribution of Elp1 fused to the NES of HIV Rev is not altered. A) Representative images of strains expressing GFP tagged Elp1 and Elp1-NES (Rev) with a Nic96-4mCherry nuclear boundary tag. The nuclear boundary (red) and GFP signals (green) were visualised by mCherry and YFP-ET channels respectively. B) Quantification of the average % nuclear and cytoplasmic pools of Elp1 and Elp1-NES(Rev). Percentages were calculated using the summed intensity of GFP and the number (n) of cells analysed for each strain is shown.

The Zymocin sensitivity of *ELP1*-NES(Rev)-GFP strains was tested by Eclipse assay (Figure 3.21A) and showed sensitivity comparable to that of wild-type *ELP1*, indicating that there was no obvious defect in Elongator function. Other phenotypes associated with Elongator dysfunction such as temperature and rapamycin sensitivity were also assayed but again there were no obvious defects (Figure 3.21B). The NES(Rev) sequence fused onto Elp1-GFP does not disrupt the tRNA wobble uridine modification function of Elongator.

Assuming that the export sequence is functional this means that the Elp1 nuclear pool is not required for tRNA modification. By extension, the addition of the nuclear export sequence may have no effect on Elp1 function because it does not alter the wild-type distribution, namely there is no physiologically relevant Elp1 nuclear pool. This is in agreement with the fact that the distribution of Elp1-NES(Rev)-GFP is not drastically altered compared to wild-type Elp1-GFP. Taking into account the fact that analysis of images in 2D would be expected to overestimate the nuclear pool, since it does not account for compartment volumes, then it is possible that the apparent nuclear pool quantified in both images may be an artefact of this. We cannot say for sure that the nuclear export sequence can work in the context of Elp1-GFP but it has been used in other work to deplete yeast proteins from the nucleus (Ohira and Suzuki, 2011).

It is also possible that independently of the basic region tested in this work, Elp1 could undergo nucleo-cytoplasmic shuttling so that in the context of this strong NES sequence no localisation defect can be assayed. There are no leucine rich NES sequences detectable in any Elongator subunits so it is not clear how any shuttling between the nucleus and cytoplasm could be facilitated. Previous work supports the

idea that Elp1 does not shuttle since sequential deletion of all known export pathways in yeast failed to cause accumulation of Elp1 in the nucleus (Rahl et al., 2005).

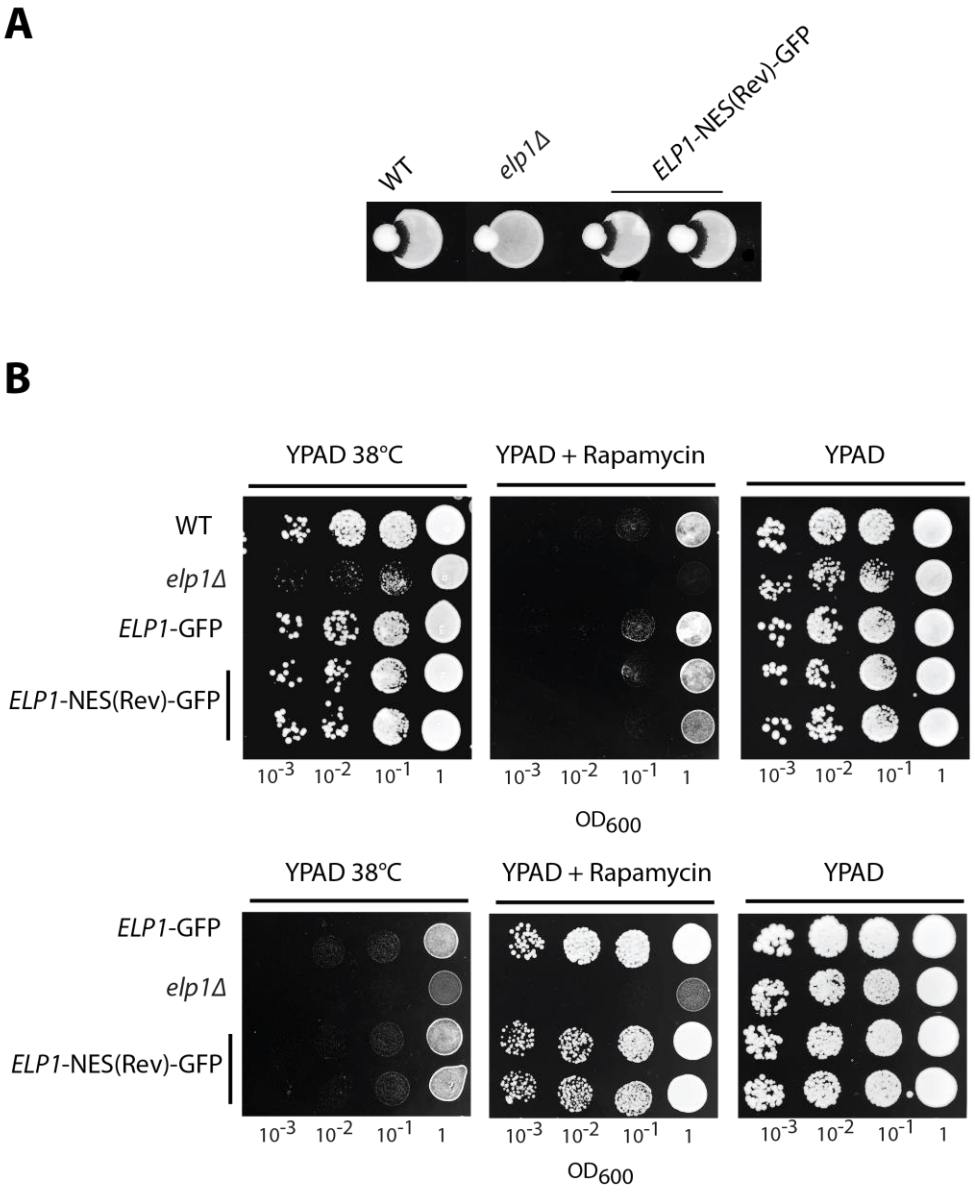

Figure 3.21: Elp1 fused to the NES of HIV Rev is functional. A) Eclipse assay of *ELP1*-NES(Rev)-GFP strains. Two *ELP1*-NES(Rev)-GFP clones were assayed alongside *ELP1*-GFP (YRDS59). WT (wild-type, BY4741) and *elp1Δ* (YRDS250) served as controls for Zymocin sensitivity and resistance respectively. B) Growth tests of two *ELP1*-NES(Rev)-GFP clones alongside *ELP1*-GFP (YRDS59), *elp1Δ* (YRDS250) at 30 °C, 38°C and on media containing 1 µg/µl of Rapamycin.

3.3.4 Fusing a nuclear localisation sequence onto Elp1 disrupts Elongator function

In previous work a nuclear localisation sequence (NLS) from the protein Cbp80 was fused onto Elp1 and shown to disrupt Elongator function (as assayed by caffiene sensitivity, Rahl et al., 2005). To confirm this result the NLS of Cbp80 was also inserted into our Elp1-GFP construct (Figure 3.22). Unlike the basic region of Elp1, the Cpb80 NLS is annotated by the program cNLS mapper but not by NLSstradeum, despite being a *bona fide* NLS (Huh et al., 2003). This illustrates the potential issues with prediction of these types of sequences.

The distribution of Elp1-NLS(Cbp80)-GFP was assayed and was found to be localised in the nucleus of the cell, indicating that this NLS can drive efficient nuclear import (Figure 3.23A). In contrast, mutating four basic amino acids in this sequence to create Elp1-NLS4A(Cbp80)-GFP resulted in a distribution that was mainly cytoplasmic. These strains were quantified alongside wild-type Elp1-GFP and Elp1-KR9A-GFP and this confirmed that Elp1-NLS(Cbp80) was mainly nuclear whereas Elp1-GFP, Elp1-KR9A-GFP and Elp1-NLS4A(Cbp80)-GFP were all cytoplasmic (Figure 3.23B). The fact that a functional NLS sequence inserted at this region can be recognised by the import machinery indicates that there is unlikely to be masking of sequences in this region due the conformation of the Elp1-GFP construct. This suggests that the NES sequence inserted at the same position should also be recognised by export machinery, though we acknowledge that masking affects could be sequence specific.

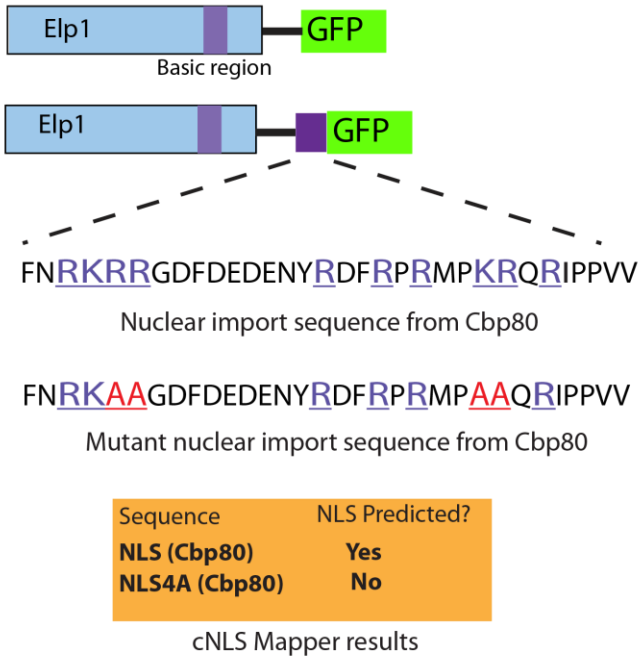

Figure 3.22: A nuclear localisation sequence from Cbp80 built into the Elp1 GFP. Schematic showing the nuclear localisation sequence (NLS) from Cbp80 fused downstream of the Elp1 C-terminus. A mutant version with four alanine substitutions was also cloned. The Cbp80 NLS sequence has basic residues highlighted in purple and alanine substitutions in red. The NLS predictor programme cNLS annotations of the Cbp80 NLS and NLS4A mutant sequences are also shown.

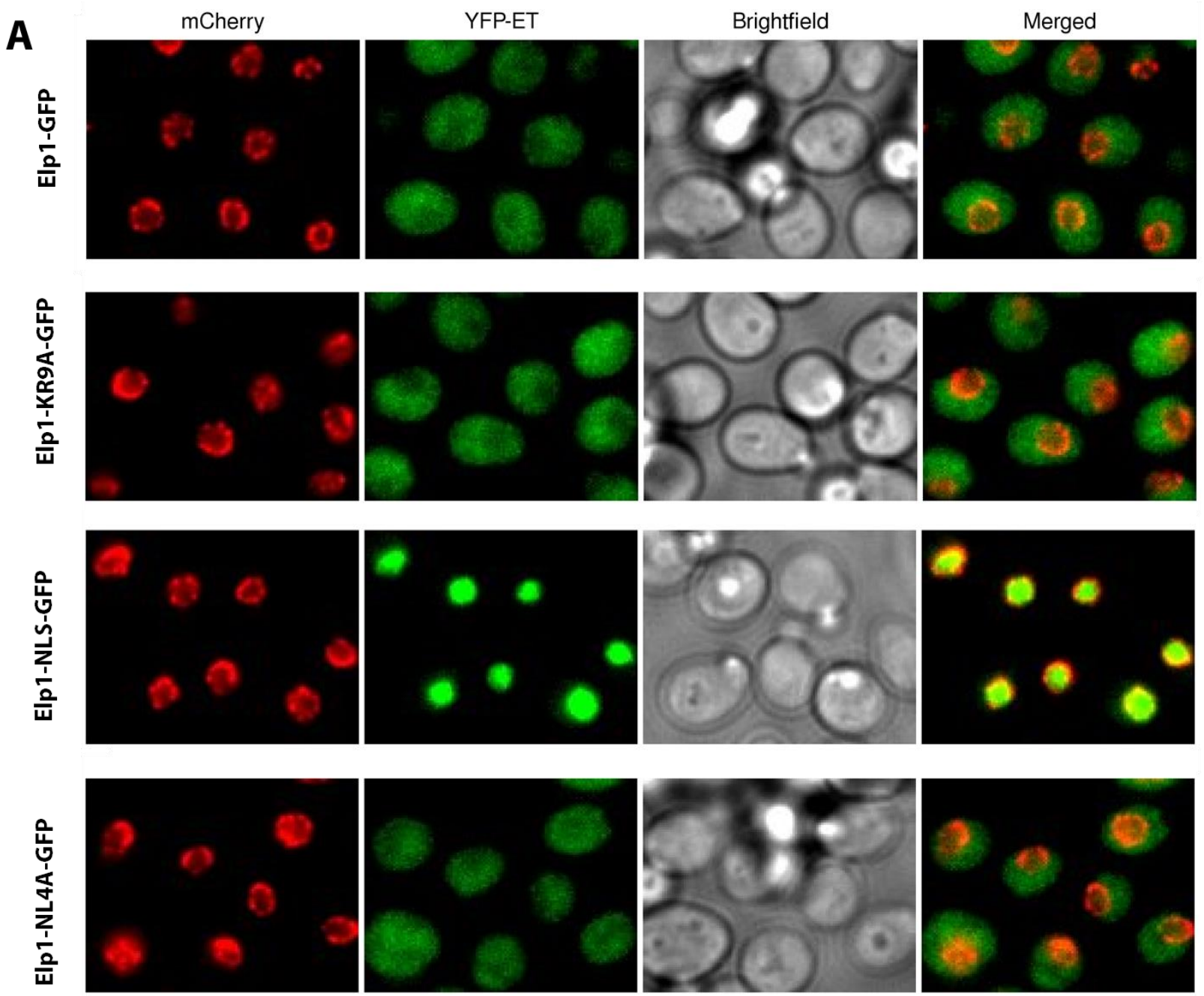

Figure 3.23: Elp1 fused to the NLS of Cbp80 is nuclear localised; See next page for figure legend.

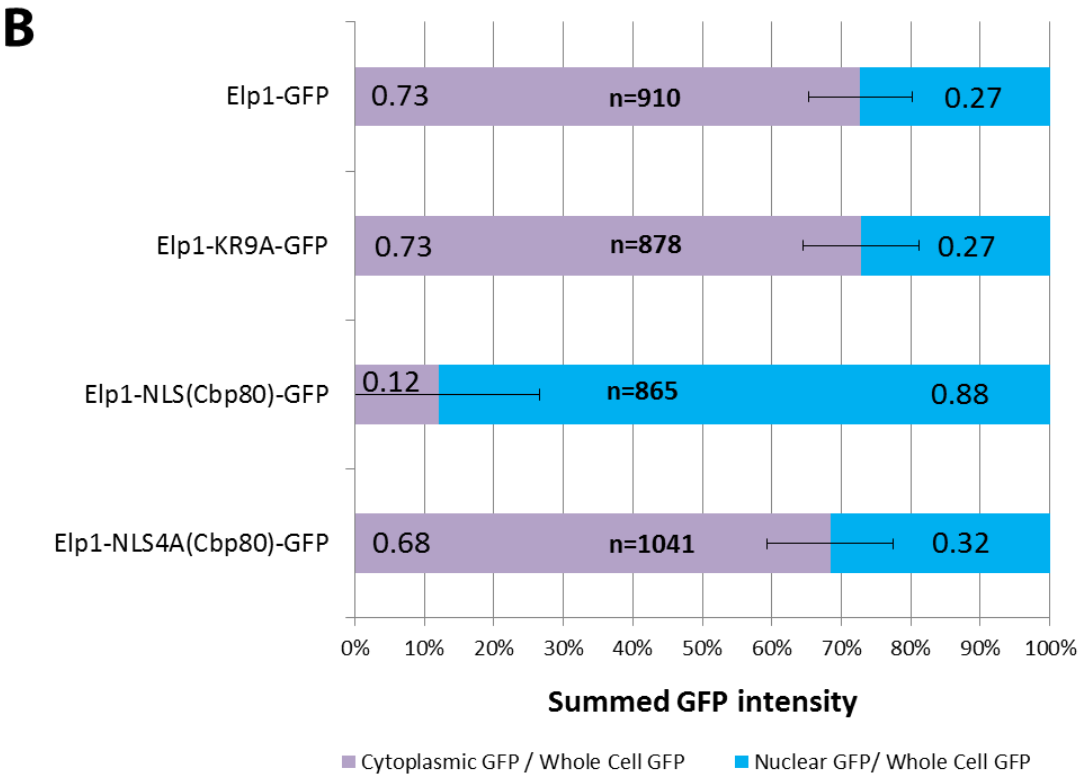

Figure 3.23: Elp1 fused to the NLS of Cbp80 is nuclear localised. A) Representative images of strains expressing GFP tagged Elp1, Elp1-KR9A, Elp1-NLS(Cbp80)-GFP, Elp1-NLS4A(Cbp80)-GFP with a Nic96-4mCherry nuclear boundary tag. The nuclear boundary (red) and GFP signals (green) were visualised by mCherry and YFP-ET channels respectively. B) Quantification of the average % nuclear and cytoplasmic pools of Elp1. Percentages were calculated using the summed intensity of GFP and the number (n) of cells analysed for each strain is shown.

The Zymocin sensitivity of *ELP1*-NLS(Cbp80)-GFP and *ELP1*-NLS4A(Cbp80)-GFP strains was checked by Eclipse assay and by using the pAE1 Zymocin expression plasmid (Figure 3.23). The *ELP1*-NLS(Cbp80)-GFP strain was resistant to Zymocin whereas the *ELP1*-NLS4A(Cbp80)-GFP strain was sensitive. The *ELP1*-NES(Rev)-GFP strain showed slight resistance compared to wild-type *ELP1*-GFP in the pAE1 assay. This suggests it may have a minor effect on Elp1 function, the conformation of the NES or increased length of the linker between GFP and the Elp1 C-terminus could cause this small defect. Nevertheless the tRNA wobble uridine modification function of Elongator, as monitored using Zymocin sensitivity, is abolished when Elp1 is trapped in the nucleus.

Taken together this data supports a role for Elongator that involves cytoplasmic rather than nuclear localisation. We have tried to deplete the nuclear pool of Elp1 using a strong nuclear export sequence (HIV Rev) and though we cannot be certain how well this works, the Elp1 protein is still functional in terms of tRNA modification. Conversely, when Elp1 is trapped in the nucleus using a strong nuclear import sequence (Cbp80) this inactivates Elongator. Coupled with the fact that the Elp1-KR9A mutant shows no defect in Elp1 localisation this would suggest that Elp1 is a *bona fide* cytoplasmic protein and that its cytoplasmic distribution is required for its tRNA modification.

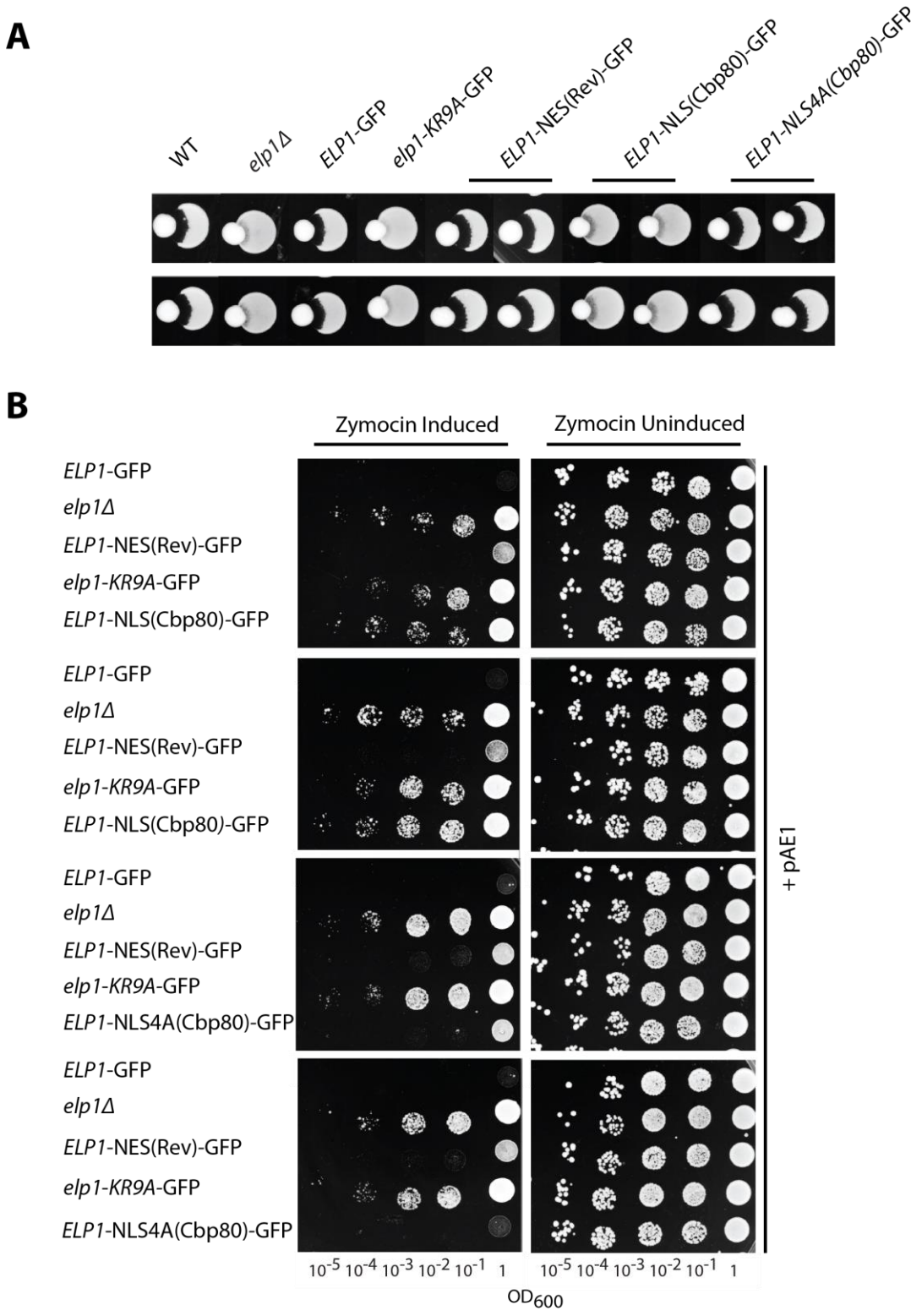

Figure 3.24: Elp1 fused to the NLS of Cbp80 is non-functional. A) Eclipse assay of various *ELP1* strains. Two clones of each strain were tested. Wild-type (WT, BY4741), *ELP1*-GFP (YRDS253) were controls for sensitivity and *elp1Δ* (YRDS250) for resistance to zymocin. B) Growth tests of various *ELP1* strains containing the pAE1 plasmid. pAE1 contains the gamma toxin subunit of Zymocin under control of a galactose inducible promoter. Zymocin expression was induced by growth on galactose and repressed on glucose. *ELP1*-GFP (YRDS59) and *elp1Δ* (YRDS250) served as controls for Zymocin sensitivity and resistance respectively.

Chapter 4: The Elp1 basic region does not affect complex assembly but is linked to C-terminal phosphorylation

4.1 Introduction

The Elongator holocomplex consists of two copies of a heterotrimeric subcomplex containing Elp1, Elp2, and Elp3 (Otero et al., 1999) together with a more salt labile subcomplex containing two copies each of Elp4, Elp5 and Elp6 (Krogan and Greenblatt, 2001, Winkler et al., 2001, Glatt et al., 2012). The Elp1 subunit has been shown to be essential for assembly of Elongator and acts as a core scaffold (Frohloff et al., 2003, Fichtner et al., 2002b). The Elp3 subunit relies on Elp1 for stability and is also required for Elongator to be assembled. In contrast, Elp2 is dispensable for core Elongator assembly but is required for binding of accessory factor Kti12 (Frohloff et al., 2003, Fichtner et al., 2002b). The Elp4-6 subunits all contain a common RecA-like NTPase fold and assemble into a heterohexameric ring structure (Glatt et al., 2012). The dodecamer holocomplex of Elongator is suggested to be assembled such that the heterohexameric ring of Elp4-6 bridges two sub-complexes of Elp1-Elp3 (see Figure 1.3, Glatt et al., 2012).

Kti12 is an accessory factor that binds to the preassembled Elongator complex and is essential for its function (Frohloff et al., 2001, Fichtner et al., 2002a, Butler et al., 1994). It is not known why Kti12 is important for the tRNA modification function of Elongator but deletion or overexpression results in Zymocin resistance, suggesting that a balance of Kti12 is required (Butler et al., 1994).

The Elp1 subunit of Elongator is also regulated by phosphorylation and it has been shown that the balance of phospho-isoforms is important for Elongator function (Mehlgarten et al., 2009, Jablonowski et al., 2004, Jablonowski et al., 2001a, Jablonowski et al., 2009). Deletion of the phosphatase *SIT4* or multicopy *KTI12* results in Elp1 'hyper' phosphorylation and inactivation of Elongator (Jablonowski et al.,

2001a, Butler et al., 1994, Frohloff et al., 2001, Fichtner et al., 2002a). Conversely, mutation of the casein kinase *HRR25* or deletion of *KTI12* results in Elp1 'hypo' phosphorylation but also inactivation (Mehlgarten et al., 2009, Jablonowski et al., 2009, Jablonowski et al., 2004, Jablonowski et al., 2001a). It has been suggested that both Kti12 and Hrr25 act together to negatively regulate Sit4 dependent Elp1 dephosphorylation. Some evidence to support this is that the Elp1 'hypo' phosphorylated form in *kti12* deletion strains persists when combined with multicopy *HRR25*, suggesting promotion of phosphorylation requires both Hrr25 and Kti12. Multicopy *KTI12* and *SIT4* in combination also restored normal phosphorylation levels (Jablonowski et al., 2004, Mehlgarten et al., 2009) suggesting these proteins may antagonise each other. Further to this Hrr25 is known to associate with Kti12 and Elp1 and the latter interaction is reduced with excess Kti12 (Mehlgarten et al., 2009). There is a clear interplay between different phospho-forms of Elp1 that is dependent on Kti12, Hrr25 and Sit4 and as of yet this is not well understood (see Figure 1.10).

Many interlinking factors may influence the tRNA wobble uridine modification function of the Elongator complex, including correct assembly of the holocomplex, interaction with accessory factors and its modification status. It was therefore important to address whether there were any differences in these properties that may be associated with or perhaps be responsible for the loss of Elongator function observed in our basic region mutant *elp1-KR9A*.

4.2 Results

4.2.1 Elongator complex assembly in Elp1-KR9A

It was possible that the Elp1 basic region could be required for the proper assembly of the Elongator holocomplex. In order to check that the Elongator complex was still assembled in the presence of the basic region mutations, Elp1-GFP and Elp1-KR9A-GFP were pulled down with GFP-Trap and interacting proteins stained with SYPRO Ruby. As a negative control GFP tagged argininosuccinate lyase (Arg4), a protein involved in arginine biosynthesis that should not interact with Elongator subunits was pulled down in parallel. This controls for non-specific interactions with the beads and the GFP tag.

There were no obvious differences in the overall assembly of the Elp1-3 subcomplex when comparing Elp1 and Elp1-KR9A and no major protein bands missing in the mutant (Figure 4.1). This implies that the interaction profile of Elp1-KR9A may not be drastically altered compared to wild-type Elp1 and that this subcomplex is still assembled. Protein bands corresponding to Elp4-6 cannot be easily assigned but are reportedly less stable interactors and could also be obscured by the large number of other small protein bands in the pulldown. It should also be noted that a faster migrating N-terminal truncated form of Elp1 is also observed in both wild-type Elp1 and Elp1-KR9A samples, this may be a degradation product or serve an as of yet unknown function (Fichtner et al., 2003).

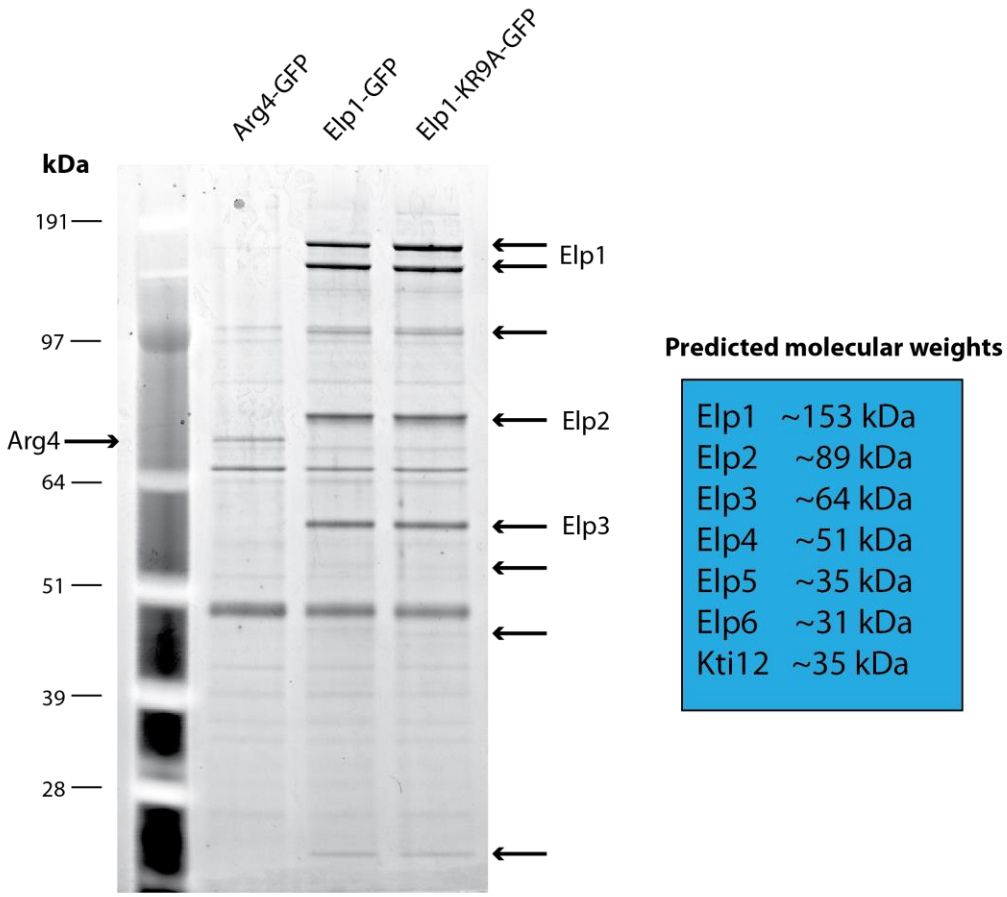

Figure 4.1: The Elp1-3 subcomplex of Elongator is assembled in the Elp1-KR9A mutant. GFP-Trap pulldowns of Arg4-GFP, Elp1-GFP and Elp1-KR9A-GFP were analysed by SDS-PAGE on a 4-12% Bis-Tris polyacrylamide gel and stained with SYPRO Ruby. The arrows indicate Elp1 associated bands and where possible the predicted identity of each band based on previous work. The faster migrating form of Elp1 is an N-terminal truncation. There are no obvious differences in the pattern of bands between Elp1 and Elp1-KR9A. The right panel shows the predicted molecular weights of each of the Elongator subunits and Kti12.

To further determine the effects of the basic region mutation in terms of complex assembly, the interaction of GFP tagged Elp1 and Elp1-KR9A with other HA tagged Elongator complex members was tested. Representative members of the two sub-complexes of Elongator, Elp3 and Elp5 respectively, together with Kti12, were HA tagged in the context of GFP tagged Elp1 or Elp1-KR9A.

Pulldowns of Elp1-GFP and Elp1-KR9A-GFP were assayed for associated HA tagged Kti12, Elp3 and Elp5 and these were each present as co-precipitants under physiological salt conditions (Fig 4.2A and E). This confirms both that the Elp1-3 subcomplex is intact and that interactions with Elp5 and Kti12 are largely unaffected by the basic region mutation. As with the previous pulldowns, Arg4-GFP was used as a negative control to show that these proteins are not associated with this nonspecific protein or with the GFP tag (Fig 4.2C).

When these interactions were analysed by densitometry, Elp1-KR9A-GFP was consistently found associated with ~30% less Elp5-3HA and ~40% less Kti12-3HA than the wild-type Elp1-GFP protein (Fig 4.3A and B). These minor defects in interaction are highly consistent and statistically significant. In contrast, the interaction between Elp1-KR9A-GFP and Elp3-3HA appears unchanged (Figure 4.3C), consistent with the previous experiment (Figure 4.1). As a positive control Elp1-1209A-GFP was also pulled down in the context of HA tagged Kti12, since this mutant was previously shown to have increased Kti12 binding (Abdel-Fattah and Stark, unpublished). As expected this phosphorylation site mutant had ~2 fold more interacting Kti12-3HA than wild-type Elp1-GFP (Figure 4.2 and 4.3A).

It is difficult to explain why such defects in Kti12 and Elp5 interactions with the Elp1-KR9A mutant were observed but it may reflect the fact that Elongator is no longer

modifying tRNA. If the complex needs to shuttle between multiple forms and is stuck due to the basic region mutations, then this may lead to reduced complex stability and/or interaction with particular subunits. It cannot be ruled out that the conformation of Elp1-KR9A may also be altered and that has subtle effects on these interactions. The differences in Kti12 association between Elp1-KR9A and Elp1-1209A mutants suggests that although both are non-functional in terms of tRNA modification (Chapter 3), the defect causing this loss of function may be distinct in both cases. These mutants may represent distinct forms of Elongator, whereas wild-type Elp1 may cycle between the two for its tRNA modification function. It is likely that Elp4 and 6 would show similar defects in their interaction with Elp1-KR9A since these subunits are assembled into a hexameric ring complex alongside Elp5 (Glatt et al., 2012). We might also expect to see no defect in Elp2 interaction based on the results for Elp3 and our previous initial assay of total complex assembly (Figure 4.1).

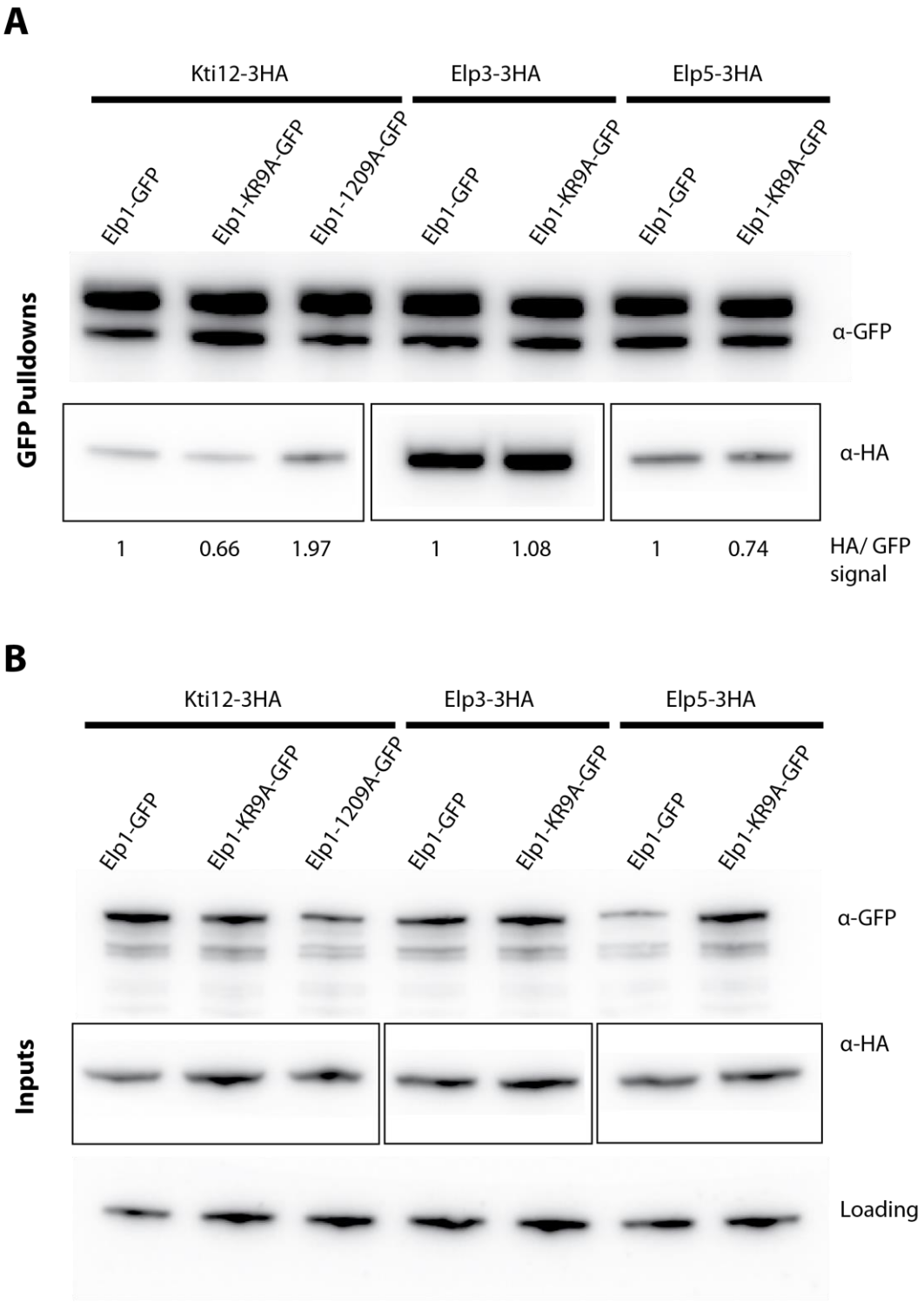

Figure 4.2: Elp1 and Elp1-KR9A show differences in Elp5 and Kti12 association; See overleaf for figure legend.

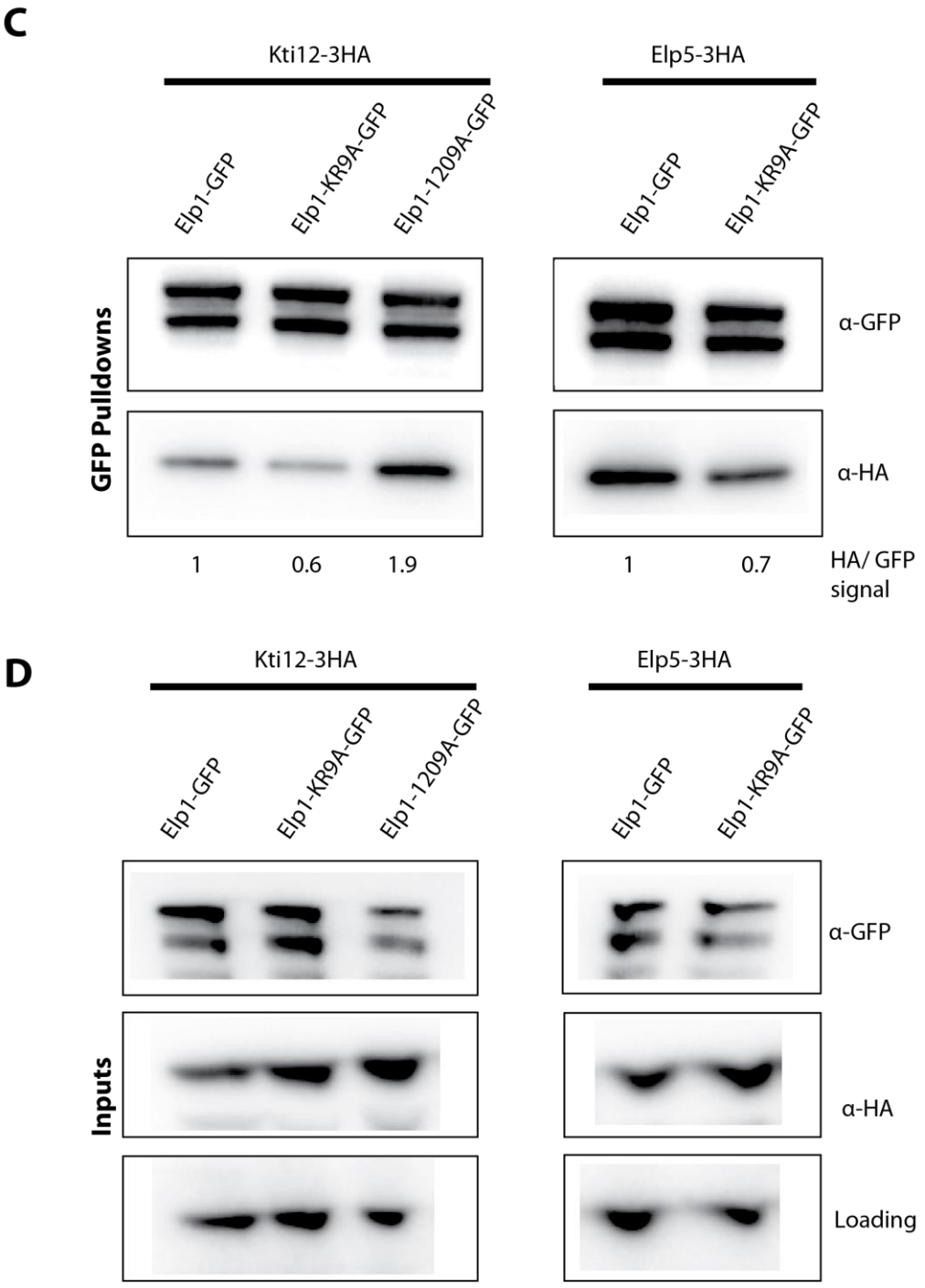

Figure 4.2: Elp1 and Elp1-KR9A show differences in Elp5 and Kti12 association; See next page for figure legend.

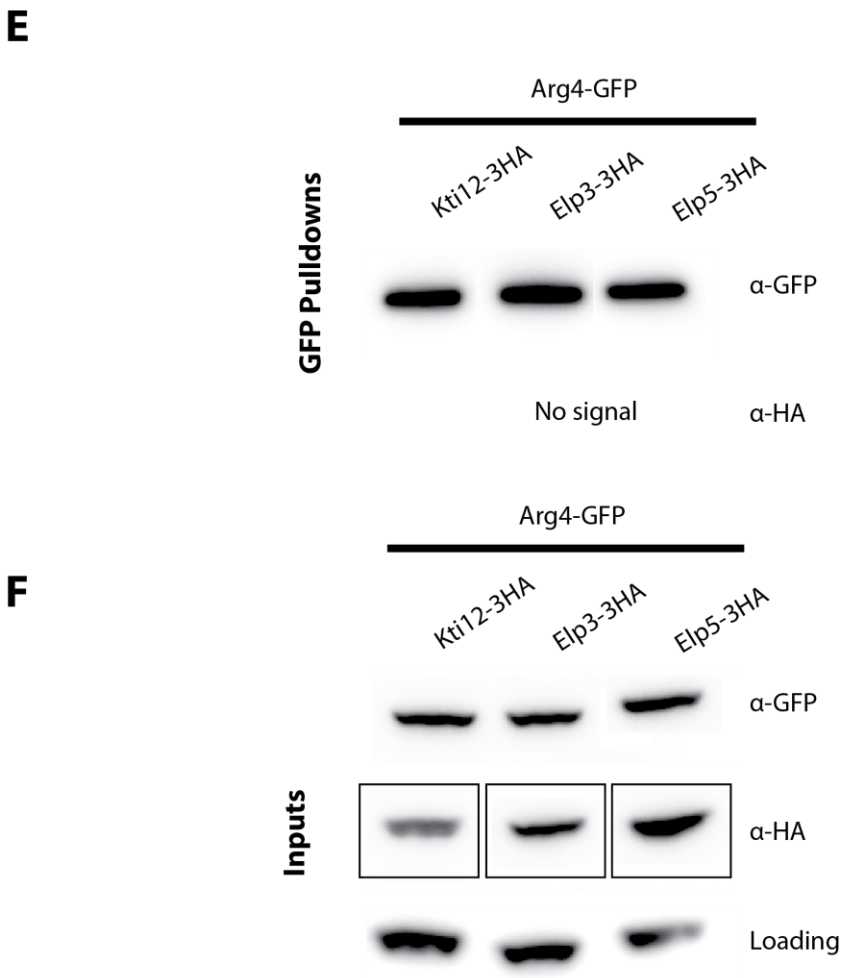

Figure 4.2: Elp1 and Elp1-KR9A show differences in Elp5 and Kti12 association. All samples were analysed by western blotting with anti-GFP and anti-HA. A) GFP-Trap pulldowns and B) inputs of Elp1-GFP and Elp1-KR9A-GFP in the context of HA tagged Kti12, Elp3 and Elp5. C) GFP-Trap pulldowns and D) inputs of Elp1-GFP and Elp1-KR9A-GFP in the context of HA tagged Kti12 and Elp5. E) GFP-Trap pulldowns and F) inputs of Arg4-GFP in the context of HA tagged Kti12, Elp3 and Elp5 as a negative control. As a loading control input blots were also analysed with anti-Cdc28. The Elp1-1209A-GFP mutant is known to bind excess Kti12 and was used as a positive control. Pulldown blots were quantified relative to wild-type Elp1 by densitometry of HA tag signals normalised by GFP tag signals.

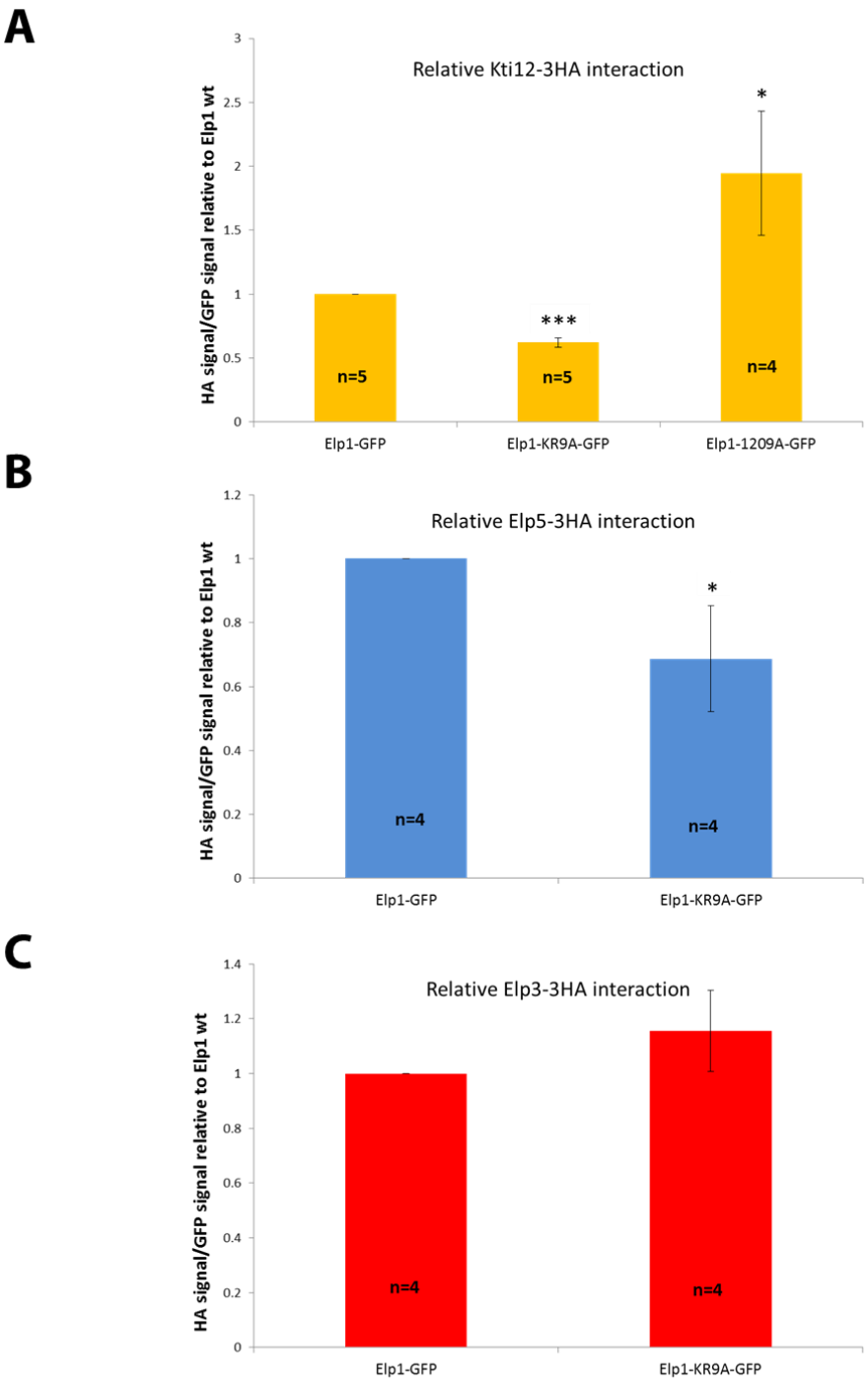

Figure 4.3: Elp1 and Elp1-KR9A show highly consistent differences in Kti12 and Elp5 association. The average relative quantification of pulldown experiments by densitometry of HA tag signals normalised by GFP tagged signals. GFP-Trap pulldowns of Elp1-GFP and Elp1-KR9A-GFP in the context of A) HA tagged Kti12 B) HA tagged Elp5 C) HA tagged Elp3. The Elp1-1209A-GFP mutant is known to bind excess Kti12 and was used as a positive control. The number (n) of independent experiments is indicated and the error bars represent the standard deviation of the average. * indicates a *p* value of < 0.05 (significant), *** indicates a *p* value < 0.001 (very highly significant). Differences in Elp3 association were not statistically significant.

It was possible that since there was a reduced interaction between Kti12 and Elp1-KR9A that the Elp1-KR9A mutant phenotype might be rescued by introducing extra copies of *KTI12*. Deletion or multicopy expression of Kti12 causes Elongator dysfunction (Butler et al., 1994) suggesting there is a balance that must be maintained for Elongator functionality. Extra copies of *KTI12* were therefore introduced on a high copy plasmid (pJHW27) and the effect on Elongator function tested by eclipse assay (Figure 4.4A).

Wild-type Elp1 strains with elevated *KTI12* gene copy became resistant to Zymocin, in agreement with previous work (Butler et al., 1994, Mehlgarten et al., 2009). The Elp1-KR9A mutant was Zymocin resistant as expected, and elevation of *KTI12* copy number did not alter this. Extra Kti12 protein cannot suppress the Elp1-KR9A defect and this is consistent with defects in Kti12 association not being the primary cause of Elongator dysfunction in this mutant. The phosphorylation site mutant Elp1-1209A also remained Zymocin resistant with extra copies of *KTI12*. The effects of *kti12Δ* in the context of these mutants were also assayed (Figure 4.4B). The wild-type Elp1 became resistant to Zymocin when *KTI12* was deleted but Elp1-KR9A and Elp1-1209A remained resistant. The balance of Kti12 is essential for Elongator function and disrupting this in the context of Elp1-KR9A does not rescue the strain's Zymocin resistant phenotype.

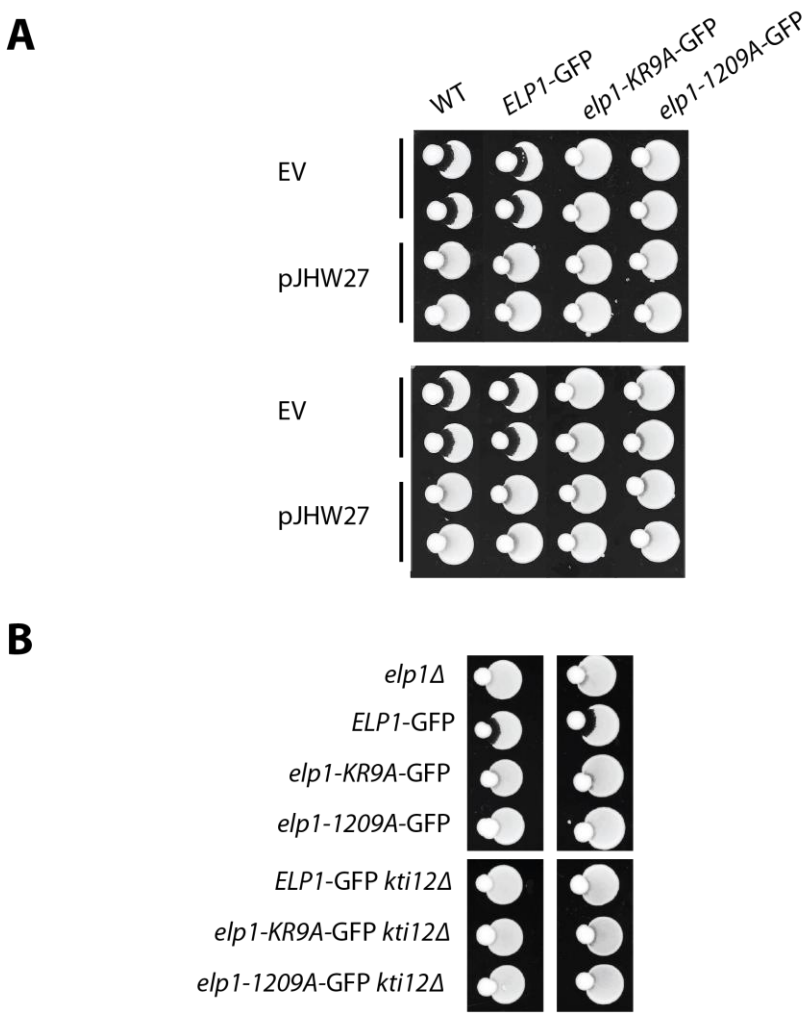

Figure 4.4: Altering the balance between Elongator and Kti12 does not rescue the Zymocin resistance of *elp1* mutants. A) Eclipse assay of WT (wild-type), *ELP1*-GFP, *elp1-KR9A*-GFP and *elp1-1209A*-GFP strains with either empty vector (EV) or a multicopy KTI12 vector (pJHW27). B) Eclipse assay of *ELP1*-GFP, *elp1-KR9A*-GFP and *elp1-1209A*-GFP strains with or without *kti12Δ.* WT (YRDS1) and *elp1*Δ (WAY034) served as controls for Zymocin sensitivity and resistance respectively.

4.2.2 Elp1 and Elp1-KR9A can associate within Elongator

Since it is now known that Elongator forms a dodecamer made up of two copies of its six subunits, it seemed possible that Elp1-KR9A could be defective in assembly into this higher order complex. To test this YCp-*ELP1*-6HA and YCp-*elp1-KR9A*-6HA plasmids were transformed into *ELP1*-GFP and *elp1-KR9A*-GFP strains to generate cells expressing two differentially tagged copies of Elp1.

Wild-type Elp1-GFP and Elp1-KR9A-GFP were pulled down using GFP-Trap and assayed for co-precipitation of the 6HA tagged versions of Elp1 (Figure 4.5). The GFP tagged wild-type Elp1 co-precipitated with Elp1-6HA as was previously reported (Glatt et al., 2012) and could also associate with Elp1-KR9A-6HA to the same degree. The GFP tagged Elp1-KR9A also co-precipitated with Elp1-6HA and Elp1-KR9A-6HA and no obvious defects in the interaction between any of the combinations were observed. There is therefore no apparent defect in Elp1 association within the Elongator complex due to the Elp1 basic region mutation.

It is interesting that there are no observable defects in Elp1 association in Elp1-KR9A, despite the fact this mutant shows a minor defect in Elp5 association. It should also be noted that Elp3 association is apparently unaffected in this mutant (Figure 4.2A). This suggests that Elp1 could associate across Elp1-3 subcomplexes independently of the Elp4-6 hexamer. To test this, these differentially tagged Elp1 pulldowns could be repeated in the context of an *elp5* deletion strain. If wild-type Elp1 shows no defect in association with a different tagged version of itself, despite the hexamer being disrupted by loss of Elp5, then this interaction is independent of bridging by the Elp4-6 subcomplex.

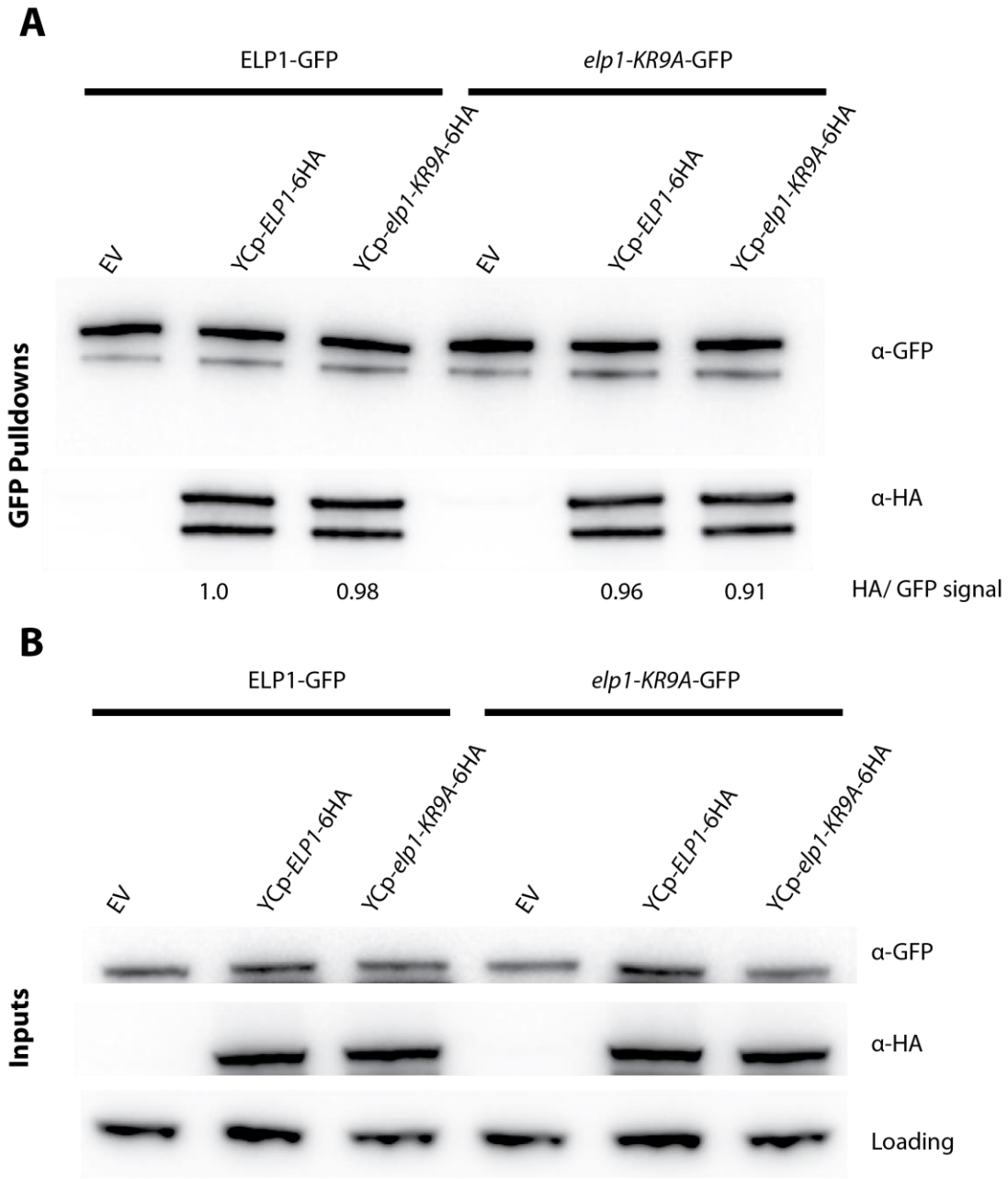

Figure 4.5: Elp1 and Elp1-KR9A can both associate as part of Elongator. All samples were analysed by western blotting with anti-GFP and anti-HA. A) GFP-Trap pulldowns and B) inputs from *ELP1*-GFP (YRDS253) and *elp1-KR9A*-GFP (YRDS255) strains containing YCp-*ELP1*-6HA or YCp-*elp1-KR9A*-6HA plasmids. As a loading control, input blots were also analysed with anti-Cdc28. Pulldown blots were quantified relative to wild-type Elp1 by densitometry of HA tag signals normalised to the GFP tag signals.

The Zymocin sensitivity of these doubly tagged Elp1 strains was tested by Eclipse assay to check that Elongator dysfunction was not caused by an excess of Elp1 expression (Figure 4.6). As shown previously, wild-type *ELP1* strains were sensitive whereas *elp1-KR9A* strains resistant to Zymocin. *ELP1*-GFP strains remain sensitive in the context of YCp-*ELP1*-6HA, so increased *ELP1* copy number is not causing any obvious defects. Interestingly, *elp1-KR9A*-GFP strains, though still largely Zymocin resistant, showed some subtle evidence of rescue by wild-type YCp-*ELP1*-6HA. When *ELP1*-GFP was combined with YCp-*elp1-KR9A*-6HA, the strain remained sensitive, but slightly less so than when combined with the wild-type YCp-*ELP1*-6HA plasmid. Strains expressing the two differentially tagged copies of Elp1-KR9A were completely resistant. The fact that the combination of Elp1-GFP with Elp1-KR9A-6HA is more functional than Elp1-*KR9A*-GFP with Elp1-6HA implies adding the 6HA tag to the Elp1 C-terminus leads to slightly less functionality than the GFP tagged version, as was observed previously (Chapter 1).

Although these effects are quite subtle, it is nonetheless clear from these experiments that both wild-type Elp1 and Elp1-KR9A compete for incorporation into Elongator despite the fact this leads to the formation of non-functional complexes. This is further evidence that there is no defect in the overall assembly of Elongator due to the Elp1 basic region mutant.

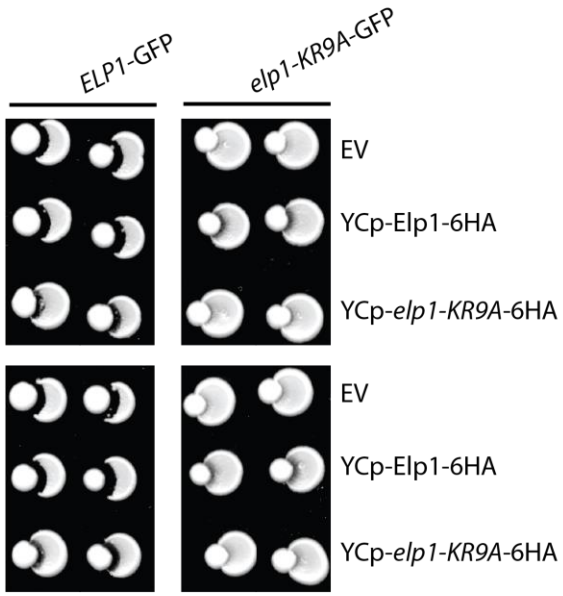

Figure 4.6: Elp1 and Elp1-KR9A compete for assembly into Elongator. Eclipse assay of *ELP1*-GFP (YRDS253) and *elp1-KR9A-GFP* (YRDS255) strains containing either empty vector (EV), YCp-*ELP1*-6HA or YCp-*elp1-KR9A*-6HA plasmids. Two replicate spots of each strain are shown.

4.2.3 The Elp1-KR9A mutant leads to increased phosphorylation at the functionally important serine-1209 site

The Elp1 subunit of Elongator is regulated by phosphorylation and the balance between phosphorylated forms is important for Elongator function (Mehlgarten et al., 2009, Jablonowski et al., 2004, Jablonowski et al., 2001a, Jablonowski et al., 2009). Further to this our lab has shown that the C-terminus of Elp1 contains functionally important phosphorylation sites by phosphopeptide mapping and mutational analysis (Abdel-Fattah and Stark, unpublished). The mutation of Elp1 C-terminal serine 1209 to alanine results in Elongator inactivation, suggesting this site is functionally essential. Mutation of this site to a phosphomimic residue (aspartic acid) partially rescues this defect (Abdel-Fattah and Stark, unpublished).

An anti-peptide antibody was raised against the 1209 phosphorylation site in order to begin investigating the possible relationship between the Elp1 basic region and phosphorylation. As expected, this antibody cannot recognise the Elp1-1209A mutant protein in which residue 1209 cannot be phosphorylated (Figure 4.7).

To test whether the Elp1-KR9A mutant was still phosphorylated at this functionally important site, Elp1-GFP and Elp1-KR9A-GFP were pulled down with GFP-Trap and probed for ser-1209 phosphorylation (Figure 4.8A). The *elp1-KR9A* mutant showed a three-fold increased phosphorylation at this site compared to wild-type Elp1-GFP. This increase in ser-1209 phosphorylation was also detected in total protein extracts of Elp1-GFP and *elp1-KR9A*-GFP (Figure 4.8C).

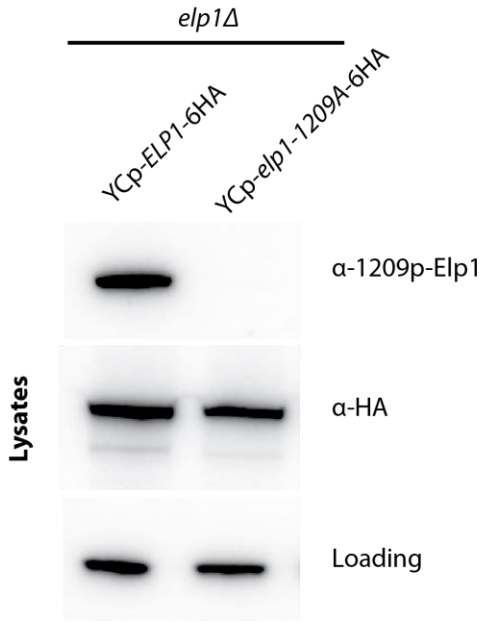

Figure 4.7: The 1209p-Elp1 antibody does not recognise the Elp1-1209A mutant protein. Protein extracts from an *elp1Δ* strain (WAY034) containing YCp-*ELP1*-6HA or YCp-*elp1-1209A*-6HA plasmids were analysed by western blotting with phosphospecific anti-phosphoserine-1209 (anti-1209p-Elp1) antibody and anti-HA. As a loading control blots were also analysed with anti-Cdc28.

Elp1-GFP and Elp1-KR9A-GFP pulldowns were also checked for general levels of phosphorylated serine as well as for ser-1209 phosphorylation (Figure 4.9). Alongside the observed increase in ser-1209 phosphorylation there was also an increase in the phospho-serine signal in Elp1-KR9A-GFP compared to wild-type Elp1. The Elp1-1209A mutant showed wild-type levels of phospho-serine. The increase in the generic anti-phospho-serine signal observed in Elp1-KR9A may be generated by recognition of ser-1209 phosphate only, since this is lost in the Elp1-1209A mutant, but it is also possible that phosphorylation of Elp1 at other sites is increased. The interplay between different specific phosphorylation sites on Elp1 is not well understood and this requires more thorough investigation, perhaps with other phosphospecific antibodies. Such work is currently ongoing in our lab.

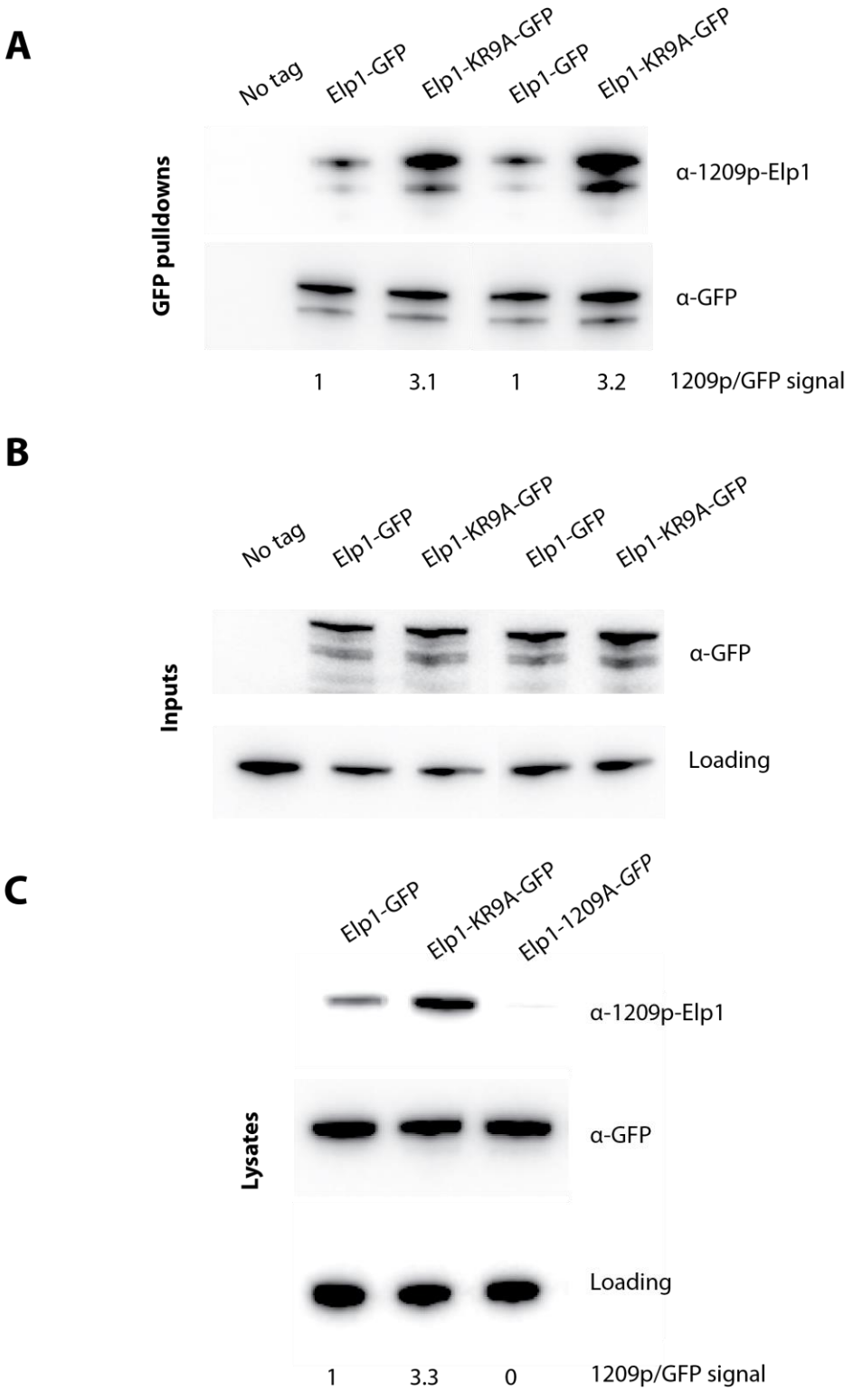

Figure 4.8: The Elp1-KR9A mutant shows increased phosphorylation at ser-1209. All samples were analysed by western blotting with anti-GFP and anti-1209p-Elp1. A) Duplicate GFP-Trap pulldowns and B) inputs of Elp1-GFP and Elp1-KR9A-GFP. C) Protein extracts from strain expressing Elp1-GFP, Elp1-KR9A-GFP and Elp1-1209A-GFP. As a loading control, input and extract blots were also analysed with anti-Cdc28. Pulldown blots were quantified relative to wild-type Elp1 by densitometry of 1209p-Elp1 signals normalised by GFP tag signals.

In Elp1-KR9A, Kti12 association was slightly defective but phosphorylation was increased compared to wild-type Elp1. In contrast, Elp1-1209A results in increased Kti12 association. This apparent inverse relationship between serine 1209 phosphorylation and Kti12 binding might suggest that phosphorylation governs Kti12 binding and release. In support of this, Hrr25 kinase dead mutants lead to 'hypo' phosphorylated Elp1 and this also results in increased binding of Kti12 to Elp1, similar to the Elp1-1209A mutant (Mehlgarten et al., 2009).

The increased phosphorylation at ser-1209 in Elp1-KR9A could be in line with the hypothesis that this mutant is trapped in a specific form that prevents tRNA modification. It is not yet clear why phosphorylation at this site is functionally relevant but it may be required to activate the complex or be involved in the mechanism of tRNA modification. The accumulation of this phosphorylated site in Elp-KR9A could indicate that this mutant is being misregulated, or could occur as a compensatory mechanism to lack of function. The basic region may also bind to phosphorylated residues in the Elp1 C-terminus and this could result in conformational changes involved in complex function. However, regardless of the mechanism, it is clear that mutation of the Elp1 basic region has some interplay with the functionally essential serine-1209 phosphorylation site.

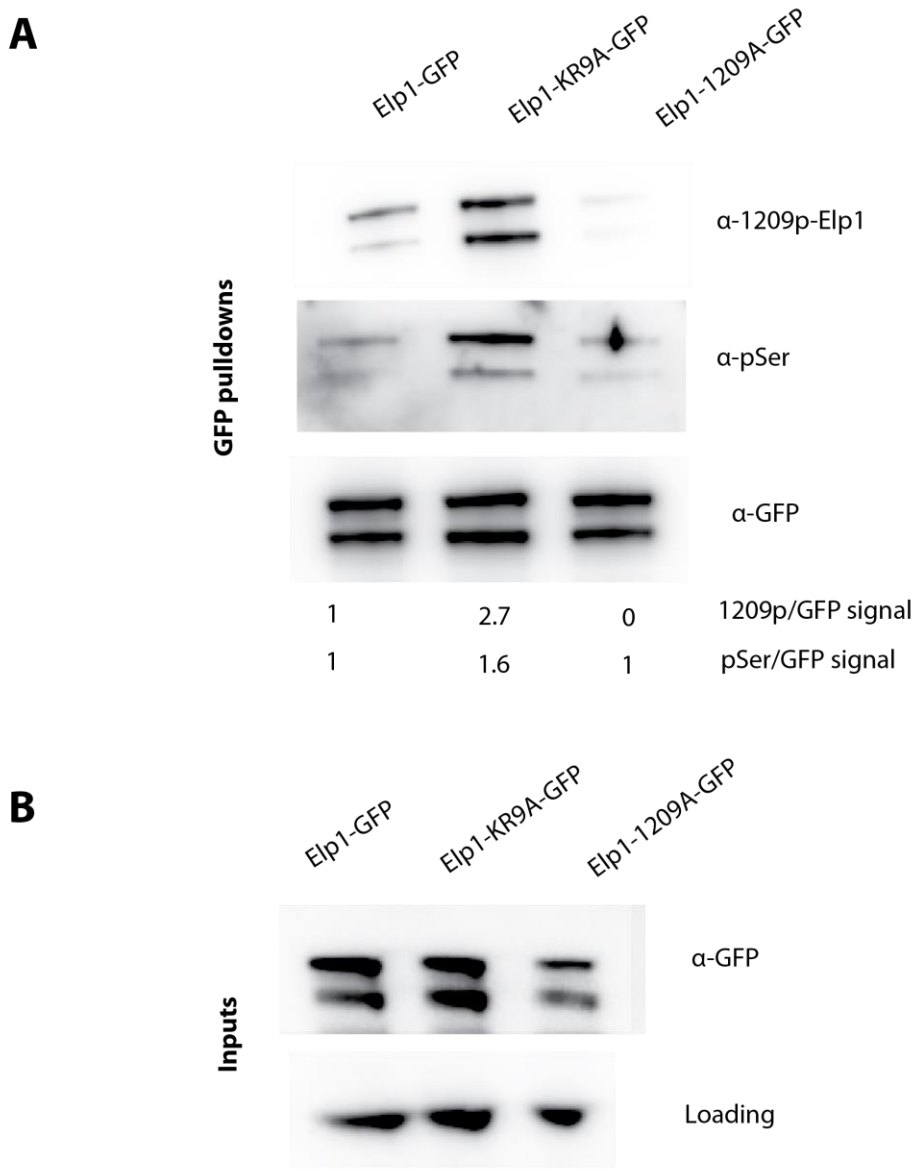

Figure 4.9: The Elp1-KR9A mutant shows increased serine phosphorylation. All samples were analysed by western blotting with anti -GFP, anti -1209p-Elp1 and anti-pSer. A) GFP-Trap pulldowns and B) inputs of Elp1-GFP, Elp1-KR9A-GFP and Elp1-1209A-GFP. As a loading control input and lysate blots were also analysed with anti-Cdc28. Pulldown blots were quantified relative to wild-type Elp1 by densitometry of 1209p-Elp1 or pSer signals normalised by GFP tag signals.

4.2.4 Analysis of Elp1 and Elp1-KR9A associated proteins

To attempt to identify any other differences between the binding profiles of Elp1-GFP and Elp1-KR9A-GFP these were affinity purified by virtue of their GFP tag and analysed by mass spectrometry for label-free quantification of associated proteins. As a control, pulldowns from untagged strains were processed in parallel. This method is qualitative rather than quantitative but would give an idea of any major differences in the interaction profile of the wild-type and mutant Elp1 proteins, especially in terms of known interactors. Any candidate binding interactions drastically altered in Elp1-KR9A relative to wild-type Elp1 could then be confirmed by further pulldowns and western blotting. A huge difference in the binding profiles of these proteins was not expected based on the fact that there were no obvious protein band changes when GFP-Trap pulldowns of Elp1-GFP and Elp1-KR9A-GFP were compared (Figure 4.1).

Using this approach, all subunits of the Elongator complex were identified associated with both Elp1-GFP and Elp1-KR9A-GFP (Table 4.1). The Elp1-3 subunits were all identified with a similar number of peptides between samples and were by far the best identified in terms of peptide number. The subunits Elp4-6 were also all identified but in most cases with only one peptide being detected. Since they are known and verified interactors this was acceptable and indicates that this subcomplex is present in the Elp1 associated fraction. However, peptides corresponding to Kti12 were not observed in any of the pulldown samples, despite associated Kti12 being readily identified by western blotting under the same pulldown conditions (Figure 4.2), this may suggest a technical issue in the identification of associated proteins.

Gene Name	Protein Name	Description	Enrichment relative to beads	Number of peptides	PEP	Coverage %
Elp1-GFP						
YLR384C	Elp1	Elongator subunit 1	0.999	75	0	64.6
YGR200C	Elp2	Elongator subunit 2	1.000	46	0	67.6
YPL086C	Elp3	Elongator subunit 3	0.997	34	0	60.9
YPL101W	Elp4	Elongator subunit 4	1.000	1	2.18E-44	15.4
YHR187W	Elp5	Elongator subunit 5	1.000	1	1.36E-15	3.9
YMR312W	Elp6	Elongator subunit 6	1.000	1	0.000422	3.7
Elp1-KR9A-GFP						
YLR384C	Elp1	Elongator subunit 1	0.999	72	0	64.4
YGR200C	Elp2	Elongator subunit 2	1.000	44	0	65.5
YPL086C	Elp3	Elongator subunit 3	0.997	35	0	61.4
YPL101W	Elp4	Elongator subunit 4	1.000	4	2.18E-44	10.3
YHR187W	Elp5	Elongator subunit 5	1.000	1	1.36E-15	3.9
YMR312W	Elp6	Elongator subunit 6	1.000	1	0.000422	3.7

Table 4.1: All Elongator subunits were detected in Elp1 and Elp1-KR9A pulldowns by mass spectrometry. Elp1-GFP and Elp1-KR9A-GFP were pulled down using GFP-Trap and precipitates analysed by mass spectrometry. The Elongator subunits were significantly enriched in pulldowns compared to untagged controls and are summarised. Enrichment is calculated by intensity in sample relative to total intensity (sample+bead control). PEP is the posterior error probability and acts as a *p* value for protein identification. Values shown here are representative of 2 independent replicates.

All the subunits of the Elongator complex were identified associated with Elp1 and Elp1-KR9A by mass spectrometry, which when taken together with the previous data confirms that there is no major defect in assembly of the holocomplex. Since Kti12 was absent and the small complex subunits were only identified with a small number of peptides, caution is needed in interpreting any other interactors identified in this analysis. Given that caveat, other interacting proteins that were identified by at least two peptides and that were enriched in the Elp1 and Elp1-KR9A pulldown samples relative to the bead control are summarised in Tables 4.2 and 4.3. In general there were less interacting proteins, meeting these criteria in Elp1-KR9A than wild-type Elp1 pulldown, this may suggest the mutant is defective in some interactions, though this would require more work to confirm.

Gene Name	Protein Name	Description	Enrichment relative to beads	Number of peptides	PEP	Coverage %	Also in Elp1-KR9A?
YJR009C	TDH2	Glyceraldehyde-3-phosphate dehydrogenase, isozyme 2	0.825	19	8.6E-145	63.3	Yes
YKL081W	TEF4	Gamma subunit of translational elongation factor eEF1B	0.824	9	0	25.5	No
YLR441C	RPS1A	Ribosomal protein 10 (rp10) of the small (40S) subunit	0.793	9	1.23E-150	48.6	No
YBR196C	PGI1	Glycolytic enzyme phosphoglucose isomerase	0.853	8	2.37E-124	17.5	No
YDR023W	SES1	Cytosolic seryl-tRNA synthetase	1.000	7	2.03E-60	25.5	Yes
YER074W; YIL069C	RPS24A/ RPS24A	Protein component of the small (40S) ribosomal subunit	0.920	7	2.91E-30	37.8	No
YER110C	KAP123	Karyopherin beta, mediates nuclear import of ribosomal proteins prior to assembly into ribosomes	0.834	6	1.9E-167	14.5	Yes
YHR064C	SSZ1	Hsp70 protein that interacts with Zuo1p (a DnaJ homolog) to form a ribosome-associated complex	0.987	6	2.47E-46	16.7	No
YGL245W	GUS1	Glutamyl-tRNA synthetase (GluRS)	1.000	5	5.69E-17	7.9	No
YPL061W	ALD6	Cytosolic aldehyde dehydrogenase	0.914	5	5.59E-39	11.8	No
YKL152C	GPM1	Tetrameric phosphoglycerate mutase	0.832	5	2.42E-41	49	No
YMR108W	ILV2	Acetolactate synthase, catalyses the first common step in isoleucine and valine biosynthesis	1.000	4	1.66E-15	7	Yes
YCL050C	APA1	AP4A phosphorylase; bifunctional diadenosine 5',5'''-P1,P4-tetraphosphate phosphorylase	1.000	4	1.36E-11	11.8	Yes
YGL253W	HXK2	Hexokinase isoenzyme 2	1.000	3	7.93E-37	12.1	No
YJL136C; YKR057W	RPS21B/ RPS21A	Protein component of the small (40S) ribosomal subunit	1.000	3	2.18E-05	25.3	No
YDR050C	TPI1	Triose phosphate isomerase	0.908	3	1.55E-105	46.8	No
YJL138C; YKR059W	TIF2/TIF1	Translation initiation factor eIF4A	0.900	3	1.24E-44	18.7	No
YML028W	TSA1	Thioredoxin peroxidase; acts as both a ribosome-associated and free cytoplasmic antioxidant	0.820	3	7.93E-84	60.2	No

YHR183W; YGR256W	GND1 /GND2	6-phosphogluconate dehydrogenase; part of the pentose phosphate pathway	0.793	3	4.50E-32	8.6	No
YER043C	SAH1	S-adenosyl-L-homocysteine hydrolase	1.000	2	3.16E-14	4.5	No
YGR162W; YGL049C	TIF4631/TIF4632	Translation initiation factor eIF4G, subunit of the mRNA cap-binding protein complex	1.000	2	8.08E-16	6	No
YNL055C	POR1	Mitochondrial porin (voltage-dependent anion channel)	1.000	2	7.92E-09	7.4	Yes
YAL051W	OAF1	Oleate-activated transcription factor	1.000	2	0.000204	5.7	No
YLR180W; YDR502C	SAM1 /SAM2	S-adenosylmethionine synthetase	1.000	2	6.91E-07	5.2	Yes
YKL080W	VMA5	Subunit C of the eight-subunit V1 peripheral membrane domain of vacuolar H+-ATPase	1.000	2	6.65E-22	11.7	Yes
YAL003W	EFB1	Translation elongation factor 1 beta	1.000	2	1.78E-05	9.7	No
YLR447C	VMA6	Subunit d of the five-subunit V0 integral membrane domain of vacuolar H+-ATPase	1.000	2	3.66E-05	8.4	No
YGR061C	ADE6	Formylglycinamidine-ribonucleotide (FGAM)-synthetase	1.000	2	7.01E-09	3.1	No
YGL234W	ADE5,7	Bifunctional enzyme of the 'de novo' purine nucleotide biosynthetic pathway	0.873	2	1.03E-91	5.5	Yes
YLR029C	RPL15A	Ribosomal 60S subunit protein L15A; binds to 5.8 S rRNA	0.821	2	5.23E-23	24	No
YNL064C	YDJ1	Type I HSP40 co-chaperone	0.804	2	4.25E-31	18.3	Yes
YPR181C	SEC23	GTPase-activating protein	1.000	2	1.25E-11	4.8	No
YIL053W; YER062C	RHR2/ HOR2	Constitutively expressed glycerol-1-phosphatase	1.000	2	1.83E-14	14.4	No

Table 4.2: Proteins enriched in wild-type Elp1 pulldowns. Elp1-GFP was pulled down using GFP-Trap and precipitates were analysed by mass spectrometry. The proteins identified that were significantly enriched in pulldowns compared to untagged controls are summarised. Enrichment is calculated by intensity in sample relative to total intensity (sample+bead control). PEP is the posterior error probability and acts as a *p* value for protein identification. Values shown here are representative of 2 independent replicates.

Gene Name	Protein Name	Description	Enrichment relative to beads	Number of peptides	PEP	Coverage %	Also in Elp1?
YJR009C	TDH2	Glyceraldehyde-3-phosphate dehydrogenase, isozyme 2	1.000	11	8.6E-145	34	Yes
YOL039W	RPP2A	Ribosomal protein P2 alpha, a component of the ribosomal stalk	0.818	5	1.98E-52	52.8	No
YLR180W; YDR502C	SAM1 /SAM2	S-adenosylmethionine synthetase	1.000	2	6.91E-07	5	Yes
YOL080C	REX4	Putative RNA exonuclease	1.000	2	0.003745	9.7	Yes
YGL060W	YBP2	Central kinetochore associated protein	1.000	2	0.000204	3.4	Yes
YNL222W	SSU72	Phosphatase and transcription/RNA-processing factor	1.000	2	0.00022	8.7	Yes
YMR004W	MVP1	Protein required for sorting proteins to the vacuole	0.758	2	0.002658	6.3	Yes

Table 4.3: Proteins enriched in Elp1-KR9A pulldowns. Elp1-KR9A-GFP was pulled down using GFP-Trap and precipitates were analysed by mass spectrometry. The peptides identified that were significantly enriched in pulldowns compared to untagged controls are summarised. Enrichment is calculated by intensity in sample relative to total intensity (sample+bead control). PEP is the posterior error probability and acts as a *p* value for protein identification. Values shown here are representative of 2 independent replicates.

In the wild-type Elp1 pulldown a number of proteins involved in Energy metabolism, tRNA metabolism and translation were identified but the significance of these hits in terms of Elongator function is not yet obvious. Two S-adenosyl methione metabolising enzymes were identified; S-adenosyl-L-homocysteine hydrolase and S-adenosylmethionine synthetase, which may warrant further investigation. These could work alongside the Radical SAM domain in Elp3 for the chemistry of the mcm^5 and ncm^5 modifications. Another interesting hit is Kap123, an importin implicated in ribosome transport. This was also found in Elp1-KR9A pulldowns with a similar number of peptides but only in one replicate, which is why it is not listed in the top hits for the mutant. While it is possible this importin could be responsible for nuclear import of Elongator, our data have shown this is not mediated by the Elp1 basic region and the fact that Kap123 was also found associated with Elp1-KR9A-GFP is consistent with this.

Although speculative, it is tempting based on wild-type Elp1 results to hypothesise that Elongator may associate with enzymes involved in energy metabolism in order to 'sense' changes in nutrients. It is also possible that the complex may accumulate around areas of active translation for its tRNA modification function or interact with ribosomal proteins to influence translation under certain conditions. The Elongator associated factor Kti11 has been shown to associate with ribosomal proteins (Fichtner et al., 2003), although it was not identified here. Since other known Elongator associated factors have not been identified then other techniques and/or conditions are required to more fully address its interacting partners. In order to quantitatively assess the differences in the interaction profile of wild-type Elp1 and Elp1-KR9A a SILAC labelling approach could be employed (Ong et al., 2002) to enable a true quantitative comparison to be made.

Although it is difficult to interpret the results for other unverified interacting proteins present in the pulldowns, the reduced number of hits in the Elp-KR9A mutant would support the idea that the complex could be trapped in a distinct form from wild-type Elp1 and that this excludes it from certain interactions. Our label free analysis of wild-type Elp1 and Elp1-KR9A associated proteins does, however, support the conclusion that the Elongator complex is assembled in the basic region mutant.

4.2.5 Creating and testing conditional Elongator "switch off" strains

The C-terminal domain of Elp1 and sites therein are functionally important for tRNA wobble uridine modification (Fichtner et al., 2003, Mehlgarten et al., 2009). This finding was exploited to create a system whereby the functionality of Elongator could be conditionally regulated in real time. This would allow investigation into the timescale for turnover of Elongator dependent tRNA modifications under Elongator "switch off" conditions. In the future this could be used to investigate the acute effects of loss Elongator function on a timescale that may reflect more accurately the type of change that might be seen if Elongator activity is subject to phosphoregulation. Proteins whose levels change or that show reduced translation when Elongator function is lost could be analysed using SILAC mass spectrometry and/or ribosome profiling (Ong et al., 2002, Ingolia et al., 2009). This could be useful since changes that result solely due to translational dysfunction may be masked in chronically adapted Elongator knockout strains where defects are likely to arise from secondary issues with long term translational defects.

A version of Elp1 in which the C-terminus is disrupted by a Tobacco Etch Virus (TEV) protease cleavage site was designed (Figure 4.10A). This was introduced by *'delitto perfetto'* into a strain that expresses TEV protease from the galactose-inducible *GAL1* promoter. The introduction of the TEV site did not interfere with Elongator function, as monitored by eclipse assays on glucose containing medium (Figure 4.10C, right panel).

The TEV cleavage system was tested by switching cells growing in log phase from raffinose to galactose-containing media. This resulted in expression of TEV protease and specific cleavage of the Elp1 C-terminus, detectable by a dramatic reduction in the C-terminal HA tag signal, within 30 min of galactose switching. The Elp1-TEV-3HA signal

was undetectable by 90 min and this persisted for the full time course (Figure 4.10B). There was no cleavage of wild-type Elp1-3HA upon induction of TEV protease and no TEV expression or Elp1-TEV cleavage in glucose containing media.

The consequences of TEV protease cleavage of Elp1 was assayed by eclipse assay on galactose containing medium (Figure 4.10C, left panel) and resulted in loss of Elongator function. The function of Elongator can therefore be disrupted by growth on galactose with this system.

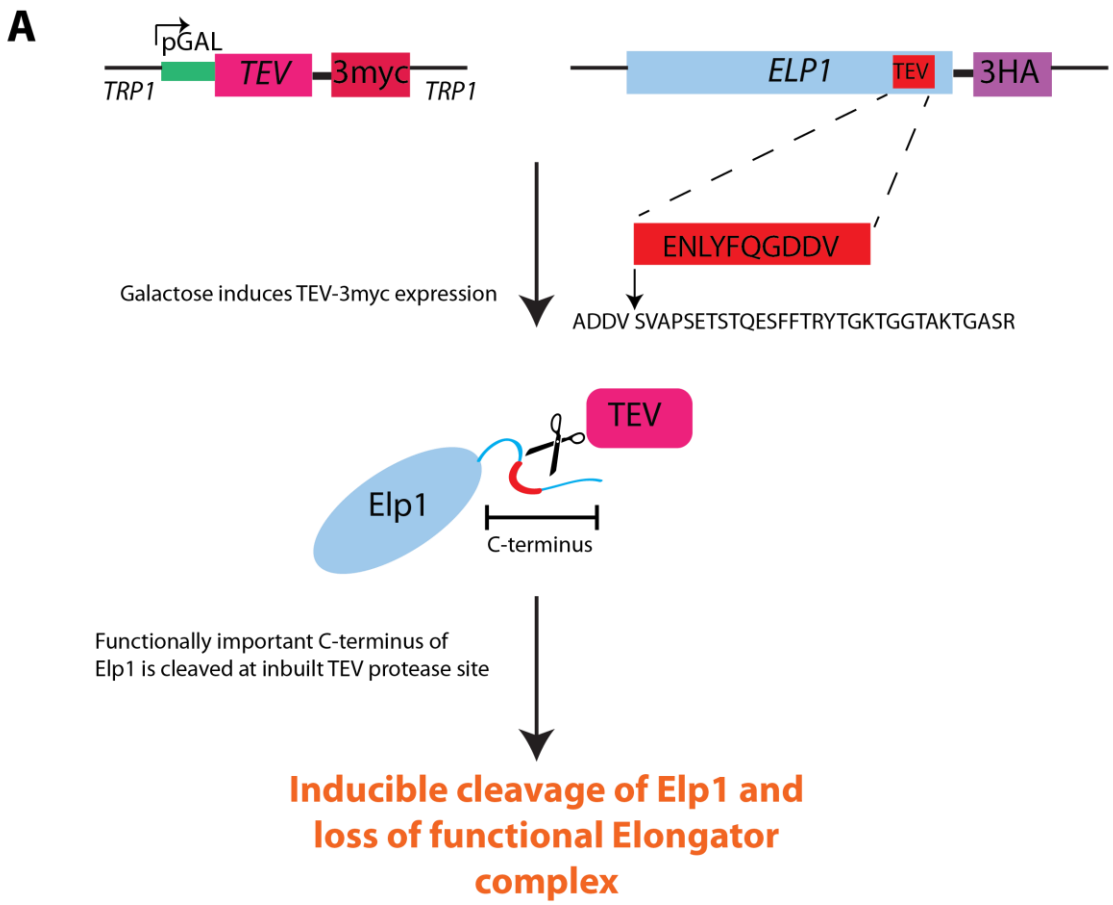

Figure 4.10: A galactose inducible TEV protease cleavage system to conditionally disrupt Elongator function; See overleaf for figure legend.

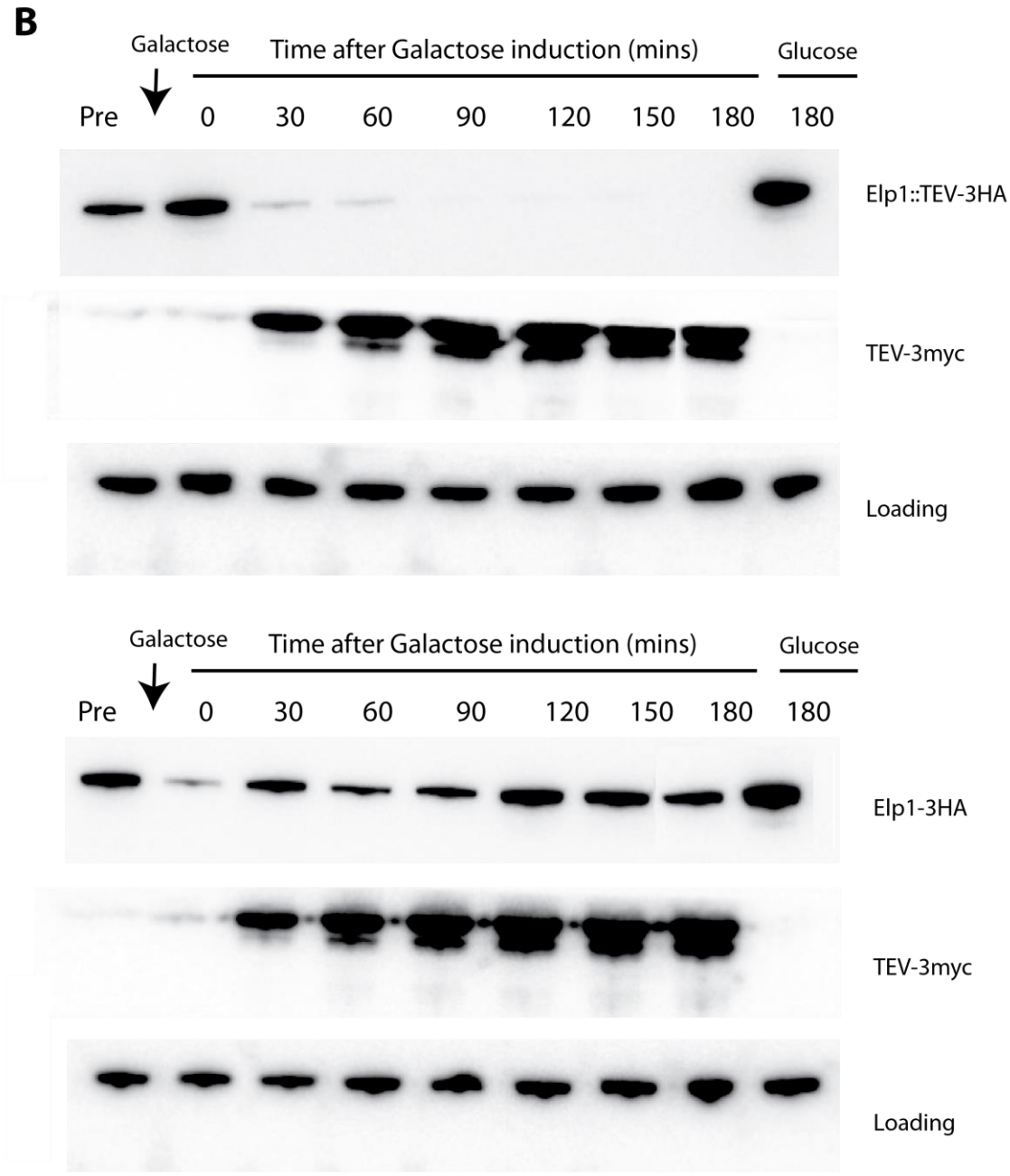

Figure 4.10: A galactose inducible TEV protease cleavage system to conditionally disrupt Elongator function; See next page for figure legend.

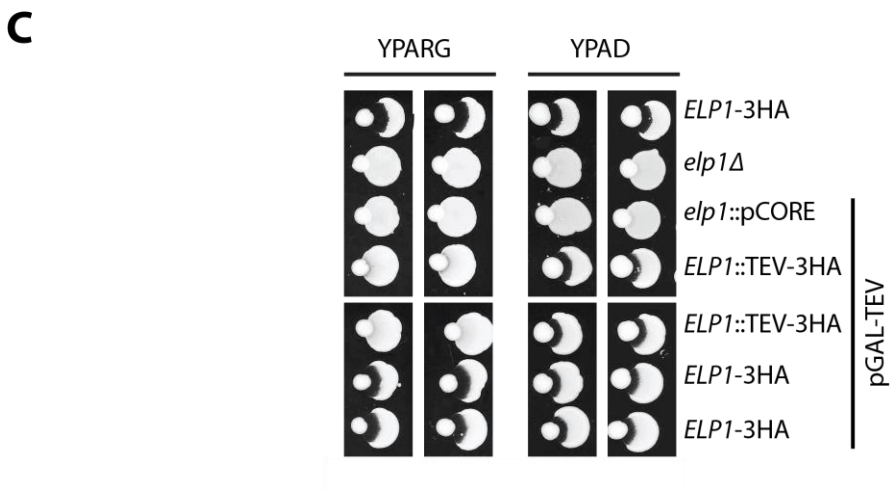

Figure 4.10: A galactose inducible TEV protease cleavage system to conditionally disrupt Elongator function. A) Schematic summary of the TEV protease cleavage system. Strains express TEV-3myc from a galactose inducible promoter as well as Elp1-3HA with a TEV cleavage site built into the C-terminus. B) Protein extracts from a galactose switching time course were analysed by western blotting with anti-Myc and anti-HA. After galactose induction TEV protease expression was detected and specific cleavage of Elp1::TEV-3HA was assayed by loss of the 3HA signal. Strains that express Elp1-3HA do not show any degradation. As a loading control blots were also analysed with anti-Cdc28. C) Eclipse assays of *ELP1*-3HA and *ELP1*::TEV-3HA strains containing inducible TEV protease on galactose (TEV on) and glucose (TEV off) containing media. Each panel shows two replicate spot and multiple clones. *ELP1*-3HA (YRDS261) and *elp1Δ* (YRDS250) strains served as controls for Zymocin sensitivity and resistance, respectively.

As an alternative means of conditional Elongator 'switch off' the Auxin inducible degron system was used (Nishimura et al., 2009). This method takes advantage of the fact that in plants there is a means by which certain transcription factors are degraded by the SCF- Ubiquitin pathway but only in the presence of the plant hormone Auxin. Substrates of this Auxin-degron system contain an Auxin inducible degron sequence (AID) which is specifically bound by this hormone. This Auxin-AID complex then binds a plant specific F-box transport inhibitor response 1 protein (Tir1) that forms a complex with the E3 ligase SCF machinery. This ultimately results in recruitment of other factors for polyubiquitation and proteasome mediated degradation of the AID containing substrate (Quint and Gray, 2006).

In other eukaryotes, including *S. cerevisiae*, the components of the SCF E3 ubiqutin ligase machinery are conserved whereas the auxin regulated components, auxin, AID and the F-box protein Tir1 are not. The existing SCF machinery in other eukaryotes can by hijacked to replicate this plant system by expression of plant Tir1 and addition of exogenous auxin. Fusing the AID sequence to a protein of interest allows it to be degraded by the endogenous proteasome in an auxin-dependant manner.

A strain was created where the *Oryza sativa* (*Os*) TIR1 gene with a C-terminal 9-myc tag was integrated at the *ADH1* locus, under the control of the *ADH1* promoter. Into this strain the AID sequence at the C-terminus of Elp1-3HA was introduced. This should allow conditional, proteasome mediated degradation of Elp1 in the presence of auxin or related compounds (Figure 4.11A).

The presence of Elp1-3HA-AID was assayed in medium in which 0.5 mM 1-Naphthalene acetic acid (NAA), an auxin related compound, was added (Figure 4.11B). A reduction in Elp1-3HA-AID could be seen after 30 min whereas Elp1-3HA was unchanged. Elp1-3HA-AID was further reduced after 90 mins but was still visible until the 360 min time point, when it can no longer be seen by western blot. The consequences of NAA-triggered loss of Elp1 on Elongator function were assessed by Eclipse assay (Figure 4.11C). When assayed on NAA containing agar at 0.25 mM and 0.5 mM, strains expressing Elp1-3HA-AID became resistant to Zymocin whereas Elp1-3HA strains remained sensitive. This system can therefore conditionally degrade the Elp1 subunit of Elongator in the presence of NAA, resulting in loss of Elongator function.

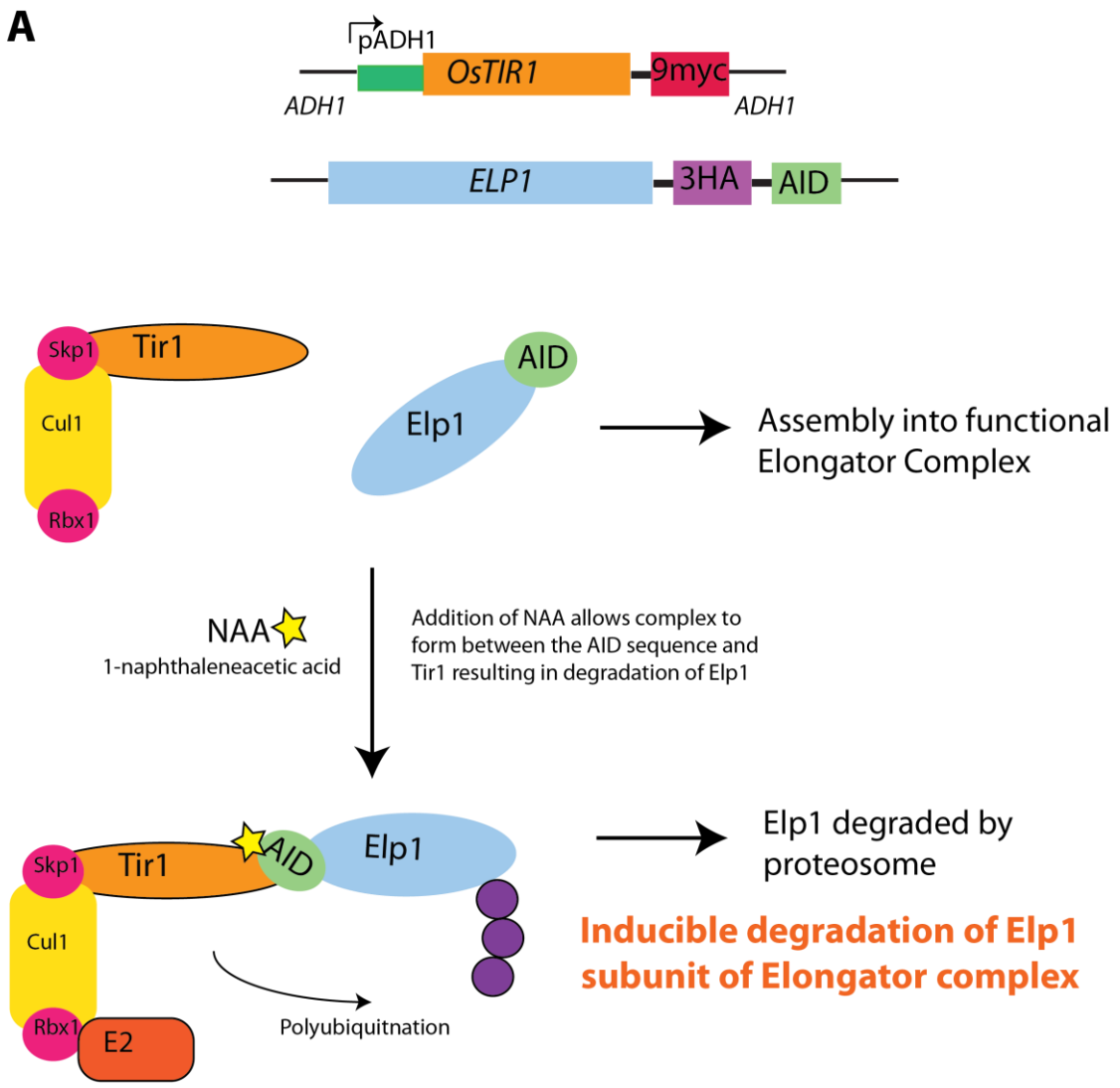

Figure 4.11: An auxin inducible degron system to conditionally disrupt Elongator function; See overleaf for figure legend.

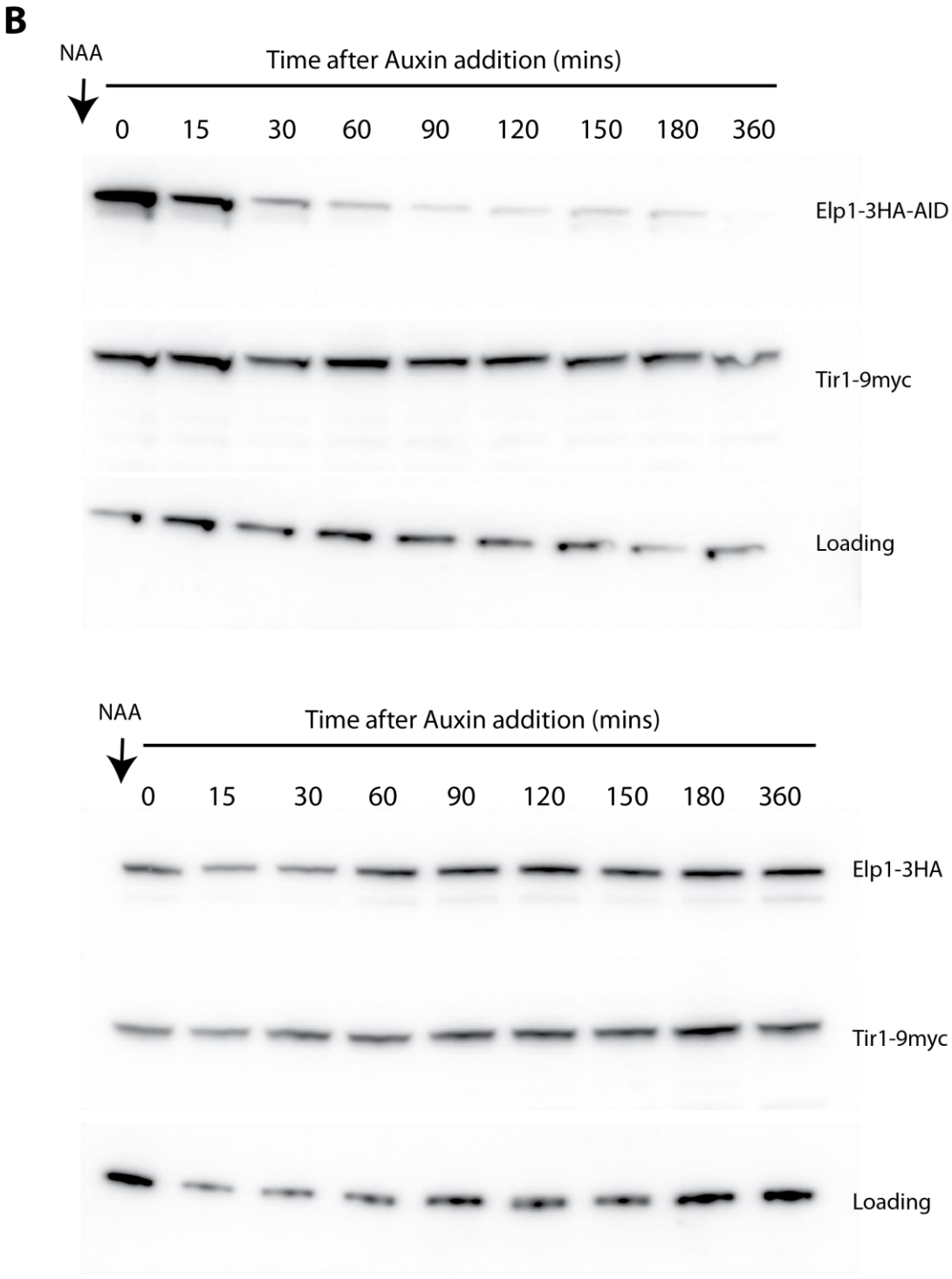

Figure 4.11: An auxin inducible degron system to conditionally disrupt Elongator function; See next page for figure legend.

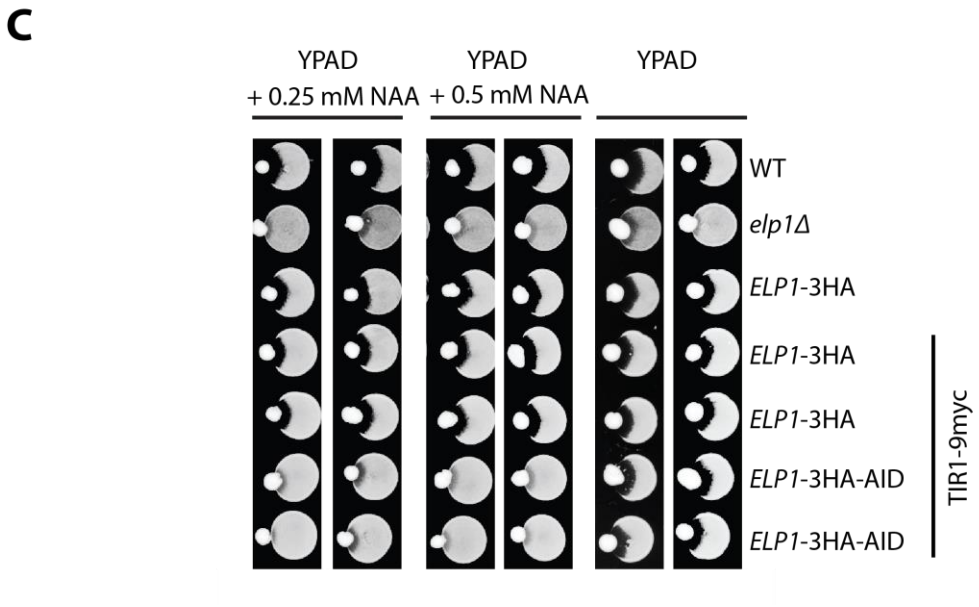

Figure 4.11: An auxin inducible degron system to conditionally disrupt Elongator function. A) Schematic summary of the auxin inducible degron system for Elp1. Strains express Tir1-9myc from the *ADH1* promoter as well as Elp1-3HA with an AID sequence built into the C-terminus. B) Lysates from the 1-Naphthalene acetic acid (NAA) time-course were analysed by western blotting with anti-Myc and anti-HA and specific degradation of Elp1-3HA-AID was assayed by loss of the 3HA signal. Strains that express wild-type Elp1-3HA show no degradation. As a loading control, input blots were also analysed with anti-Cdc28. C) Eclipse assays of strains expressing Elp1-3HA-AID and Elp1-3HA on media containing no NAA (System off), 0.25 mM and 0.5 mM NAA (System on). Each panel shows two replicate spots and multiple clones. Wild-type (WT, BY4741) and *elp1Δ* (YRDS250) strains served as controls for Zymocin sensitivity and resistance, respectively.

The timescale for degradation of Elp1 is slower than for cleavage with the TEV system (compare Figure 4.10B and Figure 4.11B). This may reflect the fact that the AID system relies on assembly of the ubiquitin-proteasome factors for loss of Elp1 and the binding of NAA to the AID sequence in Elp1, which may not be completely efficient. The cleavage of Elp1-TEV by TEV protease is probably more efficient because it only relies on the TEV protease recognising its sequence and cleaving it.

Since Elp1 acts as a scaffold, it is expected that in the AID system there is no Elongator complex formation in the absence of Elp1. In the TEV cleavage system, whether or not loss of the Elp1 C-terminus abolishes complex integrity has not yet been directly tested. However, preliminary data from our lab has implicated the N-terminus as being essential for complex assembly, since truncation causes loss of Elp3 protein stability. A deletion of the C-terminal portion, encompassing the same region as the TEV cleaved Elp1, can still bind to Elp3 suggesting that complex assembly may not be disrupted (Kozyrska and Stark, unpublished).

The two conditionally functional Elp1 systems can both be used for acute down-regulation of Elongator function to assess the turnover of the tRNA wobble uridine modifications. Once a timescale for loss of modification is established, the defects that arise from this down-regulation of Elongator function can be assessed without the complication of effects of chronic adaptation.

Chapter 5: The basic region in Elp1 is required for tRNA binding

5.1 Introduction

The conserved basic region in Elp1 is essential for the tRNA wobble uridine modification function of Elongator, but although this sequence was annotated as a putative NLS it does not appear to play a role in regulating the distribution of the Elp1 between the nucleus and cytoplasm. The Elp1 basic region is also not required for overall complex assembly but is linked to phosphorylation of the C-terminus of Elp1 at serine-1209.

Elongator was previously described as a factor required for RNA polymerase II mediated transcription (Otero et al., 1999, Wittschieben et al., 1999) and in line with this the Elongator complex was shown to interact with naked DNA and nucleosomal DNA by electromobility shift assays (EMSAs, Winkler et al., 2002). However, the functional significance of this interaction *in vivo* is now disputed since Elongator is mainly cytoplasmic and could not be found interacting with any tested genes in yeast (Pokholok et al., 2002). It was then shown that Elongator bound RNA *in vitro* with a greater specificity than DNA (Gilbert et al., 2004, Greenwood et al., 2009). The Elp3 subunit was also crosslinked to mRNAs and pre-mRNAs *in vivo* and was suggested to be in close proximity to elongating RNA transcripts despite its steady state cytoplasmic distribution (Gilbert et al., 2004, Petrakis et al., 2004). These studies implicated Elongator in nucleic acid binding but the *in vivo* function of this was remained unclear.

When it was first reported that Elongator was required for tRNA wobble uridine modifications, it was shown that the Elp1 and Elp3 subunits could be crosslinked to radiolabelled $tRNA^{Glu}_{UUC}$ but not $tRNA^{Met}_{i}$ (Huang et al., 2005). More recently, it was demonstrated that the Elp4-6 subcomplex of Elongator binds $tRNA^{Glu}_{UUC}$ by EMSA and that this binding may be regulated by ATP hydrolysis (Glatt et al., 2012). This suggests

that Elongator may play a direct role in tRNA binding and subsequent modification, though the domains required and the molecular mechanisms involved are not known.

Since the basic region in Elp1 was clearly important for Elongator function, we hypothesised that it may be involved in binding tRNA molecules to the complex for modification. Elp1 was analysed for potential RNA binding sites using the RNA/DNA binding prediction program BindN (Figure 5.1). This program attempts to predict RNA binding regions from primary sequence based on the properties of RNA binding residues from known structures (Wang and Brown, 2006). BindN highlighted the C-terminal basic region in Elp1 as being likely to bind RNA. The human Elp1 subunit was also analysed in this way and a similar putative RNA binding region was highlighted, within the conserved basic region. Arg4, a protein not known to bind RNA did not have any particular regions highlighted by BindN (data not shown). This is consistent with the hypothesis that this basic region may be required for tRNA binding.

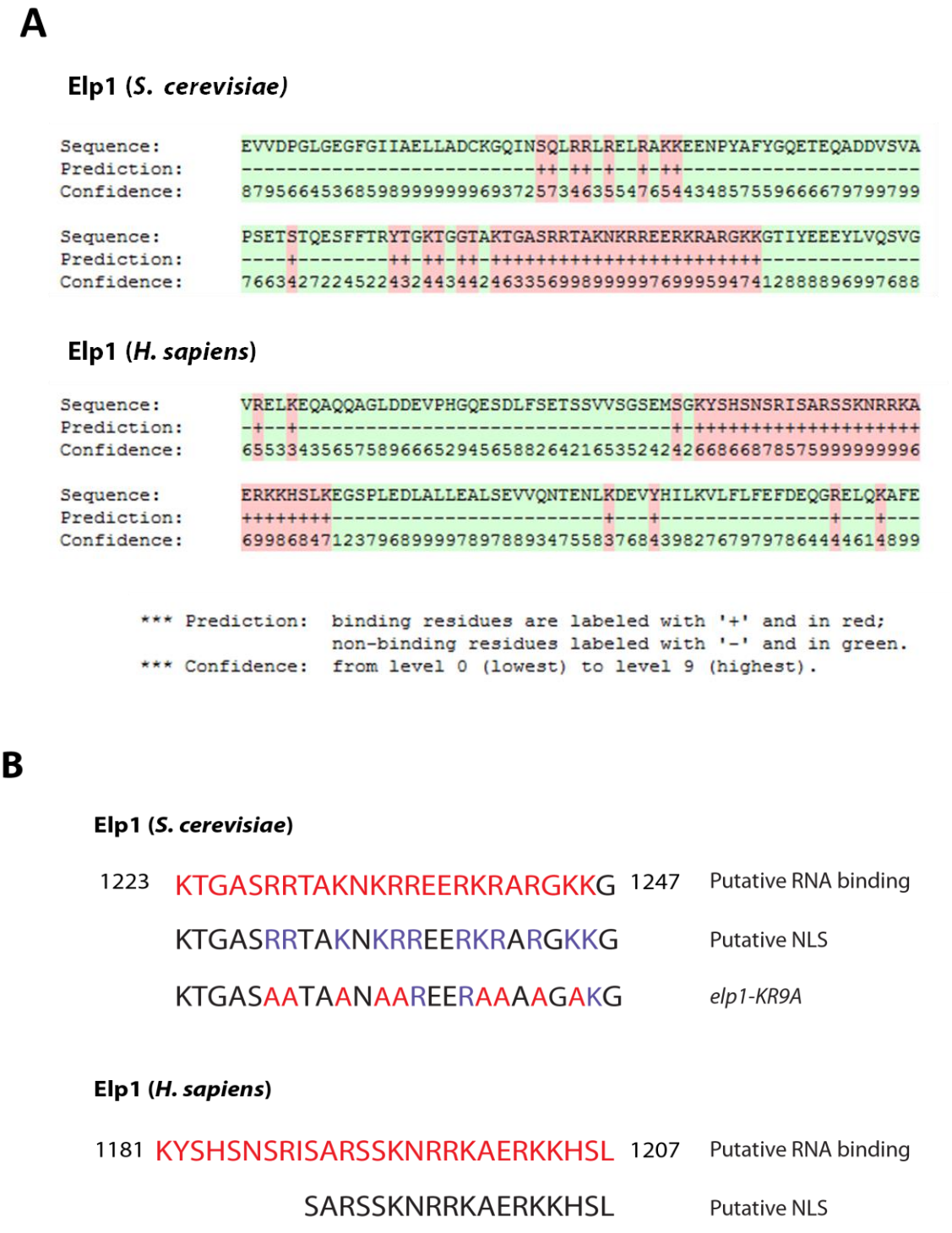

Figure 5.1. The basic region in Elp1 is annotated as a putative RNA binding domain. A) The results from a search on BindN+ (http://bioinfo.ggc.org/bindn+/) for RNA binding regions with the entire protein sequence of *S. cerevisiae* Elp1 and *H. sapiens* Elp1. This highlights (red) the basic region as putative RNA binding with several residues scoring with high confidence. B) The putative RNA binding region is compared to the putative nuclear localisation sequence (NLS) predicted by NLStradamus (http://www.moseslab.csb.utoronto.ca/NLStradamus/). The *S. cerevisiae* Elp1 putative RNA binding resides (1223-1247) overlap exactly with the putative NLS and several basic residues (purple) that are mutated (red) in the *elp1-KR9A* mutant may therefore influence RNA binding if it occurs. The *H. sapiens* Elp1 RNA binding residues (1181-1207) overlap partially with a predicted NLS.

5.2 Results

5.2.1 Expression and purification of the Elp1 C-terminal domain

We hypothesised that Elp1 may be able to bind to tRNA and that *elp1-KR9A* mutants may lose this ability due to mutation of the putative RNA binding region. To begin to address this hypothesis, recombinant Elp1 and Elp1-KR9A were required for *in vitro* binding assays. Since Elp1 is a large protein, made up of 1349 amino acids, it seemed possible that recombinant expression of the full-length protein could be problematic. Therefore the C-terminus of Elp1 (residues 730-1349), which is predicted to consist of largely alpha helices, was expressed as a GST fusion protein (Figure 5.2).

Primers were designed with built in restriction sites to amplify the region encoding the C-terminal domain of Elp1 and Elp1-KR9A from plasmid constructs for cloning into an inducible expression vector pGEX-4T-1. A sequence encoding 6 histidine residues was included in the Elp1 reverse primer to add a C-terminal His_6 tag. The pGEX-4T-1 vector contains an N-terminal Glutathione-S-transferase (GST) sequence for in frame fusion to cloned genes as well as an intervening Thrombin cleavage site for tag removal after purification. The final cloned *ELP1* and *elp1-KR9A* constructs therefore contained an N-terminal GST tag and a C-terminal His_6 tag for tandem affinity purification (GST-*ELP1-CTD*-His_6 and GST-*elp1-KR9A*-CTD-His_6). These fusion genes are under the control of the *tac* promoter, which is repressed by plasmid encoded lac repressor in the absence of lactose or other analogues (Smith and Johnson, 1988, Amann et al., 1983, GE Healthcare, 2012). *E. coli* strains grown in the presence of lactose or analogues such as IPTG direct high levels of recombinant protein expression from pGEX vectors (Studier and Moffatt, 1986).

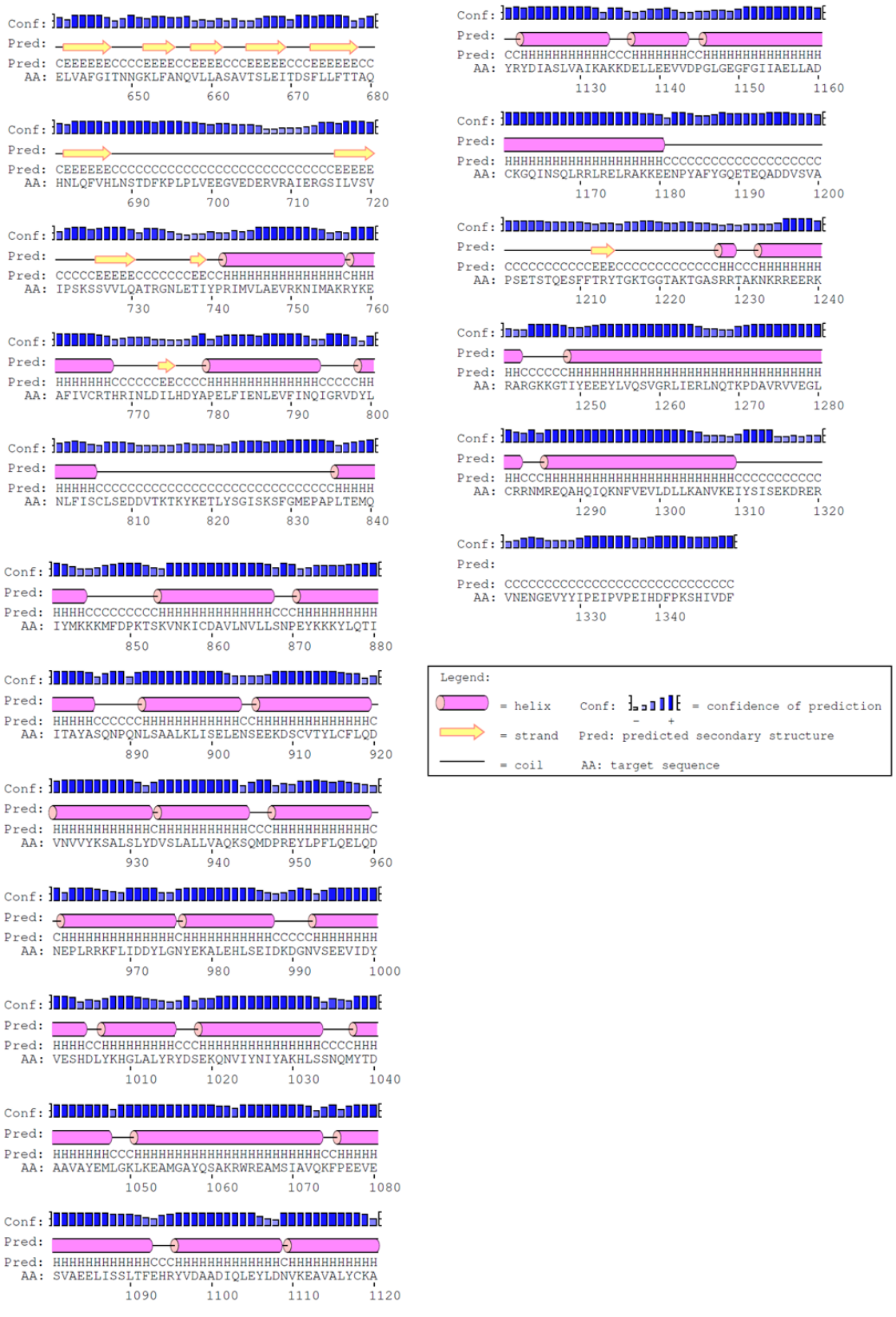

Figure 5.2: The C-terminal domain of Elp1 is predicted to be alpha-helical. The entire protein sequence of Elp1 was analysed using PSI-PRED v3.3 (http://bioinf.cs.ucl.ac.uk/psipred/) to predict its secondary structure. The C-terminal half of Elp1 was predicted to consist of alpha-helices and residues 731-1349, starting ATRG were utilised for protein expression.

Elp1 and Elp1-KR9A expression vectors were transformed into *E. coli* BL21 (DE3) and expression of the recombinant C-terminal domain was induced using auto induction medium (Studier, 2005). Auto induction medium contains a mixture of glucose, lactose and glycerol as carbon sources. Strains utilise glucose until late log phase and upon saturation begin to take up and metabolise lactose. This induces high-level expression of the *tac* promoter driven constructs upon saturation of the culture. Strains were grown at 30°C for 4-5 hours to allow for sufficient cell density and then the temperature was lowered to 25°C overnight to minimise degradation of expressed recombinant proteins.

A small sample of culture by SDS-PAGE was assayed for expression of Elp1 and Elp1-KR9A C terminal domains (Figure 5.3) and these were compared against a control GST-His_6 expressing culture. Bands of around the expected size (~ 98 kDa) for GST-Elp1-CTD-His_6 and GST- Elp1-KR9A-CTD-His_6 (from now on these will be referred to as Elp1 CTDs or fusion proteins) that were absent from the GST- His_6 lysate were observed. These samples were also checked for the presence of both tags by western blot (data not shown).

Since relatively high levels of the recombinant Elp1 fusion proteins were detectable in our strains, these were used for tandem affinity purification alongside the GST-His_6 control. Lysates were made from these strains and assayed for the presence of the Elp1 and Elp1-KR9A fusion proteins in the soluble fraction (SN) and the insoluble fraction (Pellet). The majority of the recombinant Elp1 fusion proteins appeared in the soluble fraction (Figure 5.4A) and so this was incubated with HisPur Cobalt resin for affinity purification using the C-terminal His_6 tag (Figure 5.4B).

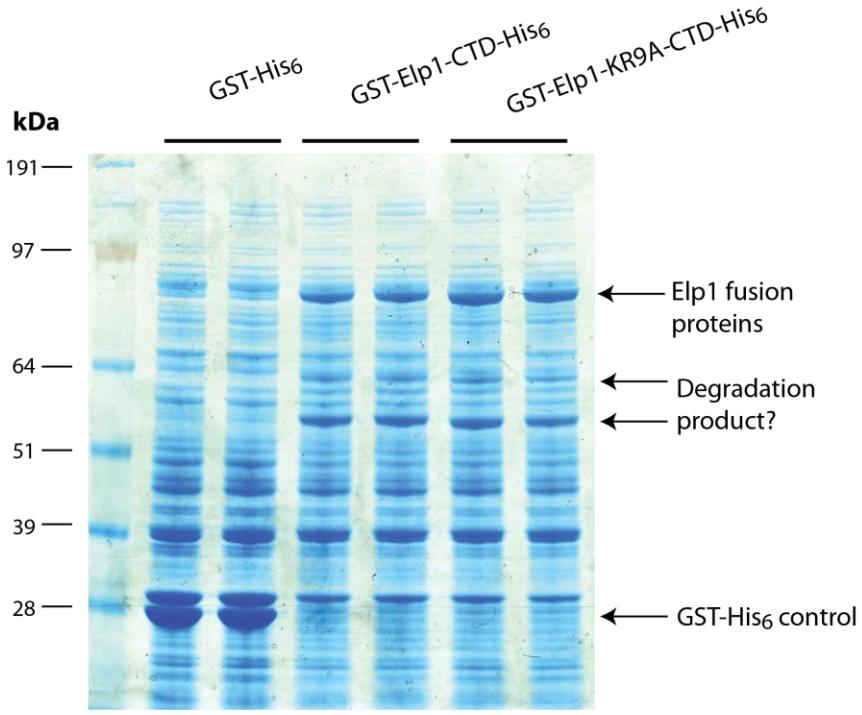

Figure 5.3: GST and His6 tagged Elp1 and Elp1-KR9A C-terminal domains were detectable upon induction of expression in *E. coli*. A small (20 µl) sample of saturated cultures in auto induction medium was boiled in an equal volume of 2× Laemmli Buffer. The samples were analysed by SDS-PAGE on a 4-12% Bis-Tris polyacrylamide gel and stained with Instant Blue. Many high abundance proteins can be stained in all samples. A unique band of around the predicted size (~ 98 kDa) of the Elp1 fusion proteins is highlighted in Elp1 and Elp1-KR9A samples along with possible degraded or truncated products. The GST-His_6 control band is also highlighted and this is known to be well expressed under these conditions.

The His_6 tag was used to purify full length Elp1 as the first step, since the GST affinity purification would isolate both full length and C-terminally truncated versions of Elp1. Small scale testing confirmed that this order of purification was the most efficient (data not shown). Binding of the Elp1 CTDs to the HisPur resin (Bead) was visualised despite there being a significant proportion remaining in the flow-through (FT). This was also the case for the GST- His_6 control, indicating that the resin was likely saturated. Other contaminating proteins were also present in the bound samples, some of which may be degraded versions of the Elp1 fusions. Excess imidazole was used to elute the His_6 tagged proteins off the resin by competition, as assayed by the 'Post Bead' samples compared to the Bead samples (Figure 5.4B).

The pooled eluates were added to glutathione resin for purification using the N-terminal GST tag (Figure 5.4C). A contaminating band was present in the bound sample between 64 and 51 kDa alongside the Elp1 and Elp1-KR9A fusion proteins. This band also appeared in the HisPur bead samples (Figure 5.4B) where it was hypothesised to be a degradation product of the fusion proteins. However, since it was also present in the glutathione bound sample it would need to have both affinity tags, so it seemed likely that it could be a bacterial chaperone as these can co-purify with recombinant proteins (GE Healthcare, 2012). Excess glutathione was used to elute the GST tagged proteins from the resin by competition and the eluates were pooled and concentrated (Figure 5.4D and Figure 5.5).

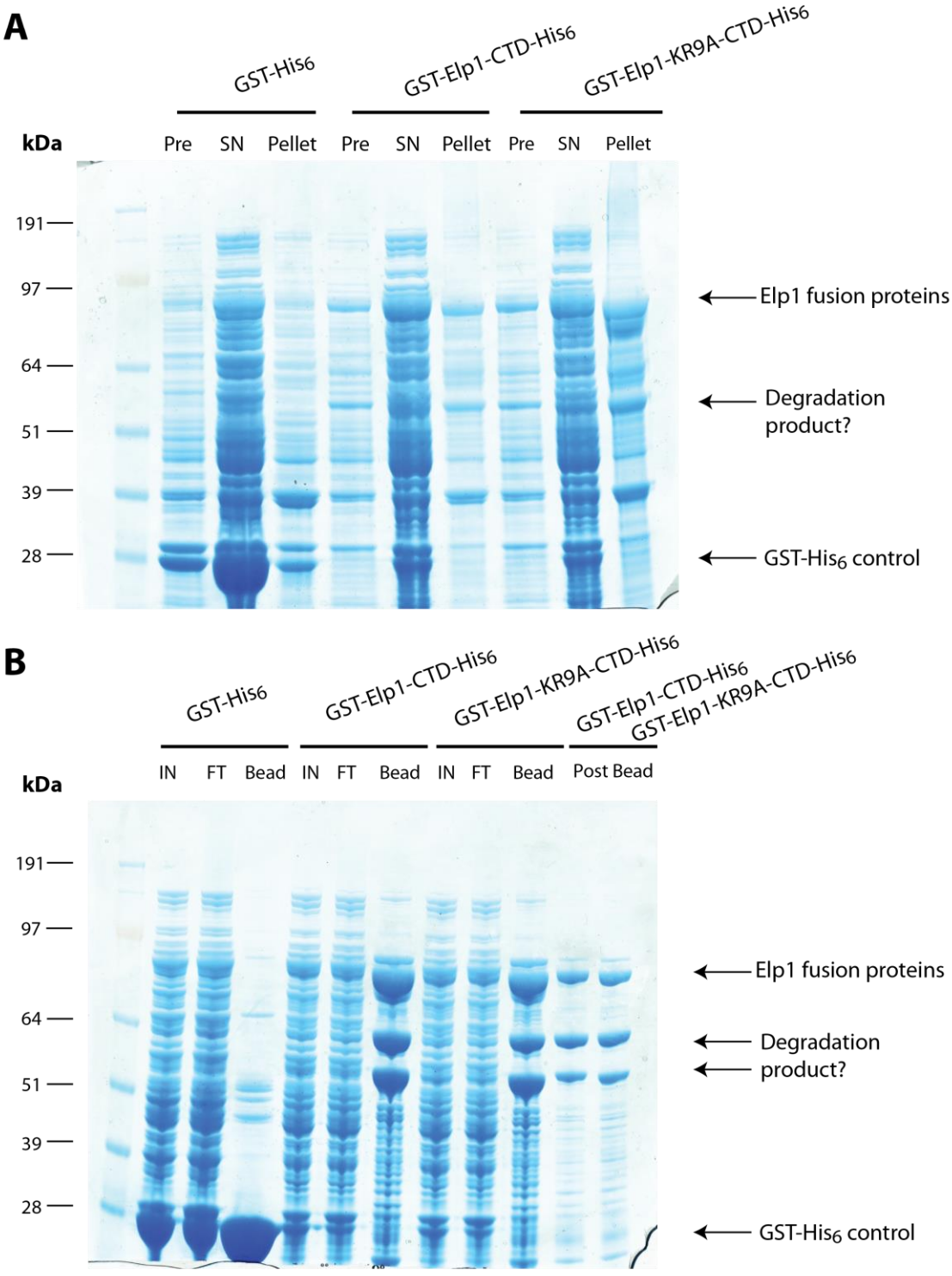

Figure 5.4: Purification scheme of Elp1 and Elp1-KR9A fusion proteins; See next page for figure legend.

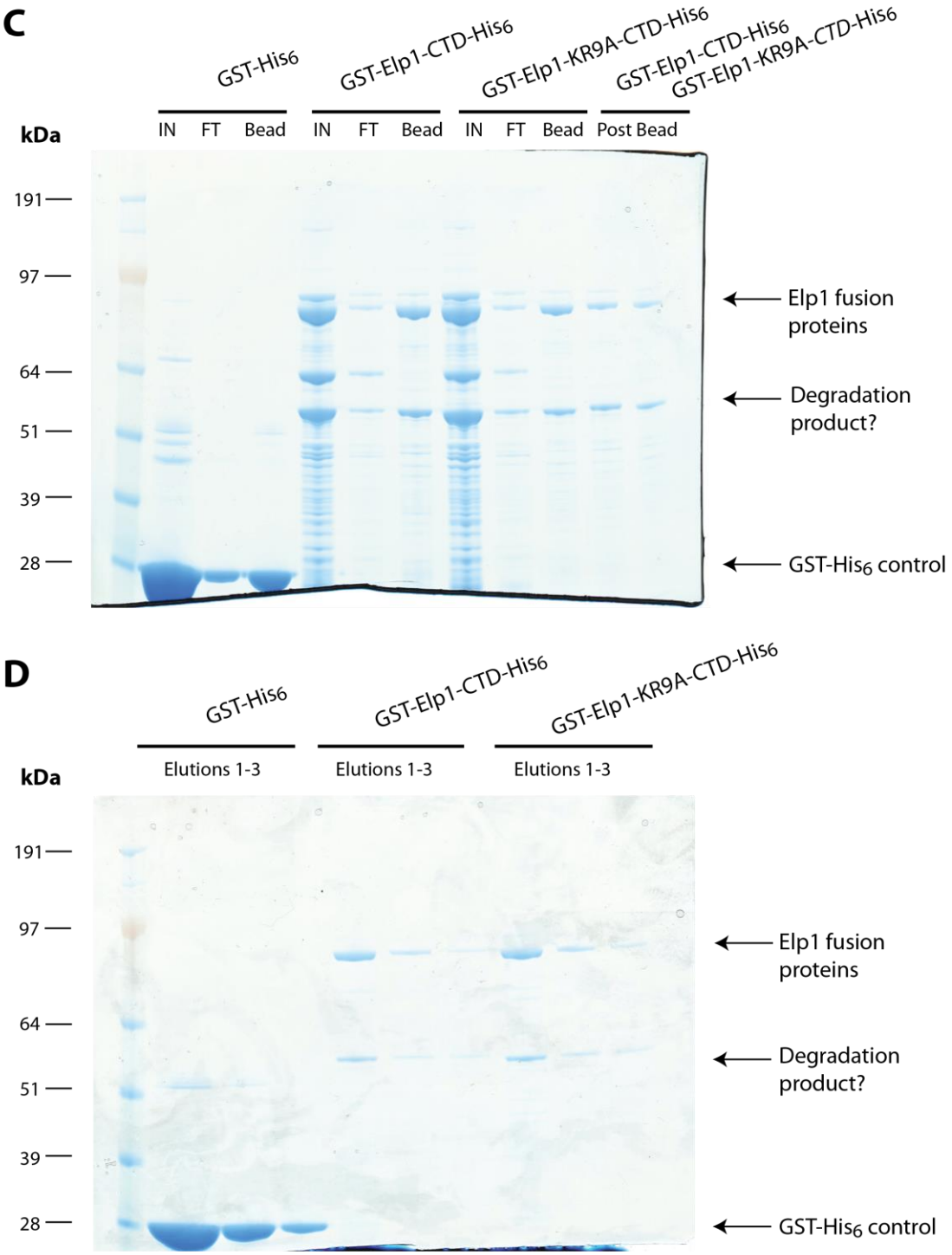

Figure 5.4: Purification scheme of Elp1 and Elp1-KR9A fusion proteins. Samples from different stages of purification were boiled in an equal volume of 2× Laemmli Buffer. The samples were analysed by SDS-PAGE on 4-12% Bis-Tris polyacrylamide gels and stained with Instant Blue. Highlighted are the Elp1 fusion proteins, putative degradation products and GST-His_6. A) Samples before lysis (Pre), supernatants of cleared lysates (SN) and insoluble proteins and debris (Pellet) were analysed. B) Lysates were added to HisPur resin for affinity purification of the His_6 tag. C) Pooled eluates from the HisPur resin were added to glutathione resin for purification of the GST tag. Samples of Inputs (IN), flow-through (FT) and Bound (Bead) fractions were analysed in both B) and C). D) Glutathione elution fractions, all three elution fractions for each sample were pooled.

The C-terminal domains of Elp1 and Elp1-KR9A were successfully purified using N-terminal GST and C-terminal His_6 tags (Figure 5.5A). In order to find out the identity of the lower molecular weight band in the Elp1 and Elp1-KR9A fusion protein samples, both full length and contaminating bands (Band 2) were sent for peptide fingerprinting by mass spectrometry. Peptides identified were matched against the recombinant protein sequence (including tags) as well as the BL21 (DE3) *E. coli* proteome.

Surprisingly, there were no significant peptide matches against *E. coli* proteins in any of the samples, indicating that the contaminating band was not a chaperone as hypothesised. Instead in all samples the vast majority of peptides identified matched Elp1 (Figure 5.5B) and this suggests that the small molecular weight band is a degradation product of Elp1. An observation made was that peptides matching the GST tag were mainly found in the full length Elp1 band and a peptide corresponding to the first 8 residues in the GST tag was not identified in the smaller band. This suggests that this could be an Elp1 degradation product that has lost all or at least part of the GST tag but that it may interact with the full-length fusion protein and hence co-purify with it.

To test this hypothesis further these samples were analysed by western blotting for presence of the GST and His_6 tags (Figure 5.6). Interestingly, a His_6 tagged protein at around the molecular weight of the contaminating band was detected. Although we could detect many smaller, lower intensity bands apart from full length with anti-GST antibody, no major GST band was detected at the molecular weight of the contaminating band. This supports the mass spectrometry data, making it very likely that the contaminating band is a degradation product of Elp1 that has lost all or part of the N-terminal GST tag.

A

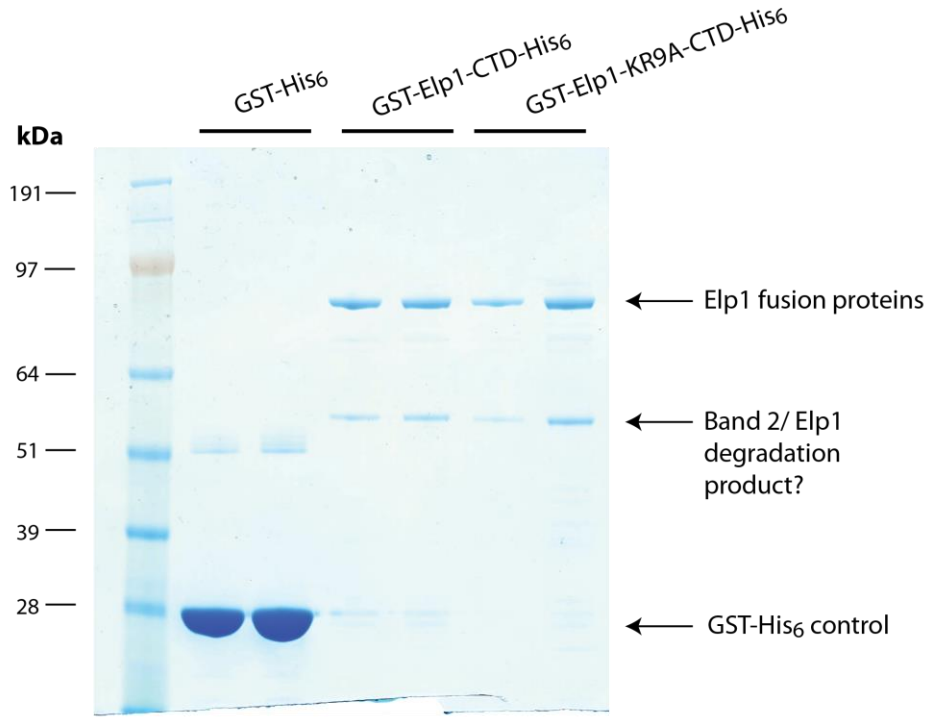

B

Sample	Peptides matching Elp1	Peptides matching GST	HIS tag peptide	First 8 aa's peptide
Elp1	63	8	Yes	Yes
Elp1 Band 2	42	2	Yes	No
Elp1-KR9A	52	8	Yes	Yes
Elp1-KR9A Band 2	48	3	Yes	No

Figure 5.5: Final purified Elp1 and Elp1-KR9A fusion proteins contain a lower molecular weight contaminating band that is likely to be a degraded version of Elp1. A) Two samples of pooled and concentrated recombinant proteins were boiled in an equal volume of 2× Laemmli Buffer, then analysed by SDS-PAGE on 4-12% Bis-Tris polyacrylamide gels and stained with Instant Blue. Highlighted are the Elp1 fusion proteins, a potential degradation product between 64 -51 kDa (Band 2) and the GST-His_6 control. B) Table summarising the results for peptide mass fingerprinting. The majority of peptides detected in all samples matched the Elp1 fusion protein sequence. The Elp1-KR9A fusion has a unique peptide that was only detected in this sample. A peptide corresponding to the first 8 residues of the GST tag was missing in Band 2 samples but in all samples a peptide corresponding to the C-terminal His tag was detected.

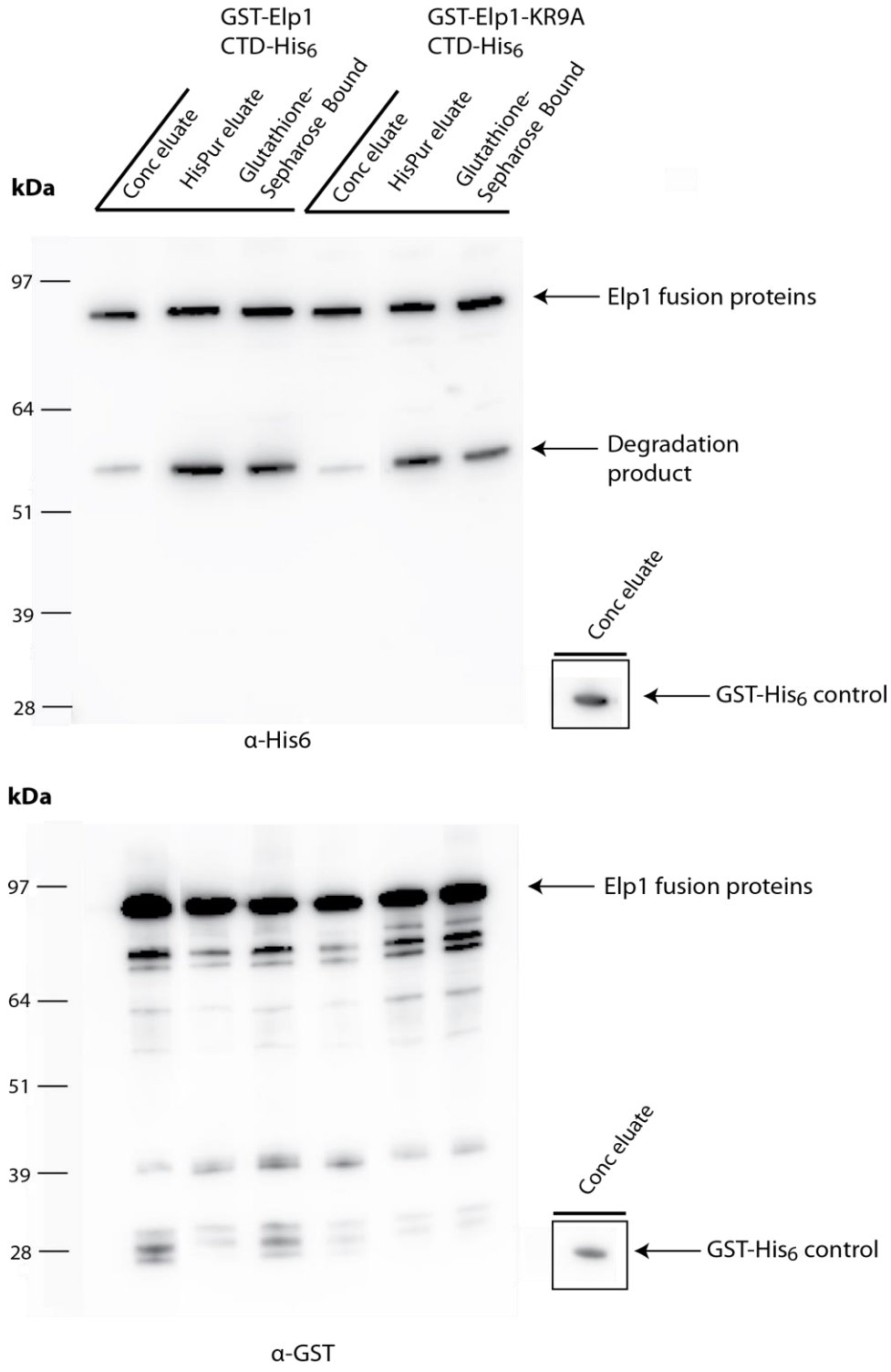

Figure 5.6: Western blotting recombinant Elp1 fusion proteins for GST and His_6 tags. The samples shown in Figures 5.4 and 5.5 were analysed by western blotting for anti-His_6 (top panel) and anti-GST (bottom Panel). The control GST-His_6 bands are indicated as controls. Major bands corresponding to Elp1 fusion proteins (where both tags were recognised) were detected as indicated. A candidate for the contaminating band was detected in anti- His_6 blots, appearing around 64-51 kDa. In the GST blot, multiple bands of lower size and intensity than the full-length fusion were detected and are likely to be other truncations or degradation products.

To further corroborate this, the samples were analysed with a non-phospho-Elp1 antibody alongside both GST and His_6 antibodies and the band pattern carefully matched across blots (Figure 5.7). A smaller molecular weight band was recognised by both the His_6 and Elp1 specific antibodies but not the GST antibody. Therefore this is a degradation product of the Elp1 fusion protein which has lost all or part of the GST tag and that is stably associated throughout tandem affinity purification. This implies that full length Elp1 fusion protein may bind to a degradation product of itself and this complex is stable through the affinity purification, despite having lost at least part of one affinity tag, most likely the N-terminal GST. We (Chapter 3) and others (Glatt et al., 2012) have shown that two copies of Elp1 can associate within Elongator and these results would indicate that the C-terminus is directly involved in this interaction. This suggests that the Elp1 subunits may directly interact with one another within Elongator.

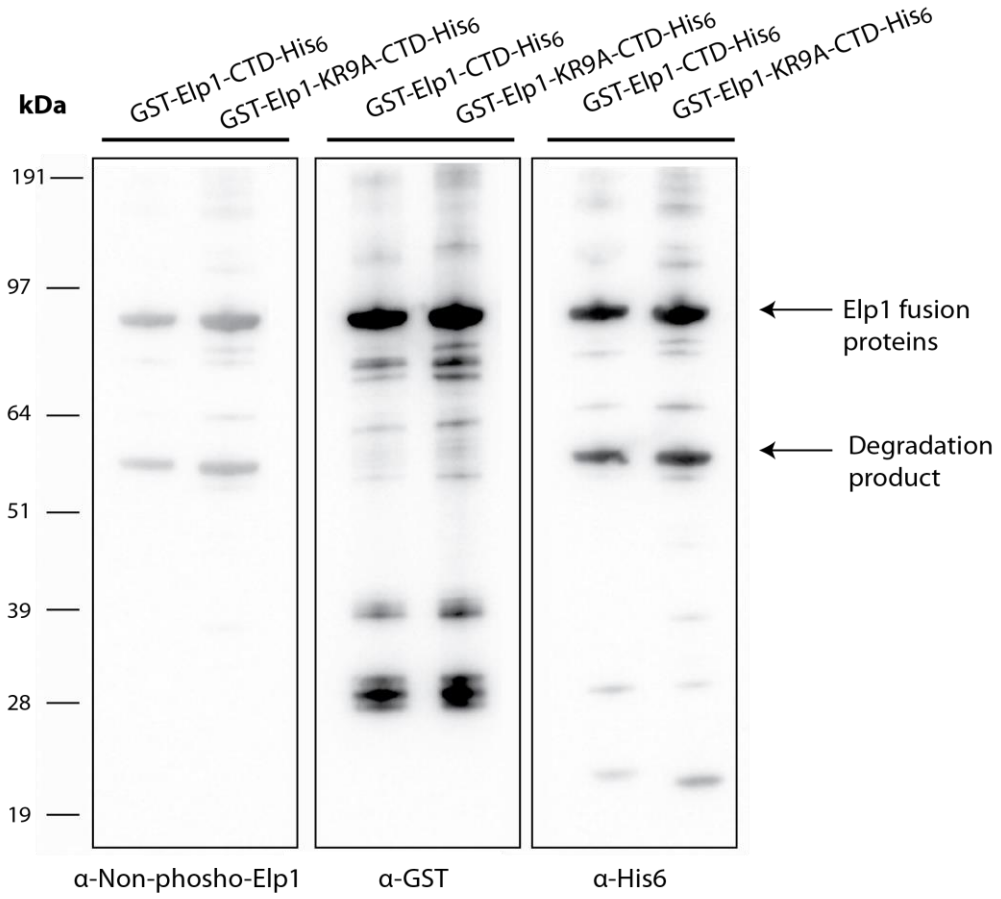

Figure 5.7: Western blotting recombinant Elp1 fusion proteins with Non-phospho-Elp1 antibody. The samples shown in Figure 5.5 were analysed by western blotting for anti-Non-phospho-Elp1 (left), anti-GST (middle) and anti-His_6 (right). Major bands corresponding to Elp1 fusion proteins (where both tags were recognised) were detected as indicated. The contaminating band, appearing around 64-51 kDa was detected by both anti-Non-phospho-Elp1 and anti- His_6 antibodies but not by the anti-GST antibody.

5.2.2 Electrophoretic mobility shift assays with Elp1 and excess tRNA

If the Elp1 basic region is a tRNA binding domain then the recombinant Elp1 C-terminal domain should bind to tRNA and the Elp1-KR9A mutation would be expected to disrupt this. Binding reactions using either recombinant GST, Elp1 or Elp1-KR9A fusion proteins and an excess of yeast tRNA were set up and analysed by native gel electrophoresis and SYBR Gold staining (Figure 5.8A). If tRNA forms a complex with any of the recombinant proteins then we would expect to see a shift in the mobility of SYBR Gold detected tRNA to a slower-migrating position on the gel compared with the free tRNA. This technique is referred to as an Electrophoretic mobility shift assay (EMSA, Hellman and Fried, 2007)

A clear tRNA shift was detected in binding reactions with the wild-type Elp1-CTD but not with the Elp1-KR9A-CTD or GST alone, despite all proteins being present at equivalent concentrations (Figure 5.8B). The wild-type Elp1-CTD shows multiple tRNA band shifts with the most intense SYBR gold staining at the top of the gel. It is possible that the complex formed between Elp1 and tRNA may not be completely stable during electrophoresis or that heterogenous complexes may exist due to multimerisation. Thus the wild-type Elp1-CTD forms a complex with tRNA and mutation of the basic region, as in Elp1-KR9A, disrupts this.

Normally, antibody against the protein of interest is added to binding reactions and if this protein is present in a shifted complex, the binding of the antibody will produce an even greater mobility shift – a 'supershift'. This is used to confirm that a protein of interest is part of the shifted complex. However, since the majority of the Elp1-tRNA complex was detected near the top of the gel it may have been impossible to resolve a supershift under our conditions.

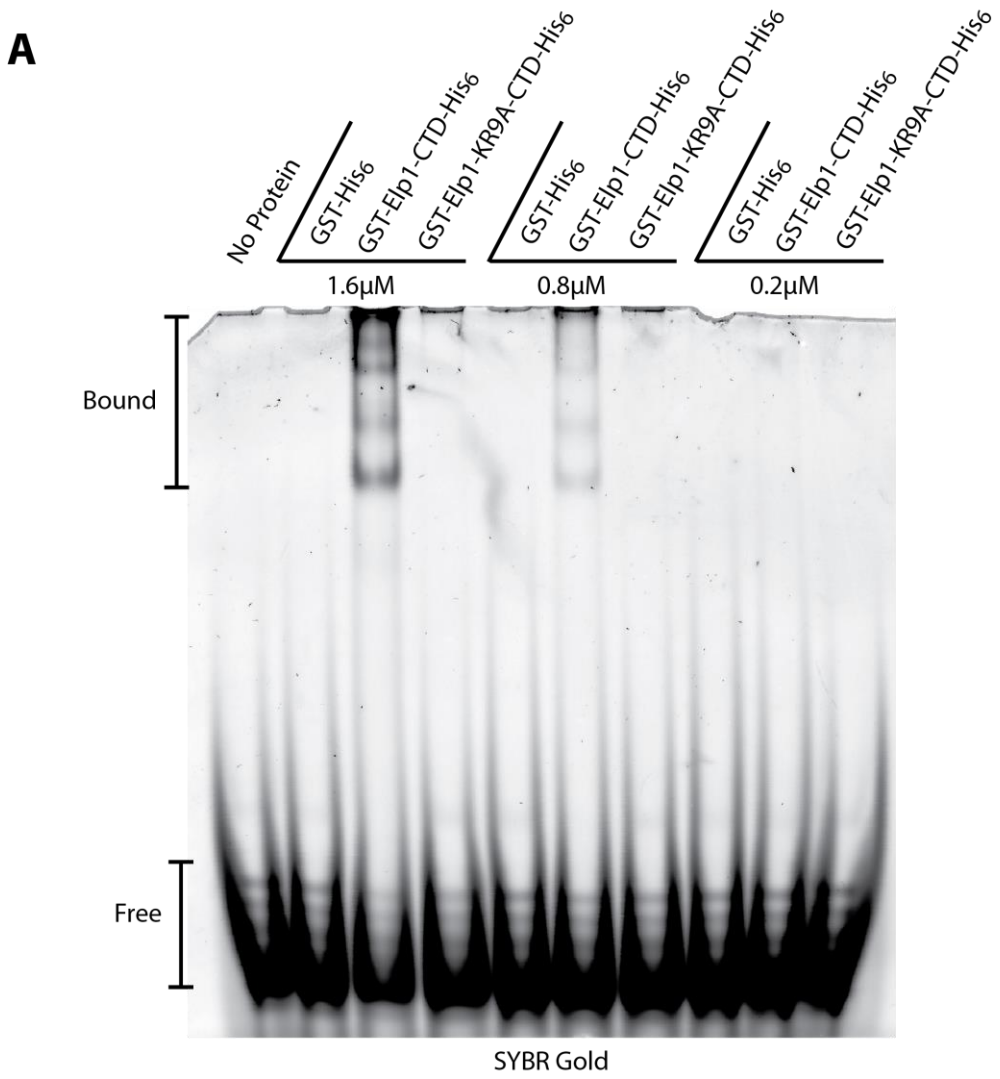

Figure 5.8: The wild-type Elp1 C-terminal domain forms a complex with tRNA but this is disrupted in Elp1-KR9A; See next page for figure legend.

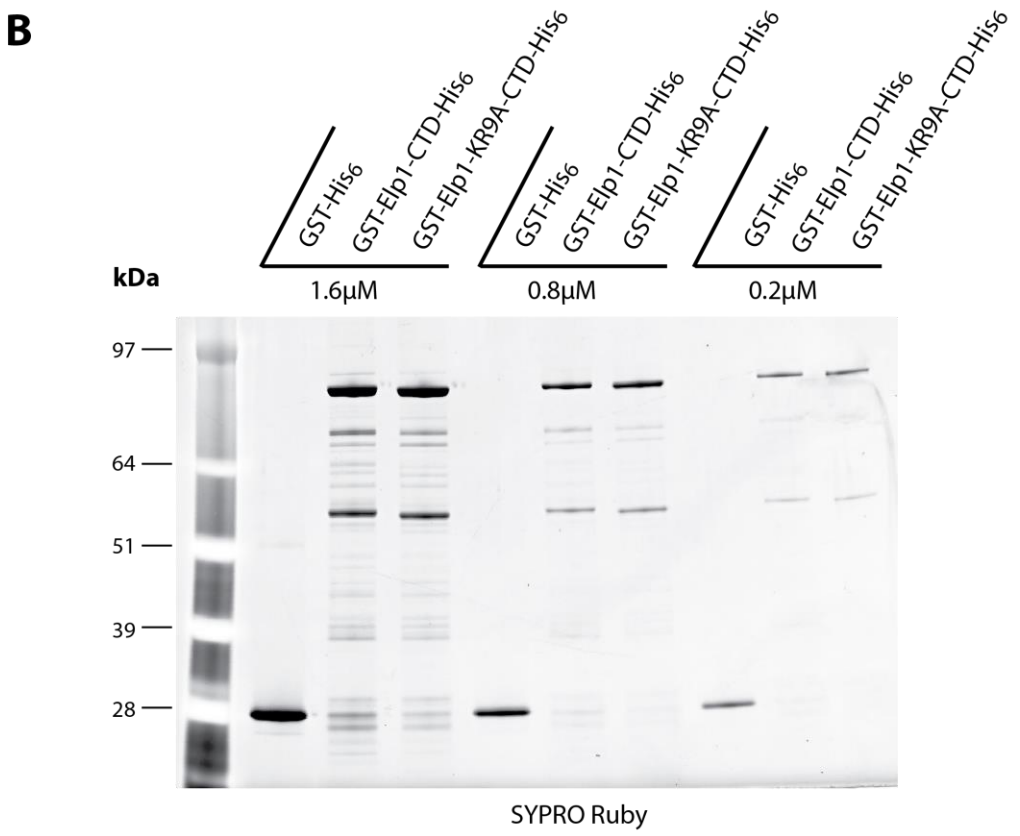

Figure 5.8: The wild-type Elp1 C-terminal domain forms a complex with tRNA but this is disrupted in Elp1-KR9A. A) EMSA using excess unlabelled tRNA and recombinant GST, Elp1-CTD and Elp1-KR9A-CTD proteins. Complexes were allowed to form between unlabelled tRNA at 0.3 µM and the indicated concentrations of recombinant proteins. Binding reactions were separated on a 6% polyacrylamide native gel and stained with SYBR Gold. B) Recombinant protein from each dilution was added to an equal volume of 2× Laemmli Buffer, boiled and analysed by SDS-PAGE on a 4-12% Bis-Tris polyacrylamide gel followed by SYPRO Ruby staining.

Instead, binding reactions were set up as previously, separated by native gel electrophoresis and then proteins present in the shifted bands were detected using western blotting (Figure 5.9). The native gel blot was probed with antibodies against the His_6 tag and the GST tag and wherever there was a shifted tRNA band, the equivalent band was also detected by both antibodies. Therefore, the Elp1-CTD was present in these shifted complexes. In the binding reactions with no tRNA, both His_6 and GST tags were observed as single bands at the top of the gel. This could be consistent with a native multimerisation of Elp1, since faster migrating bands cannot

be detected corresponding to the smaller contaminating version of Elp1 assayed during purification, however, we cannot yet conclude this based on this experiment.

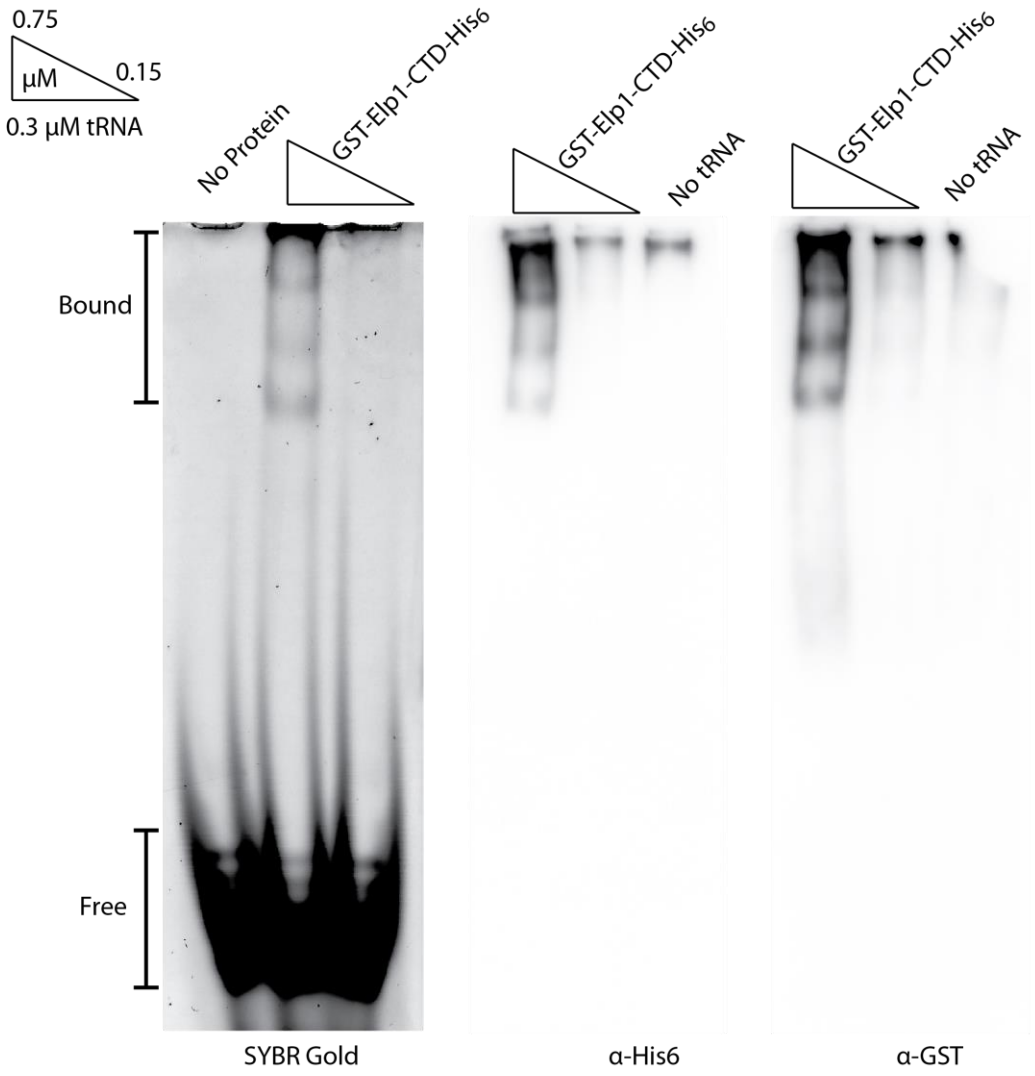

Figure 5.9: The wild-type Elp1 C-terminal domain is detectable in shifted tRNA bands. EMSA using excess unlabelled tRNA and recombinant Elp1-CTD. Complexes were allowed to form between unlabelled tRNA at 0.3 μM and the indicated concentrations of recombinant Elp1-CTD. Binding reactions were separated on a 6% polyacrylamide native gel and one part of the gel stained with SYBR Gold. The rest of the gel was treated with 0.5% SDS and transferred to nitrocellulose membrane for western blotting using anti -His_6 and anti -GST antibodies.

5.2.3 Electrophoretic mobility shifts assays with Elp1 and ^{32}P-tRNA

A complex between the wild-type Elp1 C-terminal domain and tRNA was detectable by native gel electrophoresis and SYBR Gold staining in an electrophoretic mobility shift assay, but this was not formed with the Elp1-KR9A C-terminal domain. However, in order to detect shifted tRNA using SYBR Gold, an excess concentration (0.3 µM) of unlabelled tRNA was used in each binding reaction. This excess of tRNA may artificially force the formation of complexes under physiological salt conditions. To address this yeast tRNA was radiolabelled at the 5' end with [^{32}P]-Phosphate as this allows more sensitive detection of complexes formed in binding reactions with much lower tRNA concentrations (Hellman and Fried, 2007).

Binding reactions between ^{32}P -tRNA and the Elp1-CTD were analysed by native gel electrophoresis and autoradiography. As observed previously, an Elp1-tRNA complex was detected at the top of the gel (Figure 5.10). This indicates that the complex formed between Elp1 and tRNA is not simply due to an artificial interaction caused by excess tRNA. Although there is some smearing in the shifted band, compared to the previous experiments using excess tRNA, the binding pattern was a lot less heterogeneous (compare Figure 5.8 and 5.10). This suggests that excess tRNA may have caused heterogeneous complexes to form or that the large amount of negatively charged tRNA affected the stability of the complexes during separation.

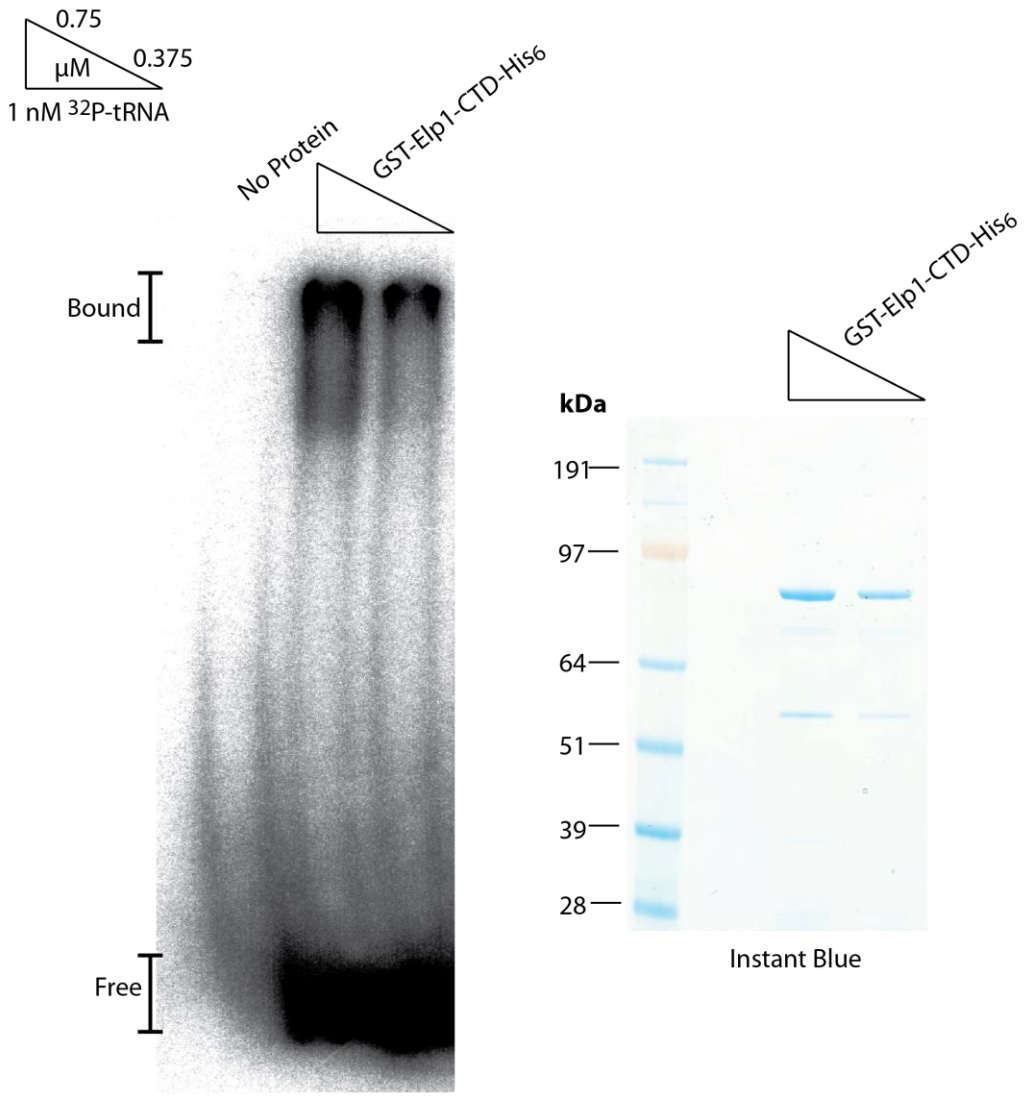

Figure 5.10: The wild-type Elp1 C-terminal domain forms a complex with radiolabelled tRNA. EMSA using ^{32}P-labelled tRNA and recombinant Elp1-CTD. Complexes were allowed to form between ^{32}P-tRNA at 1 nM and the indicated concentrations of recombinant Elp1-CTD. Binding reactions were separated on a 5% polyacrylamide native gel and analysed by autoradiography (left panel). Recombinant protein from each dilution was added to an equal volume of 2× Laemmli Buffer, boiled and analysed by SDS-PAGE on a 4-12% Bis-Tris polyacrylamide gel followed by Instant Blue staining (right panel).

Since the Elp1-tRNA complex migrated at the very top of 5% and 6% polyacrylamide native gels, further binding reactions were resolved on 4-20% polyacrylamide native gels. The reasoning was that this would allow further separation of the shifted complex without loss of the free tRNA probe. Binding reactions between ^{32}P-tRNA and GST, Elp1 and Elp1-KR9A fusion proteins was assayed by separation on 4-20% native gels and autoradiography (Figure 5.11A). A tRNA shift was resolved with wild-type Elp1-CTD binding reactions but this was absent in the GST and Elp1-KR9A-CTD binding reactions despite similar concentrations of fusion proteins being present (Figure 5.11B). The Elp1-tRNA complex still appears at the top of the gradient gel, which suggests it may be quite large since it is also unable to migrate very far though the pores of the 4% polyacrylamide region.

In order to estimate the dissociation constant (K_D) of the Elp1-tRNA complex, binding reactions were set up with a negligibly low concentration of ^{32}P-tRNA (0.1 nM) and increasing concentrations of wild-type Elp1 fusion protein ranging from 25 nM to 0.75 µM. These were resolved by native gel electrophoresis and autoradiography (Figure 5.12A and 5.12B) and the fraction of bound tRNA quantified by densitometry. The values of the % bound fraction were plotted against the protein concentration and this was fitted to a non-linear sigmoidal curve (Figure 5.12C). The calculated K_D was 0.37 µM and therefore the dissociation constant of the complex formed between Elp1 and tRNA was estimated to be in the low micromolar range. However, for a more accurate dissociation constant measurement more replicates are required. A potential issue with these calculated values is that the protein concentrations were determined based on the calculated extinction coefficient of GST-Elp1-His_6, but this is not a completely pure preparation and this could lead to under estimation.

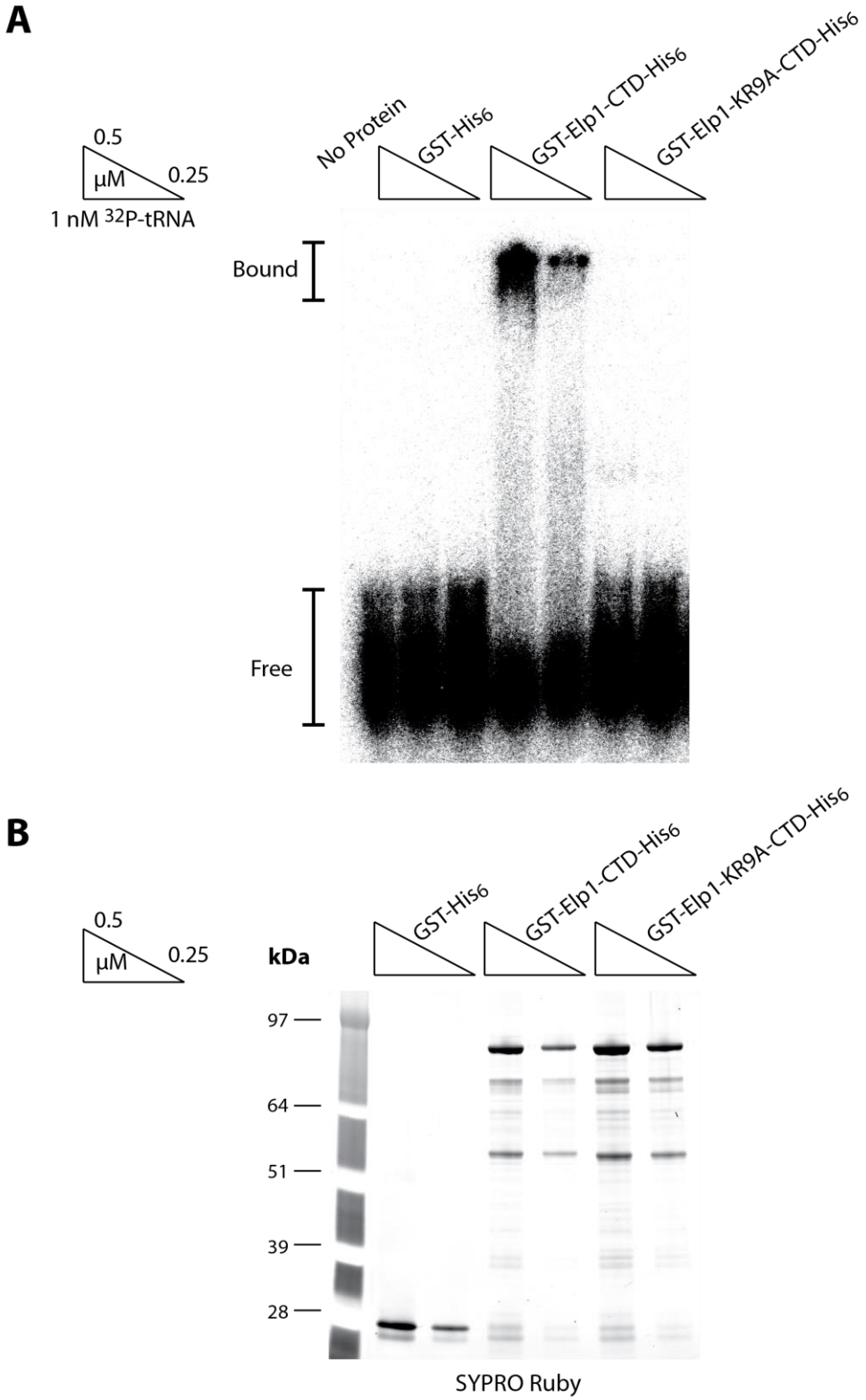

Figure 5.11: The wild-type Elp1 C-terminal domain forms a complex with radiolabelled tRNA that is disrupted in the Elp1-KR9A mutant. A) Electromobility shift assay using ^{32}P-labelled tRNA and recombinant GST, Elp1 and Elp1-KR9A fusion proteins. Complexes were allowed to form between ^{32}P-tRNA at 1 nM and the indicated concentrations of fusion proteins. Binding reactions were separated on a 4-20% polyacrylamide native gel and analysed by autoradiography. B) Recombinant protein from each dilution was added to an equal volume of 2× Laemmli Buffer, boiled and analysed by SDS-PAGE on a 4-20% Bis-Tris polyacrylamide gel followed by SYPRO Ruby staining.

The spreading of the bound bands at higher protein concentrations also make accurate quantification by densitometry technically difficult. The stoichiometry of binding is also not yet known but in some cases the value of the hill coefficient (b) calculated from fitted binding curves can indicate the stoichiometry of binding (Weiss, 1997). This value was calculated to be ~2 in this experiment, suggesting that the Elp1 CTD could interact with tRNA as a dimer. This could be more accurately determined with stoichiometric binding reactions using a constant excess of unlabelled tRNA containing a small concentration of ^{32}P-tRNA and increasing molar concentrations of protein. Plotting the fraction of bound tRNA against the concentration of protein/tRNA equivalents allows the stoichiometry to be determined based on fitting to saturation binding curves (Ryder et al., 2008).

Binding reactions were set up using ^{32}P-tRNA and either GST-His_6, Elp1-CTD or Elp1-KR9A-CTD but this time these were resolved on a 1.5% agarose gel, followed by autoradiography (Figure 5.13). Using this format, a shifted Elp1-tRNA complex that migrated nearer the middle of the gel was resolved and as previously, this shift was absent in GST-His_6 and Elp1-KR9A-CTD binding reactions. This format may therefore be more appropriate for further analysis of the complex since it can now be better resolved through the larger pores formed by agarose.

Taken together, these data demonstrate that the C-terminal domain of Elp1 forms a complex with tRNA and that Elp1-KR9A, in which the basic region of Elp1 is mutated, has lost the ability to form this complex. We propose that this basic region in Elp1 is a well-conserved RNA binding domain.

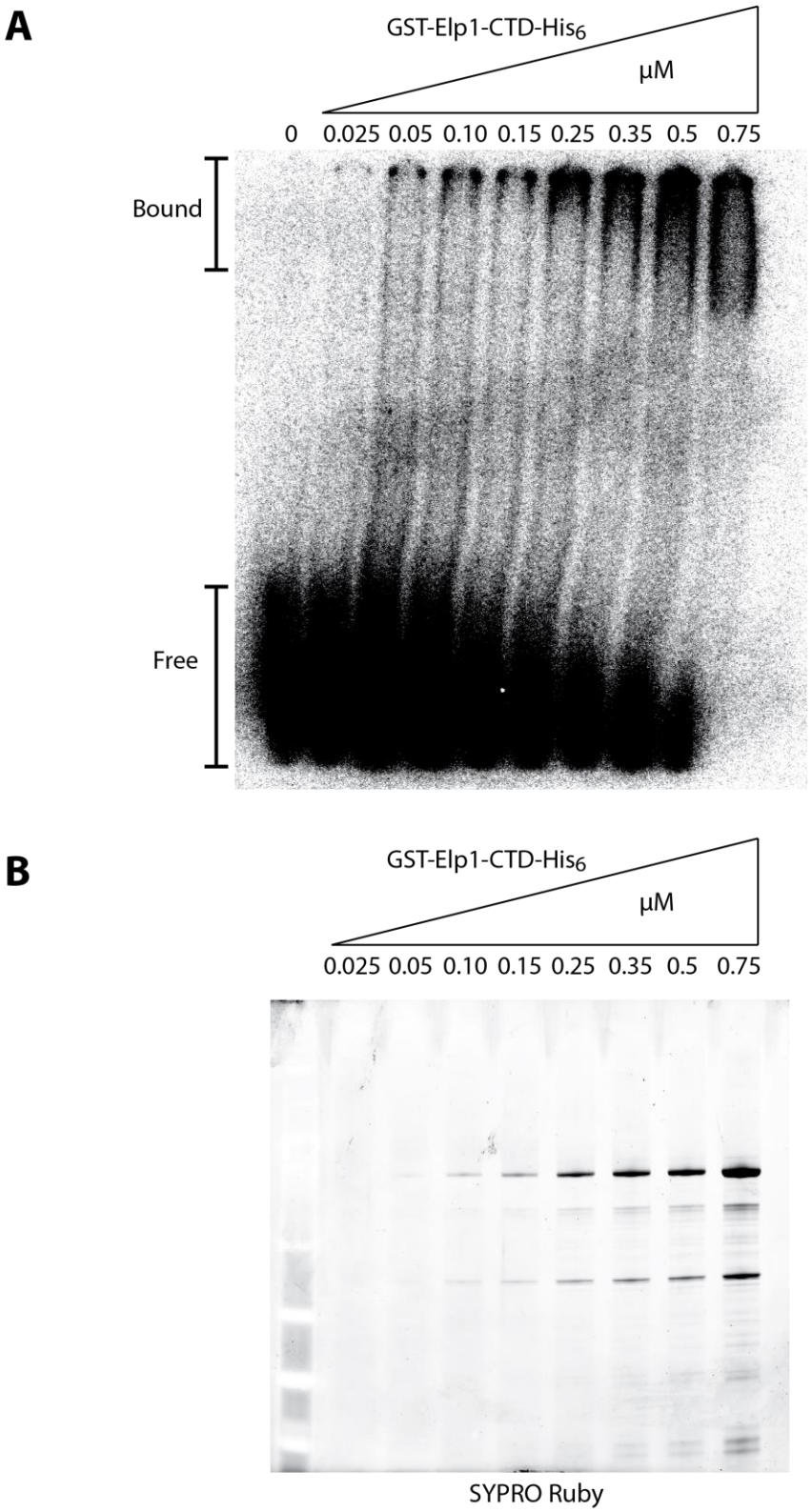

Figure 5.12: The wild-type Elp1 C-terminal domain and tRNA form a complex with a K_D in the low micromolar range; See next page for figure legend

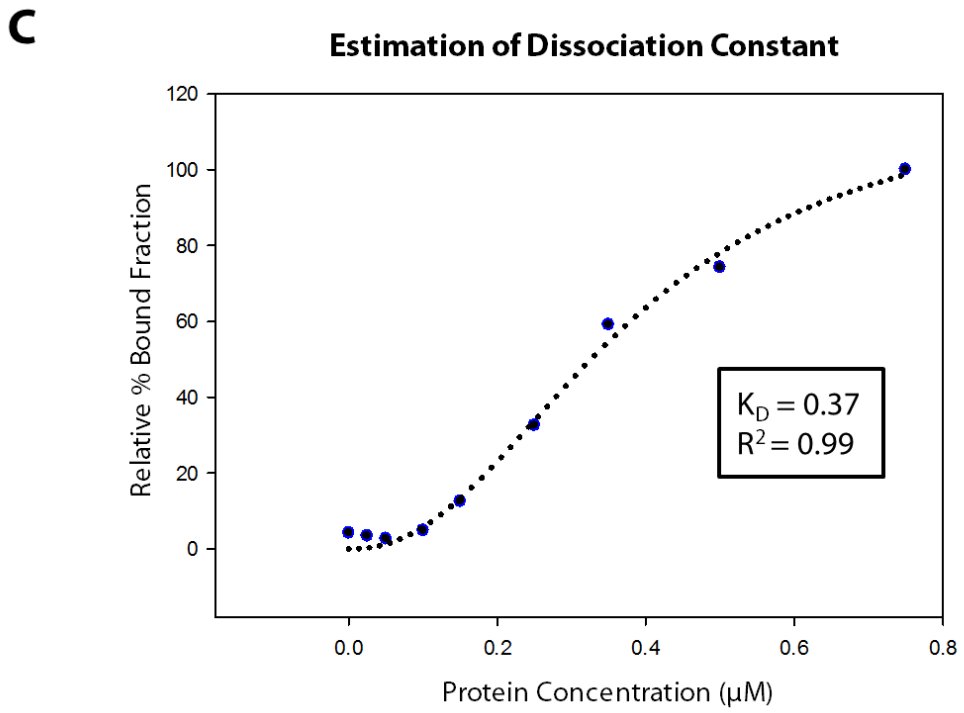

Figure 5.12: The wild-type Elp1 C-terminal domain and tRNA form a complex with a K_D in the low micromolar range. A) EMSA using ^{32}P-labelled tRNA and increasing concentrations of recombinant Elp1-CTD. Complexes were allowed to form between ^{32}P-tRNA at 0.1 nM and the indicated concentrations of protein. Binding reactions were separated on a 4-20% polyacrylamide native gel and analysed by autoradiography. B) Recombinant protein from each dilution was added to an equal volume of 2× Laemmli Buffer, boiled and analysed by SDS-PAGE on a 4-12% Bis-Tris polyacrylamide gel followed by SYPRO Ruby staining. C) % Bound fraction shifts in the mobility of ^{32}P-tRNA were quantified by densitometry and plotted against the protein concentration (µM) of Elp1 C-terminal domain. A sigmoidal curve was fitted to the data ($f = (a*b)^b/c^b+x^b$) as indicated by the dotted line and the r^2 values and calculated K_D are shown. The K_D is estimated from the protein concentration at which binding is 50% of the maximal value.

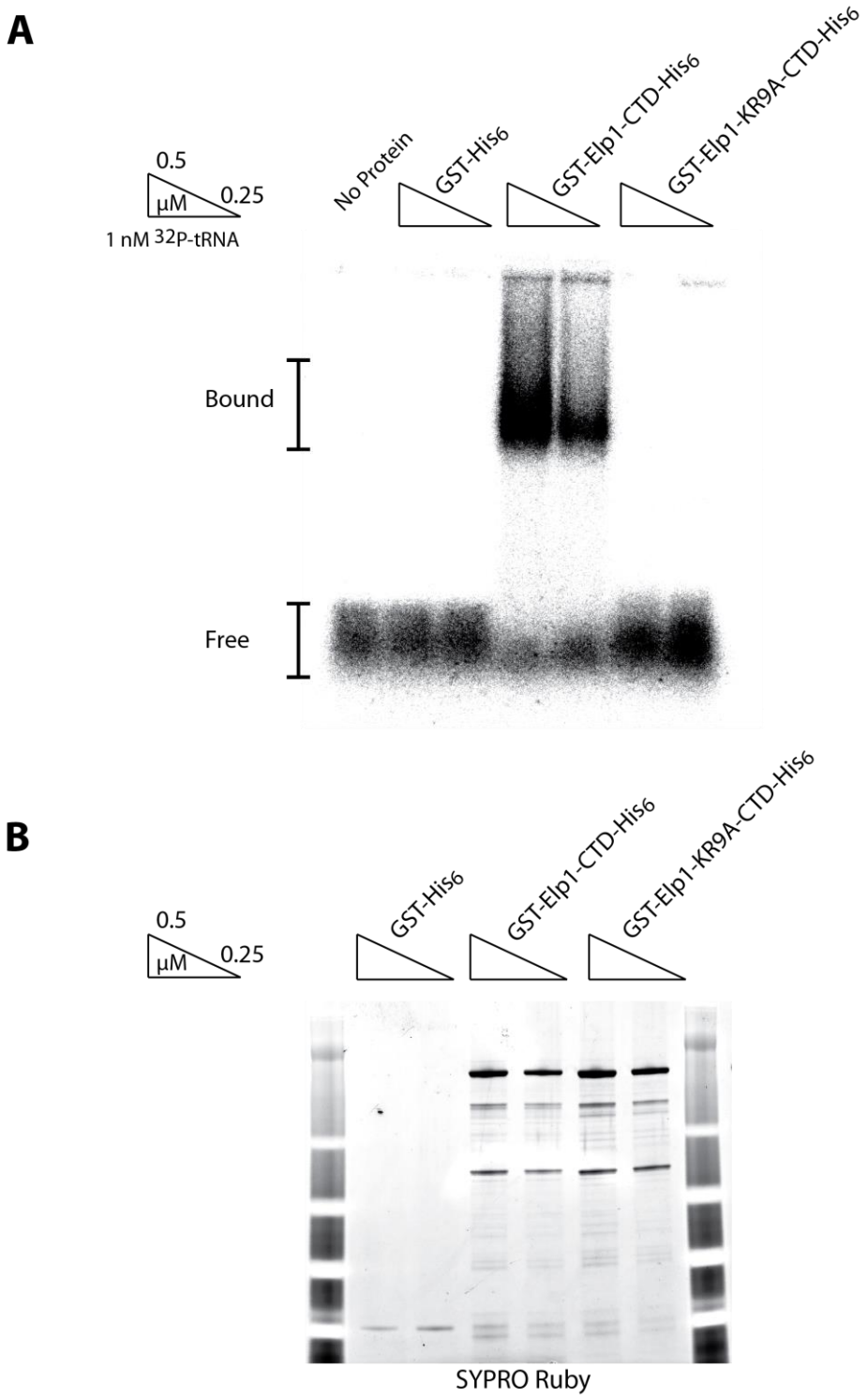

Figure 5.13: The wild-type Elp1 C-terminal domain forms a complex with radiolabelled tRNA that can be resolved by 1.5% agarose electrophoresis. A) EMSA using ^{32}P-labelled tRNA and recombinant GST-His_6, Elp1 and Elp1-KR9A fusion proteins. Complexes were allowed to form between ^{32}P-tRNA at 1 nM and the indicated concentrations of recombinant proteins. Binding reactions were separated on a 1.5 % native agarose gel and analysed by autoradiography. B) Recombinant protein from each dilution was added to an equal volume of 2× Laemmli Buffer, boiled and analysed by SDS-PAGE on a 4-12% Bis-Tris polyacrylamide gel followed by SYPRO Ruby staining.

5.2.4 Specificity of the Elp1-tRNA interaction

Previous work has demonstrated interactions between the Elongator complex and nucleic acids, such DNA and mRNA. In order to test the specificity of the interaction between the Elp1 fusion proteins and tRNA, competition binding experiments were carried out to assay whether any other types of nucleic acid could compete effectively with tRNA for binding to Elp1.

Binding reactions with the Elp1 C-terminal domain and 1 nM ^{32}P-tRNA were set up as previously but this time the formation of complexes was challenged with a variety of competitors (Figure 5.14). Since it is known that non-specific competitors added to binding reactions can decrease even specific interactions if added at a sufficiently high concentration, especially when using purified proteins, competitors were carefully titrated at incremental concentrations.

Heparin, a negatively charged polysaccharide that is often used to purify nucleic acid binding proteins and inhibit RNA polymerase binding to DNA (Wallin and Maenpaa, 1979, Carey et al., 2012) was tested first as a competitor in the binding reaction. Heparin has the highest net negative charge of any known biological molecule, and yet it was unable to significantly compete the Elp1-tRNA interaction at 0.5 nM or 1 nM, although at a 5-fold molar excess (5 nM) it reduced the complex formation by around 60%. The interaction between the Elp1 C-terminal domain and tRNA is resistant to heparin when present at similar molar concentrations but the tRNA binding by Elp1 may be quite dependent on electrostatic charge interactions, which cause its disruption at higher molar excess of heparin. Given heparin's high negative charge density and the fact it is known to be a strong interactor with nucleic acid binding proteins this is not entirely surprising. Polyuridylic acid (poly(U)) was also used as a

competitor since contrary to tRNA, this is an RNA which should have no secondary structure. This was supplied as a potassium salt and the length of each poly(U) tract is not known but is expected to be very heterogeneous. Therefore, half, equivalent and 5 times the gram concentration of tRNA was titrated in as competitor. Poly(U) did not significantly compete the Elp1-tRNA complex at any of these concentrations. Since it was also shown in previous work that Elp1 could bind DNA, we also tested ssDNA (22bp oligonucleotide) as a competitor. No significant competition of the Elp1-tRNA complex by ssDNA was detected, although there may be some small loss of complex at a 5-fold molar excess when quantified by densitometry. These results demonstrate that the Elp1 C-terminal domain preferentially binds tRNA over unstructured RNA and ssDNA.

These competition experiments are in agreement with previous work using the recombinant Elp4-6 hexamer, which formed a complex with tRNA but not poly(U) or ssDNA (Glatt et al., 2012). Taken together the complex between the Elp1 C-terminal domain and tRNA is stable to competition from the other nucleic acids tested, suggesting specificity for tRNA. Extra stability and specificity may be imparted within the context of the entire Elongator complex where other subunits, such as the hexameric subcomplex, may also make interactions with the tRNA molecule (Glatt et al., 2012).

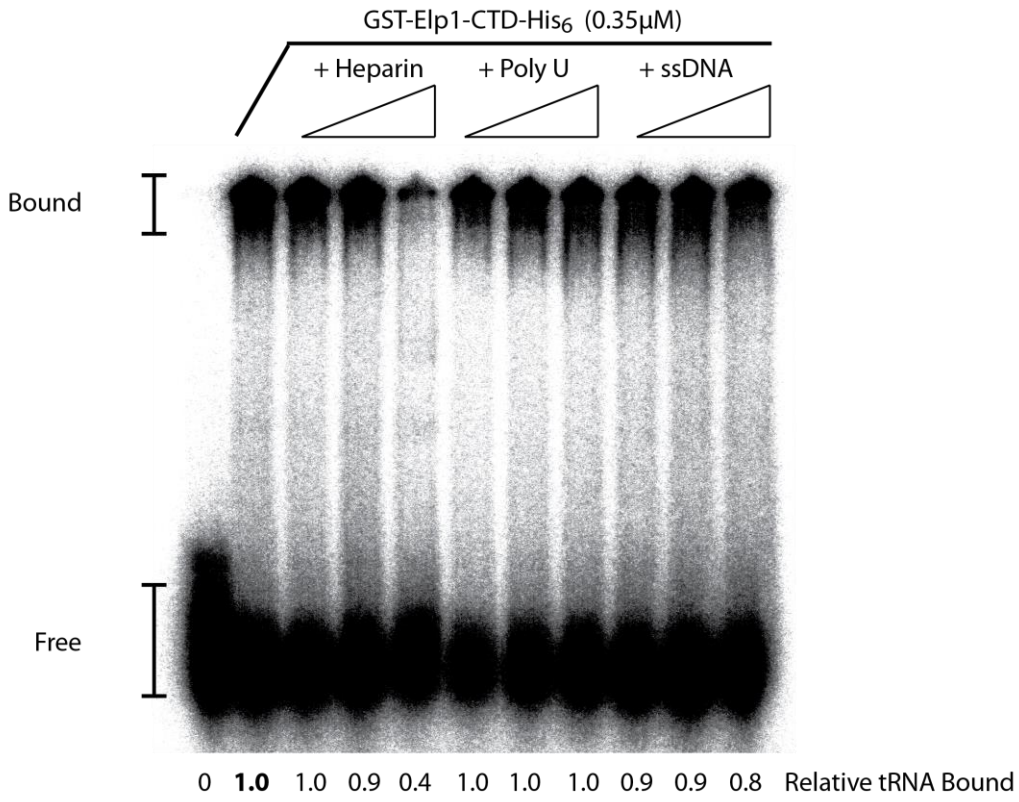

Figure 5.14: The complex formed between the Elp1 C-terminal domain and tRNA is not competed by other types of nucleic acid. EMSA using ^{32}P-labelled tRNA and recombinant Elp1-CTD. Binding reactions were incubated with ^{32}P-tRNA at 1 nM and the indicated concentrations of recombinant proteins but were challenged with increasing concentrations of unlabelled competitor. The competitor concentrations were; Heparin and ssDNA: 0.5, 1.0 and 5 nM; poly(U): 12.5, 25, 125 pg/µl. Binding reactions were separated on a 4-20% polyacrylamide native gel and analysed by autoradiography. Shifts in the mobility of ^{32}P -tRNA were quantified relative to those seen the absence of competitor by densitometry.

5.2.5 Analysis of Elp1 association with endogenous tRNA

The Elp1 basic region may be important for the binding of tRNA to the Elongator complex based on *in vitro* EMSA assays with the recombinant C-terminal domain. However, we also wanted to address whether a defect in tRNA binding to Elongator *in vivo* could be observed. Previous work has demonstrated that immunoprecipitated Elp1 and Elp3 subunits can be crosslinked to exogenous tRNA (Huang et al., 2005) but the association of the complex with endogenous tRNA has never been demonstrated.

To test whether Elp1 was associated with endogenous tRNAs, Elp1-GFP was pulled down using GFP-Trap and then RNA extracted from the precipitate (Figure 5.15A). The associated RNAs were assayed by northern blotting using a probe against $tRNA^{Gln}_{UUG}$, which receives the Elongator dependent mcm^5s^2 modification (Figure 5.15B). To act as positive controls glutamine tRNA synthetase (Gln4), which is known to bind $tRNA^{Gln}$ (Grant et al., 2013, Grant et al., 2012), and cytoplasmic export protein 1 (Cex1), which is involved in the tRNA nuclear export pathway (McGuire and Mangroo, 2007), were used.

There was an enrichment of $tRNA^{Gln}_{UUG}$ associated with the Elp1-GFP pulldown compared to the untagged control, indicating that this tRNA associates with Elongator *in vivo*. The Gln4-GFP control also shows enrichment of $tRNA^{Gln}_{UUG}$, this is one of its two substrate tRNAs in yeast. No association of $tRNA^{Gln}_{UUG}$ with Cex1-GFP was seen despite it being annotated as a tRNA binding protein. It is possible that Cex1-GFP may bind tRNA too transiently to see enrichment under these conditions. There is more enrichment of $tRNA^{Gln}_{UUG}$ in the Gln4-GFP pulldown compared with the Elp1-GFP pulldown, but this may be because Gln4 binds only two tRNA substrates whereas

Elongator may be associated with any one of up to eleven different substrate tRNAs, which could reduce the $tRNA^{Gln}_{UUG}$ specific signal significantly.

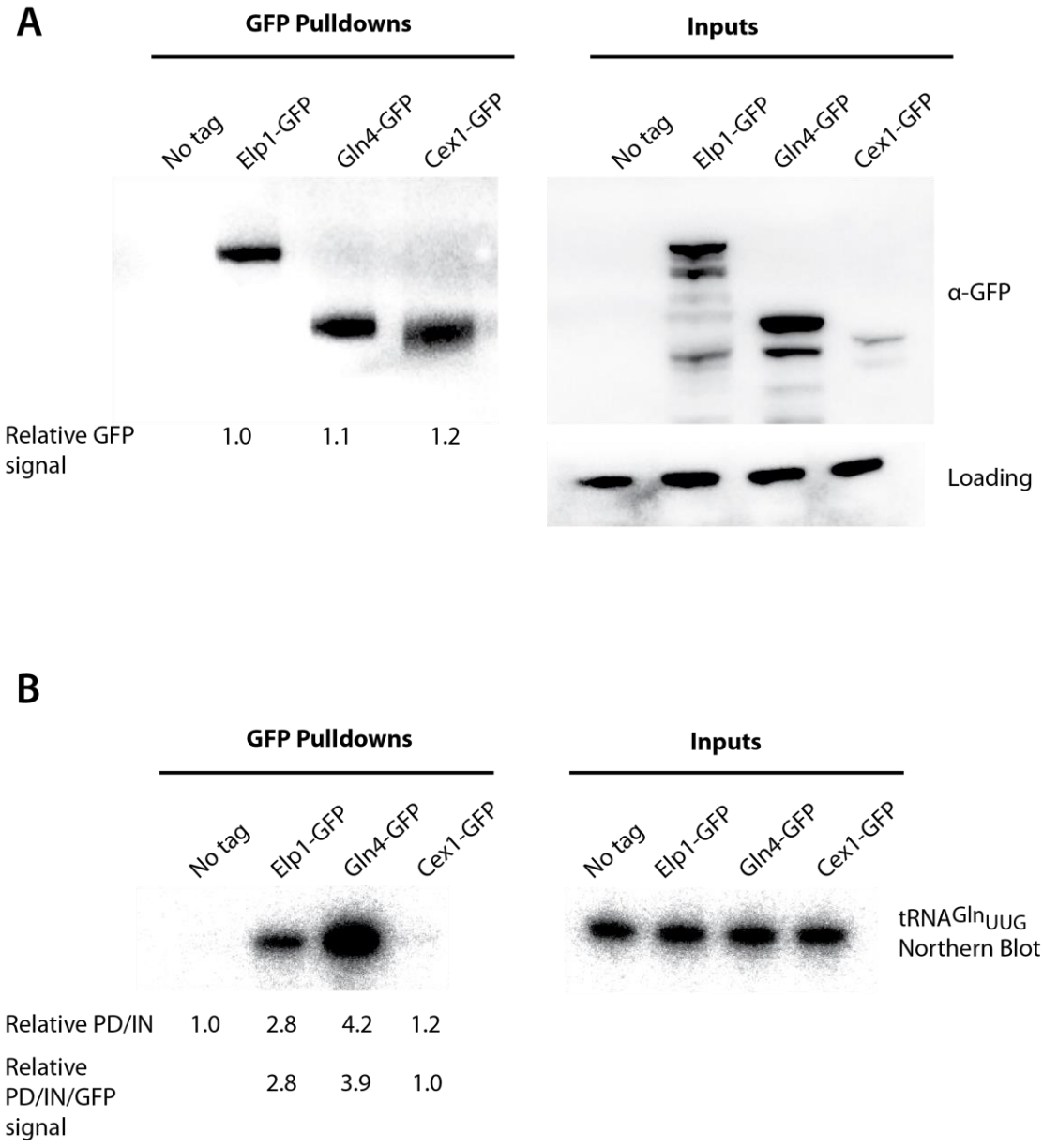

Figure 5.15: Elp1 associates with $tRNA^{Gln}_{UUG}$. A) GFP pulldowns (left panel) and inputs (right panel) from untagged, Elp1-GFP, Gln4-GFP and Cex1-GFP expressing strains were analysed by western blotting with anti-GFP. The relative GFP pulldown signal was quantified by densitometry. B) RNA was extracted from GFP pulldown (left panel) and input (right panel) samples and analysed by northern blotting using a probe against $tRNA^{Gln}_{UUG}$. The relative $tRNA^{Gln}_{UUG}$ signal was quantified by densitometry and normalised by input signals. This PD/IN value was also divided by GFP signals to take into account the efficiency of GFP pulldown.

The Elp1-KR9A basic region mutant has a defect in tRNA wobble uridine modification (Chapter 3) and furthermore there was no detectable binding of tRNA to the recombinant C-terminal domain of Elp1 in this mutant (Sections 5.2.3 and 5.2.4). To assay whether there was an *in vivo* defect in the association of $tRNA^{Gln}_{UUG}$ with the basic region mutant, Elp1-KR9A-GFP and Elp1-GFP were pulled down with GFP-Trap and RNA was extracted from the precipitates (Figure 5.16A). As a negative control, argininosuccinate lyase (Arg4) was used, this should not associate with tRNA and controls for the presence of the GFP tag. The association of $tRNA^{Gln}_{UUG}$ with Elp1-GFP, Elp1-KR9A-GFP and Arg4-GFP was analysed by northern blotting (Figure 5.16B). No enrichment of $tRNA^{Gln}_{UUG}$ in Arg4-GFP was observed compared with the untagged control, but as previously we could see an enrichment in the wild-type Elp1-GFP precipitate. There was no enrichment of $tRNA^{Gln}_{UUG}$ with Elp1-KR9A-GFP and this implies that the basic region mutation disrupts tRNA binding to the complex.

To analyse the specificity of this interaction, northern blots were reprobed for $tRNA^{Lys}_{CUU}$, which is not modified in an Elongator dependent manner (Figure 5.16C). There was still enrichment of $tRNA^{Lys}_{CUU}$ in wild-type Elp1-GFP samples and this suggests that the association is not specific for Elongator modified tRNAs under our conditions. This is consistent with previous work that showed association of the Elp4-6 hexamer with tRNA was unchanged regardless of which base was present in the wobble position (Glatt et al., 2012). It was suggested based on this that Elongator does not discriminate between tRNAs it binds but rather has a proofreading mechanism that determines which ones are modified (Glatt et al., 2012). In contrast, other work has shown that Elp1 and Elp3 could only be crosslinked to $tRNA^{Glu}$ and not $tRNA^{Met}_{i}$, implying that there might be some specificity for wobble uridine-containing tRNAs (Huang et al., 2005). However, since the structure of initiator tRNAs is slightly different,

having for example an A-U base pair at the top of the acceptor stem, three G-C base pairs in the anticodon stem and the sequence -GAUC- in place of -GrTψC- in the TψC loop this may not have been the best control to use in the latter work (Basavappa and Sigler, 1991, Kapp et al., 2006).

The total associated RNA from the above pulldowns was also run on a small RNA gel and visualised by SYBR Gold staining (Figure 5.16D). In the wild-type Elp1 pulldown a clear enrichment in the tRNA band was seen compared with the other samples. However, we could also see enrichment for what we assume are the 28S RNA and 18S ribosomal RNA bands, as well as dark staining at the top of the gel implying that other larger RNAs are also present. It has been shown by crosslinking that Elongator associates with mRNAs and this cannot ruled out based on our data (Gilbert et al., 2004). However, it is also possible that these RNAs are associated with other proteins that interact with Elongator, for example Elongator interacts with RNA Polymerase II in lysates (Otero et al., 1999, Wittschieben et al., 1999), although the true *in vivo* significance of this is disputed. Ribosomal proteins were also identified in our mass spectrometry pulldown analysis, which was carried out under the same conditions as these RNA pulldowns (Chapter 2). This makes interpretation of the true specificity of Elongator *in vivo* quite difficult and other methods may be required to complement this work. However, these RNA pulldown experiments do provide preliminary evidence to support the idea that that Elp1 associates with endogenous tRNAs and that this association depends on the basic region of Elp1, since the Elp1-KR9A allele blocks tRNA enrichment in the GFP precipitates.

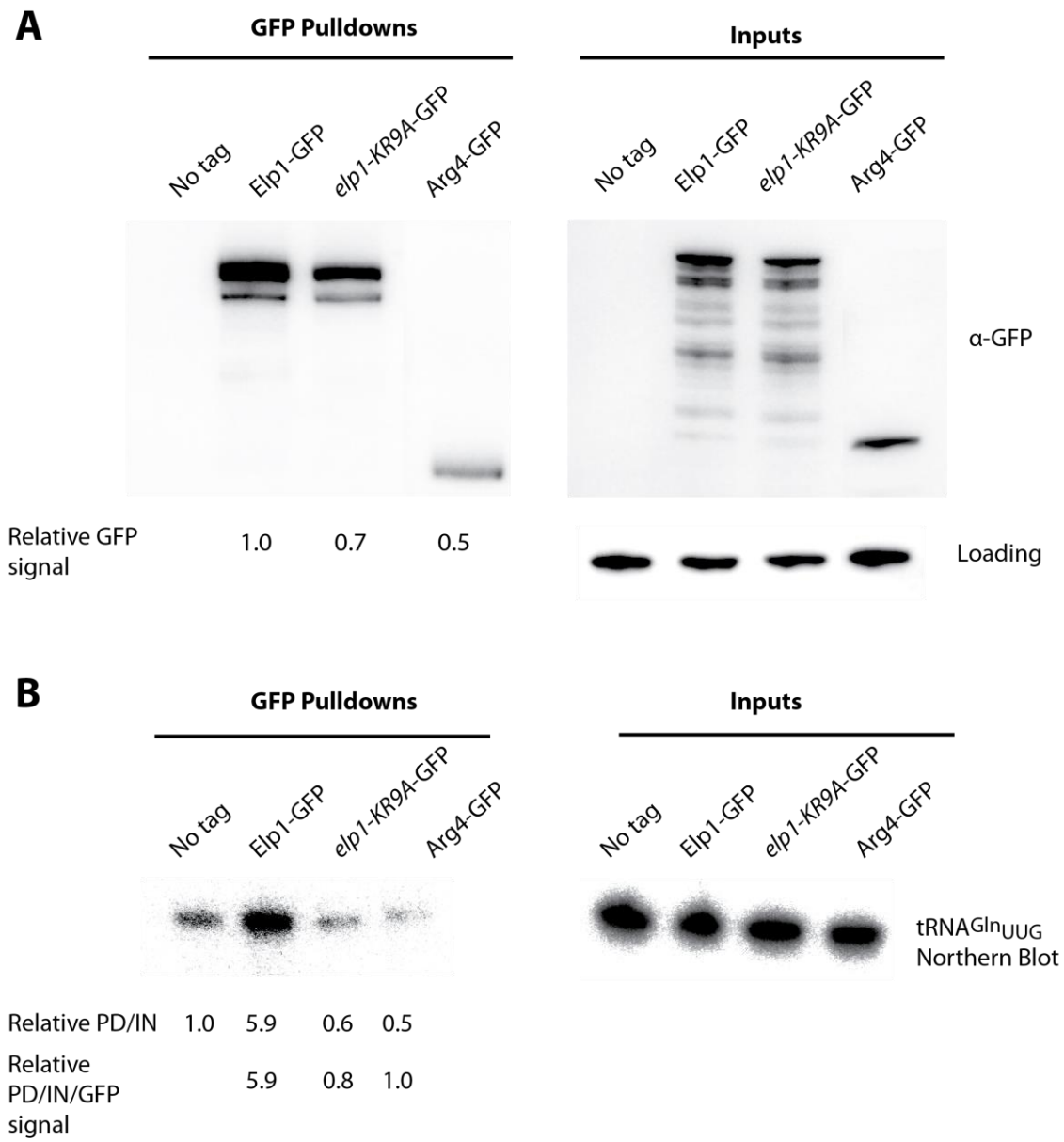

Figure 5.16: Elp1 association with tRNA$^{Gln}_{UUG}$ is disrupted in the Elp1-KR9A mutant; See next page for figure legend.

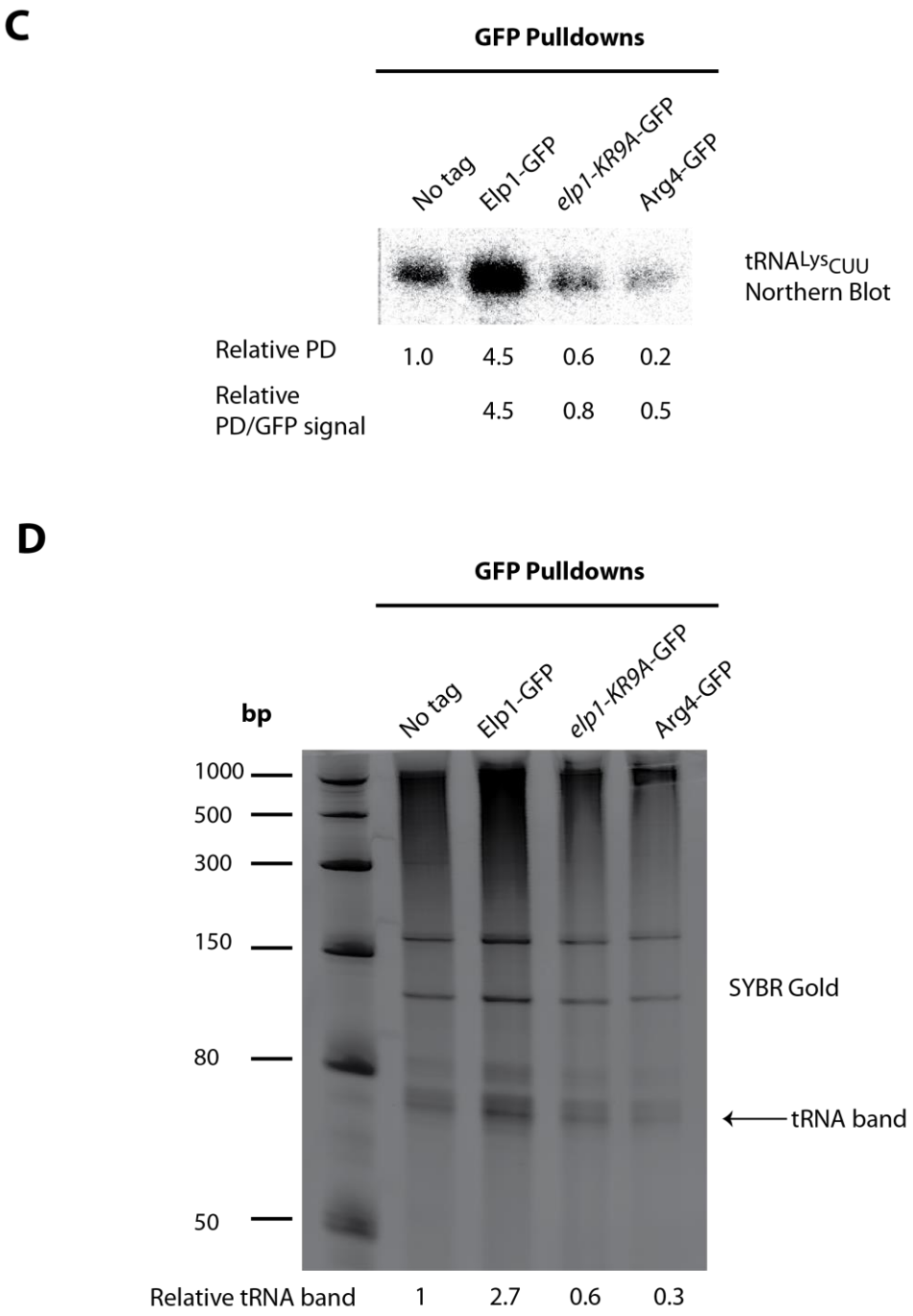

Figure 5.16: Elp1 association with $tRNA^{Gln}_{UUG}$ is disrupted in the Elp1-KR9A mutant. A) GFP pulldowns (left panel) and inputs (right panel) from untagged, Elp1-GFP, Elp1-KR9A and Arg4-GFP expressing strains were analysed by western blotting with anti-GFP. The relative GFP pulldown signal was quantified by densitometry. B) RNA was extracted from GFP pulldown (left panel) and input (right panel) samples and analysed by northern blotting with a probe for $tRNA^{Gln}_{UUG)}$. C) Northern blots were reprobed with $tRNA^{Lys}_{CUU}$. In both B) and C) the relative $tRNA^{Gln}_{UUG}$ and $tRNA^{Lys}_{CUU}$ signals were quantified by densitometry and normalised by input signals. This PD/IN value was also divided by GFP signals to take into account the efficiency of GFP pulldown. D) Total associated RNA was analysed by separation on a 10% TBE-Urea gel and staining with SYBR Gold. The tRNA band is indicated and the relative signals were quantified by densitometry.

Chapter 6: Discussion

6.1 A basic region in the Elp1 subunit of Elongator is essential for wobble uridine tRNA modification

The Elp1 subunit of the Elongator complex contains a lysine/arginine-rich basic region in the C-terminal domain that is highly conserved across eukaryotes and was previously annotated as a putative nuclear localisation sequence (Fichtner et al., 2003). Since it was originally thought that Elongator played a role in transcription, a nuclear function, this was in line with the proposed function of the complex. However, it was then shown that the Elongator subunits were all mainly localised in the cytoplasm of cells and that the major function of the complex was likely to be in tRNA wobble uridine modification, which is thought to occur in the cytoplasm (Pokholok et al., 2002, Huang et al., 2005, Hopper and Phizicky, 2003). It therefore became less clear why the Elp1 subunit would contain a highly conserved basic region if its role was indeed to direct nuclear import. It was still thought possible that nuclear import could be important to the tRNA modification function of Elongator, despite its steady state cytoplasmic localisation, because deletion of the gene encoding a karyopherin, Kap120, was found to confer Zymocin resistance (Fichtner et al., 2003). However, this mutant has since been shown to have normal levels of Elongator dependent tRNA modification and so must be defective in Zymocin uptake or activation (Huang et al., 2008).

In order to address the role of this basic region in Elp1 we created alanine mutations throughout this sequence. Mutation of nine basic residues in this region to alanine, as in *elp1-KR9A*, caused Zymocin resistance and loss of Elongator dependent *SUP4 ochre* suppressor function, both phenotypes of which were comparable in severity to those shown by an *elp1* deletion strain. This indicates that the levels of Elongator dependent

tRNA modification in this mutant are very low. Mutations of the proximal (first half) basic residues in this region, as in *elp1-KR5A*, caused Zymocin resistance but only a minor defect in Elongator dependent *SUP4 ochre* suppression. Mutations of the distal (second half) basic residues, as in *elp1-KR4A*, were wild-type in terms of Elongator dependent *SUP4 ochre* suppression but showed some level of Zymocin resistance, though less than *elp1-KR9A* and *elp1-KR5A* mutant strains. Since the *elp1-KR9A* mutations confer a more severe phenotype than mutations in either the proximal or distal sequence alone then the entire region must be important for the tRNA modification function of Elongator.

Despite the *elp1-KR9A* mutations being of comparable severity to an *elp1* knockout in terms of the above assays, other phenotypes associated with Elongator dysfunction do not appear to be as severe. There was no obvious temperature sensitivity phenotype compared to an *elp1* knockout in any of the basic region mutants or in functionally important phosphorylation site mutants, *elp1-1209A* or *elp1-1198A-1202A*. Therefore, the presence of non-functional Elp1 gives a less severe temperature sensitivity phenotype than deletion of this subunit. The assayed temperature sensitivity of *elp1*Δ is fairly subtle and so any small level of tRNA modification in point mutants compared with a complete *ELP1* knockout may allow this phenotype to become less pronounced. In the absence of Elongator no mcm^5U is detected and there is a reduction in the levels of the s^2 modification on mcm^5s^2U receiving tRNAs (Huang et al., 2005). Urm1 is responsible for the incorporation of the s^2 group and it is possible that there may be some interplay between Urm1 and Elongator, although this has never been fully investigated. Assembly of a non-functional Elongator complex may support higher levels of the Urm1 catalysed s^2 modification, allowing for a slightly higher level of tRNA function, although this is speculative.

In agreement with previous work, multicopy expression of hypomodified $tRNA^{Lys}_{UUU}$ and $tRNA^{Gln}_{UUG}$ rescued the temperature sensitivity of the *elp1*Δ deletion strain (Esberg et al., 2006). This implies that this phenotype is caused by reduced translational function of these hypomodified tRNAs in particular. Multicopy expression of the hypomodified tRNA is expected to rescue this defect by increasing the available pool of these tRNAs for decoding, thereby compensating for the effects of reduced binding of these tRNAs to the ribosome A-site.

Hypersensitivity to rapamycin was assayed in *elp1-KR9A* mutants but this was less severe than that shown by an *elp1* knockout strain. Unlike temperature sensitivity, rapamycin sensitivity in *elp1* knockouts was not suppressed by increased expression of the hypomodified tRNAs. It is possible that other Elongator dependent tRNAs may rescue this defect, although this has not yet been tested. Hypersensitivity to rapamycin may occur due to a more severe translational defect caused by concurrent loss of Elongator dependent tRNA modifications and the rapamycin induced down-regulation of protein synthesis. It was also reported that rapamycin treatment causes nuclear accumulation of spliced tRNAs in yeast (Pierce et al., 2010), so it is possible that this may deplete the pool available for translation and worsen the effects of lack of tRNA modifications.

Deletion of Urm1 has previously been shown to confer similar, though less severe phenotypes compared with Elongator dysfunction. This was proposed to be due to the fact that Elongator targets eleven wobble uridine containing tRNAs, whereas Urm1 only targets three (see Figure 1.9). In *urm1* deletion strains rapamycin hypersensitivity does show rescue by the hypomodified tRNAs (Leidel et al., 2009). Since the same

tRNAs failed to rescue the phenotype in *elp1* deletion strains, this suggests that the Elongator phenotype could be more severe in terms of its effects on translation.

There may also be another aspect to the phenotypes caused by Elongator dysfunction. In yeast *elp3Δ* and *urm1Δ* cells recent work has demonstrated a weak induction of the Gcn4 signalling pathway caused by increased translation of the *GCN4* mRNA (Zinshteyn and Gilbert, 2013). In brief, Gcn4 is a transcription factor that is translationally regulated by stress and nutrient availability. The *GCN4* mRNA contains upstream open reading frames (uORFs) that repress Gcn4 ORF translation by preferential ribosome binding at these upstream regions. The major pathway of Gcn4 up-regulation occurs in low nutrient availability, when increased levels of uncharged tRNAs directly activate the protein kinase Gcn2, which in turn phosphorylates the initation factor eIF2. This prevents the reformation of eIF2 ternary complexes and leads to decreased efficiency of translation initiation. This results in a general decrease in protein synthesis, but causes a concurrent increase in Gcn4 translation due to the skipping of uORFs on its mRNA transcript. Increased levels of the Gcn4 transcription factor cause transcriptional induction of a number of genes required to maintain homeostasis during amino acid starvation (Hinnebusch, 2005).

In *elp3Δ* and *urm1Δ* cells there is an increase in transcription and translation of certain Gcn4 targets but the major pathway of Gcn4 activation governed by increased eIF2 phosphorylation is apparently unaffected. The authors of this work suggest that a distinct mechanism is increasing the efficiency of Gcn4 translation and this could be occurring due to signalling by the hypomodified tRNAs directly, although how this occurs is not yet understood (Zinshteyn and Gilbert, 2013). It is possible that lack of tRNA modification could be sensed by an unknown pathway that causes cellular

responses. In yeast, mutations that result in inappropriate nuclear accumulation of tRNAs are associated with upregulation of Gcn4 translation, independent of eIF2 phosphorylation (Qiu et al., 2000). It is possible that hypomodification of tRNAs resulting from lack of Elongator function causes them to accumulate in the nucleus and that this contributes to aberrant signalling. It is also possible that alterations in metabolites occurring due to lack of tRNA modifications may cause perturbations in signalling pathways, though both these suggestions are highly speculative.

A double deletion of *GCN4* and *ELP3* with concurrent multicopy expression of the hypomodified $tRNA^{Lys}_{UUU}$ and $tRNA^{Gln}_{UUG}$ gives partial rescue of the rapamycin hypersensitivity phenotype, suggesting that disruption of cellular signalling pathways may also contribute to certain Elongator phenotypes (Zinshteyn and Gilbert, 2013). Although preliminary, an analysis of Elp1-GFP associated proteins by mass spectrometry identified three ribosome proteins of the 40S subunit as well as the initiation factor eIF4A and elongation factors eEF1B and eEFB1. If these interactions can be confirmed they may support the idea that Elongator function could be linked to translation in other ways that are independent of tRNA function, though for now this is speculative.

Taken together, this illustrates that thresholds for the detection of a particular Elongator phenotype are distinct due to the potentially complex underlying causes resulting from lack of tRNA modification, which are not yet fully understood.

6.2 Mutations in the Elp1 basic region do not disrupt the nucleo-cytoplasmic distribution of Elp1

The basic region of Elp1 was annotated as a bipartite type NLS sequence that in isolation could direct the nuclear import of GFP (Fichtner et al., 2003). We confirmed this NLS function using the Elp1 C-terminal domain and demonstrated that mutations in this basic region disrupt this nuclear import function. The fact that *elp1-KR9A, elp1-KR5A* and *elp1-KR4A* alleles all showed similar GFP distributions in this assay is interesting since the severity of phenotypes displayed by these mutants are distinct. The distal *elp1-KR4A* mutant is the most functional of these mutant alleles conferring only a slight Zymocin resistance phenotype. This indicates that tRNA modification in this strain is less defective compared with the other basic region mutants. However, the defect in nuclear import appears to be comparably severe across these mutants. This is consistent with the tRNA modification defects resulting from mutations in the Elp1 basic region not being due to a defect in nuclear import in the context of the full length polypeptide.

The distribution of Elp1-GFP between the nucleus and cytoplasm was assayed and as reported previously found to be mainly cytoplasmic (Pokholok et al., 2002, Huh et al., 2003). If the basic region functioned to drive nuclear import then mutation of this region should cause a clear defect in the distribution of Elp1 at steady state. However, we could not detect any obvious defects in the distribution of the Elp1-KR9A, Elp1-KR5A or Elp1-KR4A GFP fusion proteins compared to wild-type Elp1-GFP. Quantification of images allowed a small nuclear pool of Elp1 to be demonstrated, ~25% of the total Elp1 in a wild-type strain, but this was not disrupted by any basic region mutations, which would be expected if the basic region was required for

nuclear import of the subunit. Therefore the basic region of Elp1 does not function as a nuclear localisation sequence in the context of the full-length protein.

We also hypothesised that functionally important phosphorylation sites, which lie upstream of the Elp1 basic region, could potentially regulate the localisation of Elp1. It would be expected that if these sites regulated distribution of the complex then phosphorylation site mutations would disrupt this and cause an obvious defect in localisation. The effect of the *elp1-1209A* mutation on the distribution of Elp1 between the nucleus and cytoplasm was assayed but no obvious changes were observed to suggest this site regulates localisation.

In yeast, the cytoplasmic localisation of Elongator subunits has been reported in a number of studies (Pokholok et al., 2002, Huh et al., 2003). However, the localisation of the accessory factor Kti12 is less well defined. The Yeast GFP collection annotates Kti12 as cytoplasmic but the distribution of Kti12-GFP in these images appears to be uniform throughout the cell, whereas cells expressing GFP tagged Elongator subunits have a weakly-fluorescent nucleus as in the images presented in this work (Huh et al., 2003). The localisation of Kti12-GFP was therefore determined and although the majority was observed to be cytoplasmic there was a higher relative nuclear pool of Kti12 compared to that of Elp1. Since it was formally possible that Kti12 may influence the localisation of the Elongator, the distribution of Elp1-GFP and Elp1-KR9A-GFP between the nucleus and cytoplasm was assayed in a *kti12* deletion background but no obvious changes were seen in comparison with *KTI12* wild-type controls.

The role(s) of phosphorylation sites in Elp1 and of the accessory factor Kti12 in terms of Elongator-dependent tRNA wobble uridine modification remain to be defined but these do not appear to function through affecting Elp1 localisation. Although the Elp1

basic region can direct nuclear import in isolation, in the context of the full length Elp1 subunit this property does not appear to be functionally relevant. However, the basic region is nonetheless essential for wobble uridine tRNA modification.

6.3 The cytoplasmic localisation of Elp1 is essential for Elongator's tRNA modification function

The Elongator subunits all share a cytoplasmic localisation but in agreement with our work a small nuclear pool has also been reported (Pokholok et al., 2002, Fichtner et al., 2002b, Rahl et al., 2005). It is clear that mutations in the basic region of Elp1 do not disrupt this steady state nuclear pool. However, this small pool of nuclear localised Elp1 may nevertheless contribute to function. To test this, the classical NES sequence from HIV Rev was cloned between Elp1 and the GFP tag and this should actively deplete any nuclear localised Elp1 to give a cytoplasmic distribution at steady state. The distribution of Elp1-NES(Rev)-GFP showed no clear differences in distribution compared to wild-type Elp1-GFP. This could imply that there is little to no nuclear Elp1 under steady state conditions, although we cannot rule out that this sequence may not function in the context of Elp1. The addition of the NES(Rev) sequence also did not cause any major defect in Elongator function as assayed by Zymocin sensitivity, consistent with the tRNA modification function of Elongator requiring a cytoplasmic localisation.

To confirm this, a *bona fide* nuclear localisation sequence was cloned between Elp1 and the GFP tag. As expected this Elp1-NLS(Cbp80)-GFP construct was localised to the nucleus and consequently resulted in Zymocin resistance comparable to that of an *elp1*

deletion mutant. Taken together, these results are in support of the cytoplasmic localisation of Elongator being required for its tRNA wobble uridine modification function.

It is possible that the small nuclear pool of Elp1 quantified through analysis of our images represents some form of unaccountable background signal rather than a genuine nuclear pool. Images taken in 3D could not be quantified because of problems with GFP and mCherry photobleaching but we have observed that in these images the apparent GFP nuclear pool assayed in Elp1-GFP, Elp1-KR9A-GFP and Elp1-NES(Rev)-GFP expressing strains is visibly bleached after the first z-section resulting in a black hole in the image, whereas cytoplasmic GFP signals are still detectable throughout the image stack. The 2D analysis of cells will also overestimate the nuclear pool since it does not take into account compartment volume. It is possible that a low level of degraded or unfolded Elp1-GFP could account for this nuclear pool.

In other work both fluorescent protein tagging and immunolocalisation with antibodies against endogenous Elongator subunits have been used to assay localisation (Rahl et al., 2005, Fichtner et al., 2002b, Pokholok et al., 2002, Holmberg et al., 2002). We and others have also tested different methods of sample preparation, such as different fixation methods or using live cells (Rahl et al., 2005, Kim et al., 2002). Arguably since these separate experimental conditions all indicate low levels of nuclear Elongator then this may not a technical artefact.

It is possible that other basic sequences in Elp1 could influence its distribution. The programme cNLS Mapper does not annotate the Elp1 basic region as a bipartite NLS, but it does pick up a possible monopartite NLS with a score of 7.5. A score of 7-8 indicates possible partial nuclear localisation of a protein, and can be compared with

the *bona fide* bipartite NLS of Cbp80 that is given a score of 9.5 by cNLS Mapper. However, this putative monopartite sequence occurs in the N-terminus of Elp1 within a region predicted to fold into a beta sheet and so it may not be accessible to the cell's import machinery. For comparison, the tRNA binding protein Gln4 has a similar cytoplasmic localisation to Elp1 (Huh et al., 2003) and also has a monopartite NLS predicted by cNLS mapper with a score of 7. If these sequences could interact with the importin machinery in the context of the full length polypeptide they may allow a small nuclear pool of these enzymes to form. Neither of the predicted monopartite NLS sequences in these proteins conform exactly to the monopartite NLS consensus sequence so it is unclear whether these could be functionally significant in the context of these proteins. However, it is formally possible that these short basic sequences could allow a small nuclear pool of these tRNA modification enzymes to exist in yeast. There are no other putative NLS sequences identified by cNLS mapper in any of the other Elongator subunits or accessory factors.

In worms, mice and flies, Elongator subunits have also been reported to be cytoplasmic but the extent to which any nuclear Elongator is detectable is also unclear (Chen et al., 2009a, Lin et al., 2013, Creppe et al., 2009, Kim et al., 2002, Holmberg et al., 2002). In worms no apparent nuclear pool of Elp1 was detectable and there was no overlap between Elp1 and nuclear localised RNA Pol II in mice (Chen et al., 2009a, Lin et al., 2013). In human cells the consensus appears to be that the complex is predominantly cytoplasmic, although there may be a small nuclear pool of Elongator subunits as assayed by both immunolocalisation and fluorescent tagging of Elp subunits (Kim et al., 2002, Holmberg et al., 2002, Close et al., 2012b). Fractionation of HEK293 cell lysates followed by western blotting for Elp5 detected ~14% of the protein in the nuclear fraction (Close et al., 2012b). However, this would require further work

to confirm for the other larger Elongator subunits, since it is possible that this represents a pool of Elp5 that is not assembled into Elongator and that may be freely diffusible between the compartments due to its small size.

We cannot completely rule out that Elp1 may undergo nucleo-cytoplasmic shuttling under steady state conditions and this could have masked the effect of the strong NES sequence. However, since addition of the HIV Rev NES did not affect the nucleo-cytoplasmic distribution, this would require wild-type Elp1 nuclear export to occur at a similar rate as that which occurs in the Elp1-NES construct, implying that a strong nuclear export sequence would have to be present in either wild-type Elp1 or another Elp subunit. Nuclear import must also be occurring independently of the Elp1 basic region, since its mutation does not affect the steady state distribution. It is not immediately clear how shuttling would be mediated since the nuclear pool of Elp1 would have to be maintained at low levels to support cytoplasmic wobble uridine tRNA modification and there are no obvious nuclear export sequences in Elp1 or any other Elongator subunits. Previous work has also shown that sequential deletion of known yeast nuclear export pathways, including the Crm1 export pathway, also does not disrupt the steady state distribution of Elp1 (Rahl et al., 2005). However, it is true that this does not take into account redundancy between these pathways or export by a yet unknown pathway.

It is known that in yeast mature tRNAs constitutively shuttle between the nucleus and the cytoplasm and this may serve as a proofreading mechanism, preventing damaged or improperly folded tRNAs from being exported back into the cytoplasm for use in translation (Takano et al., 2005, Phizicky and Hopper, 2010b). It is formally possible that a small nuclear pool of Elongator may increase the efficiency of tRNA modification

by allowing modifications to occur in both compartments. In support of this, work unrelated to studies of Elongator assayed the modification status of a tRNA species that had apparently never been exported to the cytoplasm and the ncm^5U modification was detected (Ohira and Suzuki, 2011). The re-export of mature yeast tRNAs is sensitive to nutrient status since amino acid, glucose and nitrogen starvation conditions cause nuclear accumulation of certain tRNA species. However, the localisation of Elongator subunits has been tested under various stress conditions, including nitrogen starvation (Rahl et al., 2005, Tkach et al., 2012, Breker et al., 2013). Under these conditions there were no apparent differences in the cytoplasmic distribution of Elongator subunits. Although further work may be required to confirm that there are not some more subtle changes occurring, it does suggest that if Elongator does shuttle then this may be independent of tRNA localisation, and so the immediate benefit of this to the yeast cell is not clear.

It seems formally possible based on our data that there is a small pool of nuclear localised Elp1 but how this is maintained and its functional significance is not apparent. Whether or not a small nuclear pool of Elp1 does exist *in vivo* is ultimately out with the scope of this project. It is clear that localisation is not being disrupted by mutation of the Elp1 basic region and that the major Elongator pool involved in wobble uridine tRNA modification is cytoplasmic.

6.4 Elongator is still assembled in the Elp1-KR9A mutant

In the context of the Elp1 basic region mutant Elp1-KR9A, the overall assembly of the Elongator complex was largely unaffected. The Elp1-3 subcomplex was detected in GFP tagged Elp1 and Elp1-KR9A pulldowns and all subunits were detected by mass spectrometry. HA-tagged Elp3, Elp5 and Kti12 proteins were also each present as co-precipitants in GFP tagged Elp1 and Elp1-KR9A pulldowns. Since there were no apparent losses of any Elongator subunit interactions then the basic region of Elp1 is unlikely to encompass a binding domain involved in complex assembly. However, there were subtle differences in the association of the Elp5 subunit and Kti12 with Elp1-KR9A binding ~30% and ~40% less of each, respectively. These defects could occur because the complex is non-functional and as a result the stability of certain interactions may be reduced.

If Elongator cycles between multiple forms in order to bind, modify and release a tRNA molecule then a mutation that disrupts this mechanism could cause the complex to stall in a particular conformation. The Elp5 subunit has been shown to be an integral, though less stable component of the Elongator complex along with Elp4 and Elp6. These associate together into a hexameric ring complex and so any defect in the association of the Elp5 subunit with Elp1-KR9A should theoretically be shared with the Elp4 and Elp6 subunits (Glatt et al., 2012). Rather than forming a static structure it is expected that the hexameric ring complex would be involved in cycles of conformational changes, as in other members of the RecA-like NTPase superfamily, though this has not been confirmed (Lyubimov et al., 2011). Assuming this is the case, reduced association of Elp5 with Elp1-KR9A may occur due to an arrest in the mechanism of action of Elongator, resulting in reduced or stalled cycling of the

hexamer. It is also still possible that part of a binding domain for these subunits has been disrupted by the basic region mutations causing reduced association, since involvement of the Elp1 C-terminus in the interaction between the Elp1-3 subcomplex and the Elp4-6 hexamer has never been directly tested.

Mutation of the essential serine phoshorylation site at position 1209 to alanine causes a similar level of defect in Elongator function as the Elp1-KR9A mutation. However, this Elp1-1209A mutant showed a ~2 fold increased Kti12 association compared to wild-type Elp1. This is in contrast to reduced Kti12 association in the Elp1-KR9A mutant and suggests that the cause of Elongator dysfunction in these mutants is distinct. If Elongator does cycle between Kti12-associated and free forms, our data would be consistent with the basic region and phosphorylation site mutants having distinct effects on the balance of these different forms. It would be interesting to test whether the other Elongator accessory factor Kti11 and its binding partner Kti13 share the same pattern of association in these mutants.

If defective Kti12 association was the primary defect in the Elp1 basic region mutant we reasoned that increasing the levels of Kti12 might rescue this defect and give a more functional Elongator complex. However, multicopy *KTI12* did not rescue the Zymocin resistant phenotype of Elp1-KR9A and this is consistent with the minor defects in Kti12 association not being the major cause of dysfunctional Elongator in this mutant, rather this may occur as a secondary consequence. It is also possible that if the Elp1-KR9A mutation has disrupted part of the Kti12 binding domain then this might prevent rescue by extra copies of Kti12. However, since it was previously shown that truncation of the Elp1 C-terminus, including the basic region (deletion of residues 1229-1349), still supported Kti12 association to the same degree as wild-type Elp1

(Fichtner et al., 2002b), it seems unlikely that the basic region is a major determinant of Kti12 interaction.

The Elongator holocomplex has been proposed to be assembled using two copies of each of the six Elongator subunits to form a dodecamer (Figure 1.3, Glatt et al., 2012). It was possible that the Elp1 basic region may be important for integration into this higher order complex and so to test this, GFP pulldowns in strains with two differentially tagged versions of Elp1 and Elp1-KR9A were carried out. Both tagged versions of Elp1 and Elp1-KR9A could associate to a similar degree in various combinations, so that the Elp1-KR9A mutant was able to associate with a differentially tagged wild-type Elp1 and Elp1-KR9A protein. Concurrent expression of both wild-type Elp1 and Elp1-KR9A alleles in the same cell caused partial Zymocin resistance, indicating the formation of both functional and non-functional complexes. Therefore the basic region mutant could compete with the wild-type Elp1 for incorporation into Elongator.

Interestingly, when purifying recombinant Elp1 and Elp1-KR9A C-terminal domains from *E. coli* a degraded version of the Elp1 fusion proteins was stably associated during both tandem affinity steps despite the apparent loss of an affinity tag in the shorter version, as judged by Western blotting. This suggests that the dimerization of Elp1 may occur directly via its C-terminal domain and provides further evidence that the basic region mutant does not disrupt this association. If this type of dimerisation occurs in the context of Elongator then our view of Elongator assembly would need to revised. Rather than two copies of Elp1-3 being bridged by an Elp4-6 hexamer, two copies of Elp1 may also directly associate with each other via the flexible C-terminal domain. This would be supported by the fact that there is no defect in Elp1-KR9A association

with a differentially tagged version of itself or Elp3, despite this mutant having a minor defect in Elp5 association. This is consistent with the Elp1 subunits associating independently of the Elp4-6 hexamer. Previous data from our lab has shown that the N-terminal domain of Elp1 is essential for complex assembly, since the Elp3 interaction is lost when this domain is truncated. Conversely, deletion of the Elp1 C-terminal domain (deletion of amino acids 1198-1349) appears to be dispensable for this interaction (Kozyrska and Stark, unpublished). Our data may be consistent with the Elp1 C-terminal domain being essential in formation of the higher order dodecamer structure of Elongator and thus not completely dispensable for holocomplex assembly.

Taken together, mutation of the Elp1 basic region does not disrupt the overall assembly of the Elongator holocomplex but does reduce the association of the Elp5 subunit and of Kti12.

6.5 The Elp1-KR9A mutant has increased ser-1209 phosphorylation

The Elp1 basic region mutant was assayed for phosphorylation at the functionally important ser-1209 site. Compared with wild-type Elp1, the Elp1-KR9A mutant had ~three fold more phosphorylation at this site. A more modest increase in general phosphorylated serine was also detected in Elp1-KR9A mutant. The fact that the Elp1 basic region mutant has an elevated pool of phospho-1209-Elp1 compared with wild-type Elp1 is in line with the hypothesis that it could be trapped in a specific form.

The wild-type Elp1 showed a weak generic phosphorylated serine signal that was also detected in Elp1-1209A mutants. This is in agreement with other data from our lab in which other phosphorylation sites have also been mapped (Figure 1.11); Ser-1209 is not the sole phosphorylation site in Elp1. The increase in phosphorylated serine observed in Elp1-KR9A could be due to the increased phosphorylation at ser-1209 alone but it also possible that other phosphorylation sites are affected. Mutation of ser-1209 to a phosphomimetic aspartic acid residue (Elp1-1209D) results in partial Zymocin sensitivity and so restores some functionality (Abdel-Fattah and Stark, unpublished). This suggests that this phosphorylation site could perhaps serve to activate the complex or prime phosphorylation at other surrounding sites. The increased phosphorylation at this site in Elp1-KR9A could therefore also be occurring as a compensatory mechanism for lack of Elongator function.

In the Elp1-1209A mutant, Kti12 association with Elongator is increased and this may be a general trend that occurs when Elp1 is in a 'hypo' phosphorylated state, since deletion or mutation of the Hrr25 kinase also causes Elp1 'hypo' phosphorylation and increased Kti12 association(Mehlgarten et al., 2009). Deletion of *KTI12* results in Elp1 'hypo' phosphorylation and disrupts the ability of Hrr25 to associate with Elongator. In contrast Elp1-KR9A shows increased phosphorylation and a reduced Kti12 association.

It is not yet understood which kinases may act on the Elp1 C-terminus but previous work suggests that although both Kti12 and Hrr25 influence this there must also be other factors that impinge on Elp1 phosphorylation. When *KTI12* and *SIT4* are both expressed in multicopy, a wild-type balance of Elp1 phospho-forms is observed and this is also the case in strains with a simultaneous Hrr25 kinase dead allele and *SIT4* deletion. To fit with these observations it was therefore suggested that Kti12 and

Hrr25 may act to down-regulate Sit4 function in order to maintain a balance of phosphorylation on the Elp1 subunit (Mehlgarten et al., 2009). It is possible that Kti12 could bind to Sit4 directly and inhibit its function and this may underlie the 'hyper' and 'hypo' phosphorylation of Elp1 in multicopy *KTI12* and *kti12* deletion strains, respectively (Jablonowski et al., 2004). It would be interesting to test whether 'hyper' phosphorylation caused by a deletion of Sit4 would also lead to reduced Kti12 association with Elp1 as was observed in Elp1-KR9A. The Sit4 phosphatase may also be less associated with the Elp1-KR9A mutant and this may underlie the increased phosphorylation assayed in this mutant.

A speculative model for the complex interplay between Kti12 and Elp1 phosphorylation may explain some of the observations so far made in our lab and in the literature. Elp1 dephosphorylation at certain sites may cause a conformational change that allows it to bind a tRNA molecule. Once tRNA is bound to the complex, Kti12 may then be released from Elongator, at which point Elp1 undergoes phosphorylation at certain sites, thereby preventing further Kti12 association. Kti12 may mediate Sit4 activity to regulate its own binding and release from the complex and other kinases, such as Hrr25 may also impinge on this. In this model balanced phosphorylation regulates the mechanism of tRNA binding and modification by Elongator and mutations that disrupt a part of this cycle could cause stalling in certain forms. This assumes that Elongator is a highly dynamic complex that undergoes multiple conformational changes for the binding, modification and release of tRNA.

It is also possible that certain phosphorylation sites serve to activate or inactivate the function of the complex rather than cycling between phosphorylated and dephosphorylated states as part of the mechanism. The pattern of phosphorylation

could promote or enhance the association of accessory factors to increase the efficiency of tRNA modification. The balanced forms seen in the wild-type Elp1 may represent various states and all or nothing disruption of this balance causes dysfunction.

The Elp1 basic region may also be required for a conformational change that involves interaction between this positively charged region and the upstream phosphorylation sites when they are phosphorylated and hence negatively charged. This may be intimately involved in the mechanism of tRNA binding and release and/or regulation of the tRNA modification reaction. By extension, it is possible that Elp1 binds to tRNA when upstream phosphorylation sites are dephosphorylated and releases tRNA when the region becomes highly phosphorylated. Testing this hypothesis would require a better knowledge of the interplay between Elp1 C-terminal phosphorylation sites. Determining whether the basic region may be involved in more extensive conformational changes during the mechanism of tRNA modification would likely require structural studies.

The complex interplay between different phosphorylation sites in the Elp1 subunit and the role of the various accessory factor proteins is as of yet still elusive (see Figure 1.10 and 1.11). However, there is a clear interplay between the Elp1 basic region mutations and phosphorylation at the functionally important ser-1209 site.

6.6 Conditional regulation of Elongator function using Elp1 "switch off" strains

We and others have demonstrated that the C-terminal domain of Elp1 is important for tRNA wobble uridine modification (Fichtner et al., 2003, Mehlgarten et al., 2009). This was utilised to create strains in which Elongator function could be "switched off" either by conditional cleavage of the Elp1 C-terminal domain by TEV protease or by using the auxin inducible degron system to direct Elp1 for conditional proteosomal degradation. These strains will allow real time analysis of the timescale for loss of tRNA modifications and the acute changes in protein translation that are expected to occur as a result.

The loss of mcm^5 and ncm^5 modifications due to lack of Elongator function has been shown not to affect the steady state stability of the tRNA molecule, so it is expected that the hypomodified tRNAs will persist but have reduced function in translation (Bjork et al., 2007). It is not known how quickly the modifications will begin to disappear once Elongator function is lost since it is thought that tRNAs have an extremely long half-life in the cell (Hopper and Phizicky, 2003). A time course experiment of Elp1 degradation coupled to analysis of modified tRNA nucleosides will allow the levels of these Elongator dependent modifications to be monitored in real-time. Information as to how long after Elongator "switch off" the modifications are no longer detected will direct future experiments, where the aim would be to assay acute changes in protein expression occurring due to defects in the translational function of hypomodified tRNAs. Protein expression changes can be monitored by SILAC coupled mass spectrometry to identify changes in protein levels, while ribosome profiling can be used to determine which mRNAs may spend an increased amount of time being

translated compared to wild-type strains (Ong et al., 2002, Ingolia et al., 2009). These datasets can be compared to corresponding mRNA expression to account for transcriptional changes and then the patterns of codon usage across mRNAs showing a translational defect could be studied.

It is expected that mRNAs enriched in AAA or CAA codons, that are translated by $tRNA^{Lys}_{UUU}$ and $tRNA^{Gln}_{UUG}$ respectively, will be enriched in mRNAs where expression is down-regulated because the hypomodified versions of these tRNAs can rescue nearly all phenotypes associated with Elongator dysfunction assayed so far (Esberg et al., 2006). Other work that has begun to address the translational defects associated with Elongator has assayed these types of codon bias in proteins that rely on Elongator for their expression (Bauer et al., 2012, Fernandez-Vazquez et al., 2013, Rezgui et al., 2013).

Certain changes in protein expression may be masked in chronically adapted strains where an Elongator subunit has been deleted due to up-regulation of other pathways or transcriptional changes that compensate for any translational defects. It has been suggested that defects in charging of hypomodified tRNAs may be masked in Elongator deletion strains by increased expression of their charging enzymes and that hypomodified tRNAs may also impinge on cellular signalling pathways directly contributing to phenotypes arising from lack of modifications, although how this is mediated is not yet understood (Zinshteyn and Gilbert, 2013). Investigating the turnover and acute affects occurring due to lack of Elongator dependent tRNA modifications may help address this and other changes that are masked in Elongator deletion strains by secondary effects or adaptations.

Elongator function could conceivably be regulated, such as by phosphorylation, as a means of modulating gene expression. Our lab has already mapped functionally important sites within the C-terminus of Elp1 (Figure 1.11). Knowledge of the timescale for turnover of tRNA modifications upon loss of Elongator function would give a better idea of how Elongator regulation might be utilised *in vivo*. For example if tRNA modifications were undetectable within a short timescale then Elongator could be regulated dynamically, for example by nutrient availability or extracellular signals. This means that kinases and phosphatases upstream of Elongator may regulate tRNA modifications in response to changing conditions in order to cause translational changes that affect the proteome. This may allow certain mRNAs to be translated normally under normal growth conditions but be primed for translational inefficiency under conditions where Elongator dependent tRNA modifications are decreased. If tRNA modifications are quite persistent once Elongator function is lost then it is also still possible that this type of regulation may function in longer-term scenarios such as during certain growth phases, and in higher eukaryotes may be relevant to developmental stages.

6.7 The Elp1 basic region is required for tRNA binding

Since the Elp1 basic region is essential to the function of the Elongator complex but is not involved in nuclear import, it seemed possible that it could be required for interaction with tRNA. The basic residues lysine and arginine are commonly known to be involved in interactions with nucleic acids and this region was annotated using BindN, which predicts putative RNA binding regions from primary sequence based on mathematical modelling with known RNA-protein structures (Nadassy et al., 1999, Draper, 1999, Jones et al., 2001, Wang and Brown, 2006)

Although it is not yet known if Elongator is involved directly in tRNA modification it seems likely that this is the primary role of the complex at least in yeast (Esberg et al., 2006, Huang et al., 2005). Purified Elongator was previously shown to bind ssRNA *in vitro* with a higher affinity than linear dsDNA, suggesting that the complex possessed RNA binding domains or motifs (Gilbert et al., 2004, Greenwood et al., 2009). More recently it was shown that immunoprecipitated Elp1 and Elp3 subunits can be crosslinked to exogenous $tRNA^{Glu}_{UUC}$ and that the recombinant Elp4-6 hexamer forms a complex with tRNA in EMSA assays (Huang et al., 2005, Glatt et al., 2012).

The discovery that the Elp4-6 hexamer can bind tRNA is the first major evidence that Elongator is directly involved in tRNA modifications. The small subcomplex binds tRNA only when all three subunits are present, therefore the binding determinants for tRNA are formed across the subunit interfaces. The complex has a calculated K_D for tRNA binding of 1.2-1.4 μM and does not form a complex with poly(U) or ssDNA. The interaction with tRNA is competed by addition of tRNA anticodon loop, suggesting that this region of the tRNA contains all or part of the recognition sites for the hexamer (Glatt et al., 2012). In general members of the RecA-like NTPase superfamily bind

nucleic acids using positively charged binding surfaces within the central ring of the hexamer (Lyubimov et al., 2011). The Elp4-6 hexamer does not contain a similar binding surface, but mutation of two amino acids within a protruding loop in Elp5 reduced tRNA binding to the hexamer (Glatt et al., 2012). This suggests a different mechanism for binding to the tRNA anticodon loop that does not rely on charge interactions, although other subunits of Elongator may contribute to this *in vivo*. Interestingly, the Elp4-6 hexamer was shown to bind $tRNA^{Glu}$ with a similar affinity regardless of the identity of the base at the wobble position of the anticodon loop. This suggests that the specificity for wobble uridine modification may be imparted during the modification reaction itself rather than by discriminatory binding to Elongator. The Elp4-6 hexamer also has a basal ATPase activity, which has been proposed to regulate tRNA binding and release coupled to dynamic movement of this subcomplex (Glatt et al., 2012).

The recombinant C-terminal domain of Elp1 and Elp1-KR9A was purified for use in EMSA binding assays with yeast tRNA in order to determine firstly whether Elp1 was involved in tRNA binding and secondly whether the Elp1 basic region was required for this. The wild-type Elp1 C-terminal domain formed a complex with yeast tRNA but this ability was lost in the Elp1-KR9A mutant. We propose that the conversed Elp1 basic region is involved in binding tRNA molecules to the Elongator complex.

Preliminary work calculated that the K_D of the Elp1 C-terminal domain and tRNA complex is in the low micromolar range (~0.37 μM) and demonstrated that this complex is resistant to competition from ssDNA and poly(U). The complex formed between the wild-type Elp1 C-terminal domain and tRNA appears quite large (~130 kDa would be expected for 1:1 complex of Elp1 fusion protein and tRNA) since it is

poorly resolved in 4% polyacrylamide gels. However, migration in a native gel is not directly related to the molecular mass of protein or complex, factors such as the overall charge and mass of a complex will affect this (Hellman and Fried, 2007). It seems likely that Elp1 could bind to tRNA as a dimeric complex, since we and others have shown association between differentially tagged Elp1 proteins *in vivo*, and our work has suggested this occurs directly through the C-terminal domain. In order to confirm that the native Elp1 C-terminus is associated as a dimer we could use crosslinking and native gel electrophoresis to determine whether a ladder of dimeric and monomeric Elp1 can be observed. Stoichiometry of binding experiments could also be carried out using a known concentration of unlabelled tRNA mixed with a small amount of radiolabelled tRNA for binding reactions with the Elp1 C-terminal domain. The molar ratio of protein/RNA equivalents required to saturate the shift in the radiolabelled pool can be used to estimate the stoichiometry of binding by fitting the % bound curve to theoretical saturation curves (Ryder et al., 2008).

Although we have shown that the Elp1 C-terminal domain in isolation associates with tRNA, it seems likely that other subunits may also contribute to the overall affinity and specificity of the Elongator complex, especially in view of the data presented by Glatt and coworkers. Competition experiments with different regions of a tRNA molecule such as the anticodon loop, the DHU loop and the TΨC loop (see figure 1.4) will be used to determine which region of the molecule interacts with Elp1. It might be expected that the Elp1 C-terminus binds to a part of the tRNA molecule distinct from that which interacts with the Elp4-6 hexamer in order to anchor it within the complex. However, although speculative, it is also possible that the flexible Elp1 C-terminus may bind tRNA and translocate it into an Elongator reaction centre where Elp3 is likely to be involved in the modification. In this scenario, Elp1 could be involved in imparting

some specificity to the modification reaction by discriminating between the anticodon loops of different tRNA species.

The Elp1 basic region must contribute important binding determinants to the interaction with tRNA since mutations that replace the positively charged amino acids across this sequence disrupt tRNA binding. It has been shown that arginine and lysine residues are enriched in nucleic acid binding motifs and that these amino acids can make multiple types of interactions with nucleic acids, including electrostatic contacts with the negatively charged sugar phosphate backbone (Jones et al., 2001, Draper, 1999). It is difficult based on primary structure to predict exactly what types of interactions are lost in Elp1-KR9A since protein and nucleic acid binding can typically rely on electrostatic interactions, hydrogen bonding and van der Waals forces between amino acids, nucleotide bases and the sugar phosphate backbone. The secondary structure of RNA also creates more diverse interaction surfaces for proteins than is typically found in DNA so the types of contacts made are not easily predicted (Jones et al., 2001, Draper, 1999). It is still also possible that an alteration in the secondary structure of Elp1-KR9A could contribute to loss of tRNA binding. However, the Elp1 basic region resides across the junction between a region of random coli and alpha-helix in the predicted Elp1 secondary structure (see Figure. 1.2) and the mutations in Elp1-KR9A do not alter this prediction.

To determine whether the Elp1 basic region disrupts tRNA binding *in vivo*, Elp1 and Elp1-KR9A were pulled down and associated RNAs analysed by northern blot. Wild-type Elp1 co-precipitated $tRNA^{Gln}_{UUG}$ whereas only background levels were detected in association with Elp1-KR9A. The basic region therefore appears to be important for tRNA binding to Elongator *in vivo*. To test specificity of the association of wild-type

Elp1 with tRNA, co-precipitation of $tRNA^{Lys}_{CUU}$, which is not a substrate for Elongator-dependent modification, was also assayed. The wild-type Elp1 still showed enrichment for this non-substrate tRNA, suggesting that association is not specific for Elongator-dependent tRNAs under our conditions. This may support the hypothesis suggested by Glatt and co-workers, that specificity may be mediated once tRNA is bound to the complex rather than by discriminatory binding, but more work is required to confirm this.

Although preliminary, the loss of tRNA association with Elp1-KR9A *in vivo* supports the importance of this region for the association of tRNA with Elongator and suggests that other subunits cannot compensate for loss of this region. In the future to address the same question, pulldowns of Elongator and crosslinking to exogenous tRNA could be carried out in an analogous manner to the experiments carried out by Byström and co-workers (Huang et al., 2005) to confirm whether the reported association with tRNA is lost in Elp1-KR9A.

Taken together, we have shown that the Elp1 basic region is required for tRNA binding to the C-terminal domain of Elp1 and therefore forms a highly conserved tRNA binding motif in Elongator.

6.8 Perspectives and future work

The Elp1 subunit of Elongator contains a highly conserved C-terminal basic region and this work has shown that this is essential for wobble uridine tRNA modification. This region was previously annotated as a nuclear localisation sequence but in the context of the full length Elp1 polypeptide does not influence its distribution. The Elp1 basic region is also not required for the overall assembly of Elongator but mutations in this domain do cause increased phosphorylation at a functionally important upstream serine. The wild-type Elp1 C-terminal domain forms a complex with tRNA that is disrupted by mutation of residues in the basic region, suggesting that the true role of this region is in tRNA binding.

Future work will be directed towards identifying the binding determinants within the tRNA molecule that are important for interaction with the Elp1 and attempting to address whether this binding shows any specificity towards substrate tRNAs containing a uridine at the wobble position. It seems likely that the Elp1 C-terminal domain associates as a dimer and that this may create an interface for the binding of tRNA. Although more work is required to confirm this, if Elp1 does dimerise directly through the C-terminal domain then in the future the determinants for this can be analysed by mutational analysis. This will allow us to address whether this dimerization is essential for tRNA binding.

Since the Elp1 basic region is important for tRNA association this could explain some of the other differences observed in the Elp1-KR9A mutant when compared with wild-type Elp1. A defect in tRNA binding to Elongator would be expected to arrest the mechanism of the complex, which is in line with the hypothesis that the Elp1-KR9A mutant protein may be trapped in a specific form that alters its interactions with other

subunits and accessory factors. The modification of tRNA by Elongator may proceed by dynamic alterations in conformation that transiently alter subunit contacts and interactions with accessory factors. In this scenario the wild-type Elp1 would be expected to cycle between different conformations during the mechanism of tRNA binding, modification and release. The Elp1-KR9A mutant is assembled into Elongator but cannot bind tRNA and so it may be trapped in a substrate binding-incompetent form. This could explain the decreased association with Kti12 and Elp5 if the complex was less stable without bound tRNA or if it makes tighter transient associations with these proteins later in the modification reaction. If phosphorylation is also involved in driving this mechanism then this could also account for the increased ser-1209 phosphorylation observed in the basic region mutant. A better understanding of how Elongator interacts with tRNA and the interplay of this with accessory factors and Elp1 phosphorylation would help to clarify this model.

Since Kti12 association is reduced in the Elp1-KR9A mutant then it would be interesting to determine whether Kti11 and Kti13 are also similarly affected. Since phosphorylation of Elp1-KR9A is increased it seems possible that the activity of Sit4 phosphatase could also be misregulated. Kti12 has been hypothesised to regulate the activity of Sit4 perhaps by direct association with the phosphatase or its SAP binding partners. Analysing the associations of Sit4, Hrr25 and Kti12 with each other and with this basic region mutant may reveal more about the interplay between these factors.

Another hypothesis which has not yet been tested is that Kti12 may itself bind and/or modify tRNA molecules, perhaps alongside Kti11 and Kti13 and could bring them to the Elongator complex for further modification. Kti12 has an N-terminal P-loop motif and is closely related to O-phosphoseryl-tRNA^{sec} kinase (PSTK), which has both a kinase

activity and binds to tRNA (Araiso et al., 2009). Interestingly, PSTK acts as a dimer, which might imply that Kti12 could adopt a similar conformation although this is speculative. The accessory proteins Kti11 and 13 may also be involved in the activation of the tRNA before modification by Elongator. Kti11 has a zinc finger motif which is often found in nucleic acid binding proteins and Kti13 has been suggested to act as GEF protein which may regulate the function of Kti12 (Chen and Varani, 2005, Fichtner and Schaffrath, 2002). In order to study what other Elongator subunits or accessory factors may be involved in tRNA binding, recombinant proteins could be made and similar analysis of complex formation by EMSA carried out. It would be especially interesting to determine whether Kti12 participates in tRNA modifications directly or as a regulator of Elongator.

The mechanism of cm^5 tRNA modification at the wobble uridine position still remains to be determined, though the Radical SAM and HAT domains of Elp3 are expected to be involved. An interesting finding in this work was that two SAM metabolic enzymes that could participate in this mechanism were identified in association with Elp1. This would require further work to confirm whether it represents a true association before any further studies to determine how these may impinge on Elongator function. More work is also needed to understand the function of Elp1 C-terminal domain phosphorylation since a balance between different phosphorylated forms appears to be essential. The interplay between certain phosphorylation sites and other putative kinases that may impinge on them is currently under investigation in our lab.

A summary of the complex regulation of the Elongator complex illustrating the known functional interactions and factors important for Elongator function is presented in Figure 6.1. The work presented in this thesis has contributed to this by demonstrating

that the Elp1 C-terminal domain contains a conserved basic region that is essential for the wobble uridine tRNA modification function of the Elongator complex and that this is likely to be mediated by its role as a tRNA binding region.

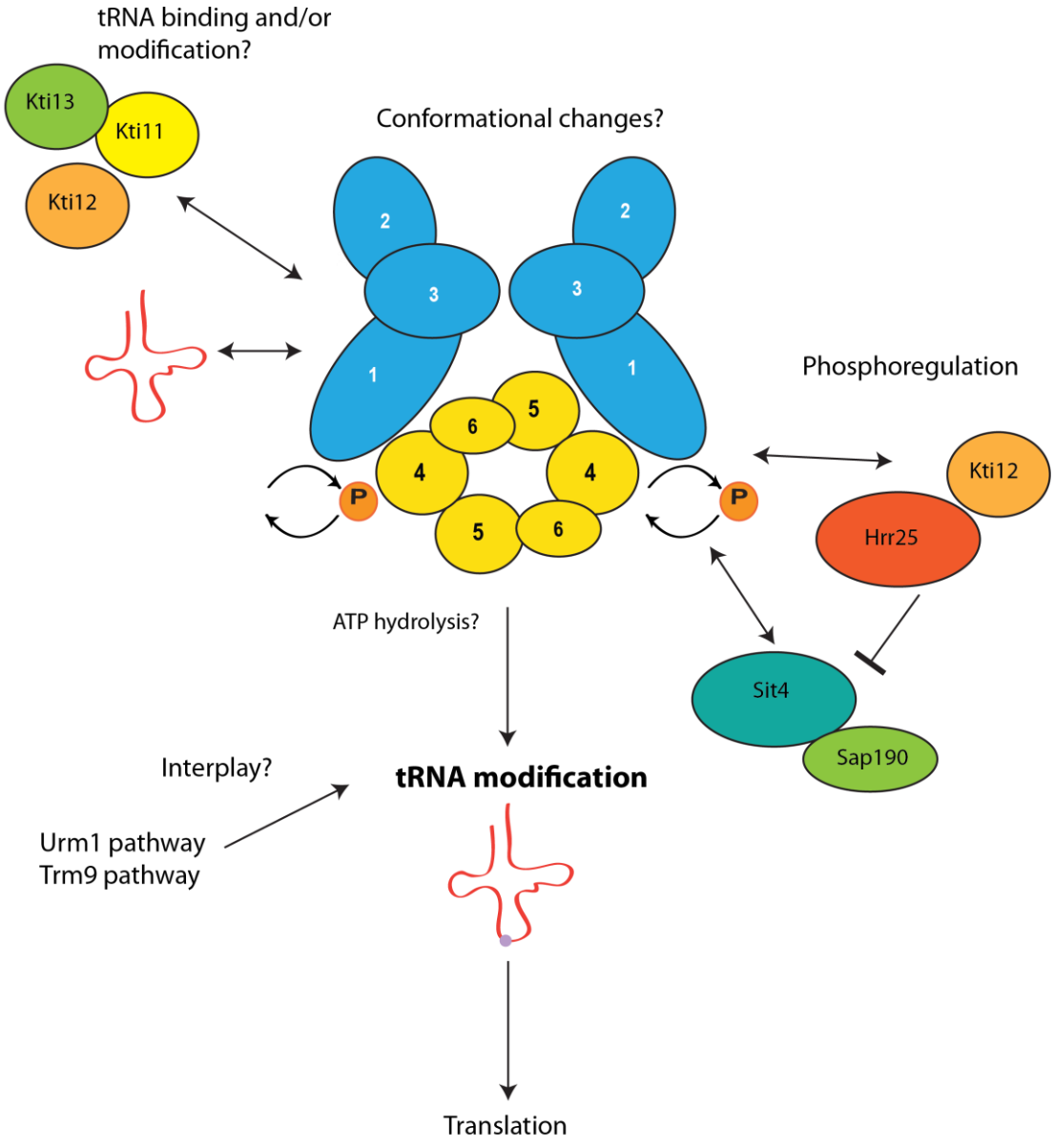

Figure 6.1: The complex regulation of the yeast Elongator complex. Double headed arrows denote putative transient associations with substrate tRNA and accessory factors and orange balls denote Elp1 phosphorylation. Note that the Elongator cartoon shown is not representative of the exact contacts between all subunits.

References

AGARWALLA, S., KEALEY, J. T., SANTI, D. V. & STROUD, R. M. 2002. Characterization of the 23 S ribosomal RNA m5U1939 methyltransferase from Escherichia coli. *J Biol Chem,* 277**,** 8835-40.

AGRIS, P. F. 2008. Bringing order to translation: the contributions of transfer RNA anticodon-domain modifications. *EMBO reports,* 9**,** 629-35.

AGRIS, P. F., VENDEIX, F. A. & GRAHAM, W. D. 2007. tRNA's wobble decoding of the genome: 40 years of modification. *J Mol Biol,* 366**,** 1-13.

AKELLA, J. S., WLOGA, D., KIM, J., STAROSTINA, N. G., LYONS-ABBOTT, S., MORRISSETTE, N. S., DOUGAN, S. T., KIPREOS, E. T. & GAERTIG, J. 2010. MEC-17 is an alpha-tubulin acetyltransferase. *Nature,* 467**,** 218-22.

ALBERTS, B. 2008. How Cells Read the Genome: From DNA to Protein. *Molecular biology of the cell.* 5th ed. New York: Garland Science.

ALLAN, C., BUREL, J. M., MOORE, J., BLACKBURN, C., LINKERT, M., LOYNTON, S., MACDONALD, D., MOORE, W. J., NEVES, C., PATTERSON, A., PORTER, M., TARKOWSKA, A., LORANGER, B., AVONDO, J., LAGERSTEDT, I., LIANAS, L., LEO, S., HANDS, K., HAY, R. T., PATWARDHAN, A., BEST, C., KLEYWEGT, G. J., ZANETTI, G. & SWEDLOW, J. R. 2012. OMERO: flexible, model-driven data management for experimental biology. *Nature methods,* 9**,** 245-53.

AMANN, E., BROSIUS, J. & PTASHNE, M. 1983. Vectors bearing a hybrid trp-lac promoter useful for regulated expression of cloned genes in Escherichia coli. *Gene,* 25**,** 167-78.

AMBERG, D. C., BURKE, D. & STRATHERN, J. N. 2005. *Methods in yeast genetics: a Cold Spring Harbor Laboratory course manual*, Cold Spring Harbor Laboratory Pr.

ANDERSON, S. L., COLI, R., DALY, I. W., KICHULA, E. A., RORK, M. J., VOLPI, S. A., EKSTEIN, J. & RUBIN, B. Y. 2001. Familial dysautonomia is caused by mutations of the IKAP gene. *Am J Hum Genet,* 68**,** 753-8.

ANGELES DE LA TORRE-RUIZ, M., TORRES, J., ARINO, J. & HERRERO, E. 2002. Sit4 is required for proper modulation of the biological functions mediated by Pkc1 and the cell integrity pathway in Saccharomyces cerevisiae. *J Biol Chem,* 277**,** 33468-76.

ANTON, B. P., SALEH, L., BENNER, J. S., RALEIGH, E. A., KASIF, S. & ROBERTS, R. J. 2008. RimO, a MiaB-like enzyme, methylthiolates the universally conserved Asp88 residue of ribosomal protein S12 in Escherichia coli. *Proc Natl Acad Sci U S A,* 105**,** 1826-31.

ARAISO, Y., SHERRER, R. L., ISHITANI, R., HO, J. M., SOLL, D. & NUREKI, O. 2009. Structure of a tRNA-dependent kinase essential for selenocysteine decoding. *Proc Natl Acad Sci U S A,* 106**,** 16215-20.

ARNDT, K. T., STYLES, C. A. & FINK, G. R. 1989. A suppressor of a HIS4 transcriptional defect encodes a protein with homology to the catalytic subunit of protein phosphatases. *Cell,* 56**,** 527-37.

BAR, C., ZABEL, R., LIU, S., STARK, M. J. & SCHAFFRATH, R. 2008. A versatile partner of eukaryotic protein complexes that is involved in multiple biological processes: Kti11/Dph3. *Mol Microbiol,* 69**,** 1221-33.

BASAVAPPA, R. & SIGLER, P. B. 1991. The 3 A crystal structure of yeast initiator tRNA: functional implications in initiator/elongator discrimination. *Embo J,* 10**,** 3105-11.

BAUER, F. & HERMAND, D. 2012. A coordinated codon-dependent regulation of translation by Elongator. *Cell cycle,* 11**,** 4524-9.

BAUER, F., MATSUYAMA, A., CANDIRACCI, J., DIEU, M., SCHELIGA, J., WOLF, D. A., YOSHIDA, M. & HERMAND, D. 2012. Translational control of cell division by Elongator. *Cell reports,* 1**,** 424-33.

BEGLEY, U., DYAVAIAH, M., PATIL, A., ROONEY, J. P., DIRENZO, D., YOUNG, C. M., CONKLIN, D. S., ZITOMER, R. S. & BEGLEY, T. J. 2007. Trm9-catalyzed tRNA modifications link translation to the DNA damage response. *Mol Cell,* 28**,** 860-70.

BERG, J. M., TYMOCZKO, J. L. & STRYER, L. 2007. Protein Synthesis. *Biochemistry.* 6th ed. New York: W. H. Freeman.

BJÖRK, G. R. 1995. Biosynthesis and function of modified nucleosides. *In:* SÖLL, D. & RAJBHANDARY, U. (eds.) *tRNA : structure, biosynthesis, and function*

Washington, D.C.: ASM Press.

BJORK, G. R., HUANG, B., PERSSON, O. P. & BYSTROM, A. S. 2007. A conserved modified wobble nucleoside (mcm5s2U) in lysyl-tRNA is required for viability in yeast. *Rna,* 13**,** 1245-55.

BREKER, M., GYMREK, M. & SCHULDINER, M. 2013. A novel single-cell screening platform reveals proteome plasticity during yeast stress responses. *The Journal of cell biology,* 200**,** 839-50.

BUTLER, A. R., O'DONNELL, R. W., MARTIN, V. J., GOODAY, G. W. & STARK, M. J. 1991a. Kluyveromyces lactis toxin has an essential chitinase activity. *Eur J Biochem,* 199**,** 483-8.

BUTLER, A. R., PORTER, M. & STARK, M. J. 1991b. Intracellular expression of Kluyveromyces lactis toxin gamma subunit mimics treatment with exogenous toxin and distinguishes two classes of toxin-resistant mutant. *Yeast,* 7**,** 617-25.

BUTLER, A. R., WHITE, J. H., FOLAWIYO, Y., EDLIN, A., GARDINER, D. & STARK, M. 1994. Two Saccharomyces cerevisiae genes which control sensitivity to G1 arrest induced by Kluyveromyces lactis toxin. *Mol Cell Biol,* 14**,** 6306.

BUTLER, A. R., WHITE, J. H. & STARK, M. J. 1991c. Analysis of the response of Saccharomyces cerevisiae cells to Kluyveromyces lactis toxin. *Journal of general microbiology,* 137**,** 1749-57.

CAREY, M. F., PETERSON, C. L. & SMALE, S. T. 2012. Experimental strategies for the identification of DNA-binding proteins. *Cold Spring Harbor protocols,* 2012**,** 18-33.

CHAN, C. T., DYAVAIAH, M., DEMOTT, M. S., TAGHIZADEH, K., DEDON, P. C. & BEGLEY, T. J. 2010. A quantitative systems approach reveals dynamic control of tRNA modifications during cellular stress. *PLoS Genet,* 6**,** e1001247.

CHEISHVILI, D., MAAYAN, C., COHEN-KUPIEC, R., LEFLER, S., WEIL, M., AST, G. & RAZIN, A. 2011. IKAP/Elp1 involvement in cytoskeleton regulation and implication for familial dysautonomia. *Hum Mol Genet,* 20**,** 1585-94.

CHEN, C., HUANG, B., ANDERSON, J. T. & BYSTROM, A. S. 2011a. Unexpected accumulation of ncm(5)U and ncm(5)S(2) (U) in a trm9 mutant suggests an additional step in the synthesis of mcm(5)U and mcm(5)S(2)U. *PloS one,* 6**,** e20783.

CHEN, C., HUANG, B., ELIASSON, M., RYDEN, P. & BYSTROM, A. S. 2011b. Elongator complex influences telomeric gene silencing and DNA damage response by its role in wobble uridine tRNA modification. *PLoS Genet,* 7**,** e1002258.

CHEN, C., TUCK, S. & BYSTROM, A. S. 2009a. Defects in tRNA modification associated with neurological and developmental dysfunctions in Caenorhabditis elegans elongator mutants. *PLoS Genet,* 5**,** e1000561.

CHEN, Y. & VARANI, G. 2005. Protein families and RNA recognition. *The FEBS journal,* 272**,** 2088-97.

CHEN, Y. T., HIMS, M. M., SHETTY, R. S., MULL, J., LIU, L., LEYNE, M. & SLAUGENHAUPT, S. A. 2009b. Loss of mouse Ikbkap, a subunit of elongator, leads to transcriptional deficits and embryonic lethality that can be rescued by human IKBKAP. *Mol Cell Biol,* 29**,** 736-44.

CHINENOV, Y. 2002. A second catalytic domain in the Elp3 histone acetyltransferases: a candidate for histone demethylase activity? *Trends in biochemical sciences,* 27**,** 115-7.

CLOSE, P., EAST, P., DIRAC-SVEJSTRUP, A. B., HARTMANN, H., HERON, M., MASLEN, S., CHARIOT, A., SODING, J., SKEHEL, M. & SVEJSTRUP, J. Q. 2012a. DBIRD complex integrates alternative mRNA splicing with RNA polymerase II transcript elongation. *Nature,* 484**,** 386-9.

CLOSE, P., GILLARD, M., LADANG, A., JIANG, Z., PAPUGA, J., HAWKES, N., NGUYEN, L., CHAPELLE, J. P., BOUILLENNE, F., SVEJSTRUP, J., FILLET, M. & CHARIOT, A. 2012b. DERP6 (ELP5) and C3ORF75 (ELP6) regulate tumorigenicity and migration of melanoma cells as subunits of Elongator. *J Biol Chem,* 287**,** 32535-45.

CLOSE, P., HAWKES, N., CORNEZ, I., CREPPE, C., LAMBERT, C. A., ROGISTER, B., SIEBENLIST, U., MERVILLE, M. P., SLAUGENHAUPT, S. A., BOURS, V., SVEJSTRUP, J. Q. & CHARIOT, A. 2006. Transcription impairment and cell migration defects in elongator-depleted cells: implication for familial dysautonomia. *Mol Cell,* 22**,** 521-31.

COCHELLA, L., BRUNELLE, J. L. & GREEN, R. 2007. Mutational analysis reveals two independent molecular requirements during transfer RNA selection on the ribosome. *Nature structural & molecular biology,* 14**,** 30-6.

COLLIER, R. J. 2001. Understanding the mode of action of diphtheria toxin: a perspective on progress during the 20th century. *Toxicon : official journal of the International Society on Toxinology,* 39**,** 1793-803.

COLLUM, R. G., BRUTSAERT, S., LEE, G. & SCHINDLER, C. 2000. A Stat3-interacting protein (StIP1) regulates cytokine signal transduction. *Proc Natl Acad Sci U S A,* 97**,** 10120-5.

CREPPE, C., MALINOUSKAYA, L., VOLVERT, M. L., GILLARD, M., CLOSE, P., MALAISE, O., LAGUESSE, S., CORNEZ, I., RAHMOUNI, S., ORMENESE, S., BELACHEW, S., MALGRANGE, B., CHAPELLE, J. P., SIEBENLIST, U., MOONEN, G., CHARIOT, A. & NGUYEN, L. 2009. Elongator controls the migration and differentiation of cortical neurons through acetylation of alpha-tubulin. *Cell,* 136**,** 551-64.

CRICK, F. H. 1966. Codon--anticodon pairing: the wobble hypothesis. *J Mol Biol,* 19**,** 548-55.

CUAJUNGCO, M. P., LEYNE, M., MULL, J., GILL, S. P., LU, W., ZAGZAG, D., AXELROD, F. B., MAAYAN, C., GUSELLA, J. F. & SLAUGENHAUPT, S. A. 2003. Tissue-specific reduction in splicing efficiency of IKBKAP due to the major mutation associated with familial dysautonomia. *Am J Hum Genet,* 72**,** 749-58.

DEFRAIA, C. & MOU, Z. 2011. The role of the Elongator complex in plants. *Plant signaling & behavior,* 6**,** 19-22.

DEPHOURE, N., HOWSON, R. W., BLETHROW, J. D., SHOKAT, K. M. & O'SHEA, E. K. 2005. Combining chemical genetics and proteomics to identify protein kinase substrates. *Proc Natl Acad Sci U S A,* 102**,** 17940-5.

DI COMO, C. J. & ARNDT, K. T. 1996. Nutrients, via the Tor proteins, stimulate the association of Tap42 with type 2A phosphatases. *Genes & development,* 10**,** 1904-16.

DINGWALL, C. & LASKEY, R. A. 1986. Protein import into the cell nucleus. *Annual review of cell biology,* 2**,** 367-90.

DOUVILLE, J., DAVID, J., FORTIER, P. K. & RAMOTAR, D. 2004. The yeast phosphotyrosyl phosphatase activator protein, yPtpa1/Rrd1, interacts with Sit4 phosphatase to mediate resistance to 4-nitroquinoline-1-oxide and UVA. *Curr Genet,* 46**,** 72-81.

DRAPER, D. E. 1999. Themes in RNA-protein recognition. *J Mol Biol,* 293**,** 255-70.

ESBERG, A., HUANG, B., JOHANSSON, M. J. & BYSTROM, A. S. 2006. Elevated levels of two tRNA species bypass the requirement for elongator complex in transcription and exocytosis. *Mol Cell,* 24**,** 139-48.

FELLOWS, J., ERDJUMENT-BROMAGE, H., TEMPST, P. & SVEJSTRUP, J. Q. 2000. The Elp2 subunit of elongator and elongating RNA polymerase II holoenzyme is a WD40 repeat protein. *J Biol Chem,* 275**,** 12896-9.

FERNANDEZ-VAZQUEZ, J., VARGAS-PEREZ, I., SANSO, M., BUHNE, K., CARMONA, M., PAULO, E., HERMAND, D., RODRIGUEZ-GABRIEL, M., AYTE, J., LEIDEL, S. & HIDALGO, E. 2013. Modification of tRNA(Lys) UUU by Elongator Is Essential for Efficient Translation of Stress mRNAs. *PLoS Genet,* 9**,** e1003647.

FICHTNER, L., FROHLOFF, F., BURKNER, K., LARSEN, M., BREUNIG, K. D. & SCHAFFRATH, R. 2002a. Molecular analysis of KTI12/TOT4, a Saccharomyces cerevisiae gene required for Kluyveromyces lactis zymocin action. *Mol Microbiol,* 43**,** 783-91.

FICHTNER, L., FROHLOFF, F., JABLONOWSKI, D., STARK, M. J. & SCHAFFRATH, R. 2002b. Protein interactions within Saccharomyces cerevisiae Elongator, a complex essential for Kluyveromyces lactis zymocicity. *Mol Microbiol,* 45**,** 817-26.

FICHTNER, L., JABLONOWSKI, D., SCHIERHORN, A., KITAMOTO, H. K., STARK, M. J. & SCHAFFRATH, R. 2003. Elongator's toxin-target (TOT) function is nuclear localization sequence dependent and suppressed by post-translational modification. *Mol Microbiol,* 49**,** 1297-307.

FICHTNER, L. & SCHAFFRATH, R. 2002. KTI11 and KTI13, Saccharomyces cerevisiae genes controlling sensitivity to G1 arrest induced by Kluyveromyces lactis zymocin. *Mol Microbiol,* 44**,** 865-75.

FISCHER, U., HUBER, J., BOELENS, W. C., MATTAJ, I. W. & LUHRMANN, R. 1995. The HIV-1 Rev activation domain is a nuclear export signal that accesses an export pathway used by specific cellular RNAs. *Cell,* 82**,** 475-83.

FORNEROD, M., OHNO, M., YOSHIDA, M. & MATTAJ, I. W. 1997. CRM1 is an export receptor for leucine-rich nuclear export signals. *Cell,* 90**,** 1051-60.

FREY, P. A., HEGEMAN, A. D. & RUZICKA, F. J. 2008. The Radical SAM Superfamily. *Critical reviews in biochemistry and molecular biology,* 43**,** 63-88.

FRITZ, C. C. & GREEN, M. R. 1996. HIV Rev uses a conserved cellular protein export pathway for the nucleocytoplasmic transport of viral RNAs. *Current biology : CB,* 6**,** 848-54.

FROHLOFF, F., FICHTNER, L., JABLONOWSKI, D., BREUNIG, K. D. & SCHAFFRATH, R. 2001. Saccharomyces cerevisiae Elongator mutations confer resistance to the Kluyveromyces lactis zymocin. *Embo J,* 20**,** 1993-2003.

FROHLOFF, F., JABLONOWSKI, D., FICHTNER, L. & SCHAFFRATH, R. 2003. Subunit communications crucial for the functional integrity of the yeast RNA polymerase II elongator (gamma-toxin target (TOT)) complex. *J Biol Chem,* 278**,** 956-61.

FU, D., BROPHY, J. A., CHAN, C. T., ATMORE, K. A., BEGLEY, U., PAULES, R. S., DEDON, P. C., BEGLEY, T. J. & SAMSON, L. D. 2010. Human AlkB homolog ABH8 Is a tRNA methyltransferase required for wobble uridine modification and DNA damage survival. *Mol Cell Biol,* 30**,** 2449-59.

GARDINER, J., BARTON, D., MARC, J. & OVERALL, R. 2007. Potential role of tubulin acetylation and microtubule-based protein trafficking in familial dysautonomia. *Traffic,* 8**,** 1145-9.

GE HEALTHCARE, L. S. 2012. GST Gene Fusion System.

GIETZ, R. D. & AKIO, S. 1988. New yeast-Escherichia coli shuttle vectors constructed with in vitro mutagenized yeast genes lacking six-base pair restriction sites. *Gene,* 74**,** 527-534.

GIETZ, R. D. & WOODS, R. A. 2002. Transformation of yeast by lithium acetate/single-stranded carrier DNA/polyethylene glycol method. *Methods in enzymology,* 350**,** 87-96.

GILBERT, C., KRISTJUHAN, A., WINKLER, G. S. & SVEJSTRUP, J. Q. 2004. Elongator interactions with nascent mRNA revealed by RNA immunoprecipitation. *Mol Cell,* 14**,** 457-64.

GLATT, S., LETOQUART, J., FAUX, C., TAYLOR, N. M., SERAPHIN, B. & MULLER, C. W. 2012. The Elongator subcomplex Elp456 is a hexameric RecA-like ATPase. *Nature structural & molecular biology,* 19**,** 314-20.

GLATT, S. & MULLER, C. W. 2013. Structural insights into Elongator function. *Current opinion in structural biology,* 23**,** 235-42.

GOEHRING, A. S., RIVERS, D. M. & SPRAGUE, G. F., JR. 2003. Urmylation: a ubiquitin-like pathway that functions during invasive growth and budding in yeast. *Mol Biol Cell,* 14**,** 4329-41.

GOLD-VON SIMSON, G. & AXELROD, F. B. 2006. Familial dysautonomia: update and recent advances. *Current problems in pediatric and adolescent health care,* 36**,** 218-37.

GRANT, T. D., LUFT, J. R., WOLFLEY, J. R., SNELL, M. E., TSURUTA, H., CORRETORE, S., QUARTLEY, E., PHIZICKY, E. M., GRAYHACK, E. J. & SNELL, E. H. 2013. The Structure of Yeast Glutaminyl-tRNA Synthetase and Modeling of Its Interaction with tRNA. *J Mol Biol*.

GRANT, T. D., SNELL, E. H., LUFT, J. R., QUARTLEY, E., CORRETORE, S., WOLFLEY, J. R., SNELL, M. E., HADD, A., PERONA, J. J., PHIZICKY, E. M. & GRAYHACK, E. J. 2012. Structural conservation of an ancient tRNA sensor in eukaryotic glutaminyl-tRNA synthetase. *Nucleic Acids Res,* 40**,** 3723-31.

GREENWOOD, C., SELTH, L. A., DIRAC-SVEJSTRUP, A. B. & SVEJSTRUP, J. Q. 2009. An iron-sulfur cluster domain in Elp3 important for the structural integrity of elongator. *J Biol Chem,* 284**,** 141-9.

GROVE, T. L., BENNER, J. S., RADLE, M. I., AHLUM, J. H., LANDGRAF, B. J., KREBS, C. & BOOKER, S. J. 2011. A radically different mechanism for S-adenosylmethionine-dependent methyltransferases. *Science,* 332**,** 604-7.

HAWKES, N. A., OTERO, G., WINKLER, G. S., MARSHALL, N., DAHMUS, M. E., KRAPPMANN, D., SCHEIDEREIT, C., THOMAS, C. L., SCHIAVO, G., ERDJUMENT-BROMAGE, H., TEMPST, P. & SVEJSTRUP, J. Q. 2002. Purification and characterization of the human elongator complex. *J Biol Chem,* 277**,** 3047-52.

HELLMAN, L. M. & FRIED, M. G. 2007. Electrophoretic mobility shift assay (EMSA) for detecting protein-nucleic acid interactions. *Nature protocols,* 2**,** 1849-61.

HINNEBUSCH, A. G. 2005. Translational regulation of GCN4 and the general amino acid control of yeast. *Annual review of microbiology,* 59**,** 407-50.

HO, Y., GRUHLER, A., HEILBUT, A., BADER, G. D., MOORE, L., ADAMS, S. L., MILLAR, A., TAYLOR, P., BENNETT, K., BOUTILIER, K., YANG, L., WOLTING, C., DONALDSON, I., SCHANDORFF, S., SHEWNARANE, J., VO, M., TAGGART, J., GOUDREAULT, M., MUSKAT, B., ALFARANO, C., DEWAR, D., LIN, Z., MICHALICKOVA, K., WILLEMS, A. R., SASSI, H., NIELSEN, P. A., RASMUSSEN, K. J., ANDERSEN, J. R., JOHANSEN, L. E., HANSEN, L. H., JESPERSEN, H., PODTELEJNIKOV, A., NIELSEN, E., CRAWFORD, J., POULSEN, V., SORENSEN, B. D., MATTHIESEN, J., HENDRICKSON, R. C., GLEESON, F., PAWSON, T., MORAN, M. F., DUROCHER, D., MANN, M., HOGUE, C. W., FIGEYS, D. & TYERS, M. 2002. Systematic identification of protein complexes in Saccharomyces cerevisiae by mass spectrometry. *Nature,* 415**,** 180-3.

HO, Y., MASON, S., KOBAYASHI, R., HOEKSTRA, M. & ANDREWS, B. 1997. Role of the casein kinase I isoform, Hrr25, and the cell cycle-regulatory transcription factor, SBF, in the transcriptional response to DNA damage in Saccharomyces cerevisiae. *Proc Natl Acad Sci U S A,* 94**,** 581-6.

HOEKSTRA, M. F., DHILLON, N., CARMEL, G., DEMAGGIO, A. J., LINDBERG, R. A., HUNTER, T. & KURET, J. 1994. Budding and fission yeast casein kinase I isoforms have dual-specificity protein kinase activity. *Mol Biol Cell,* 5**,** 877-86.

HOLMBERG, C., KATZ, S., LERDRUP, M., HERDEGEN, T., JAATTELA, M., ARONHEIM, A. & KALLUNKI, T. 2002. A novel specific role for I kappa B kinase complex-associated protein in cytosolic stress signaling. *J Biol Chem,* 277**,** 31918-28.

HOPPER, A. K. & PHIZICKY, E. M. 2003. tRNA transfers to the limelight. *Genes & development,* 17**,** 162-80.

HORVATH, A. & RIEZMAN, H. 1994. Rapid protein extraction from Saccharomyces cerevisiae. *Yeast,* 10**,** 1305-1310.

HUANG, B., JOHANSSON, M. J. & BYSTROM, A. S. 2005. An early step in wobble uridine tRNA modification requires the Elongator complex. *Rna,* 11**,** 424-36.

HUANG, B., LU, J. & BYSTROM, A. S. 2008. A genome-wide screen identifies genes required for formation of the wobble nucleoside 5-methoxycarbonylmethyl-2-thiouridine in Saccharomyces cerevisiae. *Rna,* 14**,** 2183-94.

HUH, W. K., FALVO, J. V., GERKE, L. C., CARROLL, A. S., HOWSON, R. W., WEISSMAN, J. S. & O'SHEA, E. K. 2003. Global analysis of protein localization in budding yeast. *Nature,* 425**,** 686-91.

INGOLIA, N. T., GHAEMMAGHAMI, S., NEWMAN, J. R. & WEISSMAN, J. S. 2009. Genome-wide analysis in vivo of translation with nucleotide resolution using ribosome profiling. *Science,* 324**,** 218-23.

JABLONOWSKI, D., BUTLER, A. R., FICHTNER, L., GARDINER, D., SCHAFFRATH, R. & STARK, M. J. 2001a. Sit4p protein phosphatase is required for sensitivity of Saccharomyces cerevisiae to Kluyveromyces lactis zymocin. *Genetics,* 159**,** 1479-89.

JABLONOWSKI, D., FICHTNER, L., MARTIN, V. J., KLASSEN, R., MEINHARDT, F., STARK, M. J. & SCHAFFRATH, R. 2001b. Saccharomyces cerevisiae cell wall chitin, the Kluyveromyces lactis zymocin receptor. *Yeast,* 18**,** 1285-99.

JABLONOWSKI, D., FICHTNER, L., STARK, M. J. & SCHAFFRATH, R. 2004. The yeast elongator histone acetylase requires Sit4-dependent dephosphorylation for toxin-target capacity. *Mol Biol Cell,* 15**,** 1459-69.

JABLONOWSKI, D., TAUBERT, J. E., BAR, C., STARK, M. J. & SCHAFFRATH, R. 2009. Distinct subsets of Sit4 holophosphatases are required for inhibition of Saccharomyces cerevisiae growth by rapamycin and zymocin. *Eukaryot Cell,* 8**,** 1637-47.

JABLONOWSKI, D., ZINK, S., MEHLGARTEN, C., DAUM, G. & SCHAFFRATH, R. 2006. tRNAGlu wobble uridine methylation by Trm9 identifies Elongator's key role for zymocin-induced cell death in yeast. *Mol Microbiol,* 59**,** 677-88.

JOHANSEN, L. D., NAUMANEN, T., KNUDSEN, A., WESTERLUND, N., GROMOVA, I., JUNTTILA, M., NIELSEN, C., BOTTZAUW, T., TOLKOVSKY, A., WESTERMARCK, J., COFFEY, E. T., JAATTELA, M. & KALLUNKI, T. 2008. IKAP localizes to membrane ruffles with filamin A and regulates actin cytoskeleton organization and cell migration. *Journal of cell science,* 121**,** 854-64.

JOHANSSON, M. J., ESBERG, A., HUANG, B., BJORK, G. R. & BYSTROM, A. S. 2008. Eukaryotic wobble uridine modifications promote a functionally redundant decoding system. *Mol Cell Biol,* 28**,** 3301-12.

JONA, G., WITTSCHIEBEN, B. O., SVEJSTRUP, J. Q. & GILEADI, O. 2001. Involvement of yeast carboxy-terminal domain kinase I (CTDK-I) in transcription elongation in vivo. *Gene,* 267**,** 31-6.

JONES, S., DALEY, D. T., LUSCOMBE, N. M., BERMAN, H. M. & THORNTON, J. M. 2001. Protein-RNA interactions: a structural analysis. *Nucleic Acids Res,* 29**,** 943-54.

KAFADAR, K. A., ZHU, H., SNYDER, M. & CYERT, M. S. 2003. Negative regulation of calcineurin signaling by Hrr25p, a yeast homolog of casein kinase I. *Genes & development,* 17**,** 2698-708.

KALHOR, H. R. & CLARKE, S. 2003. Novel methyltransferase for modified uridine residues at the wobble position of tRNA. *Mol Cell Biol,* 23**,** 9283-92.

KAPLAN, D. L. & O'DONNELL, M. 2003. Rho factor: transcription termination in four steps. *Current biology : CB,* 13**,** R714-6.

KAPP, L. D., KOLITZ, S. E. & LORSCH, J. R. 2006. Yeast initiator tRNA identity elements cooperate to influence multiple steps of translation initiation. *Rna,* 12**,** 751-64.

KELLOGG, D. R. & MURRAY, A. W. 1995. NAP1 acts with Clb1 to perform mitotic functions and to suppress polar bud growth in budding yeast. *The Journal of cell biology,* 130**,** 675-85.

KIM, J. H., LANE, W. S. & REINBERG, D. 2002. Human Elongator facilitates RNA polymerase II transcription through chromatin. *Proc Natl Acad Sci U S A,* 99**,** 1241-6.

KIRKPATRICK, D. & SOLOMON, F. 1994. Overexpression of yeast homologs of the mammalian checkpoint gene RCC1 suppresses the class of alpha-tubulin mutations that arrest with excess microtubules. *Genetics,* 137**,** 381-92.

KONG, S. E., KOBOR, M. S., KROGAN, N. J., SOMESH, B. P., SOGAARD, T. M., GREENBLATT, J. F. & SVEJSTRUP, J. Q. 2005. Interaction of Fcp1 phosphatase with elongating RNA polymerase II holoenzyme, enzymatic mechanism of action, and genetic interaction with elongator. *J Biol Chem,* 280**,** 4299-306.

KOSUGI, S., HASEBE, M., MATSUMURA, N., TAKASHIMA, H., MIYAMOTO-SATO, E., TOMITA, M. & YANAGAWA, H. 2009a. Six classes of nuclear localization signals specific to different binding grooves of importin alpha. *J Biol Chem,* 284**,** 478-85.

KOSUGI, S., HASEBE, M., TOMITA, M. & YANAGAWA, H. 2009b. Systematic identification of cell cycle-dependent yeast nucleocytoplasmic shuttling proteins by prediction of composite motifs. *Proc Natl Acad Sci U S A,* 106**,** 10171-6.

KOUSKOUTI, A. & TALIANIDIS, I. 2005. Histone modifications defining active genes persist after transcriptional and mitotic inactivation. *Embo J,* 24**,** 347-57.

KROGAN, N. J. & GREENBLATT, J. F. 2001. Characterization of a six-subunit holo-elongator complex required for the regulated expression of a group of genes in Saccharomyces cerevisiae. *Mol Cell Biol,* 21**,** 8203-12.

KROGAN, N. J., KIM, M., AHN, S. H., ZHONG, G., KOBOR, M. S., CAGNEY, G., EMILI, A., SHILATIFARD, A., BURATOWSKI, S. & GREENBLATT, J. F. 2002. RNA polymerase II elongation factors of Saccharomyces cerevisiae: a targeted proteomics approach. *Mol Cell Biol,* 22**,** 6979-92.

LANGE, A., MILLS, R. E., LANGE, C. J., STEWART, M., DEVINE, S. E. & CORBETT, A. H. 2007. Classical nuclear localization signals: definition, function, and interaction with importin alpha. *J Biol Chem,* 282**,** 5101-5.

LAXMAN, S., SUTTER, B. M., WU, X., KUMAR, S., GUO, X., TRUDGIAN, D. C., MIRZAEI, H. & TU, B. P. 2013. Sulfur Amino Acids Regulate Translational Capacity and Metabolic Homeostasis through Modulation of tRNA Thiolation. *Cell,* 154**,** 416-29.

LAXMAN, S. & TU, B. P. 2011. Multiple TORC1-associated proteins regulate nitrogen starvation-dependent cellular differentiation in Saccharomyces cerevisiae. *PloS one,* 6**,** e26081.

LEE, G., PAPAPETROU, E. P., KIM, H., CHAMBERS, S. M., TOMISHIMA, M. J., FASANO, C. A., GANAT, Y. M., MENON, J., SHIMIZU, F., VIALE, A., TABAR, V., SADELAIN, M. & STUDER, L. 2009. Modelling pathogenesis and treatment of familial dysautonomia using patient-specific iPSCs. *Nature,* 461**,** 402-6.

LEIDEL, S., PEDRIOLI, P. G., BUCHER, T., BROST, R., COSTANZO, M., SCHMIDT, A., AEBERSOLD, R., BOONE, C., HOFMANN, K. & PETER, M. 2009. Ubiquitin-related modifier Urm1 acts as a sulphur carrier in thiolation of eukaryotic transfer RNA. *Nature,* 458**,** 228-32.

LI, F., LU, J., HAN, Q., ZHANG, G. & HUANG, B. 2005. The Elp3 subunit of human Elongator complex is functionally similar to its counterpart in yeast. *Mol Genet Genomics,* 273**,** 264-72.

LI, Q., FAZLY, A. M., ZHOU, H., HUANG, S., ZHANG, Z. & STILLMAN, B. 2009. The elongator complex interacts with PCNA and modulates transcriptional silencing and sensitivity to DNA damage agents. *PLoS Genet,* 5**,** e1000684.

LIM, V. I. 1994. Analysis of action of wobble nucleoside modifications on codon-anticodon pairing within the ribosome. *J Mol Biol,* 240**,** 8-19.

LIN, F. J., SHEN, L., JANG, C. W., FALNES, P. O. & ZHANG, Y. 2013. Ikbkap/Elp1 deficiency causes male infertility by disrupting meiotic progression. *PLoS Genet,* 9**,** e1003516.

LIU, S., BACHRAN, C., GUPTA, P., MILLER-RANDOLPH, S., WANG, H., CROWN, D., ZHANG, Y., WEIN, A. N., SINGH, R., FATTAH, R. & LEPPLA, S. H. 2012. Diphthamide modification on eukaryotic elongation factor 2 is needed to

assure fidelity of mRNA translation and mouse development. *Proc Natl Acad Sci U S A,* 109**,** 13817-22.

LIU, S., MILNE, G. T., KUREMSKY, J. G., FINK, G. R. & LEPPLA, S. H. 2004. Identification of the proteins required for biosynthesis of diphthamide, the target of bacterial ADP-ribosylating toxins on translation elongation factor 2. *Mol Cell Biol,* 24**,** 9487-97.

LIU, S., WIGGINS, J. F., SREENATH, T., KULKARNI, A. B., WARD, J. M. & LEPPLA, S. H. 2006. Dph3, a small protein required for diphthamide biosynthesis, is essential in mouse development. *Mol Cell Biol,* 26**,** 3835-41.

LONGTINE, M. S., MCKENZIE 3RD, A., DEMARINI, D. J., SHAH, N. G., WACH, A., BRACHAT, A., PHILIPPSEN, P. & PRINGLE, J. R. 1998. Additional modules for versatile and economical PCR-based gene deletion and modification in Saccharomyces cerevisiae. *Yeast (Chichester, England),* 14**,** 953.

LOPEZ-MIRABAL, H. R., WINTHER, J. R. & KIELLAND-BRANDT, M. C. 2008. Oxidant resistance in a yeast mutant deficient in the Sit4 phosphatase. *Curr Genet,* 53**,** 275-86.

LU, J., HUANG, B., ESBERG, A., JOHANSSON, M. J. & BYSTROM, A. S. 2005. The Kluyveromyces lactis gamma-toxin targets tRNA anticodons. *Rna,* 11**,** 1648-54.

LUKE, M. M., DELLA SETA, F., DI COMO, C. J., SUGIMOTO, H., KOBAYASHI, R. & ARNDT, K. T. 1996. The SAP, a new family of proteins, associate and function positively with the SIT4 phosphatase. *Mol Cell Biol,* 16**,** 2744-55.

LYUBIMOV, A. Y., STRYCHARSKA, M. & BERGER, J. M. 2011. The nuts and bolts of ring-translocase structure and mechanism. *Current opinion in structural biology,* 21**,** 240-8.

MACARA, I. G. 2001. Transport into and out of the nucleus. *Microbiology and molecular biology reviews : MMBR,* 65**,** 570-94, table of contents.

MARMORSTEIN, R. 2001. Structure of histone acetyltransferases. *J Mol Biol,* 311**,** 433-44.

MCGUFFIN, L. J., BRYSON, K. & JONES, D. T. 2000. The PSIPRED protein structure prediction server. *Bioinformatics,* 16**,** 404-5.

MCGUIRE, A. T. & MANGROO, D. 2007. Cex1p is a novel cytoplasmic component of the Saccharomyces cerevisiae nuclear tRNA export machinery. *Embo J,* 26**,** 288-300.

MEHLGARTEN, C., JABLONOWSKI, D., BREUNIG, K. D., STARK, M. J. & SCHAFFRATH, R. 2009. Elongator function depends on antagonistic regulation by casein kinase Hrr25 and protein phosphatase Sit4. *Mol Microbiol,* 73**,** 869-81.

MEHLGARTEN, C., JABLONOWSKI, D., WRACKMEYER, U., TSCHITSCHMANN, S., SONDERMANN, D., JAGER, G., GONG, Z., BYSTROM, A. S., SCHAFFRATH, R. & BREUNIG, K. D. 2010. Elongator function in tRNA wobble uridine modification is conserved between yeast and plants. *Mol Microbiol,* 76**,** 1082-94.

MEHLGARTEN, C. & SCHAFFRATH, R. 2003. Mutant casein kinase I (Hrr25p/Kti14p) abrogates the G1 cell cycle arrest induced by Kluyveromyces lactiszymocin in budding yeast. *Molecular genetics and genomics : MGG,* 269**,** 188-96.

MEHLGARTEN, C. & SCHAFFRATH, R. 2004. After chitin docking, toxicity of Kluyveromyces lactis zymocin requires Saccharomyces cerevisiae plasma membrane H+-ATPase. *Cellular microbiology,* 6**,** 569-80.

MEHLGARTEN, C., ZINK, S., RUTTER, J. & SCHAFFRATH, R. 2007. Dosage suppression of the Kluyveromyces lactis zymocin by Saccharomyces cerevisiae ISR1 and UGP1. *FEMS yeast research,* 7**,** 722-30.

METIVIER, R., PENOT, G., HUBNER, M. R., REID, G., BRAND, H., KOS, M. & GANNON, F. 2003. Estrogen receptor-alpha directs ordered, cyclical, and combinatorial recruitment of cofactors on a natural target promoter. *Cell,* 115**,** 751-63.

MISKIEWICZ, K., JOSE, L. E., BENTO-ABREU, A., FISLAGE, M., TAES, I., KASPROWICZ, J., SWERTS, J., SIGRIST, S., VERSEES, W., ROBBERECHT, W. & VERSTREKEN, P. 2011. ELP3 controls active zone morphology by acetylating the ELKS family member Bruchpilot. *Neuron,* 72**,** 776-88.

MURPHY, F. V. T., RAMAKRISHNAN, V., MALKIEWICZ, A. & AGRIS, P. F. 2004. The role of modifications in codon discrimination by tRNA(Lys)UUU. *Nature structural & molecular biology,* 11**,** 1186-91.

NADASSY, K., WODAK, S. J. & JANIN, J. 1999. Structural features of protein-nucleic acid recognition sites. *Biochemistry,* 38**,** 1999-2017.

NELISSEN, H., DE GROEVE, S., FLEURY, D., NEYT, P., BRUNO, L., BITONTI, M. B., VANDENBUSSCHE, F., VAN DER STRAETEN, D., YAMAGUCHI, T., TSUKAYA, H., WITTERS, E., DE JAEGER, G., HOUBEN, A. & VAN LIJSEBETTENS, M. 2010. Plant Elongator regulates auxin-related genes during RNA polymerase II transcription elongation. *Proc Natl Acad Sci U S A,* 107**,** 1678-83.

NELISSEN, H., FLEURY, D., BRUNO, L., ROBLES, P., DE VEYLDER, L., TRAAS, J., MICOL, J. L., VAN MONTAGU, M., INZE, D. & VAN LIJSEBETTENS, M. 2005. The elongata mutants identify a functional Elongator complex in plants with a role in cell proliferation during organ growth. *Proc Natl Acad Sci U S A,* 102**,** 7754-9.

NGUYEN BA, A. N., POGOUTSE, A., PROVART, N. & MOSES, A. M. 2009. NLStradamus: a simple Hidden Markov Model for nuclear localization signal prediction. *BMC bioinformatics,* 10**,** 202.

NISHIMURA, K., FUKAGAWA, T., TAKISAWA, H., KAKIMOTO, T. & KANEMAKI, M. 2009. An auxin-based degron system for the rapid depletion of proteins in nonplant cells. *Nature methods,* 6**,** 917-22.

NOMA, A., SAKAGUCHI, Y. & SUZUKI, T. 2009. Mechanistic characterization of the sulfur-relay system for eukaryotic 2-thiouridine biogenesis at tRNA wobble positions. *Nucleic Acids Res,* 37**,** 1335-52.

OGLE, J. M., BRODERSEN, D. E., CLEMONS, W. M., JR., TARRY, M. J., CARTER, A. P. & RAMAKRISHNAN, V. 2001. Recognition of cognate transfer RNA by the 30S ribosomal subunit. *Science,* 292**,** 897-902.

OHIRA, T. & SUZUKI, T. 2011. Retrograde nuclear import of tRNA precursors is required for modified base biogenesis in yeast. *Proc Natl Acad Sci U S A,* 108**,** 10502-10507.

ONG, S. E., BLAGOEV, B., KRATCHMAROVA, I., KRISTENSEN, D. B., STEEN, H., PANDEY, A. & MANN, M. 2002. Stable isotope labeling by amino acids in cell culture, SILAC, as a simple and accurate approach to expression proteomics. *Molecular & cellular proteomics : MCP,* 1**,** 376-86.

OTERO, G., FELLOWS, J., LI, Y., DE BIZEMONT, T., DIRAC, A. M., GUSTAFSSON, C. M., ERDJUMENT-BROMAGE, H., TEMPST, P. & SVEJSTRUP, J. Q. 1999. Elongator, a multisubunit component of a novel RNA polymerase II holoenzyme for transcriptional elongation. *Mol Cell,* 3**,** 109-18.

PARASKEVOPOULOU, C., FAIRHURST, S. A., LOWE, D. J., BRICK, P. & ONESTI, S. 2006. The Elongator subunit Elp3 contains a Fe4S4 cluster and binds S-adenosylmethionine. *Mol Microbiol,* 59**,** 795-806.

PATIL, A., CHAN, C. T., DYAVAIAH, M., ROONEY, J. P., DEDON, P. C. & BEGLEY, T. J. 2012. Translational infidelity-induced protein stress results from a deficiency in Trm9-catalyzed tRNA modifications. *RNA biology,* 9**,** 990-1001.

PERCUDANI, R., PAVESI, A. & OTTONELLO, S. 1997. Transfer RNA gene redundancy and translational selection in Saccharomyces cerevisiae. *J Mol Biol,* 268**,** 322-30.

PETRAKIS, T. G., SOGAARD, T. M., ERDJUMENT-BROMAGE, H., TEMPST, P. & SVEJSTRUP, J. Q. 2005. Physical and functional interaction between Elongator and the chromatin-associated Kti12 protein. *J Biol Chem,* 280**,** 19454-60.

PETRAKIS, T. G., WITTSCHIEBEN, B. O. & SVEJSTRUP, J. Q. 2004. Molecular architecture, structure-function relationship, and importance of the Elp3 subunit for the RNA binding of holo-elongator. *J Biol Chem,* 279**,** 32087-92.

PETRONCZKI, M., MATOS, J., MORI, S., GREGAN, J., BOGDANOVA, A., SCHWICKART, M., MECHTLER, K., SHIRAHIGE, K., ZACHARIAE, W. & NASMYTH, K. 2006. Monopolar attachment of sister kinetochores at meiosis I requires casein kinase 1. *Cell,* 126**,** 1049-64.

PHIZICKY, E. M. & HOPPER, A. K. 2010a. tRNA biology charges to the front. *Genes & development,* 24**,** 1832-60.

PHIZICKY, E. M. & HOPPER, A. K. 2010b. tRNA biology charges to the front. *Genes & development,* 24**,** 1832.

PIERCE, J. B., ESWARA, M. B. & MANGROO, D. 2010. The ins and outs of nuclear re-export of retrogradely transported tRNAs in Saccharomyces cerevisiae. *Nucleus,* 1**,** 224-30.

PIERREL, F., DOUKI, T., FONTECAVE, M. & ATTA, M. 2004. MiaB protein is a bifunctional radical-S-adenosylmethionine enzyme involved in thiolation and methylation of tRNA. *J Biol Chem,* 279**,** 47555-63.

PLUTHERO, F. G. 1993. Rapid purification of high-activity Taq DNA polymerase. *Nucleic Acids Res,* 21**,** 4850-1.

POKHOLOK, D. K., HANNETT, N. M. & YOUNG, R. A. 2002. Exchange of RNA polymerase II initiation and elongation factors during gene expression in vivo. *Mol Cell,* 9**,** 799-809.

POLLARD, V. W. & MALIM, M. H. 1998. The HIV-1 Rev protein. *Annual review of microbiology,* 52**,** 491-532.

PONTING, C. P. 2002. Novel domains and orthologues of eukaryotic transcription elongation factors. *Nucleic Acids Res,* 30**,** 3643-52.

QIU, H., HU, C., ANDERSON, J., BJORK, G. R., SARKAR, S., HOPPER, A. K. & HINNEBUSCH, A. G. 2000. Defects in tRNA processing and nuclear export induce GCN4 translation independently of phosphorylation of the alpha subunit of eukaryotic translation initiation factor 2. *Mol Cell Biol,* 20**,** 2505-16.

QUINT, M. & GRAY, W. M. 2006. Auxin signaling. *Current opinion in plant biology,* 9**,** 448-53.

RAHL, P. B., CHEN, C. Z. & COLLINS, R. N. 2005. Elp1p, the yeast homolog of the FD disease syndrome protein, negatively regulates exocytosis independently of transcriptional elongation. *Mol Cell,* 17**,** 841-53.

RAY, P., BASU, U., RAY, A., MAJUMDAR, R., DENG, H. & MAITRA, U. 2008. The Saccharomyces cerevisiae 60 S ribosome biogenesis factor Tif6p is regulated by Hrr25p-mediated phosphorylation. *J Biol Chem,* 283**,** 9681-91.

REZGUI, V. A., TYAGI, K., RANJAN, N., KONEVEGA, A. L., MITTELSTAET, J., RODNINA, M. V., PETER, M. & PEDRIOLI, P. G. 2013. tRNA tKUUU, tQUUG, and tEUUC wobble

position modifications fine-tune protein translation by promoting ribosome A-site binding. *Proc Natl Acad Sci U S A,* 110**,** 12289-94.

ROTHBAUER, U., ZOLGHADR, K., MUYLDERMANS, S., SCHEPERS, A., CARDOSO, M. C. & LEONHARDT, H. 2008. A versatile nanotrap for biochemical and functional studies with fluorescent fusion proteins. *Molecular & cellular proteomics : MCP,* 7**,** 282-9.

RYDER, S. P., RECHT, M. I. & WILLIAMSON, J. R. 2008. Quantitative analysis of protein-RNA interactions by gel mobility shift. *Methods in molecular biology,* 488**,** 99-115.

SAMBROOK, J. & RUSSELL, D. W. 2001. *Molecular cloning: a laboratory manual*, Cold Spring Harbor Laboratory Press.

SAMBROOK, J. & RUSSELL, D. W. 2006. The inoue method for preparation and transformation of competent e. Coli: "ultra-competent" cells. *CSH protocols,* 2006.

SCHAFER, T., MACO, B., PETFALSKI, E., TOLLERVEY, D., BOTTCHER, B., AEBI, U. & HURT, E. 2006. Hrr25-dependent phosphorylation state regulates organization of the pre-40S subunit. *Nature,* 441**,** 651-5.

SELMER, M., DUNHAM, C. M., MURPHY, F. V. T., WEIXLBAUMER, A., PETRY, S., KELLEY, A. C., WEIR, J. R. & RAMAKRISHNAN, V. 2006. Structure of the 70S ribosome complexed with mRNA and tRNA. *Science,* 313**,** 1935-42.

SHERMAN, F. 2002. Getting started with yeast. *Methods in enzymology,* 350**,** 3-41.

SHERRER, R. L., O'DONOGHUE, P. & SOLL, D. 2008. Characterization and evolutionary history of an archaeal kinase involved in selenocysteinyl-tRNA formation. *Nucleic Acids Res,* 36**,** 1247-59.

SIMPSON, C. L., LEMMENS, R., MISKIEWICZ, K., BROOM, W. J., HANSEN, V. K., VAN VUGHT, P. W., LANDERS, J. E., SAPP, P., VAN DEN BOSCH, L., KNIGHT, J., NEALE, B. M., TURNER, M. R., VELDINK, J. H., OPHOFF, R. A., TRIPATHI, V. B., BELEZA, A., SHAH, M. N., PROITSI, P., VAN HOECKE, A., CARMELIET, P., HORVITZ, H. R., LEIGH, P. N., SHAW, C. E., VAN DEN BERG, L. H., SHAM, P. C., POWELL, J. F., VERSTREKEN, P., BROWN, R. H., JR., ROBBERECHT, W. & AL-CHALABI, A. 2009. Variants of the elongator protein 3 (ELP3) gene are associated with motor neuron degeneration. *Hum Mol Genet,* 18**,** 472-81.

SINGH, N., LORBECK, M. T., ZERVOS, A., ZIMMERMAN, J. & ELEFANT, F. 2010. The histone acetyltransferase Elp3 plays in active role in the control of synaptic bouton expansion and sleep in Drosophila. *Journal of neurochemistry,* 115**,** 493-504.

SLAUGENHAUPT, S. A., BLUMENFELD, A., GILL, S. P., LEYNE, M., MULL, J., CUAJUNGCO, M. P., LIEBERT, C. B., CHADWICK, B., IDELSON, M., REZNIK, L., ROBBINS, C., MAKALOWSKA, I., BROWNSTEIN, M., KRAPPMANN, D., SCHEIDEREIT, C., MAAYAN, C., AXELROD, F. B. & GUSELLA, J. F. 2001. Tissue-specific expression of a splicing mutation in the IKBKAP gene causes familial dysautonomia. *Am J Hum Genet,* 68**,** 598-605.

SMITH, D. B. & JOHNSON, K. S. 1988. Single-step purification of polypeptides expressed in Escherichia coli as fusions with glutathione S-transferase. *Gene,* 67**,** 31-40.

SOLINGER, J. A., PAOLINELLI, R., KLOSS, H., SCORZA, F. B., MARCHESI, S., SAUDER, U., MITSUSHIMA, D., CAPUANI, F., STURZENBAUM, S. R. & CASSATA, G. 2010. The Caenorhabditis elegans Elongator complex regulates neuronal alpha-tubulin acetylation. *PLoS Genet,* 6**,** e1000820.

STANSFIELD, I. A. S., M.J.R 2006. *Yeast Gene Analysis*, Academic Press.

STEITZ, T. A. 2008. A structural understanding of the dynamic ribosome machine. *Nature reviews. Molecular cell biology,* 9**,** 242-53.

STORICI, F. & RESNICK, M. A. 2006. The delitto perfetto approach to in vivo site-directed mutagenesis and chromosome rearrangements with synthetic oligonucleotides in yeast. *Methods Enzymol,* 409**,** 329-45.

STRUG, L. J., CLARKE, T., CHIANG, T., CHIEN, M., BASKURT, Z., LI, W., DORFMAN, R., BALI, B., WIRRELL, E., KUGLER, S. L., MANDELBAUM, D. E., WOLF, S. M., MCGOLDRICK, P., HARDISON, H., NOVOTNY, E. J., JU, J., GREENBERG, D. A., RUSSO, J. J. & PAL, D. K. 2009. Centrotemporal sharp wave EEG trait in rolandic epilepsy maps to Elongator Protein Complex 4 (ELP4). *Eur J Hum Genet,* 17**,** 1171-81.

STUDIER, F. W. 2005. Protein production by auto-induction in high density shaking cultures. *Protein expression and purification,* 41**,** 207-34.

STUDIER, F. W. & MOFFATT, B. A. 1986. Use of bacteriophage T7 RNA polymerase to direct selective high-level expression of cloned genes. *J Mol Biol,* 189**,** 113-30.

STUDTE, P., ZINK, S., JABLONOWSKI, D., BAR, C., VON DER HAAR, T., TUITE, M. F. & SCHAFFRATH, R. 2008. tRNA and protein methylase complexes mediate zymocin toxicity in yeast. *Mol Microbiol,* 69**,** 1266-77.

SUN, J., ZHANG, J., WU, F., XU, C., LI, S., ZHAO, W., WU, Z., WU, J., ZHOU, C. Z. & SHI, Y. 2005. Solution structure of Kti11p from Saccharomyces cerevisiae reveals a novel zinc-binding module. *Biochemistry,* 44**,** 8801-9.

SUTTON, A., IMMANUEL, D. & ARNDT, K. T. 1991. The SIT4 protein phosphatase functions in late G1 for progression into S phase. *Mol Cell Biol,* 11**,** 2133-48.

SVEJSTRUP, J. Q. 2007. Elongator complex: how many roles does it play? *Curr Opin Cell Biol,* 19**,** 331-6.

TAKANO, A., ENDO, T. & YOSHIHISA, T. 2005. tRNA actively shuttles between the nucleus and cytosol in yeast. *Science,* 309**,** 140-2.

TKACH, J. M., YIMIT, A., LEE, A. Y., RIFFLE, M., COSTANZO, M., JASCHOB, D., HENDRY, J. A., OU, J., MOFFAT, J., BOONE, C., DAVIS, T. N., NISLOW, C. & BROWN, G. W. 2012. Dissecting DNA damage response pathways by analysing protein localization and abundance changes during DNA replication stress. *Nature cell biology,* 14**,** 966-76.

TOKUNAGA, M., KAWAMURA, A. & HISHINUMA, F. 1989. Expression of pGKL killer 28K subunit in Saccharomyces cerevisiae: identification of 28K subunit as a killer protein. *Nucleic Acids Res,* 17**,** 3435-46.

TUMAITIS, T. D. & LANE, B. G. 1970. Differential labelling of the carboxymethyl and methyl substituents of 5-carboxymethyluridine methyl ester, a trace nucleoside constituent of yeast transfer RNA. *Biochimica et biophysica acta,* 224**,** 391-403.

VAN MULLEM, V., WERY, M., WERNER, M., VANDENHAUTE, J. & THURIAUX, P. 2002. The Rpb9 subunit of RNA polymerase II binds transcription factor TFIIE and interferes with the SAGA and elongator histone acetyltransferases. *J Biol Chem,* 277**,** 10220-5.

VERSEES, W., DE GROEVE, S. & VAN LIJSEBETTENS, M. 2010. Elongator, a conserved multitasking complex? *Mol Microbiol,* 76**,** 1065-9.

WALKER, J., KWON, S. Y., BADENHORST, P., EAST, P., MCNEILL, H. & SVEJSTRUP, J. Q. 2011. Role of elongator subunit Elp3 in Drosophila melanogaster larval development and immunity. *Genetics,* 187**,** 1067-75.

WALLIN, E. A. & MAENPAA, P. H. 1979. RNA polymerases from avian liver. Isolation and fractionation by heparin-sepharose chromatography. *Acta chemica Scandinavica. Series B: Organic chemistry and biochemistry,* 33**,** 519-27.

WANG, L. & BROWN, S. J. 2006. BindN: a web-based tool for efficient prediction of DNA and RNA binding sites in amino acid sequences. *Nucleic Acids Res,* 34**,** W243-8.

WATERHOUSE, A. M., PROCTER, J. B., MARTIN, D. M., CLAMP, M. & BARTON, G. J. 2009. Jalview Version 2--a multiple sequence alignment editor and analysis workbench. *Bioinformatics,* 25**,** 1189-91.

WEISS, J. N. 1997. The Hill equation revisited: uses and misuses. *FASEB J,* 11**,** 835-41.

WINKLER, G. S., KRISTJUHAN, A., ERDJUMENT-BROMAGE, H., TEMPST, P. & SVEJSTRUP, J. Q. 2002. Elongator is a histone H3 and H4 acetyltransferase important for normal histone acetylation levels in vivo. *Proc Natl Acad Sci U S A,* 99**,** 3517-22.

WINKLER, G. S., PETRAKIS, T. G., ETHELBERG, S., TOKUNAGA, M., ERDJUMENT-BROMAGE, H., TEMPST, P. & SVEJSTRUP, J. Q. 2001. RNA polymerase II elongator holoenzyme is composed of two discrete subcomplexes. *J Biol Chem,* 276**,** 32743-9.

WITTSCHIEBEN, B. O., FELLOWS, J., DU, W., STILLMAN, D. J. & SVEJSTRUP, J. Q. 2000. Overlapping roles for the histone acetyltransferase activities of SAGA and elongator in vivo. *Embo J,* 19**,** 3060-8.

WITTSCHIEBEN, B. O., OTERO, G., DE BIZEMONT, T., FELLOWS, J., ERDJUMENT-BROMAGE, H., OHBA, R., LI, Y., ALLIS, C. D., TEMPST, P. & SVEJSTRUP, J. Q. 1999. A novel histone acetyltransferase is an integral subunit of elongating RNA polymerase II holoenzyme. *Mol Cell,* 4**,** 123-8.

XU, D., HUANG, W., LI, Y., WANG, H., HUANG, H. & CUI, X. 2012. Elongator complex is critical for cell cycle progression and leaf patterning in Arabidopsis. *The Plant journal : for cell and molecular biology,* 69**,** 792-808.

YAN, F., LAMARRE, J. M., ROHRICH, R., WIESNER, J., JOMAA, H., MANKIN, A. S. & FUJIMORI, D. G. 2010. RlmN and Cfr are radical SAM enzymes involved in methylation of ribosomal RNA. *Journal of the American Chemical Society,* 132**,** 3953-64.

YARIAN, C., MARSZALEK, M., SOCHACKA, E., MALKIEWICZ, A., GUENTHER, R., MISKIEWICZ, A. & AGRIS, P. F. 2000. Modified nucleoside dependent Watson-Crick and wobble codon binding by tRNALysUUU species. *Biochemistry,* 39**,** 13390-5.

ZABEL, R., BAR, C., MEHLGARTEN, C. & SCHAFFRATH, R. 2008. Yeast alpha-tubulin suppressor Ats1/Kti13 relates to the Elongator complex and interacts with Elongator partner protein Kti11. *Mol Microbiol,* 69**,** 175-87.

ZHANG, W., ZHANG, J., XU, C., WANG, T., ZHANG, X. & TU, X. 2009. Solution structure of Urm1 from Trypanosoma brucei. *Proteins,* 75**,** 781-5.

ZINK, S., MEHLGARTEN, C., KITAMOTO, H. K., NAGASE, J., JABLONOWSKI, D., DICKSON, R. C., STARK, M. J. & SCHAFFRATH, R. 2005. Mannosyl-diinositolphospho-ceramide, the major yeast plasma membrane sphingolipid, governs toxicity of Kluyveromyces lactis zymocin. *Eukaryot Cell,* 4**,** 879-89.

ZINSHTEYN, B. & GILBERT, W. V. 2013. Loss of a Conserved tRNA Anticodon Modification Perturbs Cellular Signaling. *PLoS Genet,* 9**,** e1003675.

Appendix

Reagent List

[γ-^{32}P]ATP (6000Ci/mmol)	Perkin-Elmer
1-Naphthaleneacetic acid	Sigma-Aldrich
Acetic Acid	AnalaR NORMAPUR
Acetone	AnalaR NORMAPUR
AEBSF	Melford
Ampicillin	Formedium
Anarctic phosphatase	New England Biolabs
Antibodies	See Table 1.2
Beta mercaptoethanol	Sigma-Aldrich
Bis-Tris Gels	Novex
Bradford reagent	Pierce
Bromophenol Blue	Sigma-Aldrich
$CaCl_2$	AnalaR NORMAPUR
Concanavalin A	Sigma-Aldrich
Cyanogen bromide-activated-Sepharose 4B	GE Healthcare
Dialysis membrane	SpectoPOR
Dithiothreitol	Formedium
DNA gBlocks	Integrated DNA technologies
DNA Hyperladder I	Bioline
DNA Oligo primers and probes	Sigma-Aldrich
DNase I	Sigma-Aldrich
DNase I (RNAse free)	Fermentas
dNTPs	Fermentas
ECL	Millipore
EDTA	AnalaR NORMAPUR

Fast alkaline phosphatase	Fermentas
G418	Formedium
Galactose 20 %	Media Services
Gel extraction kit	QIAGEN
Gel pilot loading dye	QIAGEN
Glass beads 0.5 mm	Biospec products
Glucose 20 %	Media Services
Glutathione Sepharose-4 Fast Flow	GE Healthcare
Glycine	AnalaR NORMAPUR
Glycogen (RNase free)	Fermentas
HEPES	Formedium
Herring Sperm DNA	Sigma-Aldrich
HisPur Cobalt Resin	Thermo Scientific
Hydrochloric Acid	AnalaR NORMAPUR
Imidazole	Sigma-Aldrich
Instant Blue	Expedeon
Lithium Acetate	Sigma-Aldrich
Lithium Chloride 8M	Sigma-Aldrich
Lysozyme from egg white	Sigma-Aldrich
Methanol	AnalaR NORMAPUR
$MgCl_2$	Sigma-Aldrich
$MgCl_2$ 1 M (RNase free)	Ambion
MOPS 20 x	Novex
NuPage Antioxidant	Novex
Pefecthyb plus hybridisation buffer	Sigma-Aldrich
Phosphate buffered saline 10 x	Media Services
PhosSTOP tablets	Roche
Phusion DNA polymerase kit	Finnzymes
pJET1.2 vector kit	Fermentas

Plasmid purification kit	Bioline
Polyethylene Glycol	Sigma-Aldrich
Polyuridylic acid potassium salt	Sigma-Aldrich
Potassium Hydroxide	AnalaR NORMAPUR
Protease Inhibitor tablets (EDTA free)	Roche
Raffinose 20 %	Media Services
Rapamycin	Sigma-Aldrich
Rapid DNA ligation kit	Roche
Reduced Glutathione	Sigma-Aldrich
Restriction enzymes	New England Biolabs or Fermentas
Ribolock RNAse inhibitor	Fermentas
RNA Oligos	Integrated DNA technologies
Saline-sodium citrate (SSC) 20 x	Sigma-Aldrich
SDS	Sigma-Aldrich
Sepharose 4B beads	Sigma-Aldrich
Sodium acetate 3 M pH 5.5 (RNAse free)	Ambion
Sodium Carbonate	GPR RectaPur
Sodium Chloride 5M	Media Services
Sodium Fluoride	AnalaR NORMAPUR
Sodium Hydroxide	Sigma-Aldrich
Sodium Orthovanadate	Sigma-Aldrich
Sodium-Beta-Glycerophosphate	Alfa Aesar
SYBR safe	Invitrogen
SYPRO Ruby	Molecular Probes
T4 polynucleotide kinase kit	Fermentas
TAE 50 x	Media services
Taq Polymerase Buffer 10 x	Fermentas
TBE 10 x (Ultrapure)	Novex
TBE UREA loading dye 2x	Novex

TBE-Urea Gels	Novex
TE buffer (RNAse free)	Ambion
Thrombin from Bovine Plasma	Sigma-Aldrich
Tripure reagent	Roche
Tris Base	Calbiochem
Tris Buffered Saline 10 x	Media services
Triton-X100	VWR
Tween-20	VWR
Ultrapure Agarose	Invitrogen
Yeast tRNA	Sigma-Aldrich
Zymolyase-T	Seika gaku Corp

Primers and Probes used in this study

i) Primers for Gene Manipulation

Amplify *ELP1* Knockout cassette

ELP1 _F1

ATAGTAATGAAAAGCGATGCCTAGGCAAGAAACAGTACAAATGCCTAATGGCTTCGGATCCCCGGGTTAATTAA

ELP1 _R1

CTTTCTTTACGAGCACTATAGACAGTAATTTATATAACTAAGAAAATGGTATGCGAATTCGAGCTCGTTTAAAC

Amplify *KTI12* Knockout cassette

KTI12_A

AGTTGCAAATCATTATGTCATTCCT

KTI12_D

TCATAATAACCATCATAGCCAACCT

Amplified from Euroscarf knockout strain containing *kti12Δ*::KanMX4

Amplify region encoding Elp1 or Elp1 mutant CTD for cloning into pUG34 vector

ELP1Cterm_F

CACCACTAGTGAGAACCCATACGCCTTTTATGGC

ELP1Cterm_R

GCACCTCGAGAAAATGGTATGCTCAAAAATCAACAATATGACTCTTAGGGAAATC

Amplify CORE cassette for integration into *ELP1*

ELP1_P1_Cterm

GGTTTAGGCGAAGGTTTTGGTATAATTGCAGAATTACTCGCCGATTGTAAAGGCGAGCTCGTTTTCGACACTGG

ELP1_P2_Cterm

CAAAGTTCTTTTGAATTTGGTGAGCTTGCTCTCTCATGTTTCGTCTACAAAGACCCTCCTTACCATTAAGTTGATC

Amplify *ELP1* fragment for 'delitto perfetto'

ELP1_fragment_F

GCTTCTCTTGTGGCGATAAAGG

ELP1_fragment_R

TCTCTGGAACAGGTATTTCTGGG

Amplify region encoding Elp1 or Elp1 mutant CTD for cloning into pGEX4T-1

EcoR1_ELP1_F

GCTAGCGAATTCGCCACACGTGGTAATCTAGAAAC

ELP1_HIStag_Xho1_R

GTCACGATCTCGAGTTATCAATGGTGGTGGTGATGGTGAAAATCAACAATATGACTCTTAGGG

Amplify cassette for NIC96 tagging with 4mcherry

NIC96-4mcherry_ F

AGAATGCCAAGGGAAACGTACAGCACTTTAATTAATATAGACGTCTCTCTATACGCTGCAGGTCGACGG

NIC96-4mcherry_ R

GCGCATACTGATATATAGATATAAACAAAAATATACAATATTTAAAAAAAGAATTCGAGCTCGTTTAAA
C

Amplify cassette for Elp1 C-terminal tagging with GFP

ELP1-Linker-F2

CCCAGAAATACCTGTTCCAGAGATTCATGATTTCCCTAAGAGTCATATTGTTGATTTTGGTTCTGCTGGT
TCAGCTGCGGGTTCAGGACGGATCCCCGGGTTAATTAA

Amplify cassette for Elp1-HA C-terminal tagging with Auxin degron sequence

IAA17_F

CGTCCCGGACTATGCAGGATCCTATCCATATGACGTTCCAGATTACGCTCGTACGCTGCAGGTCGAC

IAA17_R

CTTTCTTTACGAGCACTATAGACAGTAATTTATATAACTAAGAAAATGGTATGCATCGATGAATTCGAGC
TCG

Amplify cassette for Arg4 C-terminal tagging with GFP

ARG4_L_F2

CGCTAAATCTGCTGTATTGAAGCAATTGGATAATTTGAAATCCCAATTAAATGGTTCTGCTGGTTCAGCT
GCGGGTTCAGGACGGATCCCCGGGTTAATTAA

ARG4_R1

GAAGTCCTAGAAGTACCAGACCTGATGAAATTCTTGCGCATAACGTCGCCATCTGGAATTCGAGCTCGTTTAAAC

Amplify cassette for Kti12 C-terminal tagging with GFP

KTI12_L_F2

GATCAAGATAGGATCGGTCCGCTTTTCGCTGATTATCTTAACAAAAACTTGAATGGTTCTGCTGGTTCAGCTGCGGGTTCAGGACGGATCCCCGGGTTAATTAA

KTI1212_R1

CAAGCAAATTTCGTCTTGCCATTTACCTTCTGATATTAATCACATGTATATCGAATTCGAGCTCGTTTAAAC

Amplify cassette for Elp5 C-terminal tagging with GFP

ELP5_F2

GAGTACGAAAAGGATGACGATTATGATGAAGAGGATCCATATGAGGATCCCTTTGGTTCTGCTGGTTCAGCTGCGGGTTCAGGACGGATCCCCGGGTTAATTAA

ELP5_R1

CGTAGTTTACATAATCTGGAAGCACTCACTATTTACCATCAGTTTCTACTTTGAATTCGAGCTCGTTTAAAC

Amplify cassette for Elp3 C-terminal tagging with GFP

ELP3_L_F2

CTATGGTAAACTAGGATATGAACTAGACGGTCCATACATGTCGAAAAGAATTGGTTCTGCTGGTTCAGCTGCGGGTTCAGGACGGATCCCCGGGTTAATTAA

ELP3_R1

CTGCTTGGAAAACCGGCCATGTCGGCGGCACATAAAAGTTCTATTTACCTGAATTCGAGCTCGTTTAAAC

ii) <u>Primers for Verification of Strains</u>

Verify *ELP1* Knockout

ELP1_A

CTGTTAAAAGATCCCGTCATTGATA

KO10

CGCACGTCAAGACTGTC

Verify *KTI12* Knockout

KTI12_D

TCATAATAACCATCATAGCCAACCT

RDS_KanMX_R

GCCTCTTCCGACCATCA

Verify CORE cassette integration into *ELP1*

PELP1R

GGGAAATCATGAATCTCTGG

KO10

CGCACGTCAAGACTGTC

ELP1SEQ3

GATGGCGTGAGGCCATGTCC

KanMX_R

GCCTCTTCCGACCATCA

Verify *ELP1* 'delitto perfetto' replacement of CORE

Elp1_Verfication_F

CCAGAGGAAGTTGAGTCAGTCGC

Elp1_ Verfication_R

GATTGTGTGGACAGGTAATGGTTG

ELP1_D

CTAAAGGATATTGCCAGAACTCAAA

Verify Nic96-4mcherry C-terminal tagging

NIC96_C

ACGAAGACGGCAGAATATATGATAG

NatR_B

TGGTGAAGGACCCATCCAG

Verify Elp1-HA C-terminal tagging with Auxin degron sequence

0080_NAT1-5 (kind gift from Tomo Tanaka)

TGGAGGTCACCAACGTCAAC

0595_ELP1_D

CTAAAGGATATTGCCAGAACTCAAA

ELP1_C

TTATATCCCAGAAATACCTGTTCCA

NatR_B

TGGTGAAGGACCCATCCAG

Verify integration of TIR1-9myc at the ADH1 locus

ADH1_A

GAAGAGGAAACAGCAATAGGG

TIR1_R

GAAGCTGAAGATGTGCTCCAC

RDS_Int_F

CAAACCGCCTCTCCCCG

tADH-REVSEQ

CCTAAGAGTCACTTTAAAATTTGTATACAC

Verify presence of TEV-3myc at the TRP1 locus

Cal_F

GCAAACCGCCTCTCCCC

TRP1_A

AGAGACCAATCAGTAAAAATCAACG

Verify integration of *SUP4 ochre* suppressor system at *his3Δ1* locus

HIS3_A

TGACGACTTTTTCTTAATTCTCGTT

NatR_B

TGGTGAAGGACCCATCCAG

Verify C-terminal tagging

ELP1_C

TTATATCCCAGAAATACCTGTTCCA

ELP5_C

GGGTGCTATTGTTTATGAGTACG

KTI12_C

GATCCGTTGAGTAAGGGCTTAC

ARG4_C

GCTGAAAGACTTGGTCTAAGCG

ELP3_Calt

CCAAAGAGACATTCCAATGCC

GLN4_C

GATAAGGATTCCAAAGAAGTGTGTAG

CEX1_C

CCTAGCACCAAGAAACATTGC

Gene specific forward primers listed above are used with the following reverse primers;

KO10

CGCACGTCAAGACTGTC

tADH-REVSEQ

CCTAAGAGTCACTTTAAAATTTGTATACAC

iii) <u>Sequencing Primers</u>

Sequence across *ELP1* 'delitto perfetto' replacement of CORE

Elp1_Sequencing_F

GTCAGTCGCAGAAGAGTTG

Sequence across region encoding Elp1 CTD for pUG34 cloning

pJET1.2_F

CGACTCACTATAGGGAGAGCGGC

Sequence across region encoding Elp1 CTD cloned into pGEX4T-1

GST-FORSEQ

CGACCATCCTCCAAAATCG

YIPLAC-INTF

CATGTGTCAGAGGTTTTCACCGT

iv) Primers as insert DNA

Nuclear export sequence of HIV(Rev) insert

NES_F

GATCCCCGGGTTAATTAACTTGCCTCCATTAGAGAGGTTAACCCTTGATAT

NES_R

ATCAAGGGTTAACCTCTCTAATGGAGGCAAGTTAATTAACCCGGG

v) 'gBlocks'

Nuclear localisation sequence from Cbp80 for cloning into pFa6a-GFP(s65T)-HIS3MX

GCTGAAGCTTCGTACGCTGCAGGTCGACGGATCCCCGGGTTAATTAACTTTAATAGAAAAAGAAGAGG
AGACTTCGATGAAGATGAAAATTACCGTGATTTTAGGCCTCGCATGCCTAAAAGACAGAGAATCCCACC
TGTTGTAAGTAAAGGAGAAGAACTTTTCACTGGAGTTGTCCCAATTCTTGTTGAATTAGATGGTGATGT
TAATGGGCACAAATTTTCTGTCAGTGGAGAGGGTGAAGGTGATGCAACATACGGAAAACTTACCCTTA
AATTTATTTGCACTACTGGAAAACTACCTGTTCCATGGCCAACACTTGTCACTACTTTCACTTATGGTGTT
CAATGCTTTTCAAGATACCCAGATCATATGAAACGGCATGACTTTTTCAAGAGTGCCATGCCCGAAGGT
TATGTACAGGAAAGAACTATATTTTTCAAAGATGACGGGAACTACAAG

Mutant Nuclear import sequence from Cbp80 for cloning into pFa6a-GFP(s65T)-HIS3MX

GCTGAAGCTTCGTACGCTGCAGGTCGACGGATCCCCGGGTTAATTAACTTTAATAGAAAAGCAGCCGG
AGACTTCGATGAAGATGAAAATTACCGTGATTTTAGGCCTCGCATGCCTGCAGCCCAGAGAATCCCACC
TGTTGTAAGTAAAGGAGAAGAACTTTTCACTGGAGTTGTCCCAATTCTTGTTGAATTAGATGGTGATGT
TAATGGGCACAAATTTTCTGTCAGTGGAGAGGGTGAAGGTGATGCAACATACGGAAAACTTACCCTTA
AATTTATTTGCACTACTGGAAAACTACCTGTTCCATGGCCAACACTTGTCACTACTTTCACTTATGGTGTT
CAATGCTTTTCAAGATACCCAGATCATATGAAACGGCATGACTTTTTCAAGAGTGCCATGCCCGAAGGT
TATGTACAGGAAAGAACTATATTTTTCAAAGATGACGGGAACTACAAG

vi) Oligonucleotide DNA Probes

Detection of tRNA by Northern blot

tRNAGlnUUG

GTCCGGATCAAAACCGAAAGTGATAACCACTACAC

tRNALysCUU

GAACCCCTAACCTTATGATTAAGAGTCATACGCG

vii) Competitor Oligonucleotides

ssDNA Competitor

Arg4_C

GCTGAAAGACTTGGTCTAAGC

Plasmids used in this study

The table below summarises plasmids used or generated in this study. In addition, selected plasmid maps are shown with important sequence features.

Appendix Table 1. Plasmids used and/or generated in this study.

Plasmid Name	Description	Source
pAE1	Expression plasmid for Zymocin gamma subunit under the control of the *GAL1-10* promoter	A. Edlin
pCORE	Plasmid for amplification of CORE cassette containing *KlURA3* and KanMX4	F. Storici
YCplac181	Multicopy expression plasmid used as an empty vector control for pJHW27	M. Stark
pJHW27	Multicopy expression plasmid containing yeast *KTI12* gene	M. Stark
pRS425	Multicopy expression plasmid used as an empty vector control for pRS425-tK(UUU)-tQ(UUG)	A. Bystrom
pRS425-tK(UUU)-tQ(UUG)	Multicopy plasmid containing yeast tK(UUU) and tQ(UUG) genes for tRNA overexpression	A. Bystrom
pSB1	*SUP4 ochre* suppressor system plasmid containing *URA3*, *SUP4* and NatRMX genes	S. Bandau
pSB3	*SUP4 ochre* suppressor system plasmid containing $ura3^{oc22}$, *SUP4* and NatRMX genes	S. Bandau
pT909	Plasmid for amplification of C-terminal 4mCherry tagging cassette containing Nat1 marker	T.Tanaka
pT1075	*OsTIR1*-9myc under the control of the *ADH1* promoter and containing the URA3 marker	T.Tanaka
pT1450	Plasmid for amplification of IAA17 AID degron sequence tagging cassette containing NatNT2 marker	T.Tanaka
yCplac111	Expression plasmid used as empty vector control for ycplac111-*ELP1*-6HA and related plasmids	D.Gietz
yCplac111-ELP1-6HA	Expression plasmid containing *ELP1*-6HA	D. Jablonowski

yCplac111-*elp1*-6HA	Expression plasmids containing *elp1*-6HA mutants[1]	DNA2.0
pFa6a-GFP(S65T)-HIS3MX6	Plasmid for amplification of C-terminal GFP tagging cassette	M. S. Longtine
pFa6a-NES-GFP(S65T)-HIS3MX6	NES from HIV Rev protein cloned in frame upstream of GFP	This study
pFa6a-NLS-GFP(S65T)-HIS3MX6	NLS from Cbp80 protein cloned in frame upstream of GFP	This study
pFa6a-NLS4A-GFP(S65T)-HIS3MX6	NLS from Cbp80 protein with 4 alanine substitutions cloned in frame upstream of GFP	This study
pUG34	Expression plasmid for N-terminal eGFP tagged fusion proteins expressed from a MET25 promoter	J.Hegemann
pUG34-ELP1 CTD	Region encoding Elp1 C-terminal domain cloned into pUG34 for fusion protein expression	This study
pUG34-*elp1-KR9A* CTD	Region encoding Elp1-KR9A C-terminal domain cloned into pUG34 for fusion protein expression	This study
pUG34-*elp1-KR5A* CTD	Region encoding Elp1-KR5A C-terminal domain cloned into pUG34 for fusion protein expression	This study
pUG34-*elp1-KR4A* CTD	Region encoding Elp1-KR4A C-terminal domain cloned into pUG34 for fusion protein expression	This study
pGEX-4T-1	Bacterial expression plasmid for GST tagged fusion proteins	A. Lamond
pGEX-6T-His_6	Bacterial expression plasmid for GST-His_6 tagged fusion proteins	T. Owen-Hughes
pGEX4T-1-*ELP1*-CTD-His_6	Sequence encoding Elp1 C-terminal domain cloned into pGEX4T-1 for bacterial fusion protein expression	This study
pGEX4T-1-*elp1-KR9A*-CTD-His_6	Sequence encoding Elp1-KR9A C-terminal domain cloned into pGEX4T-1 for bacterial fusion protein expression	This study

[1] Various plasmids containing mutant versions of *elp1* were synthesised by DNA2.0 as described in Section 2.1.11.

i) pAE1

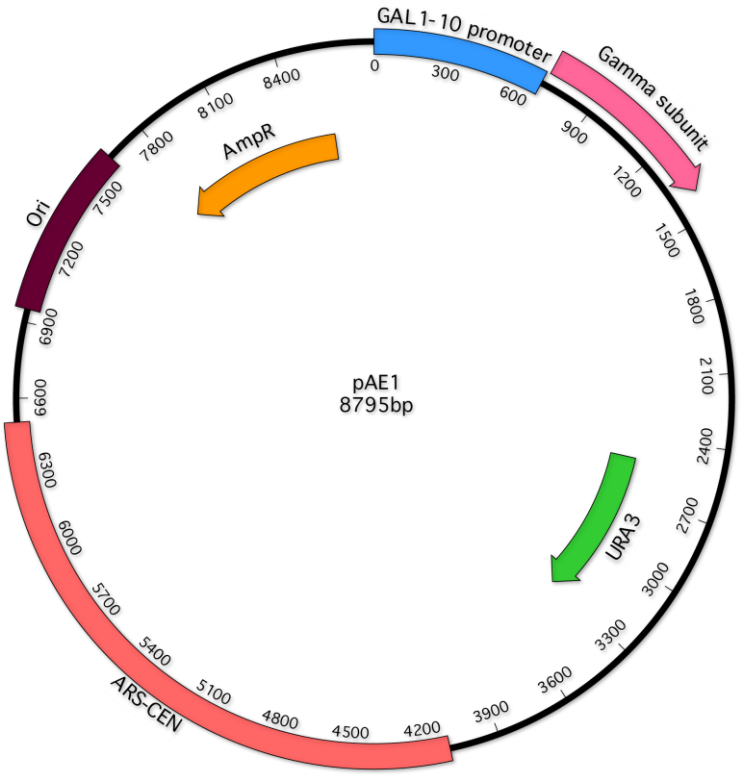

ii) pCORE

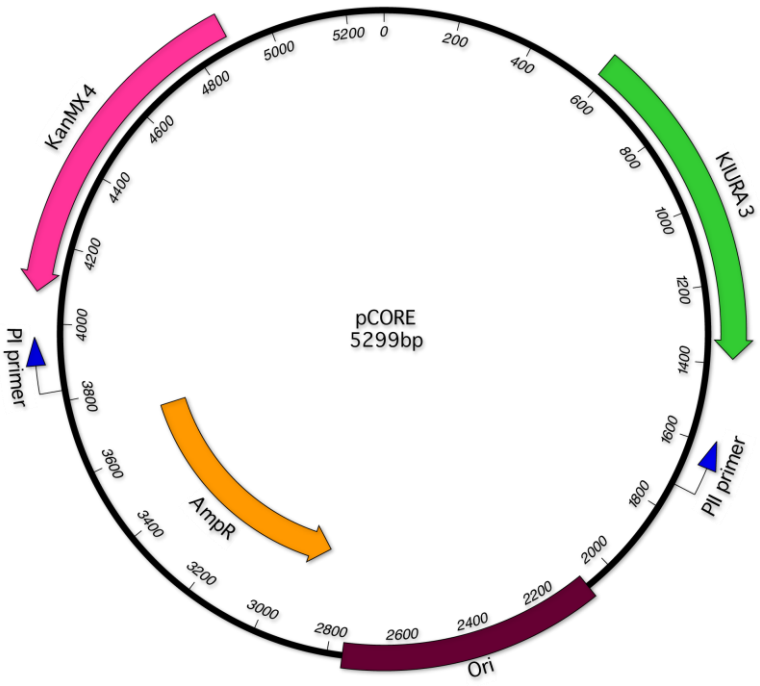

iii) pJHW27

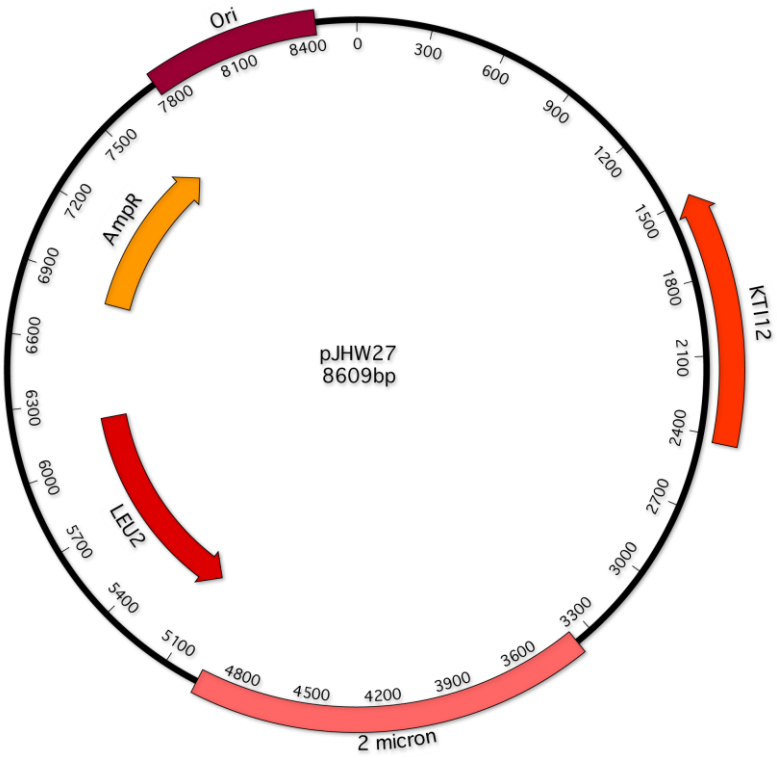

iv) pRS425-tK(UUU)-tQ(UUG)

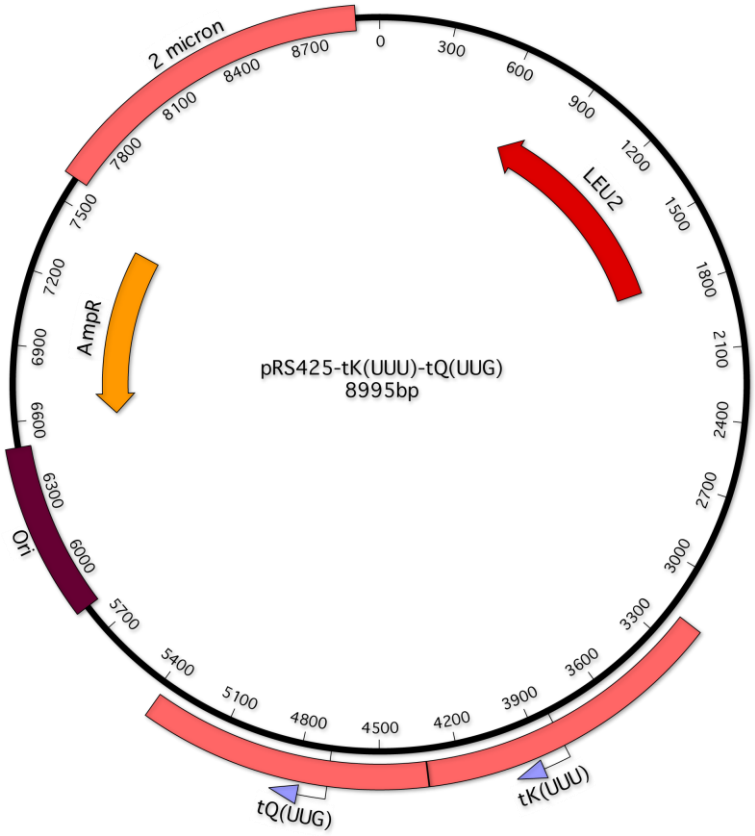

v) pSB3

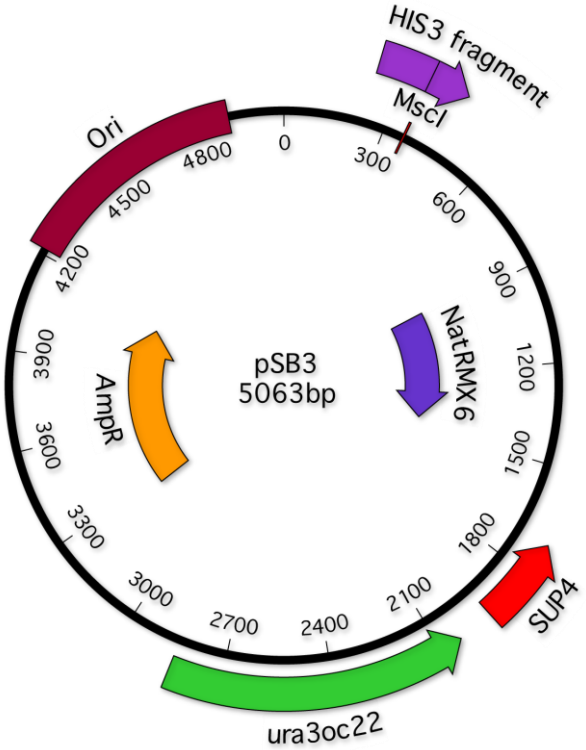

vi) ycplac111-ELP1-6HA

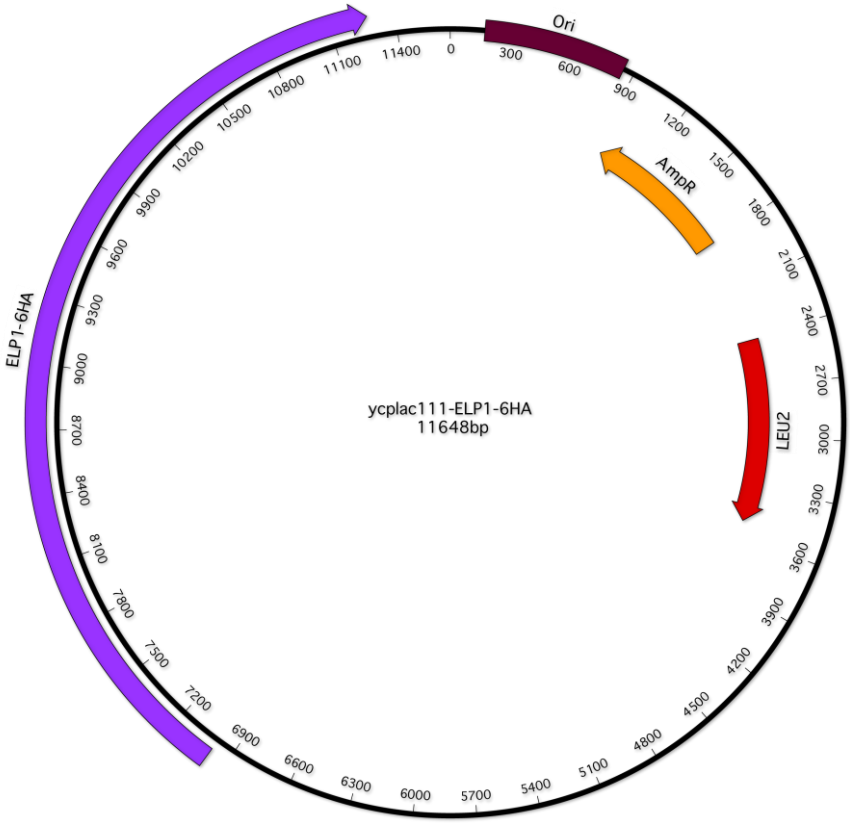

vii) pFa6a-NES-GFP(S65T)-HIS3MX6

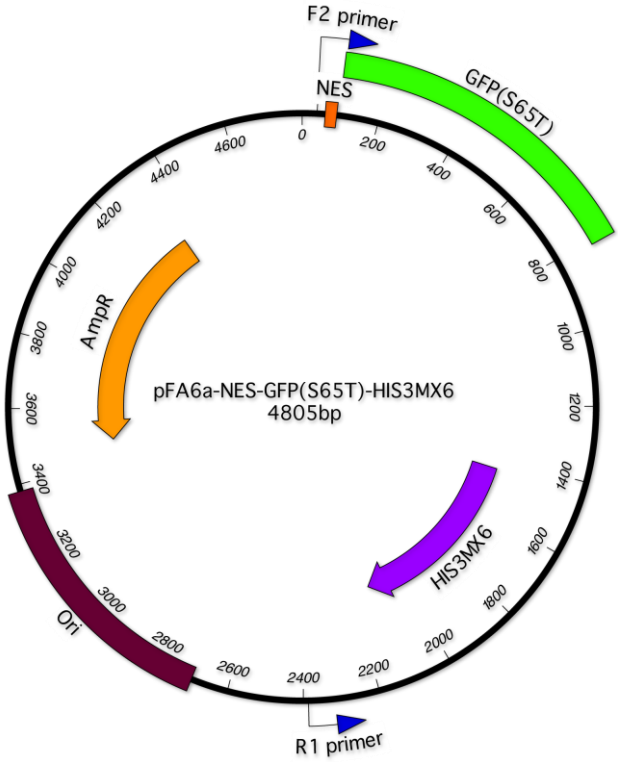

viii) pFa6a-NLS-GFP(S65T)-HIS3MX6

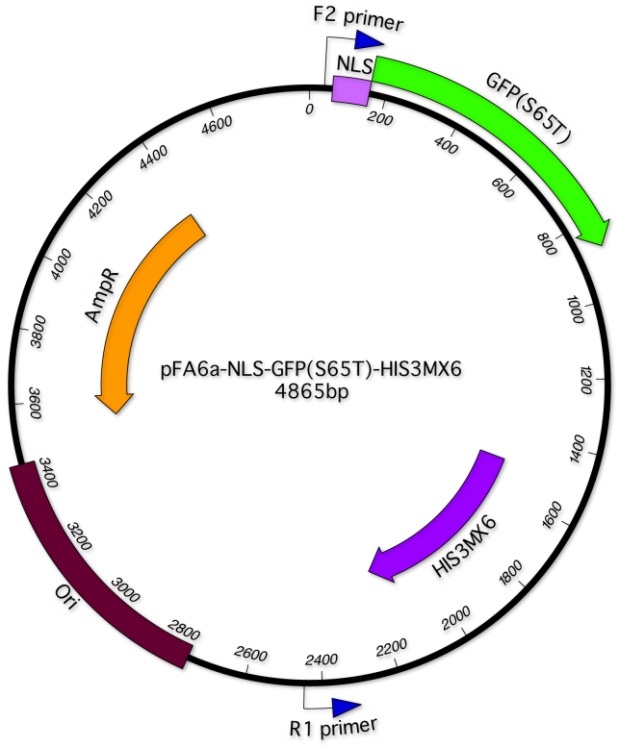

ix) pUG34-ELP1-CTD

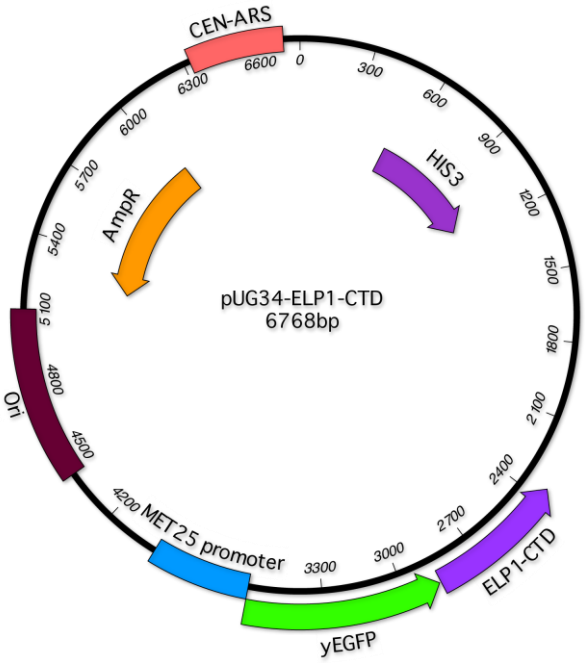

x) pGEX4T-1-*ELP1*-CTD-His$_6$

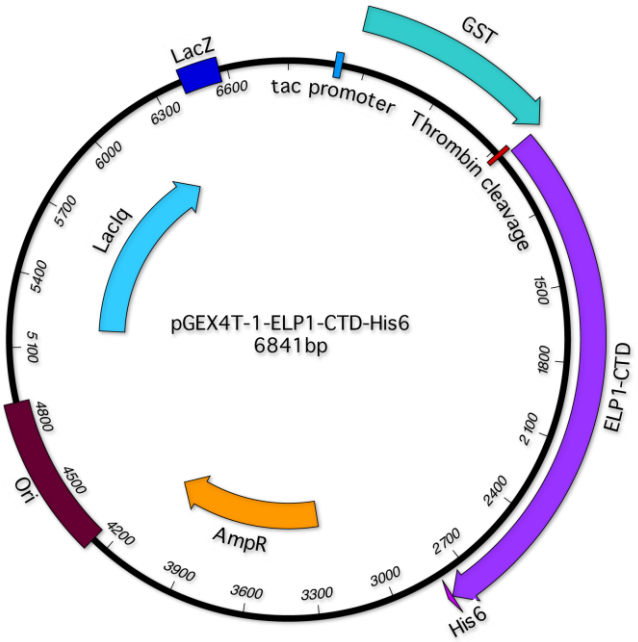

Media Recipes

The following recipes were used by Media Services, University of Dundee. All media and reagents provided are sterilised by autoclaving at 121 °C.

i) Yeast Media

Yeast extract-Peptone-Adenine-Dextrose (YPAD)

Per litre

Yeast extract (Merck)	10 g
Peptone (LabM)	20 g
Adenine Hydrochloride	0.01% (v/v)
Glucose	2% (v/v)
Granulated agar (BD Difco)	20 g (For plates only)
Deionised water	Up to 1 l

For eclipse assays Roth agar is used instead of BD granulated agar. Glucose is replaced with Raffinose and Galactose for YPARG and Raffinose for YPAR.

Synthetic complete (SC) or Drop out (DOA)

Per litre

Yeast nitrogen base (BD Difco)	6.7 g
Adenine (if required)	0.0074% (v/v)
Glucose	2% (v/v)
Granulated agar (BD Difco)	20 g (For plates only)
NaOH	1 mM (For plates only)
Appropriate Drop out mix (see below)	
Deionised water	Up to 1 l

For SC media- Synthetic complete drop out mix is added

For DOA media –Appropriate drop out mix is added with omittion of the required amino acids or nucleobases.

The final concentrations of amino acids and nucleobases used in yeast SC media are listed below.

Adenine Sulphate	20 µg/ml
Uracil	20 µg/ml
L-Tryptophan	20 µg/ml
L-Histidine HCl	20 µg/ml
L-Arginine HCl	20 µg/ml
L Methionine	20 µg/ml
L-Tyrosine	30 µg/ml
L-Leucine	100 µg/ml
L-Isoleucine	30 µg/ml
L-Lysine	30 µg/ml
L-Phenylalinine	50 µg/ml
L-Glutamic acid	100 µg/ml
L-Aspartic Acid	100 µg/ml
L-Valine	150 µg/ml
L-Threonine	200 µg/ml
L-Serine	400 µg/ml

Glucose-Nutrient-Agar (GNA)

Per litre

Nutrient Broth(BD Difco)	30 g
Yeast extract (BD Difco)	10g
Granulated agar (BD Difco)	20 g
Glucose	5% (v/v)
Deionised water	Up to 1 l

Sporulation Agar (VB)

Per litre

Sodium acetate	8.2 g
Potassium chloride	1.9 g
Sodium chloride	1.2 g
Granulated agar (BD Difco)	15 g
Magnesium sulphate	1.4 mM
Deionised water	Up to 1 l

ii) Bacterial media

Luria Browth (LB)

Per litre

LB granules (Merck)	25 g
Deionised water	Up to 1 l

Super optimal browth with catabolite repression (SOC)

Per litre

Tryptone (BD Difco)	20 g
Yeast Extract (BD Difco)	5 g
KCl	250 mM
NaCl	10 mM
$MgSO_4.7H_2O$	10 mM
$MgCl_2.6H_2O$	10 mM
Glucose	20 mM
Select Agar (Invitrogen)	12 g (plates only)
Deionised water	Up to 1 l

Autoinduction media

Per litre

Oxoid tryptone	10 g
Yeast Extract (Merck)	5 g
$MgSO_4$	1 mM
50 x 5052	20 ml
Glycerol	5 g
Glucose	0.5 g
a-lactose	2 g
$(NH_4)_2SO_4$	3.3 g
KH_2PO_4	6.8 g
Na_2HPO_4	7.1 g
Deionised water	Up to 1 l

iii) Drug working concentrations

ClonNAT	100 µg/ml
G418	200 µg/ml
Rapamycin	1 µg/ml
Ampicillin	100 µg/ml

iv) Reagents made by media services

10 x Tris buffered Saline (TBS)

Per litre

Tris	1 M
NaCl	1.4 M
Conc HCl	approx. 60ml (to pH 7.4)
Deionised water	Up to 1 l

50 x TAE

Per litre

Trizma Base (Sigma)	2 M
Glacial Acetic Acid	57.1 ml
EDTA	50 mM
Deionised water	Up to 1 l

10 x Phosphate buffered saline (PBS)

Per litre

NaCl	80 g
KCl	2 g
Na_2HPO_4	14.4 g
KH_2PO_4	2.4 g
Deionised water	Up to 1 l